Targeting glycolysis in endothelial cells to prevent intraplaque neovascularization and atherogenesis in mice

Perrotta, P.

Targeting glycolysis in endothelial cells to prevent intraplaque neovascularization and atherogenesis in mice

Paola Perrotta

Targeting glycolysis in endothelial cells to prevent intraplaque neovascularization and atherogenesis in mice

PROEFSCHRIFT

ter verkrijging van
de graad van Doctor aan de Universiteit Leiden,
op gezag van Rector Magnificus Prof.dr.ir. H. Bijl,
volgens besluit van het College voor Promoties
te verdedigen op woensdag 24 Maart 2021
klokke 15:00 uur

door

Paola Perrotta

geboren op 11 September 1986

te Bari, Italië

Promotores

Prof. Dr. P.H.A. Quax	*Leiden University Medical Center*
Prof. Dr. W. Martinet	*University of Antwerp*

Co-promotor

Dr. M.R. de Vries	*Leiden University Medical Center*

Promotiecommissie

Prof. Dr. G.R.Y. De Meyer	*University of Antwerp*
Prof. Dr. W. Jukema	*Leiden University Medical Centre*
Prof. Dr. J. Hamming	*Leiden University Medical Centre*
Dr. I. Bot	*University of Leiden*

The research described in this thesis has been a collaborative effort of the Laboratory of Physiopharmacology from the University of Antwerp and the Department of Vascular Surgery in Leiden Medical University Centre from Leiden University. The research was financially supported by the Horizon 2020 program of the European Union – Marie Sklodowska Curie actions – ITN – MOGLYNET [grant number 675527] and the University of Antwerp (DOCPRO-BOF).

Financial support by the Dutch Heart Foundation for the publication of this thesis is gratefully acknowledged.

“Science knows no country, because knowledge belongs to humanity, and is the torch which illuminates the world”.

Louis Pasteur

Cover Image: Microscopic image of a vein graft with intraplaque neovessels
Cover design: Paola Perrotta

Printed by: Arte grafica, Lecce (Italy)

Table of Contents

Abbreviations:

AA: aortic arch
ApoE: apolipoprotein E
ATP: adenosine triphosphate
CA: carotid artery
CD31: cluster of differentiation 31
CPT1: carnitine palmitoyltransferase 1A
CHD: coronary heart disease
DCM : dichloromethane
DMSO: dimethylsulfoxide
EC: endothelial cell
EF: ejection fraction
ECM : extracellular matrix
FAO: fatty acid oxidation
FAS : fatty acid synthesis
Fbn: fibrillin
FDG: fluorodeoxyglucose
FGF: fibroblast growth factor receptor
FS: fractional shortening
F-1,6-P_2 : fructose -2,6-bisphosphate
F-6-P: fructose-6-phosphate
GAPDH: Glyceraldehyde-3-Phosphate Dehydrogenase
GLUT: Glucose transporter
HAEC: human aortic endothelial cell
HDL: high-density lipoprotein
HE: haematoxylin-eosin
HIF: hypoxian inducible factor
HK: Hexokinase
HMG-CoA: 3-hydroxy-3-methylglutaryl-coenzyme A
HUVEC: Human umbilical vein endothelial cell
ICAM-1: intercellular cell adhesion molecule
iDISCO: immunolabeling-enabled 3D Imaging of Solvent Cleared Organs

IL: interleukin

iNOS: inducible nitric oxide synthase

IP/PI: intra-plaque

IVRT: isovolumic relaxion time

i.p.: intraperitoneal

i.v.: intravenous

KLF2: Kruppel Like Factor 2

α-KG: α-ketoglutaric acid

LDH: lactate dehydrogenase

LDL: low-density lipoprotein

LDLR: LDL receptor

LV: left ventricular

LVID: left ventricular internal diameter

MI: myocardial infarction

MMP: matrix metalloproteinase

NADH: nicotinamide adenine dinucleotide

OOA: oxalacetate

Ox: oxidized

PAD: peripheral arterial disease

PDGF: platelet-derived growth factor

PET: positron emission tomography

PFK-1: 6-phosphofructo-1 -kinase

PFKFB3: 6-phosphofructo-2-kinase/fructose-2,6-bisphosphatase 3

PF: platelet factor

PFPE: paraformaldehyde fixed paraffin embedded

PGI: phosphoglucose isomerase

Plgf: placenta growth factor

PCSK9: Proprotein convertase subtilisin/kexin type 9

PGK: phosphoglycerate kinase

SMC: smooth muscle cell

TCFA : thin cap fibroatheroma

TGF-β: transforming growth factor-β

TIA: transient ischaemic attack

TNF-α: Tumor necrosis factor alfa

VCAM-1 : vascular cell adhesion molecule-1

VEGF: vascular endothelial growth factor

VEGFR : VEGF receptor

vWF: von Willebrand factor

WD : western-type diet

WT: wild type

3PO: 3-(3-pyridinyl)-1-(4-pyridinyl)-2-propen-1-one

3D: three dimensional

Chapter 1

General introduction

Atherosclerosis

Atherosclerosis is a progressive inflammatory disease characterized by formation of lipid plaques inside the arterial vessel wall. Over time, plaque building can cause narrowing of the arterial lumen and lead to atherosclerotic vascular disease (i.e. coronary artery disease, peripheral artery disease).[1]

Although plaques often remain stable for years, they can also rapidly evolve to become unstable and rupture. This sudden event triggers intraluminal thrombus formation that can cause major adverse cardiovascular events such as acute coronary syndrome (ACS), myocardial infarction (MI) and stroke.[2 3] Elevated levels of low-density lipoprotein (LDL) in plasma is a major risk factor of atherosclerosis. LDL accumulates in the sub-endothelial space of the arterial wall and progressively undergoes oxidative modifications to form oxidized LDL (oxLDL).[4] This induces an inflammatory response characterized by overexpression of chemotactic proteins such as monocyte chemoattractant protein-1 (MCP-1), and adhesion molecules (vascular cell adhesion molecule-1 [VCAM-1], E-selectin and P-selectin) by endothelial cells (ECs).[5, 6] These adhesion molecules promote the infiltration of blood-carried monocytes into the inflamed arterial wall. After differentiation into macrophages, these cells engulf oxLDL and transform into foam cells which contribute to plaque development by secreting multiple mediators of the inflammatory process in the vessel wall.[7] The inflammatory response also promotes recruitment of circulating monocytes and T-cells that stimulate the migration of vascular smooth muscle cells (VSMCs) from the tunica media into the sub-endothelial space where they exhibit abnormally high proliferation and secrete extracellular matrix proteins that also contribute to atheroma growth.[5]

Advanced human plaques are characterized by a large necrotic core, many lipid-laden and activated macrophages, few VSMCs, intraplaque (IP) neovascularisation and haemorrhages, and a thin fibrous cap that separates the plaque from the blood stream.[8-10] Rupture of the fibrous cap of such high-risk vulnerable plaques leads to luminal thrombosis, arterial occlusion or embolism in distant vascular beds, resulting in MI, stroke or sudden death.[11] Figure 1 summarizes the components that can be usually found around the site of the atherosclerotic plaque.

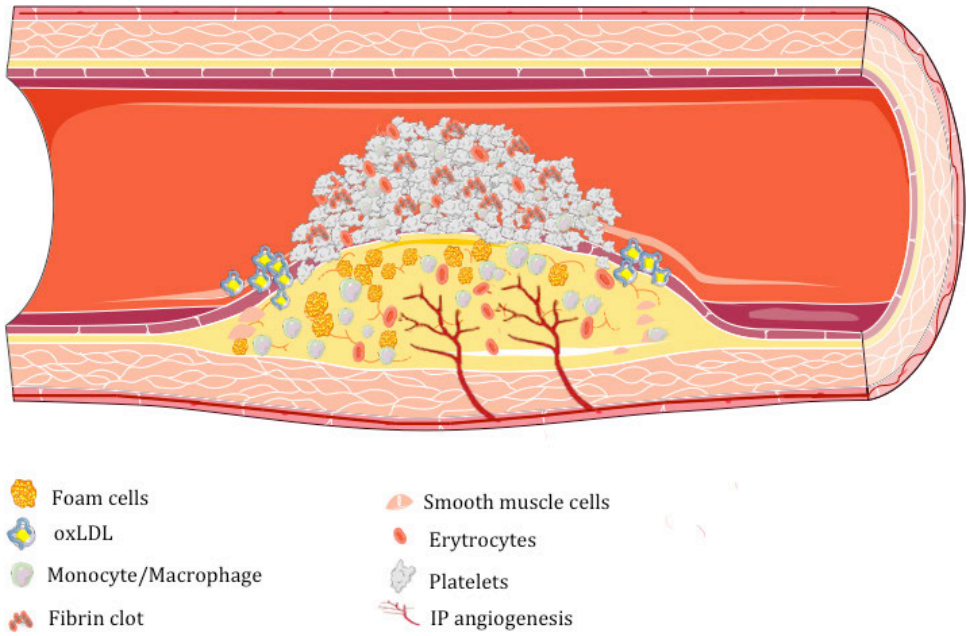

Figure 1. Schematic representation of the commonly observed components during various stages of plaque progression.

Endothelial cell dysfunction and subsequent accumulation of low-density lipoproteins (LDL) in the intima of the vessel wall are the early step of atherosclerotic plaque formation. The expression of adhesion molecules on the endothelium stimulates the recruitment of monocytes and T cells into the subendothelial space. After differentiation, macrophages turn into foam cells by “ingesting” oxidized LDL. The migration of vascular smooth muscle cells from the media into the plaque is promoted by growth factors and cytokines, derived from macrophages and T cells. Subsequent production of collagen results in the formation of a thick, protective fibrous cap. In response to hypoxia, immature intraplaque microvessels penetrate into the plaque. The atherosclerotic plaque becomes vulnerable because of a thinning fibrous cap and the formation of a large necrotic core. Plaque rupture exposes pro-coagulant material to the blood, thereby triggering thrombus formation.

Intraplaque neovascularization in advanced atherosclerosis

Intraplaque (IP) angiogenesis is a complex process that depends on the equilibrium between several pro- and anti-angiogenic molecules.[12] The presence of hypoxia in advanced atherosclerotic plaques correlates with IP angiogenesis in human carotid

arteries.[13-15] The response to low O_2 is mostly mediated by Hypoxia-inducible factors (HIFs), a family of transcription factors that control the expression of multiple pro-angiogenic mediators including vascular endothelial growth factor (VEGF), angiopoietin-1, angiopoietin-2, Tie2, platelet-derived growth factor (PDGF), basic fibroblast growth factor (bFGF), and monocyte chemoattractant protein–1 (MCP-1). Activation of HIF pathway induces localized angiogenesis by enhancing vascular permeability, endothelial cell proliferation, sprouting, migration, adhesion and tube formation.[16] From a molecular point of view, HIFs are heterodimeric proteins composed of one α and one β subunits. The α chain confers oxygen sensing to the complex and its expression is hypoxia-dependent. Each subunit has three isoforms expressed by three different genes, HIF-1α, 2α,3α and HIF-1β, HIF-2β HIF-3β HIF-1α and HIF-1β are widely expressed in normal tissues. The beta chain (three isoforms) is constitutively expressed and works as an aryl receptor nuclear translocator. Under normoxic conditions, the synthesized HIF-1α is rapidly degraded and the co-activators are blocked by oxygen-dependent enzymes; the prolyl-hydroxylases domain (PHD) enzymes. During hypoxia, PHD activity is reduced, allowing the dimerization of HIF-1α and HIF-1β. This active complex translocate to the nucleus where it binds to DNA and promotes transcription of downstream genes important for angiogenesis.[17, 18] Furthermore, it has been shown that HIF1α induces a switch from oxidative phosphorylation towards glycolysis which in turn regulates EC rearrangement during vessel sprouting.[19]

Besides hypoxia, inflammation is a strong inducer of angiogenesis as it promotes the synthesis of various angiogenic factors. During acute inflammation, several pro-angiogenic molecules can induce cell permeability, contributing to the infiltration of leukocytes in the inflammatory core and thereby provoking chronic inflammation.[20] Because the newly formed vessels growing into the plaque are immature, they are inherently leaky, permitting inflammatory cell infiltration and influx of blood constituents (including erythrocytes and blood platelets) into the plaque (Figure 2).[21] Moreover, IP neovessels can promote the entry of leukocytes into the plaque by upregulation of adhesion molecules such as ICAM-1 and VCAM-1.[22] The increased release of matrix metalloproteinases from activated macrophages and proteases secreted from mast cells cause further damage to the microvessels and facilitate IP haemorrhage.[23, 24]IP neovascularization also increases the risk of blood

haemorrhage inside the plaque which promotes plaque progression and instability.[25,26]

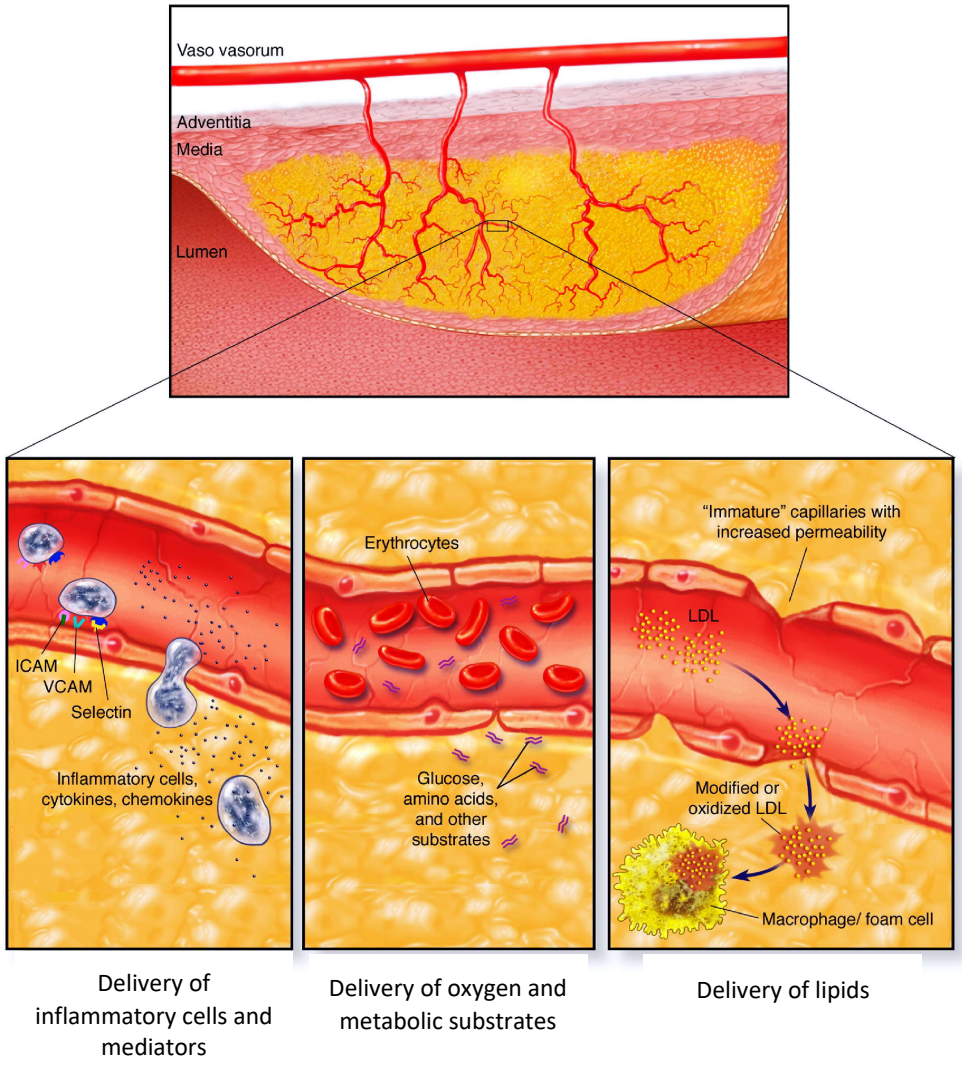

Figure 2. Contribution of intraplaque neovessels to plaque destabilization. (Adapted from Doyle et al. [27])

IP neovessels are often leaky and show high expression of vascular cell adhesion molecule 1 (VCAM-1) and intercellular adhesion molecule 1 (ICAM-1). These conditions further facilitate the entry of pro-inflammatory cells, erythrocytes and low-density lipoprotein (LDL) in the plaque microenvironment.

Intraplaque neovascularization: a novel therapeutic target in advanced atherosclerotic plaques

Thanks to cholesterol-lowering drugs (such as statins), the lifespan and wellbeing of patients has significantly improved. Recently, several new therapies have also emerged to treat high-risk patients (e.g. PCSK9 monoclonal antibodies to reduce the residual cholesterol risk).[28-31] However, a large group of patients does not fully benefit from current lipid-lowering strategies.[32] Indeed, despite major advances in cardio- and cerebrovascular research, plaque rupture remains the leading cause of acute events.[33, 34] Therefore, additional therapy that reduces atherosclerosis or prevents plaque rupture and its complications is needed.

Recent evidence suggests that IP angiogenesis promotes atherosclerosis progression and plaque destabilization.[35] Indeed, clinical data have found a strong association between IP angiogenesis and progressive unstable vascular disease.[8] Autopsy studies, for example, revealed a higher density of IP vasa vasorum microvessels in symptomatic (ruptured) plaques compared to asymptomatic ones.[24, 35] A comprehensive review of the published studies about the evidence and the impact of IP angiogenesis in human atherosclerosis progression can be found in **chapter 2** of this thesis**.**

Glycolysis inhibition as a novel approach to block IP angiogenesis and to promote plaque stability

Glycolysis is a metabolic process that converts glucose into two molecules of pyruvate and generates 2 molecules of ATP (adenosine triphosphate), 2 NADH (reduced nicotinamide adenine dinucleotide), and two water molecules (Figure 3).

Recent studies have demonstrated that proliferating ECs mainly rely on high glycolytic activity (>200-fold higher than glucose, fatty acid and glutamine oxidation), to generate up to 85% of the total cellular ATP content.[36] Although anti-VEGFA therapy has been widely used to inhibit neovascularization in oncology and eye

disease, modulation of EC metabolism has recently shown beneficial effects in cancer research, and this approach may represent an attractive new strategy to inhibit neovascularization in atherosclerosis as well.[37, 38] Further details about this approach are described in **chapter 2** of this thesis**.**

Vascular endothelial growth factor receptor-2 (VEGFR-2) signalling and expression of glucose transporter-1 (GLUT-1) as well as that of glycolytic enzymes, such as phosphofructo-2-kinase/fructose-2,6-bisphosphatases (PFKFB3) are increased in ECs under inflammatory conditions, (Figure 3).[39, 40] PFKFB3 is a key enzyme that modulates glycolytic flux and it has also been shown to promote EC migration. Deletion of this enzyme in ECs leads to defects in angiogenesis both *in vitro* and *in vivo.*[41]

Furthermore, it has been demonstrated that in ECs, normal atheroprotective blood flow increases the activity of the flow-responsive transcription factor Kruppel Like Factor 2 (KLF2) which, in addition to increasing VE-cadherin expression and barrier function, transcriptionally represses PFKFB3 expression and lowers glycolytic rates to sustain EC quiescence. Atheroprone turbulent flow lowers KLF2 activity and VE-cadherin levels, and upregulates PFKFB3 expression causing increased glycolysis and EC activation. Additionally, in atheroprone regions, low shear stress and oxLDL induce miR-92a expression to lower KLF2 levels.[39] Based on these findings, PFKFB3 could play an important role also on atherosclerotic plaques stabilization.

Previous studies in the oncological field presented a small molecule 3PO [3-(3-pyridinyl)-1-(4-pyridinyl)-2-propen-1-one], which transiently inhibits glycolysis in proliferating ECs and impairs pathological angiogenesis in vivo without interfering with the metabolism of healthy cells.[42] 3PO targets the hyper-metabolism that is induced when ECs switch from quiescence to proliferation and migration.[43]

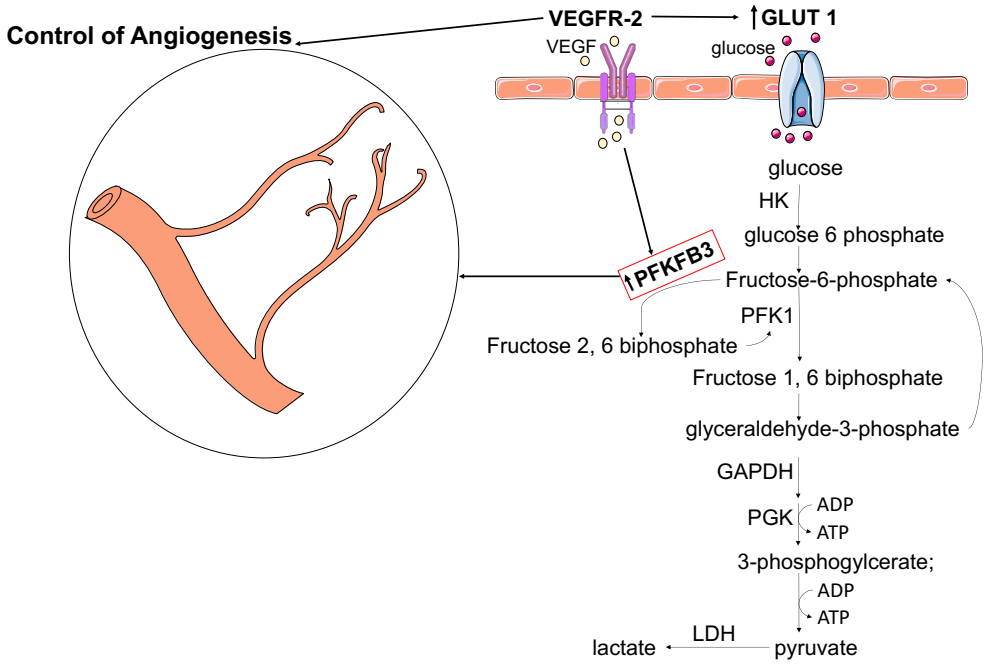

Figure 3. ***Glycolysis in ECs and its relation with angiogenesis***. Activated angiogenic endothelial cells rely mostly on glycolysis for ATP generation. Indeed, VEGFR-2 signalling (a major proangiogenic factor) increases the expression also of GLUT-1 as well as of other glycolytic enzymes, such as PFKFB3. HK (Hexokinase); PFK1 (Phosphofructokinase-1); GAPDH (Glyceraldehyde-3-Phosphate Dehydrogenase).

Animal models that develop vulnerable plaques with intraplaque angiogenesis

According to the American Heart Association (AHA), a 'vulnerable plaque' is defined as a lesion susceptible to complications, and identifies all thrombosis-prone plaques and those ones with a high probability of undergoing rapid progression. These plaques are often modestly stenotic lesions with specific morphological characteristics including a large core of lipid deposits, IP neovessels, necrotic cell debris and macrophages producing matrix-degrading enzymes such as metalloproteinases, with thinning of the fibrous cap.

These lesions as described above, are prone to rupture and may cause acute cardiovascular complications.[44]

In vivo studies with experimental animal models are essential to gain detailed insight into the molecular mechanisms of atherosclerotic plaque vulnerability and to develop better diagnostic and therapeutic tools for imaging IP neovessels. Over the years the most extensively characterized strains are apolipoprotein E-knockout ($ApoE^{-/-}$) mice and low-density lipoprotein receptor-knockout ($LDLr^{-/-}$) mice.[45] Although these models have permitted the study of atherogenic processes, to date they often do not develop vulnerable plaques with IP neovessels. This limitation can be overcome using the $ApoE^{-/-}Fbn1^{C1039G+/-}$ strain or other established mouse model of atherosclerosis (e.g.,$ApoE^{-/-}$, APOE*3-Leiden) that undergo vein grafting procedure. **Chapter 3** of this thesis presents all the current animal models of atherosclerosis including the animal models that have been used for the experimental work of this thesis, namely $ApoE^{-/-}Fbn1^{C1039G+/-}$ mice and regular $ApoE^{-/-}$ mice (with or without vein grafting).

Apolipoprotein E-deficient Fibrillin-1 mutant ($ApoE^{-/-}Fbn1^{C1039G+/-}$) mice

The extracellular matrix of atherosclerotic plaques is a complex network of predominantly elastin and collagen, which is essential to provide structural, adhesive and biochemical signalling support to the vessel wall. In elastic arteries, elastin is the most abundant protein. The elastic fibres comprise the elastin core, which is surrounded by a mantle of fibrillin-rich microfibrils.[46] The elastic-fibre-associated microfibrils have as the main structural component fibrillin-1, a large glycoprotein of about 350 kDa, whose major role is in binding and sequestering growth factors, such as transforming growth factor-β (TGF-β), as well as providing the scaffold for the deposition and the cross-linking of elastin.[47, 48]

Recently, our group reported the effect of an impaired elastin structure of the vessel wall on the progression of atherosclerosis by cross-breeding $ApoE^{-/-}$ mice with mice containing a heterozygous mutation ($C1039G^{+/-}$) in the fibrillin-1 (Fbn1) gene.[48] Mutations in the Fbn1 gene lead to the Marfan syndrome, a genetic disorder characterized by fragmentation of elastic fibres.[49] This results in increased arterial stiffening, elevated pulse pressure and progressive aortic dilatation.[48, 50, 51]

Moreover, the mutation leads to the development of highly unstable plaques in ApoE$^{-/-}$ mice, resulting in spontaneous plaque rupture with clinical end-points such as MI and sudden death.[48, 52] Importantly, these events do not – or only very occasionally – occur in ApoE$^{-/-}$ mice on a Western-type diet or in ApoE$^{-/-}$Fbn1$^{C1039G+/-}$ mice fed a normal diet.[52, 53] These findings underscore the importance of elastin fragmentation in combination with a Western-type diet as prerequisites for atherosclerotic plaque rupture in mice.

ApoE$^{-/-}$Fbn1$^{C1039G+/-}$ mice have significantly larger plaques with a highly unstable phenotype, characterized by a large necrotic core (occupying about 30% of total plaque area), and a strongly diminished collagen content. Accelerated atherogenesis in these mice is likely the result of enhanced vascular inflammation, leading to increased monocyte attraction, oxidation and accumulation of lipids.[54]

Extensive neovascularisation and IP haemorrhages consistently occur in the brachiocephalic and common carotid arteries of ApoE$^{-/-}$Fbn1$^{C1039G+/-}$ mice on Western-type diet. These features are rarely seen in murine atherosclerosis models but are known to highly affect plaque progression and vulnerability in humans.[35] In ApoE$^{-/-}$Fbn1$^{C1039G+/-}$ mice on a Western-type diet, IP neovessels, likely arising from adventitial vasa vasorum, clearly sprout out of the media.[55, 56] Neovessels are not only present at the base of the plaque but are also frequently observed in its centre, similar to the human pathology.[35, 56] Angiogenesis requires extracellular matrix degradation by proteases, including MMPs, to enable EC migration into the surrounding tissue.[57] In addition, degradation of the extracellular matrix induces the release of sequestered angiogenic factors such as vascular endothelial growth factor (VEGF) and TGF-β,[57, 58] also observed in ApoE$^{-/-}$Fbn1$^{C1039G+/-}$ mice on Western-type diet. The extent of neovascularisation in ApoE$^{-/-}$Fbn1$^{C1039G+/-}$ mice correlates with the degree of elastin fragmentation in the vessel wall. However, degradation of the extracellular matrix alone is not sufficient to induce neovascularisation in atherosclerotic plaques, because neovessels are not present in plaques of ApoE$^{-/-}$Fbn1$^{C1039G+/-}$ mice on a normal diet. Moreover, the presence of IP erythrocytes near neovessels at the base of the plaque points to intraplaque haemorrhages, substantiating ruptured neovessels as a source of IP bleeding.[35, 58, 59] Erythrocytes are important sources of free cholesterol, thereby increasing necrotic core size. Hence, neovascularisation, besides supplying plaques with leukocytes and

lipoproteins, can promote focal plaque expansion when neovessels rupture or become thrombotic.[35, 59, 60] These observations in ApoE$^{-/-}$Fbn1$^{C1039G+/-}$ mice are in line with current concepts of human vulnerable plaques. Therefore, ApoE$^{-/-}$Fbn1$^{C1039G+/-}$ mice on a Western-type diet offer the opportunity to investigate the role of key factors involved in plaque destabilisation, including IP neovascularisation, which will provide more insight into the mechanisms of plaque disruption and potential targets for therapeutic interventions.[52, 61-63]

Vein grafting in Apolipoprotein E deficient mice

Vein bypass grafting is a cardiovascular surgical practice for revascularization of occluded atherosclerotic arteries. The great saphenous veins are normally used as conduits for bypassing the occlusion.[64] Multiple lines of evidence show that 40% of the patients suffer from bypass failure within eight years and about 10% of all vein grafts fail due to acute thrombosis as a result of technical problems and de-endothelializations.[65-67] The high failure rate is due to the fact that veins grafted into an arterial environment undergo a complex vascular remodeling process resulting in intimal hyperplasia, which can lead to the rupture of the graft. These events are due to complex, dynamic interactions between various cell populations including ECs, mesenchymal smooth muscle-type cells, macrophages, activated thrombocytes and infiltrating inflammatory cells.[64, 66-68]

An important role in vein graft remodeling and subsequent rupture is played by ECs which have the ability to switch between a mature quiescent and an angiogenic state.[69] In recent years several mouse vein graft models have been described. These models vary in the location in which the graft is placed, primary in the carotid artery or the aorta. One of the most frequently used models for vein graft disease is the model described for the first time by the group of Xu [70] and currently used also by our group. In this model, the caval vein of a donor mouse is interpositioned in the carotid artery of a receiver mouse (Figure 4).

When this procedure is performed in apolipoprotein E-knockout mice (ApoE$^{-/-}$) or ApoE3*Leiden mice, a vein graft with high unstable lesions and IP angiogenesis is formed.[71] It has been demonstrated that these neovessels in vein graft lesions are dysfunctional, immature and they contribute to make the plaque bigger and unstable

by enhancing leukocyte recruitment and accumulation of cholesterol and platelets.[72, 73] Therefore vein grafting in ApoE$^{-/-}$ mice is an interesting and useful model to study potential therapeutic strategies in order to stabilize atherosclerotic lesions.

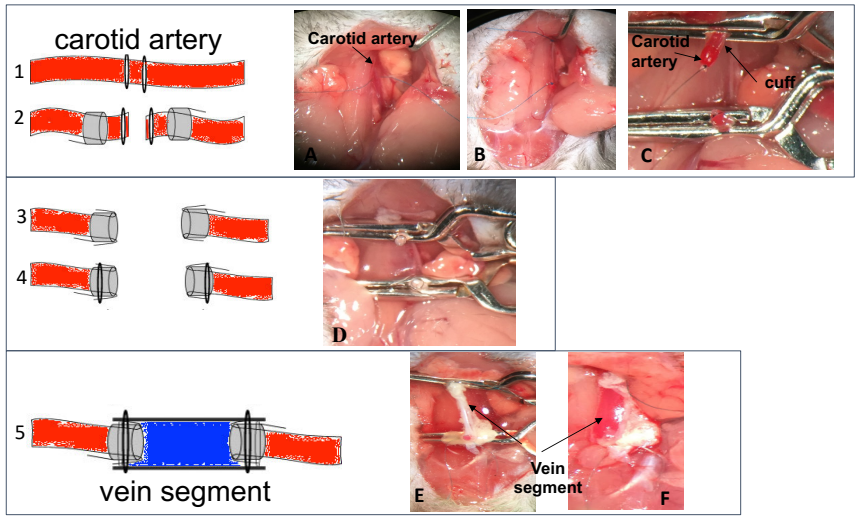

Figure 4. On the left side (1-5) : schematic overview of the different steps during vein graft surgery; on the right side (A-F): representative pictures of the procedures

1-2 Carotid artery becomes visible after it is dissected free from the surrounding fat and tissue. It is then ligated with two 8/0 silk sutures and cut in the middle (A-B). On both the proximal and distal artery end, a nylon cuff is sleeved which is fixated on the cuff handles with hemostatic clamps (C).

3-4 The carotid artery is reverted over the cuff and is tightened with an 8/0 suture (D).

5 The caval vein is positioned over both the cuffs and fixed with ligatures (E). Clamps are then removed (F).

In vivo imaging of atherosclerosis plaques

The assessment of plaque vulnerability with non-invasive imaging methods has become critically important for the diagnosis of rupture-prone plaques. Non-invasive computed tomography (CT) angiography and Doppler ultrasound are commonly used in the clinical practice to assign patient to medical or surgical intervention in presence of carotid atherosclerosis.[74] However, these methods mostly rely on

stenosis and often do not take into account other plaque parameters associated with high risk of rupture. For instance, it has been shown that significant atheroma burden with a high risk of subsequent cardiac events may arise even in absence of luminal stenosis due to outward artery remodeling.[75] Other imaging techniques, such as intravascular ultrasound (IVUS), optical coherence tomography (OCT) and near-infrared spectroscopy (NIRS), can provide a limited plaque characterization but, unfortunately, they are invasive and thus not ideal in early-diagnosis or follow-up.

To date Positron Emission Tomography (PET) is one imaging method that overcomes the previous limitation because it can detect and quantify the pathophysiological processes associated with atherogenesis and subsequent risk of plaque destabilization.[74, 76]

PET imaging as discussed in **chapter 7** is regularly used in the oncological field, and since 2002 has been used as research tool to measure pathophysiological processes in atherosclerosis.[77] [78] This imaging methodology shows higher sensitivity allowing better visualization of biological and biochemical processes involved in the development of atherosclerotic plaques. Although there is no optimal PET tracer for routine clinical imaging, numerous pathways and targets have been studied for PET imaging of atherosclerosis such as glycolysis, cell membrane metabolism (phosphatidylcholine synthesis), integrin αvβ3, low density lipoprotein (LDL) receptors (LDLr), natriuretic peptide clearance receptors (NPCRs), fatty acid synthesis, VCAM-1, macrophages, platelets, etc. Among the PET radiotracers that have been studied, only 18F-FDG has been approved for clinical use. However, carotid artery imaging using 18F-FDG PET is challenging due to the low spatial resolution of PET (≈ 4 mm in human PET and 1,2 mm in rodent PET), cardiac motion and myocardial spill over.[78] [79] To address the latter limitation, new imaging targets and radiotracers with lower unspecific myocardial uptake are currently under investigation. Non-invasive diagnosis and follow-up tools could also help in risk stratification and evaluation of the efficacy of anti-atherosclerotic therapies. **In chapter 7** the development of a new radiotracer that targets PFKFB3 enzyme in atherosclerosis is reported. This novel radiotracer (18F-radiolabeled PFKFB3-targeted ligand) has been tested in two mouse atherosclerosis models that develop rupture-prone plaques and has shown promising results.

The “low” spatial resolution of PET imaging often limits its use in preclinical studies where the characterization of atherosclerosis plaque progression and structure need to perform in small animals. To overcome this limitation, intravital microscopy (IVM) has been recently investigated. This method consists of high-resolution hardware able to study the microvasculature and explore cellular events in small sized animals using several light microscopy techniques such as widefield fluorescence, confocal, two-photon (2P).[80]

Ex-vivo imaging of atherosclerosis plaques

Although conventional histology is the gold standard for analysis of plaque morphology, it shows several limitations for assessing the three-dimensional (3D)-architecture of IP neovascularization. In every optical and microscopic technique, the capability of imaging deep into a biological sample is conditioned by the limited penetration depth of light within biological tissues that are optical media characterized by high turbidity.[81]

In **chapter 8**, a novel method of 3D reconstruction is described. This is based on immunolabeling-enabled 3D Imaging of Solvent Cleared Organs (iDISCO) and confocal microscopy. The technique is applied for the characterization of IP neovessels in $ApoE^{-/-}Fbn1^{C1039G+/-}$ an established atherosclerosis mouse model characterized by the presence of advanced plaques with evident IP neovascularization.

iDISCO is an optical clearing method that renders biological samples more transparent (‘cleared’) and allows such cleared segments to be visualized using confocal microscopy. [82] Application of this method to atherosclerotic arteries resulted in the visualization of the delicate IP neovascularization in carotid plaques. Furthermore, quantitative measurements of the neovessels entering the plaque can be obtained by using 3D analysis software.

This method may represent a useful tool for studies that aim to determine whether there is a causal relationship between the presence of intraplaque neovessel structures and atherogenesis or between angiogenic stimuli and plaque angiogenesis.

Aim of the thesis

Atherosclerosis is the main underlying condition that promotes the onset of cardiovascular disease, a leading cause in mortality in the western world.[32] Mounting evidence suggests that IP neovascularization can promote atherosclerosis progression and plaque destabilization in advanced stage. [24, 35]

The overall aim of this thesis is to investigate the biological role of IP neovascularization in atherosclerosis progression and plaque stability. In this context, ECs highly rely on glycolysis to sustain their activated pro-angiogenic behavior.[35, 69] Accordingly, this thesis also investigates whether **inhibition of EC glycolysis would be a novel target to prevent atherogenesis and/or atherosclerotic plaque destabilization.**

Thesis outline

Chapter 2 consists of a review in which we discuss the potential pharmacological strategies to inhibit IP angiogenesis. In particular, we focused our attention on inhibition of vascular endothelial growth factor signalling, inhibition of glycolytic flux, and inhibition of fatty acid oxidation. In **chapter 3** of this thesis, we review the animal models that have contributed to the understanding of atherosclerosis and its clinical consequences, and that have allowed significant improvement in atherosclerotic treatment.

Proliferating ECs in inflammatory conditions generate up to 85% of their ATP from glycolysis,[35, 69] thus targeting this pathway could be a promising approach. Indeed, IP neovascularization might represent a novel therapeutic treatment to promote plaque stabilization on top of the lipid-lowering therapies. Therefore, we investigate in **chapter 4** whether pharmacological inhibition of glycolytic flux by the small molecule 3PO [3-(3-pyridinyl)-1-(4-pyridinyl)-2-propen-1-one] had a beneficial effect on plaque stability. The effect on general metabolism was first studied and then effects on IP angiogenesis, plaque composition and plaque formation in $ApoE^{-/-}$ $Fbn1^{C1039G+/-}$ mice were determined. The molecular pathway behind the in vivo effect was also studied. In **chapter 5,** we further investigate whether 3PO-mediated

glycolysis inhibition is directly related to its direct binding to PFKFB3 (6-phosphofructo-2-kinase/fructose-2,6-bisphosphatase).

In **chapter 6,** we study the effect of specific endothelial PFKFB3 deletion in vein graft lesions of $ApoE^{-/-}$ mice. Firstly, the effect on general metabolism after PFKFB3 endothelial specific deletion was evaluated. Thereafter, IP angiogenesis and composition of vein graft lesions were analysed. Furthermore, in this chapter we evaluate in this chapter the effect of endothelial PFKFB3 deletion on native atherosclerosis.

Chapter 7 consists of a study performed in collaboration with the University of Aberdeen (UK) to investigate the uptake of a novel PFKFB3-targeted PET (Positron emission tomography) tracer ($[^{18}F]$ZCDD083) for atherosclerotic plaque imaging in $ApoE^{-/-}Fbn1^{C1039G+/-}$ mice and $ApoE^{-/-}$ mice.

Although conventional histology is the gold standard for analysis of plaque morphology, it shows several limitations for assessing the three-dimensional (3D)-architecture of IP neovascularization. Therefore, we describe in **chapter 8** a novel method based on iDISCO (immunolabeling-enabled 3D Imaging of Solvent Cleared Organs) and confocal microscopy, for a 3D reconstruction of IP angiogenesis in $ApoE^{-/-}Fbn1^{C1039G+/-}$ mice. Finally, **chapter 9** provides a summarizing discussion of the different chapters and future perspectives.

References

1. Falk E. Pathogenesis of atherosclerosis. *J Am Coll Cardiol*. 2006;47:C7-12
2. Sriranjan RS, Tarkin JM, Evans NR, Chowdhury MM, Rudd JH. Imaging unstable plaque. *Q J Nucl Med Mol Imaging*. 2016;60:205-218
3. Townsend N, Wilson L, Bhatnagar P, Wickramasinghe K, Rayner M, Nichols M. Cardiovascular disease in europe: Epidemiological update 2016. *Eur Heart J*. 2016;37:3232-3245
4. Hoogeveen RC, Gaubatz JW, Sun W, Dodge RC, Crosby JR, Jiang J, Couper D, Virani SS, Kathiresan S, Boerwinkle E, Ballantyne CM. Small dense low-density lipoprotein-cholesterol concentrations predict risk for coronary heart disease: The atherosclerosis risk in communities (aric) study. *Arterioscler Thromb Vasc Biol*. 2014;34:1069-1077
5. Fuster JJ, Castillo AI, Zaragoza C, Ibáñez B, Andrés V. Animal models of atherosclerosis. *Progress in Molecular Biology and Translational Science*. 2012:1-23
6. Tabas I, García-Cardeña G, Owens GK. Recent insights into the cellular biology of atherosclerosis. *J Cell Biol*. 2015;209:13-22
7. Sakakura K, Nakano M, Otsuka F, Ladich E, Kolodgie FD, Virmani R. Pathophysiology of atherosclerosis plaque progression. *Heart, Lung and Circulation*. 2013;22:399-411
8. Crombag G, Schreuder F, van Hoof RHM, Truijman MTB, Wijnen NJA, Voo SA, Nelemans PJ, Heeneman S, Nederkoorn PJ, Daemen JH, Daemen M, Mess WH, Wildberger JE, van Oostenbrugge RJ, Kooi ME. Microvasculature and intraplaque hemorrhage in atherosclerotic carotid lesions: A cardiovascular magnetic resonance imaging study. *J Cardiovasc Magn Reson*. 2019;21:15
9. Sluimer JC, Kolodgie FD, Bijnens AP, Maxfield K, Pacheco E, Kutys B, Duimel H, Frederik PM, van Hinsbergh VW, Virmani R, Daemen MJ. Thin-walled microvessels in human coronary atherosclerotic plaques show incomplete endothelial junctions relevance of compromised structural integrity for intraplaque microvascular leakage. *J Am Coll Cardiol*. 2009;53:1517-1527

10. Pfeiler S, Gerdes N. Atherosclerosis: Cell biology and lipoproteins - focus on anti-inflammatory therapies. *Curr Opin Lipidol*. 2018;29:53-55
11. Berliner JA, Navab M, Fogelman AM, Frank JS, Demer LL, Edwards PA, Watson AD, Lusis AJ. Atherosclerosis: Basic mechanisms : Oxidation, inflammation, and genetics. *Circulation*. 1995;91:2488-2496
12. Potente M, Gerhardt H, Carmeliet P. Basic and therapeutic aspects of angiogenesis. *Cell*. 2011;146:873-887
13. Sluimer JC, Daemen MJ. Novel concepts in atherogenesis: Angiogenesis and hypoxia in atherosclerosis. *J Pathol*. 2009;218:7-29
14. Depre C, Havaux X, Wijns W. Neovascularization in human coronary atherosclerotic lesions. *Cathet Cardiovasc Diagn*. 1996;39:215-220
15. Ogata A, Kawashima M, Wakamiya T, Nishihara M, Masuoka J, Nakahara Y, Ebashi R, Inoue K, Takase Y, Irie H, Abe T. Carotid artery stenosis with a high-intensity signal plaque on time-of-flight magnetic resonance angiography and association with evidence of intraplaque hypoxia. *J Neurosurg*. 2017;126:1873-1878
16. Zimna A, Kurpisz M. Hypoxia-inducible factor-1 in physiological and pathophysiological angiogenesis: Applications and therapies. *Biomed Res Int*. 2015;2015:549412
17. Parma L, Peters HAB, Baganha F, Sluimer JC, de Vries MR, Quax PHA. Prolonged hyperoxygenation treatment improves vein graft patency and decreases macrophage content in atherosclerotic lesions in apoe3*leiden mice. *Cells*. 2020;9
18. Majmundar AJ, Wong WJ, Simon MC. Hypoxia-inducible factors and the response to hypoxic stress. *Mol Cell*. 2010;40:294-309
19. Wong BW, Marsch E, Treps L, Baes M, Carmeliet P. Endothelial cell metabolism in health and disease: Impact of hypoxia. *EMBO J*. 2017;36:2187-2203
20. Fleiner M, Kummer M, Mirlacher M, Sauter G, Cathomas G, Krapf R, Biedermann BC. Arterial neovascularization and inflammation in vulnerable patients: Early and late signs of symptomatic atherosclerosis. *Circulation*. 2004;110:2843-2850

21. Finn AV, Jain RK. Coronary plaque neovascularization and hemorrhage: A potential target for plaque stabilization? *JACC. Cardiovascular imaging*. 2010;3:41-44
22. Cheng C, Chrifi I, Pasterkamp G, Duckers HJ. Biological mechanisms of microvessel formation in advanced atherosclerosis: The big five. *Trends in cardiovascular medicine*. 2013;23:153-164
23. Kaartinen M, Penttila A, Kovanen PT. Mast cells accompany microvessels in human coronary atheromas: Implications for intimal neovascularization and hemorrhage. *Atherosclerosis*. 1996;123:123-131
24. Sedding DG, Boyle EC, Demandt JAF, Sluimer JC, Dutzmann J, Haverich A, Bauersachs J. Vasa vasorum angiogenesis: Key player in the initiation and progression of atherosclerosis and potential target for the treatment of cardiovascular disease. *Front Immunol*. 2018;9:706
25. Chistiakov DA, Orekhov AN, Bobryshev YV. Contribution of neovascularization and intraplaque haemorrhage to atherosclerotic plaque progression and instability. *Acta physiologica (Oxford, England)*. 2015;213:539-553
26. Huang X, Teng Z, Canton G, Ferguson M, Yuan C, Tang D. Intraplaque hemorrhage is associated with higher structural stresses in human atherosclerotic plaques: An in vivo mri-based 3d fluid-structure interaction study. *Biomed Eng Online*. 2010;9:86
27. Doyle B, Caplice N. Plaque neovascularization and antiangiogenic therapy for atherosclerosis. *J Am Coll Cardiol*. 2007;49:2073-2080
28. Nishikido T, Ray KK. Inclisiran for the treatment of dyslipidemia. *Expert Opin Investig Drugs*. 2018:1-8
29. Ridker PM, Everett BM, Thuren T, MacFadyen JG, Chang WH, Ballantyne C, Fonseca F, Nicolau J, Koenig W, Anker SD, Kastelein JJP, Cornel JH, Pais P, Pella D, Genest J, Cifkova R, Lorenzatti A, Forster T, Kobalava Z, Vida-Simiti L, Flather M, Shimokawa H, Ogawa H, Dellborg M, Rossi PRF, Troquay RPT, Libby P, Glynn RJ, Group CT. Antiinflammatory therapy with canakinumab for atherosclerotic disease. *N Engl J Med*. 2017;377:1119-1131

30. Nordestgaard BG, Nicholls SJ, Langsted A, Ray KK, Tybjaerg-Hansen A. Advances in lipid-lowering therapy through gene-silencing technologies. *Nat Rev Cardiol*. 2018
31. Seidah NG, Abifadel M, Prost S, Boileau C, Prat A. The proprotein convertases in hypercholesterolemia and cardiovascular diseases: Emphasis on proprotein convertase subtilisin/kexin 9. *Pharmacol Rev*. 2017;69:33-52
32. Herrington W, Lacey B, Sherliker P, Armitage J, Lewington S. Epidemiology of atherosclerosis and the potential to reduce the global burden of atherothrombotic disease. *Circ Res*. 2016;118:535-546
33. Libby P. Mechanisms of acute coronary syndromes and their implications for therapy. *New England Journal of Medicine*. 2013;368:2004-2013
34. Michel JB, Martin-Ventura JL, Nicoletti A, Ho-Tin-Noe B. Pathology of human plaque vulnerability: Mechanisms and consequences of intraplaque haemorrhages. *Atherosclerosis*. 2014;234:311-319
35. Virmani R, Kolodgie FD, Burke AP, Finn AV, Gold HK, Tulenko TN, Wrenn SP, Narula J. Atherosclerotic plaque progression and vulnerability to rupture: Angiogenesis as a source of intraplaque hemorrhage. *Arterioscler. Thromb. Vasc. Biol.* 2005;25:2054-2061
36. De Bock K, Georgiadou M, Carmeliet P. Role of endothelial cell metabolism in vessel sprouting. *Cell metabolism*. 2013;18:634-647
37. Pircher A, Treps L, Bodrug N, Carmeliet P. Endothelial cell metabolism: A novel player in atherosclerosis? Basic principles and therapeutic opportunities. *Atherosclerosis*. 2016;253:247-257
38. Ali L, Schnitzler JG, Kroon J. Metabolism: The road to inflammation and atherosclerosis. *Curr Opin Lipidol*. 2018;29:474-480
39. Stapor P, Wang X, Goveia J, Moens S, Carmeliet P. Angiogenesis revisited - role and therapeutic potential of targeting endothelial metabolism. *J Cell Sci*. 2014;127:4331-4341
40. Treps L, Conradi LC, Harjes U, Carmeliet P. Manipulating angiogenesis by targeting endothelial metabolism: Hitting the engine rather than the drivers-a new perspective? *Pharmacol Rev*. 2016;68:872-887

41. Xu Y, An X, Guo X, Habtetsion TG, Wang Y, Xu X, Kandala S, Li Q, Li H, Zhang C, Caldwell RB, Fulton DJ, Su Y, Hoda MN, Zhou G, Wu C, Huo Y. Endothelial pfkfb3 plays a critical role in angiogenesis. *Arterioscler Thromb Vasc Biol*. 2014;34:1231-1239
42. Schoors S, De Bock K, Cantelmo AR, Georgiadou M, Ghesquiere B, Cauwenberghs S, Kuchnio A, Wong BW, Quaegebeur A, Goveia J, Bifari F, Wang X, Blanco R, Tembuyser B, Cornelissen I, Bouche A, Vinckier S, Diaz-Moralli S, Gerhardt H, Telang S, Cascante M, Chesney J, Dewerchin M, Carmeliet P. Partial and transient reduction of glycolysis by pfkfb3 blockade reduces pathological angiogenesis. *Cell metabolism*. 2014;19:37-48
43. Granchi C, Minutolo F. Anticancer agents that counteract tumor glycolysis. *ChemMedChem*. 2012;7:1318-1350
44. Stefanadis C, Antoniou CK, Tsiachris D, Pietri P. Coronary atherosclerotic vulnerable plaque: Current perspectives. *J Am Heart Assoc*. 2017;6
45. Gargiulo S, Gramanzini M, Mancini M. Molecular imaging of vulnerable atherosclerotic plaques in animal models. *Int J Mol Sci*. 2016;17
46. Kielty CM, Sherratt MJ, Shuttleworth CA. Elastic fibres. *J Cell Sci*. 2002;115:2817-2828
47. Judge DP, Dietz HC. Marfan's syndrome. *Lancet*. 2005;366:1965-1976
48. Van Herck JL, De Meyer GRY, Martinet W, Van Hove CE, Foubert K, Theunis MH, Apers S, Bult H, Vrints CJ, Herman AG. Impaired fibrillin-1 function promotes features of plaque instability in apolipoprotein e-deficient mice. *Circulation*. 2009;120:2478-2487
49. Judge DP, Biery NJ, Keene DR, Geubtner J, Myers L, Huso DL, Sakai LY, Dietz HC. Evidence for a critical contribution of haploinsufficiency in the complex pathogenesis of marfan syndrome. *Journal of Clinical Investigation*. 2004;114:172-181
50. Mariko B, Pezet M, Escoubet B, Bouillot S, Andrieu J-P, Starcher B, Quaglino D, Jacob M-P, Huber P, Ramirez F, Faury G. Fibrillin-1 genetic deficiency leads to pathological ageing of arteries in mice. *Journal of Pathology*. 2011;224:33-44

51. Medley TL, Cole TJ, Gatzka CD, Wang WY, Dart AM, Kingwell BA. Fibrillin-1 genotype is associated with aortic stiffness and disease severity in patients with coronary artery disease. *Circulation*. 2002;105:810-815
52. Van der Donckt C, Van Herck JL, Schrijvers DM, Vanhoutte G, Verhoye M, Blockx I, Van Der Linden A, Bauters D, Lijnen HR, Sluimer JC, Roth L, Van Hove CE, Fransen P, Knaapen MW, Hervent AS, De Keulenaer GW, Bult H, Martinet W, Herman AG, De Meyer GRY. Elastin fragmentation in atherosclerotic mice leads to intraplaque neovascularization, plaque rupture, myocardial infarction, stroke, and sudden death. *European Heart Journal*. 2015;36:1049-1058
53. Van der Donckt C, Roth L, Vanhoutte G, Blockx I, Bink DI, Ritz K, Pintelon I, Timmermans JP, Bauters D, Martinet W, Daemen MJ, Verhoye M, De Meyer GRY. Fibrillin-1 impairment enhances blood–brain barrier permeability and xanthoma formation in brains of apolipoprotein e-deficient mice. *Neuroscience*. 2015;295:11-22
54. Fulop T, Larbi A, Fortun A, Robert L, Khalil A. Elastin peptides induced oxidation of ldl by phagocytic cells. *Pathologie Biologie*. 2005;53:416-423
55. Moulton KS, Olsen BR, Sonn S, Fukai N, Zurakowski D, Zeng X. Loss of collagen xviii enhances neovascularization and vascular permeability in atherosclerosis. *Circulation*. 2004;110:1330-1336
56. Rademakers T, Douma K, Hackeng TM, Post MJ, Sluimer JC, Daemen MJAP, Biessen EAL, Heeneman S, van Zandvoort MAMJ. Plaque-associated vasa vasorum in aged apolipoprotein e-deficient mice exhibit proatherogenic functional features in vivo. *Arterioscler. Thromb. Vasc. Biol.* 2013;33:249-256
57. Raffetto JD, Khalil RA. Matrix metalloproteinases and their inhibitors in vascular remodeling and vascular disease. *Biochemical Pharmacology*. 2008;75:346-359
58. de Nooijer R, Verkleij CJ, von der Thüsen JH, Jukema JW, van der Wall EE, van Berkel TJ, Baker AH, Biessen EA. Lesional overexpression of matrix metalloproteinase-9 promotes intraplaque hemorrhage in advanced lesions but not at earlier stages of atherogenesis. *Arterioscler. Thromb. Vasc. Biol.* 2005;26:340-346

59. Kockx MM, Cromheeke KM, Knaapen MW, Bosmans JM, De Meyer GRY, Herman AG, Bult H. Phagocytosis and macrophage activation associated with hemorrhagic microvessels in human atherosclerosis. *Arterioscler Thromb Vasc Biol*. 2003;23:440-446
60. Sluimer JC, Kolodgie FD, Bijnens APJJ, Maxfield K, Pacheco E, Kutys B, Duimel H, Frederik PM, van Hinsbergh VWM, Virmani R, Daemen MJAP. Thin-walled microvessels in human coronary atherosclerotic plaques show incomplete endothelial junctions. *Journal of the American College of Cardiology*. 2009;53:1517-1527
61. Roth L, Rombouts M, Schrijvers DM, Martinet W, De Meyer GRY. Cholesterol-independent effects of atorvastatin prevent cardiovascular morbidity and mortality in a mouse model of atherosclerotic plaque rupture. *Vascul Pharmacol*. 2016;80:50-58
62. Roth L, Rombouts M, Schrijvers DM, Lemmens K, De Keulenaer GW, Martinet W, De Meyer GRY. Chronic intermittent mental stress promotes atherosclerotic plaque vulnerability, myocardial infarction and sudden death in mice. *Atherosclerosis*. 2015;242:288-294
63. Roth L, Van Dam D, Van der Donckt C, Schrijvers DM, Lemmens K, Van Brussel I, De Deyn PP, Martinet W, De Meyer GRY. Impaired gait pattern as a sensitive tool to assess hypoxic brain damage in a novel mouse model of atherosclerotic plaque rupture. *Physiol Behav*. 2015;139:397-402
64. Virmani R, Atkinson JB, Forman MB. Aortocoronary saphenous vein bypass grafts. *Cardiovasc Clin*. 1988;18:41-62
65. Motwani JG, Topol EJ. Aortocoronary saphenous vein graft disease: Pathogenesis, predisposition, and prevention. *Circulation*. 1998;97:916-931
66. de Vries MR, Simons KH, Jukema JW, Braun J, Quax PH. Vein graft failure: From pathophysiology to clinical outcomes. *Nat Rev Cardiol*. 2016;13:451-470
67. Yahagi K, Kolodgie FD, Otsuka F, Finn AV, Davis HR, Joner M, Virmani R. Pathophysiology of native coronary, vein graft, and in-stent atherosclerosis. *Nat Rev Cardiol*. 2016;13:79-98
68. de Vries MR, Quax PHA. Inflammation in vein graft disease. *Front Cardiovasc Med*. 2018;5:3

69. Eelen G, de Zeeuw P, Simons M, Carmeliet P. Endothelial cell metabolism in normal and diseased vasculature. *Circ Res*. 2015;116:1231-1244
70. Zou Y, Dietrich H, Hu Y, Metzler B, Wick G, Xu Q. Mouse model of venous bypass graft arteriosclerosis. *Am J Pathol*. 1998;153:1301-1310
71. Dietrich H, Hu Y, Zou Y, Huemer U, Metzler B, Li C, Mayr M, Xu Q. Rapid development of vein graft atheroma in apoe-deficient mice. *Am J Pathol*. 2000;157:659-669
72. Parma L, Baganha F, Quax PHA, de Vries MR. Plaque angiogenesis and intraplaque hemorrhage in atherosclerosis. *Eur J Pharmacol*. 2017;816:107-115
73. de Vries MR, Quax PH. Plaque angiogenesis and its relation to inflammation and atherosclerotic plaque destabilization. *Curr Opin Lipidol*. 2016;27:499-506
74. Birmpili P, Porter L, Shaikh U, Torella F. Comparison of measurement and grading of carotid stenosis with computed tomography angiography and doppler ultrasound. *Ann Vasc Surg*. 2018;51:217-224
75. Ward MR, Pasterkamp G, Yeung AC, Borst C. Arterial remodeling. Mechanisms and clinical implications. *Circulation*. 2000;102:1186-1191
76. MacAskill MG, Newby DE, Tavares AAS. Frontiers in positron emission tomography imaging of the vulnerable atherosclerotic plaque. *Cardiovasc Res*. 2019;115:1952-1962
77. Mammatas LH, Verheul HM, Hendrikse NH, Yaqub M, Lammertsma AA, Menke-van der Houven van Oordt CW. Molecular imaging of targeted therapies with positron emission tomography: The visualization of personalized cancer care. *Cell Oncol (Dordr)*. 2015;38:49-64
78. Hammad B, Evans NR, Rudd JHF, Tawakol A. Molecular imaging of atherosclerosis with integrated pet imaging. *J Nucl Cardiol*. 2017;24:938-943
79. Tarkin JM, Joshi FR, Rajani NK, Rudd JH. Pet imaging of atherosclerosis. *Future Cardiol*. 2015;11:115-131
80. Marcu L, Hillman EMC. In vivo optical imaging / intravital microscopy. *J Biophotonics*. 2017;10:760-761

81. Richardson DS, Lichtman JW. Clarifying tissue clearing. *Cell*. 2015;162:246-257

82. Renier N, Wu Z, Simon DJ, Yang J, Ariel P, Tessier-Lavigne M. Idisco: A simple, rapid method to immunolabel large tissue samples for volume imaging. *Cell*. 2014;159:896-910

Chapter 2

Pharmacological strategies to inhibit intraplaque angiogenesis in atherosclerosis

Perrotta P, Emini Veseli B, Van der Veken B, Roth L, Martinet W, De Meyer GRY.

Vascul Pharmacol. 2019; 112:72-78

Abstract

Atherosclerosis is a complex multifactorial disease that affects large and medium-sized arteries. Rupture of atherosclerotic plaques and subsequent acute cardiovascular complications remain a leading cause of death and morbidity in the Western world. There is a considerable difference in safety profile between a stable and a vulnerable, rupture-prone lesion. The need for plaque-stabilizing therapies is high, and for a long time the lack of a suitable animal model mimicking advanced human atherosclerotic plaques made it very difficult to make progress in this area. Evidence from human plaques indicates that intraplaque (IP) angiogenesis promotes atherosclerosis and plaque destabilization. Although neovascularization has been widely investigated in cancer, studies on the pharmacological inhibition of this phenomenon in atherosclerosis are scarce, mainly due to the lack of an appropriate animal model. By using $ApoE^{-/-}$ $Fbn1^{C1039G+/-}$ mice, a novel model of vulnerable plaques, we were able to investigate the effect of pharmacological inhibition of various mechanisms of IP angiogenesis on plaque destabilization and atherogenesis. In the present review, we discuss the following potential pharmacological strategies to inhibit IP angiogenesis: (1) inhibition of vascular endothelial growth factor signalling, (2) inhibition of glycolytic flux, and (3) inhibition of fatty acid oxidation. On the long run, IP neovascularization might be applicable as a therapeutic target to induce plaque stabilization on top of lipid-lowering treatment.

Introduction

Atherosclerosis is a chronic inflammatory disorder of the arterial wall leading to coronary artery disease, stroke and peripheral arterial disease. [1-3] Not only the size but rather the stability of atherosclerotic plaques is determinant for acute clinical implications. When a plaque develops an unstable phenotype, it is prone to rupture, which can lead to myocardial infarction, stroke and sudden death. Unstable plaques have a relatively large lipid core, high macrophage content and a thin fibrous cap. Due to cholesterol-lowering drugs the lifespan and wellbeing of patients has been significantly improved. However, a large group of patients does not fully benefit from current lipid-lowering strategies. [3] Indeed, despite major advances in cardio- and cerebrovascular research, plaque rupture remains the leading cause of acute events. Therefore, additional therapy that reduces atherosclerosis or prevents plaque rupture and its complications is needed.

Recently, several new therapies have emerged to treat high-risk patients (e.g. PCSK9 monoclonal antibodies and inclisiran to reduce the residual cholesterol risk, and canakinumab, a monoclonal antibody against interleukin-1β to reduce plaque inflammation).[4-7] However, accumulating evidence indicates that also intraplaque (IP) angiogenesis promotes atherosclerosis and plaque destabilization. Clinical data link IP angiogenesis with progressive and unstable vascular disease. Autopsy studies, for example, revealed a higher density of IP vasa vasorum microvessels in symptomatic (ruptured) plaques compared to asymptomatic ones. [8] IP angiogenesis is a complex process that depends on the equilibrium between several pro- and anti-angiogenic molecules. [9] The presence of hypoxia in advanced atherosclerotic plaques correlates with IP angiogenesis in human carotid arteries. [10-12] Besides hypoxia, inflammation is a strong inducer of angiogenesis as it promotes the synthesis of various angiogenic factors. During acute inflammation, several pro-angiogenic molecules can induce cell permeability, contributing to the infiltration of leukocytes in the inflammatory core and thereby provoking chronic inflammation. [13] Because the newly formed vessels growing into the plaque are immature, they are inherently leaky, permitting inflammatory cell infiltration and influx of blood constituents (including erythrocytes and blood platelets) into the plaque. [14] Moreover,

IP microvessels can promote the entry of leukocytes into the plaque by upregulation of adhesion molecules such as ICAM-1 and VCAM-1. [15] The increased release of matrix metalloproteinases from activated macrophages and proteases secreted from mast cells cause further damage to the microvessels and facilitate IP haemorrhage.[16] Following IP neovascularization, IP haemorrhage has been linked to plaque progression [17], making it an important hallmark of plaque instability. Based on these findings, it is well accepted that IP neovascularization plays a significant role in atherosclerotic plaque destabilization and rupture.

Neovascularization has been widely investigated in cancer, but studies on the pharmacological inhibition of this phenomenon in atherosclerosis are scarce, mainly due to the lack of a suitable animal model. Scientific knowledge on the significance of IP neovascularization in atherosclerosis was mainly acquired through human specimens. In normal human arteries, vasa vasorum are found in the adventitia and outer media since diffusion of oxygen and other nutrients from the lumen is sufficient to nourish the intimal layer and the inner media [18]. However, during atherogenesis the progressive increase in plaque size is associated with development of hypoxic regions, increased oxidative stress and inflammation, which promote the formation of IP microvessels (angiogenesis) that reach the intima and infiltrate the atherosclerotic plaque.[19] Depletion of ATP in macrophages is also an important contributor to IP angiogenesis due to the extremely high rates of energy necessary for cholesterol uptake. [20, 21] Microvessels grow from the adventitial vasa vasorum through the media into the intimal lesion. Plaques can be particularly rich in microvessels at the shoulder region and base. IP microvessels in human carotid arteries have a diameter of 2-200μm and a surface of 20-20000 μm^2 [22]. Furthermore, the thin wall of plaque microvessels lacks proper structure, in terms of elastic laminae and smooth muscle cell (SMC) support, making them leaky, fragile and prone to rupture. [23, 24] Recent evidence supports the idea that blocking IP angiogenesis may represent a new approach to decrease plaque instability and thus cardiovascular risk. For example, it has been shown that inhibition of plaque neovascularization reduces macrophage accumulation and progression of advanced atherosclerosis. [25]

Although IP neovascularization is a typical feature of advanced human atherosclerotic plaques, it is rarely observed in animal models, including Apolipoprotein deficient ($ApoE^{-/-}$) mice. [26] Therefore, a causal and straightforward relation between plaque rupture and IP neovascularization has never been confirmed due to the lack of a relevant animal model of atherosclerosis with human-like characteristics such as IP neovascularization. In the past two decades, animal models of atherosclerosis merely generated a stable plaque phenotype, while plaque rupture almost never occurred. [27] The latter implied a substantial limitation in atherosclerosis-related research. Vein grafts in ApoE*3Leiden mice were among the first lesions in animals with features resembling those of human plaques, such as intimal dissection, intramural thrombosis and IP neovascularization. [28] Because this model is based on vein graft surgery, it requires a complex intervention to induce microvessel formation via neovascularization. We reported that $ApoE^{-/-}$ mice containing a heterozygous mutation ($C1039G^{+/-}$) in the fibrillin-1 (Fbn1) gene show very pronounced atherosclerosis and a highly unstable plaque phenotype on a Western-type diet [29], leading to plaque rupture and human-like complications, such as myocardial infarction, stroke and sudden death without any surgical interventions. [30] Interestingly, $ApoE^{-/-}Fbn1^{C1039G+/-}$ mice reveal substantial IP neovascularization in the brachiocephalic artery and common carotid arteries. [30] Moreover, similar as in humans, both mature and immature microvessels are present, the latter being highly leaky. Because Fbn1 is the major structural component of the extracellular microfibrils in the vessel wall, neovascularization in $ApoE^{-/-}Fbn1^{C1039G+/-}$ mice probably occurs because elastin fragmentation allows microvessel sprouting from the adventitial vasa vasorum through the media into the intimal lesion. Moreover, the high degree of stenosis and the presence of activated macrophages likely results in IP hypoxia, and triggers the growth of new vessels from the adventitia. IP haemorrhages are frequently observed in the proximity of microvessels, suggesting that they arise from leaky and/or ruptured microvessels.

Because IP neovascularization seems to have a major causative effect on atherosclerosis and plaque destabilization in humans [8, 31-33], we investigated whether inhibition of IP neovascularization might be a useful therapy for atherosclerotic plaque stabilization. Inhibition of pathological angiogenesis has become an accepted therapeutic strategy in cancer and diabetes mellitus. [34] Only recently, studies

unveiled the importance of endothelial cell (EC) metabolism in controlling angiogenesis and maturation of microvessels, [35] also in the field of atherosclerosis, showing the novelty of this research . [26, 28, 36] In this review, we discuss the following potential pharmacological strategies to inhibit IP angiogenesis: (1) inhibition of vascular endothelial growth factor signalling, (2) inhibition of glycolytic flux, and (3) inhibition of fatty acid oxidation (Figure 1, Table 1).

Targeting IP angiogenesis through inhibition of vascular endothelial growth factor signalling

Anti-angiogenic therapy in cancer research has demonstrated that vascular endothelial growth factor (VEGF)-A is a potent initiator of neovascularization. The VEGF family, consists of five closely related members, namely VEGF-A, B, C, D and placental growth factor. VEGF-A is released by various cell types including ECs, SMCs, astrocytes and macrophages. VEGF-A drives vasculogenesis, angiogenesis and blood vessel maintenance in physiological conditions. Activation of VEGFR-2, a receptor for VEGF-A, triggers several downstream pathways that promote EC survival, permeability, migration and proliferation.[37] VEGF-A is abundantly present within advanced human coronary and carotid atherosclerotic plaques [38, 39] and elevated VEGF-A concentration likely contributes significantly to promote IP angiogenesis. VEGF-A has been clearly observed in lipid-rich coronary lesions and stenotic coronary plaques particularly in ECs and macrophages surrounding microvessels.[38] It induces EC permeability via phosphorylation of VE-cadherin, which gets internalized, resulting in a loss of EC junctions. Accordingly, VEGF-A upregulation in plaques leads to highly permeable and leaky microvessels, which fail to mature properly.

In view of the above-mentioned findings, VEGF-A can be used as a promising target to inhibit IP microvessel formation. In the last decade, there has been a substantial increase in compounds targeting VEGF or its downstream pathways to counteract angiogenic growth. Bevacizumab, a monoclonal antibody against VEGF-A, inhibits IP neovascularization with smaller atherosclerotic lesions as a result [40] (Figure 1). This finding nourished the presumption that targeting IP neovascularization might

result in more stable lesions and opened a new field of interest in the treatment of atherosclerosis. Besides antibodies against VEGF-A [40, 41], antibodies blocking VEGFR-2 (DC101) revealed smaller vein graft lesions and less IP haemorrhages in ApoE*3 Leiden mice. [42] Also the stability of the vein graft lesion was increased in DC101-treated mice, as shown by a reduction in macrophage content and an increase in collagen and SMCs.

In the clinical practise in oncology, tyrosine kinase inhibitors are an important subgroup of new anticancer compounds specifically targeting VEGFR-induced neovascularization. [43] Compounds targeting VEGFRs may provide an interesting approach to investigate the effect of inhibition of the VEGF signalling in the stabilization of atherosclerotic plaques. Axitinib is a potent and selective inhibitor of VEGFR tyrosine kinases 1, 2 and 3 (Figure 1), and is clinically used for the treatment of advanced renal cell carcinoma. [44] Given the very promising results in oncology, we evaluated the potential plaque stabilizing effects of axitinib. This compound was chosen above other anti-VEGF receptor tyrosine kinase inhibitors due to its potency and acceptable safety profile in oncology research. [26] In atherosclerotic $ApoE^{-/-}$ $Fbn1^{C1039G+/-}$ mice, axitinib (35 µg/g i.p. 4x/week for 6 weeks) significantly reduces IP neovascularization by 50 %, with subsequent less prevalence of IP haemorrhages. [45] The SMC content doubles, whereas the amount of macrophages decreases by 30 %. Because entry of monocytes and macrophages is related to leakage of microvessels, a reduction in the amount of macrophages may be a direct result of the decreased microvessel network in the plaque. In addition, overall cardiac function is improved in axitinib-treated animals (fractional shortening: 27±2 vs. 19±3 %). Moreover, the number of animals with myocardial infarction decreases by 40 %. Coronary plaque formation is present in almost all control animals whereas axitinib-treated animals show a 30 % reduction in the occurrence of coronary plaques. Taken together, inhibition of VEGF receptor signalling by axitinib attenuates IP angiogenesis and plaque destabilization in mice. [45] However, the mechanisms responsible for these observations are not fully understood. It is very likely that inhibition of VEGFR-signalling affects a combination of several processes. Improved plaque stability can be a direct consequence of the decrease in neovascularization, with less leakage of destabilizing cells into the plaque. On the other hand, VEGF can

act as an initiator of a well-organized signalling cascade, driving multiple mechanisms.[46, 47] Thus, not only the decrease in IP microvessels may account for the plaque-stabilizing effects of axitinib, also other mechanisms can be involved in determining the outcome. On the long run, it might be interesting to use VEGFR2 inhibitors as add-on therapy to statins for their plaque-stabilizing effects. Nevertheless, we must be careful because therapeutic angiogenesis is currently evaluated as a possible therapy in cardiovascular ischemic diseases, such as myocardial infarction and peripheral arterial disease. Importantly, in our study axitinib did not induce adverse effects on the heart; on the contrary, the heart function was even improved.

Endostatin, the C-terminal globular domain of collagen, is a naturally occurring anti-angiogenic protein. First discovered in Judith Folkman's lab, this protein was isolated for its ability to inhibit the proliferation of capillary ECs. Almost two decades ago, recombinant endostatin expressed in yeast was introduced into clinical trials. However, its instability diminished the efficacy. A new recombinant human endostatin, endostar, with an N-terminal modification was more stable and was at least twice as potent as compared to the parent compound. Endostar reduces inoculated tumour growth in mice by substantially inhibiting angiogenesis. [48] Endostar inhibits angiogenesis by blocking VEGF-induced tyrosine phosphorylation of VEGFR-2, but others associate its effects with decreased expression of β-catenin in the atherosclerotic artery. Suppression of angiogenesis through inhibition of Wnt/β-catenin signalling plays a major role in regulating fundamental aspects of development such as cell fate specification, proliferation, survival and overall organogenesis. [48, 49] B-catenin is a key intracellular signal transducer, which besides its role in the Wnt pathway, also binds to cadherins (VE- and N-cadherin in ECs), thus stabilizing cell-to-cell adhesion and tissue integrity. Down-regulation of the Wnt/β-catenin signalling pathway may be involved in the inhibition of angiogenesis. [49] Therefore, inhibition of the Wnt/β-catenin signalling pathway might be a future approach to inhibit IP angiogenesis. [19]

Targeting IP angiogenesis through inhibition of glycolytic flux

While VEGF and its downstream pathways have been widely investigated to regulate and to inhibit neovascularization, recent studies in the field of oncology present evidence from a different point of view. [50-52] Indeed, modulation of cell metabolism (glycolysis) has already shown beneficial effects in cancer research, and this approach could be of value in atherosclerosis as well. Proliferating ECs reveal high glycolytic activity (>200-fold higher than glucose, fatty acid and glutamine oxidation), which results in the generation of >85% of the total cellular ATP content. [53] The conversion of fructose-6-phosphate (F-6-P) to fructose-2,6-bisphosphate (F-2,6-P_2) is one of the three rate-limiting checkpoints during glycolytic flux and is modulated by 6-phosphofructo-2-kinase/fructose-2,6-bisphosphatases (PFKFBs) (Figure 1). PFKFB3-driven glycolysis is important for the migration of ECs, and knockdown of PFKFB3 in ECs exhibits defects in angiogenesis both *in vitro* and *in vivo*. [54] Interestingly, inhibition of PFKFB3 by intraperitoneal injection of the small molecule 3PO [3-(3-pyridinyl)-1-(4-pyridinyl)-2-propen-1-one] reduces vessel sprouting in EC spheroids, zebrafish embryos and the mouse retina by inhibiting EC proliferation and migration. [51] 3PO reduces F-2,6-P_2 levels by blocking PFKFB3 in its kinase domain, which in turn suppresses glycolysis (but without abrogating glycolytic side pathways such as the pentose phosphate pathway necessary for the production of NADPH). It is however important to note that the inhibition of PFKFB3 by 3PO is partial (35–40%) and transient [51], albeit sufficient to reduce neovascularization. Indeed, 3PO targets the hyper-metabolism that is induced when ECs switch from quiescence to proliferation and migration. This could have some safety implication, since inhibiting glycolysis nearly completely and permanently may also lead to ATP depletion and thus to cell toxicity. [55]

Recently, we showed that in atherosclerotic ApoE$^{-/-}$Fbn1$^{C1039G+/-}$ mice pharmacological inhibition of PFKFB3 by 3PO (50 µg/g, i.p) reduced IP neovascularization and haemorrhages by 50% in a preventive regimen and by 38 % in a curative regimen. [56] This compound had no effect on SMC, collagen and macrophage content in the plaques. Plasma VEGF-A levels decreased significantly (curative: 838±449 vs. 2871±653 pg/ml) and cardiac function improved after 10

weeks of treatment (fractional shortening 31±4 vs. 23±3 %). Thus, inhibition of PFKFB3 by 3PO significantly represses IP angiogenesis and haemorrhages in mice, demonstrating its potential in preventing plaque rupture.[56] However, up till now it is unclear whether the effects of 3PO are attributable solely to direct effects on PFKFB3 kinase. Previously, 3PO was investigated for its binding properties via computational modelling, whereas its activity was characterized via kinase activity assays. [57] However, recent evidence indicates that the specificity of 3PO for PFKFB3 is insufficient to attribute all its effects to PFKFB3 inhibition, meaning that there might be alternative mechanisms by which 3PO acts. [58] Recently, other PFKFB3 inhibitors such as PFK15 (a 3PO derivative that displays approximately 100-fold more activity against PFKFB3 than 3PO itself [58]), and indazole analogues that are structurally not related to 3PO have been developed. These drugs demonstrate high selectivity over related PFKFB3 isoforms and potent modulation of the target (IC_{50} PFKFB3: 3 nM)[59], though were not yet tested *in vivo*. Crystallographic studies highlight binding of these drugs at the ATP site of the enzyme. [59] In particular, a compound with a dimethylisoxazole substitution at the R position is a potent and selective inhibitor of PFKFB3. [59]Future studies are needed to evaluate whether these compounds are interesting as potential inhibitors of IP angiogenesis.

Targeting IP angiogenesis through inhibition of fatty acid oxidation

Recent evidence indicates that silencing or knocking out carnitine palmitoyltransferase 1a (CPT1a), a rate-determining enzyme of fatty acid oxidation (FAO), impairs vessel sprouting (but not migration) by reducing EC proliferation [60] (Figure 1). FAO is a multistep metabolic pathway during which fatty acids are broken down in order to produce energy in the cells. After the fatty acid enters into the cytosol it is transferred to the mitochondria where it undergoes β-oxidation. This process involves activation to acyl-CoA by conjugation with coenzyme A in the cytosol, conversion by carnitine palmitoyltransferase 1a (CTP1a) to acyl carnitine for transport across the mitochondrial membrane and conversion back to acyl-CoA inside the mitochondrion in which fatty acid oxidation (β-oxidation) takes place. β-oxidation involves a repeated sequence of four enzyme activities that results in the release of an acetyl-CoA unit, a molecule of FADH2 and a molecule of NADH.

Subsequently, the acetyl-CoA enters the mitochondrial tricarboxylic acid cycle where it is oxidized to CO_2 and H_2O with the generation of aspartate, used for dNTPs synthesis and essential for DNA replication in proliferating ECs. [61]

During angiogenesis ECs differentiate into “tip” (navigating) and “stalk” (proliferating) cells. While during the process of migration, tip cells seemed to rely more on a PFKFB3-driven glycolytic metabolism to rapidly produce enough ATP, during the process of proliferation, “stalk” cells depend on FAO, essential for sprout elongation. In contrast to 3PO, CPT1a deficiency does not alter ATP levels as FAO contributes to less than 5 % of the total amount of cellular ATP. Instead, FAO is important for the *de novo* synthesis of deoxyribonucleotides. [60] Thus, rather than using FAO for the production of energy, ECs use fatty acids for DNA synthesis, necessary for proliferation during vessel sprouting.[34] Therefore, a future strategy might be inhibition of IP angiogenesis by pharmacological blockade of CPT1a in ECs using etomoxir (Figure 1), which is an irreversible inhibitor of CPT1a enzyme that shows favourable effects during treatment of heart failure [62] and also reduces pathological angiogenesis in an ocular disease model. [60] Etomoxir impairs vessel sprouting [63, 64] but has not yet been tested in an animal model of atherosclerosis. However, the above-mentioned findings suggest its potential to inhibit IP angiogenesis.

Although we envision the future use of the above-mentioned strategies on top of a statin treatment, statins themselves might also partially affect IP angiogenesis. Statins reduce cholesterol levels via inhibition of hydroxymethylglutaryl coenzyme A (HMG-CoA) reductase, the rate-limiting enzyme in cholesterol biosynthesis. In addition, growing evidence indicates that statins trigger pro-angiogenic effects at low (nanomolar) concentrations and anti-angiogenic effects at higher (micromolar) concentrations. [65] They display these pleiotropic functions beyond lipid lowering. HMG-CoA reductase regulates the synthesis of mevalonic acid, a precursor of cholesterol, as well as geranyl geranylpyrophosphate (GGP). The latter intermediate seems to play an important role in the anti-angiogenic properties of statins as supplementation of GGP reverses the angiostatic effects.[65] Interestingly, atherosclerotic $ApoE^{-/-}Fbn1^{C1039G+/-}$ mice treated with atorvastatin show much less IP neovascularization as well as a reduction in cardiovascular morbidity and mortality without obvious changes in plasma cholesterol. [66] Accordingly, we presume that

patients suffering from atherosclerosis can benefit from the anti-angiogenic properties of statins, even without elevated cholesterol levels.

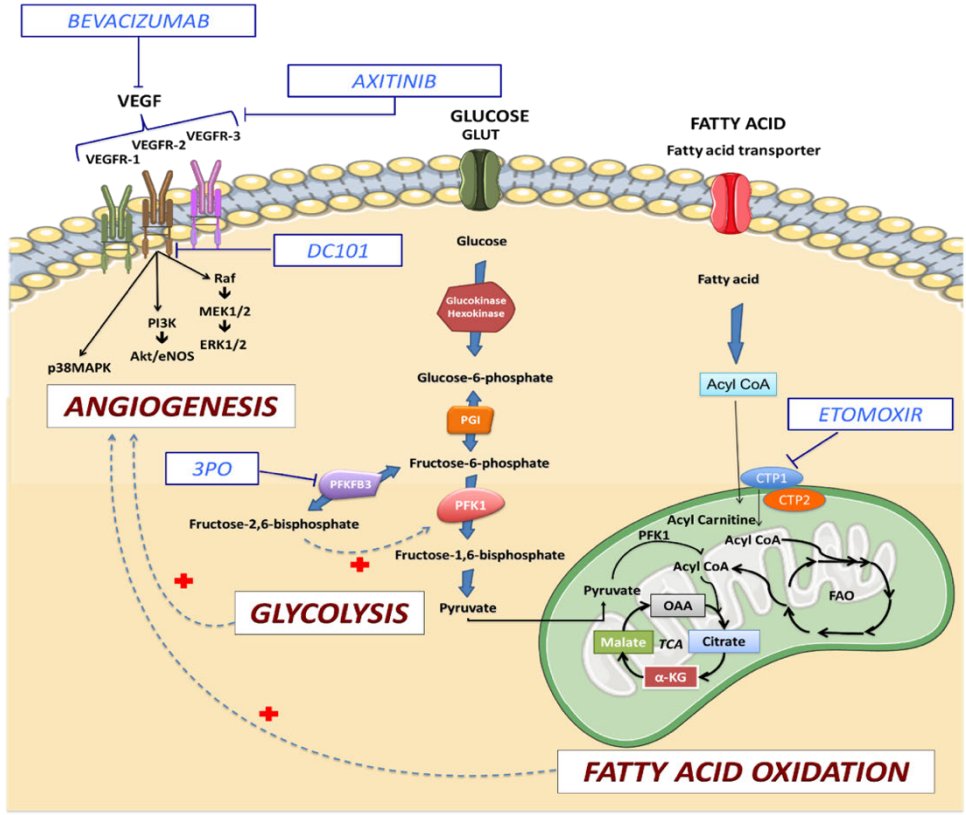

Figure 1. Overview of selected pathways in EC metabolism and their possible targets to inhibit IP angiogenesis

Schematic representation and simplified overview of selected metabolic pathways known to be involved in angiogenesis, and their respective possible targets. Vascular endothelial growth factor (VEGF) is a potent initiator of neo-angiogenesis which acts through its main receptors VEGFR1, VEGFR2 and VEGFR3. Bevacizumab inhibits VEGF-A. On the other hand, axitinib blocks VEGF receptor tyrosine kinase 1,2 and 3. DC101 is an antibody against VEGFR-2. All these targets interfere with angiogenesis.

PFKFB3 and CTP1a are key enzymes in glycolysis and FAO respectively, and are critical metabolic regulators of vessel sprouting. 3PO reduces fructose-2,6-bisphosphate levels – a potent allosteric activator of glycolysis – by blocking PFKFB3 in its kinase domain. This

inhibition is transient and partial, yet sufficient to reduce neovascularization. Pharmacological inhibition of CTP1a with small chemical compound etomoxir leads to reduced endothelial cell proliferation and defects in vessel sprouting in oncology studies. VEGF, Vascular Endothelial Growth Factor; VEGFR, Vascular Endothelial Growth Factor Receptor; eNOS, endothelial nitric oxide synthase; GLUT-1, glucose transporter 1; PGI, phosphoglucose isomerase; PFK1, 6-phosphofructokinase 1; PFKFB3, phosphofructokinase-2/fructose-2,6-bisphosphatase isoform 3; 3PO, 3-(3-pyridinyl)-1-(4-pyridinyl)-2-propen-1-one; OOA, oxalacetate; α-KG, α-ketoglutaric Acid; FAO, fatty acid oxidation; CTP1a, carnitine palmitoyltransferase 1a.

Table 1. Compounds studied to inhibit IP angiogenesis

IP angiogenesis inhibitor	**Mechanism of action**	**Animal model of IP angiogenesis**	**Reference**
Bevacizumab	Monoclonal antibody to VEGF-A	Aortic balloon denudation in hypercholesterolaemic rabbits	[40]
Axitinib	VEGFR1,2,3-inhibitor	Hypercholesterolaemic $ApoE^{-/-}Fbn1^{C1039G+/-}$ mice	[45]
DC101	VEGFR2 blocking antibody	Vein graft in hypercholesterolaemic ApoE3*Leiden mice	[42]
3PO	Glycolysis inhibitor	Hypercholesterolaemic $ApoE^{-/-}Fbn1^{C1039G+/-}$ mice	[56]
Endostar	Blocking VEGF-induced tyrosine phosphorylation of VEGFR-2, decreased expression of β-catenin	Porcine model of atherosclerosis	[49, 67]

Conclusion

In conclusion, inhibition of IP angiogenesis may represent an attracting novel pharmacological target to stabilise vulnerable atherosclerotic plaques. While an association between angiogenesis and progression of human atherosclerosis have been reported multiple times, pharmacological approaches to target this process have been started to be explored only recently. Although previous studies highlighted that pro-angiogenic therapy enhanced atherosclerosis, while anti-angiogenic therapy reduced atherosclerotic complications, the majority of *in vivo* studies in animal models of atherosclerosis were based on assessing adventitial microvessels but not IP angiogenesis. Novel, more suitable animal models such as the ones described in this review, will permit a better evaluation of this novel therapeutic target in atherosclerosis. Recent studies with these models show the ability of anti-angiogenic drugs like bevacizumab, axitinib or DC101 to inhibit IP angiogenesis in atherosclerosis and to reduce IP haemorrhage. However, further investigations will be required to explore EC metabolism as a new target in atherosclerosis as already applied in tumour angiogenesis. On the long run, this approach can lead to novel therapeutic interventions to treat patients who do not fully benefit from current lipid-lowering therapies. Furthermore, the acquired knowledge will allow a significant advance in the fundamental understanding of IP neovascularization.

Acknowledgements

This work was supported by the University of Antwerp (BOF). Paola Perrotta and Besa Emini Veseli are PhD fellows of the Horizon 2020 program of the European Union - Marie Skłodowska-Curie Actions, Innovative Training Networks (ITN), Call: H2020-MSCA-ITN-2015, NUMBER — 675527 — MOGLYNET

References

1. Lusis AJ. Atherosclerosis. *Nature*. 2000;407:233-241
2. Hansson GK. Inflammation, atherosclerosis, and coronary artery disease. *The New England journal of medicine*. 2005;352:1685-1695
3. Libby P. Mechanisms of acute coronary syndromes and their implications for therapy. *The New England journal of medicine*. 2013;368:2004-2013
4. Ridker PM, Everett BM, Thuren T, MacFadyen JG, Chang WH, Ballantyne C, Fonseca F, Nicolau J, Koenig W, Anker SD, Kastelein JJP, Cornel JH, Pais P, Pella D, Genest J, Cifkova R, Lorenzatti A, Forster T, Kobalava Z, Vida-Simiti L, Flather M, Shimokawa H, Ogawa H, Dellborg M, Rossi PRF, Troquay RPT, Libby P, Glynn RJ, Group CT. Antiinflammatory therapy with canakinumab for atherosclerotic disease. *N. Engl. J. Med.* 2017;377:1119-1131
5. Nishikido T, Ray KK. Inclisiran for the treatment of dyslipidemia. *Expert Opin Investig Drugs*. 2018:1-8
6. Nordestgaard BG, Nicholls SJ, Langsted A, Ray KK, Tybjaerg-Hansen A. Advances in lipid-lowering therapy through gene-silencing technologies. *Nat. Rev. Cardiol.* 2018
7. Seidah NG, Abifadel M, Prost S, Boileau C, Prat A. The proprotein convertases in hypercholesterolemia and cardiovascular diseases: Emphasis on proprotein convertase subtilisin/kexin 9. *Pharmacol. Rev.* 2017;69:33-52
8. Virmani R, Kolodgie FD, Burke AP, Finn AV, Gold HK, Tulenko TN, Wrenn SP, Narula J. Atherosclerotic plaque progression and vulnerability to rupture: Angiogenesis as a source of intraplaque hemorrhage. *Arteriosclerosis, thrombosis, and vascular biology*. 2005;25:2054-2061
9. Potente M, Gerhardt H, Carmeliet P. Basic and therapeutic aspects of angiogenesis. *Cell*. 2011;146:873-887
10. Sluimer JC, Daemen MJ. Novel concepts in atherogenesis: Angiogenesis and hypoxia in atherosclerosis. *J. Pathol.* 2009;218:7-29
11. Depre C, Havaux X, Wijns W. Neovascularization in human coronary atherosclerotic lesions. *Cathet Cardiovasc Diagn*. 1996;39:215-220

12. Ogata A, Kawashima M, Wakamiya T, Nishihara M, Masuoka J, Nakahara Y, Ebashi R, Inoue K, Takase Y, Irie H, Abe T. Carotid artery stenosis with a high-intensity signal plaque on time-of-flight magnetic resonance angiography and association with evidence of intraplaque hypoxia. *J. Neurosurg.* 2017;126:1873-1878
13. Fleiner M, Kummer M, Mirlacher M, Sauter G, Cathomas G, Krapf R, Biedermann BC. Arterial neovascularization and inflammation in vulnerable patients: Early and late signs of symptomatic atherosclerosis. *Circulation*. 2004;110:2843-2850
14. Finn AV, Jain RK. Coronary plaque neovascularization and hemorrhage: A potential target for plaque stabilization? *JACC. Cardiovascular imaging*. 2010;3:41-44
15. Cheng C, Chrifi I, Pasterkamp G, Duckers HJ. Biological mechanisms of microvessel formation in advanced atherosclerosis: The big five. *Trends in cardiovascular medicine*. 2013;23:153-164
16. Kaartinen M, Penttila A, Kovanen PT. Mast cells accompany microvessels in human coronary atheromas: Implications for intimal neovascularization and hemorrhage. *Atherosclerosis*. 1996;123:123-131
17. Chistiakov DA, Orekhov AN, Bobryshev YV. Contribution of neovascularization and intraplaque haemorrhage to atherosclerotic plaque progression and instability. *Acta physiologica (Oxford, England)*. 2015;213:539-553
18. Mulligan-Kehoe MJ. The vasa vasorum in diseased and nondiseased arteries. *Am. J. Physiol. Heart Circ. Physiol.* 2010;298:H295-305
19. Xu J, Lu X, Shi GP. Vasa vasorum in atherosclerosis and clinical significance. *Int. J. Mol. Sci.* 2015;16:11574-11608
20. Libby P. Atherosclerosis: The new view. *Sci. Am.* 2002;286:46-55
21. Tabas I, Garcia-Cardena G, Owens GK. Recent insights into the cellular biology of atherosclerosis. *J. Cell Biol.* 2015;209:13-22
22. Jeziorska M, Woolley DE. Local neovascularization and cellular composition within vulnerable regions of atherosclerotic plaques of human carotid arteries. *J. Pathol.* 1999;188:189-196

23. Silvestre-Roig C, de Winther MP, Weber C, Daemen MJ, Lutgens E, Soehnlein O. Atherosclerotic plaque destabilization: Mechanisms, models, and therapeutic strategies. *Circ. Res.* 2014;114:214-226
24. Kolodgie FD, Gold HK, Burke AP, Fowler DR, Kruth HS, Weber DK, Farb A, Guerrero LJ, Hayase M, Kutys R, Narula J, Finn AV, Virmani R. Intraplaque hemorrhage and progression of coronary atheroma. *N. Engl. J. Med.* 2003;349:2316-2325
25. Moulton KS, Vakili K, Zurakowski D, Soliman M, Butterfield C, Sylvin E, Lo KM, Gillies S, Javaherian K, Folkman J. Inhibition of plaque neovascularization reduces macrophage accumulation and progression of advanced atherosclerosis. *Proc. Natl. Acad. Sci. U. S. A.* 2003;100:4736-4741
26. Van der Veken B, De Meyer GRY, Martinet W. Intraplaque neovascularization as a novel therapeutic target in advanced atherosclerosis. *Expert Opin. Ther. Targets*. 2016;20:1247-1257
27. Emini Veseli B, Perrotta P, De Meyer GRA, Roth L, Van der Donckt C, Martinet W, De Meyer GRY. Animal models of atherosclerosis. *Eur. J. Pharmacol.* 2017;816:3-13
28. de Vries MR, Quax PH. Plaque angiogenesis and its relation to inflammation and atherosclerotic plaque destabilization. *Curr. Opin. Lipidol.* 2016;27:499-506
29. Van Herck JL, De Meyer GRY, Martinet W, Van Hove CE, Foubert K, Theunis MH, Apers S, Bult H, Vrints CJ, Herman AG. Impaired fibrillin-1 function promotes features of plaque instability in apolipoprotein e-deficient mice. *Circulation*. 2009;120:2478-2487
30. Van der Donckt C, Van Herck JL, Schrijvers DM, Vanhoutte G, Verhoye M, Blockx I, Van Der Linden A, Bauters D, Lijnen HR, Sluimer JC, Roth L, Van Hove CE, Fransen P, Knaapen MW, Hervent AS, De Keulenaer GW, Bult H, Martinet W, Herman AG, De Meyer GRY. Elastin fragmentation in atherosclerotic mice leads to intraplaque neovascularization, plaque rupture, myocardial infarction, stroke, and sudden death. *Eur. Heart J.* 2015;36:1049-1058

31. Pasterkamp G, van der Steen AF. Intraplaque hemorrhage: An imaging marker for atherosclerotic plaque destabilization? *Arteriosclerosis, thrombosis, and vascular biology*. 2012;32:167-168
32. Michel JB, Martin-Ventura JL, Nicoletti A, Ho-Tin-Noe B. Pathology of human plaque vulnerability: Mechanisms and consequences of intraplaque haemorrhages. *Atherosclerosis*. 2014;234:311-319
33. Kockx MM, Cromheeke KM, Knaapen MW, Bosmans JM, De Meyer GRY, Herman AG, Bult H. Phagocytosis and macrophage activation associated with hemorrhagic microvessels in human atherosclerosis. *Arterioscler. Thromb. Vasc. Biol.* 2003;23:440-446
34. Treps L, Conradi LC, Harjes U, Carmeliet P. Manipulating angiogenesis by targeting endothelial metabolism: Hitting the engine rather than the drivers-a new perspective? *Pharmacological reviews*. 2016;68:872-887
35. Cantelmo AR, Conradi LC, Brajic A, Goveia J, Kalucka J, Pircher A, Chaturvedi P, Hol J, Thienpont B, Teuwen LA, Schoors S, Boeckx B, Vriens J, Kuchnio A, Veys K, Cruys B, Finotto L, Treps L, Stav-Noraas TE, Bifari F, Stapor P, Decimo I, Kampen K, De Bock K, Haraldsen G, Schoonjans L, Rabelink T, Eelen G, Ghesquiere B, Rehman J, Lambrechts D, Malik AB, Dewerchin M, Carmeliet P. Inhibition of the glycolytic activator pfkfb3 in endothelium induces tumor vessel normalization, impairs metastasis, and improves chemotherapy. *Cancer cell*. 2016
36. Pircher A, Treps L, Bodrug N, Carmeliet P. Endothelial cell metabolism: A novel player in atherosclerosis? Basic principles and therapeutic opportunities. *Atherosclerosis*. 2016;253:247-257
37. Simons M, Gordon E, Claesson-Welsh L. Mechanisms and regulation of endothelial vegf receptor signalling. *Nat. Rev. Mol. Cell Biol.* 2016;17:611-625
38. Inoue M, Itoh H, Ueda M, Naruko T, Kojima A, Komatsu R, Doi K, Ogawa Y, Tamura N, Takaya K, Igaki T, Yamashita J, Chun TH, Masatsugu K, Becker AE, Nakao K. Vascular endothelial growth factor (vegf) expression in human coronary atherosclerotic lesions: Possible pathophysiological significance of vegf in progression of atherosclerosis. *Circulation*. 1998;98:2108-2116

39. Pelisek J, Well G, Reeps C, Rudelius M, Kuehnl A, Culmes M, Poppert H, Zimmermann A, Berger H, Eckstein HH. Neovascularization and angiogenic factors in advanced human carotid artery stenosis. *Circ J*. 2012;76:1274-1282
40. Stefanadis C, Toutouzas K, Stefanadi E, Lazaris A, Patsouris E, Kipshidze N. Inhibition of plaque neovascularization and intimal hyperplasia by specific targeting vascular endothelial growth factor with bevacizumab-eluting stent: An experimental study. *Atherosclerosis*. 2007;195:269-276
41. Pasterkamp G, van der Steen AFW. Intraplaque hemorrhage: An imaging marker for atherosclerotic plaque destabilization? *Arterioscler. Thromb. Vasc. Biol.* 2012;32:167-168
42. de Vries MR, de Jong RCM, Peters HAB, Hamming JF, Goumans MJ, Quax PHA. Vegfr2 blockade in murine vein graft results in reduced intraplaque hemorrhage and stable atherosclerotic lesions. *Atherosclerosis*. 2014;235:e161-e162
43. Gotink KJ, Verheul HMW. Anti-angiogenic tyrosine kinase inhibitors: What is their mechanism of action? *Angiogenesis*. 2009;13:1-14
44. Kelly RJ, Rixe O. Axitinib (ag-013736). *Recent results in cancer research. Fortschritte der Krebsforschung. Progres dans les recherches sur le cancer*. 2010;184:33-44
45. Van der Veken B, De Meyer GRY, Martinet W. Axitinib attenuates intraplaque angiogenesis, haemorrhages and plaque destabilization in mice. *Vascul. Pharmacol.* 2018;100:34-40
46. Matsumoto T, Claesson-Welsh L. Vegf receptor signal transduction. *Science Signaling*. 2001;2001:re21-re21
47. Ferrara N, Gerber H-P, LeCouter J. The biology of vegf and its receptors. *Nat. Med.* 2003;9:669-676
48. Wang TB, Wei XQ, Lin WH, Shi HP, Dong WG. The inhibition of endostar on the angiogenesis and growth of gastrointestinal stromal tumor xenograft. *Clin Exp Med*. 2012;12:89-95
49. Xu X, Mao W, Chen Q, Zhuang Q, Wang L, Dai J, Wang H, Huang Z. Endostar, a modified recombinant human endostatin, suppresses

angiogenesis through inhibition of wnt/beta-catenin signaling pathway. *PLoS One*. 2014;9:e107463

50. De Bock K, Georgiadou M, Schoors S, Kuchnio A, Wong BW, Cantelmo AR, Quaegebeur A, Ghesquiere B, Cauwenberghs S, Eelen G, Phng LK, Betz I, Tembuyser B, Brepoels K, Welti J, Geudens I, Segura I, Cruys B, Bifari F, Decimo I, Blanco R, Wyns S, Vangindertael J, Rocha S, Collins RT, Munck S, Daelemans D, Imamura H, Devlieger R, Rider M, Van Veldhoven PP, Schuit F, Bartrons R, Hofkens J, Fraisl P, Telang S, Deberardinis RJ, Schoonjans L, Vinckier S, Chesney J, Gerhardt H, Dewerchin M, Carmeliet P. Role of pfkfb3-driven glycolysis in vessel sprouting. *Cell*. 2013;154:651-663

51. Schoors S, De Bock K, Cantelmo AR, Georgiadou M, Ghesquiere B, Cauwenberghs S, Kuchnio A, Wong BW, Quaegebeur A, Goveia J, Bifari F, Wang X, Blanco R, Tembuyser B, Cornelissen I, Bouche A, Vinckier S, Diaz-Moralli S, Gerhardt H, Telang S, Cascante M, Chesney J, Dewerchin M, Carmeliet P. Partial and transient reduction of glycolysis by pfkfb3 blockade reduces pathological angiogenesis. *Cell Metab.* 2014;19:37-48

52. Schoors S, Bruning U, Missiaen R, Queiroz KCS, Borgers G, Elia I, Zecchin A, Cantelmo AR, Christen S, Goveia J, Heggermont W, Goddé L, Vinckier S, Van Veldhoven PP, Eelen G, Schoonjans L, Gerhardt H, Dewerchin M, Baes M, De Bock K, Ghesquière B, Lunt SY, Fendt S-M, Carmeliet P. Fatty acid carbon is essential for dntp synthesis in endothelial cells. *Nature*. 2015;520:192-197

53. De Bock K, Georgiadou M, Carmeliet P. Role of endothelial cell metabolism in vessel sprouting. *Cell metabolism*. 2013;18:634-647

54. Xu Y, An X, Guo X, Habtetsion TG, Wang Y, Xu X, Kandala S, Li Q, Li H, Zhang C, Caldwell RB, Fulton DJ, Su Y, Hoda MN, Zhou G, Wu C, Huo Y. Endothelial pfkfb3 plays a critical role in angiogenesis. *Arteriosclerosis, thrombosis, and vascular biology*. 2014;34:1231-1239

55. Granchi C, Minutolo F. Anticancer agents that counteract tumor glycolysis. *ChemMedChem*. 2012;7:1318-1350

56. Van der Veken B, De Meyer GRY, Martinet W. Inhibition of glycolysis reduces intraplaque angiogenesis in a mouse model of advanced atherosclerosis. *Atherosclerosis*. 2017;263:E23-E23
57. Clem B, Telang S, Clem A, Yalcin A, Meier J, Simmons A, Rasku MA, Arumugam S, Dean WL, Eaton J, Lane A, Trent JO, Chesney J. Small-molecule inhibition of 6-phosphofructo-2-kinase activity suppresses glycolytic flux and tumor growth. *Mol. Cancer Ther.* 2008;7:110-120
58. Clem BF, O'Neal J, Tapolsky G, Clem AL, Imbert-Fernandez Y, Kerr DA, 2nd, Klarer AC, Redman R, Miller DM, Trent JO, Telang S, Chesney J. Targeting 6-phosphofructo-2-kinase (pfkfb3) as a therapeutic strategy against cancer. *Molecular cancer therapeutics*. 2013;12:1461-1470
59. Boyd S, Brookfield JL, Critchlow SE, Cumming IA, Curtis NJ, Debreczeni J, Degorce SL, Donald C, Evans NJ, Groombridge S, Hopcroft P, Jones NP, Kettle JG, Lamont S, Lewis HJ, MacFaull P, McLoughlin SB, Rigoreau LJ, Smith JM, St-Gallay S, Stock JK, Turnbull AP, Wheatley ER, Winter J, Wingfield J. Structure-based design of potent and selective inhibitors of the metabolic kinase pfkfb3. *Journal of medicinal chemistry*. 2015;58:3611-3625
60. Schoors S, Bruning U, Missiaen R, Queiroz KC, Borgers G, Elia I, Zecchin A, Cantelmo AR, Christen S, Goveia J, Heggermont W, Godde L, Vinckier S, Van Veldhoven PP, Eelen G, Schoonjans L, Gerhardt H, Dewerchin M, Baes M, De Bock K, Ghesquiere B, Lunt SY, Fendt SM, Carmeliet P. Fatty acid carbon is essential for dntp synthesis in endothelial cells. *Nature*. 2015;520:192-197
61. Teuwen LA, Draoui N, Dubois C, Carmeliet P. Endothelial cell metabolism: An update anno 2017. *Curr. Opin. Hematol.* 2017;24:240-247
62. Bristow M. Etomoxir: A new approach to treatment of chronic heart failure. *Lancet (London, England)*. 2000;356:1621-1622
63. Wong BW, Marsch E, Treps L, Baes M, Carmeliet P. Endothelial cell metabolism in health and disease: Impact of hypoxia. *EMBO J.* 2017;36:2187-2203
64. Missiaen R, Morales-Rodriguez F, Eelen G, Carmeliet P. Targeting endothelial metabolism for anti-angiogenesis therapy: A pharmacological perspective. *Vascul. Pharmacol.* 2017;90:8-18

65. Weis M. Statins have biphasic effects on angiogenesis. *Circulation*. 2002;105:739-745

66. Roth L, Rombouts M, Schrijvers DM, Martinet W, De Meyer GRY. Cholesterol-independent effects of atorvastatin prevent cardiovascular morbidity and mortality in a mouse model of atherosclerotic plaque rupture. *Vascul. Pharmacol.* 2016;80:50-58

67. Xu X, Mao W, Chai Y, Dai J, Chen Q, Wang L, Zhuang Q, Pan Y, Chen M, Ni G, Huang Z. Angiogenesis inhibitor, endostar, prevents vasa vasorum neovascularization in a swine atherosclerosis model. *J. Atheroscler. Thromb.* 2015;22:1100-1112

Chapter 3

Animal models of atherosclerosis

Emini Veseli B, **Perrotta P**, De Meyer GRA, Roth L, Van der Donckt C, Martinet W, De Meyer GRY.

Eur J Pharmacol. 2017;816:3-13

Abstract

An ideal animal model of atherosclerosis resembles human anatomy and pathophysiology and has the potential to be used in medical and pharmaceutical research to obtain results that can be extrapolated to human medicine. Moreover, it must be easy to acquire, can be maintained at a reasonable cost, is easy to handle and shares the topography of the lesions with humans. In general, animal models of atherosclerosis are based on accelerated plaque formation due to a cholesterol-rich/Western-type diet, manipulation of genes involved in the cholesterol metabolism, and the introduction of additional risk factors for atherosclerosis. Mouse and rabbit models have been mostly used, followed by pigs and non-human primates. Each of these models has its advantages and limitations. The mouse has become the predominant species to study experimental atherosclerosis because of its rapid reproduction, ease of genetic manipulation and its ability to monitor atherogenesis in a reasonable time frame. Both Apolipoprotein E deficient ($ApoE^{-/-}$) and LDL-receptor ($LDLr^{-/-}$) knockout mice have been frequently used, but also ApoE/LDLr double-knockout, ApoE3-Leiden and PCSK9-AAV mice are valuable tools in atherosclerosis research. However, a great challenge was the development of a model in which intraplaque microvessels, haemorrhages, spontaneous atherosclerotic plaque ruptures, myocardial infarction and sudden death occur consistently. These features are present in $ApoE^{-/-}Fbn1^{C1039G+/-}$ mice, which can be used as a validated model in pre-clinical studies to evaluate novel plaque-stabilizing drugs.

Keywords: animal models, atherosclerosis, plaque rupture, ApoE, LDL receptor, PCSK9

Introduction

Atherosclerosis is a progressive inflammatory disease characterized by accumulation of lipids in the arterial vessel wall, which starts early in life. Disease progression leads to build-up of atherosclerotic plaques that cause narrowing of the arterial lumen. Atherosclerotic plaques often remain stable for years, but can rapidly become unstable, rupture and trigger thrombus formation. Accordingly, in addition to restriction of the vessel lumen, the presence of atherosclerotic plaques is linked to an increased risk of acute cardiovascular events such as myocardial infarction (MI) and stroke. The use of animal models of atherosclerosis is an essential tool to improve the understanding of the molecular mechanisms behind atherosclerotic plaque formation and progression, as well as the occurrence of plaque rupture and its associated cardiovascular events. Moreover, animal models allow to assess novel pharmacological treatments that can prevent or slow down the onset of atherosclerosis. In general, animal models for atherosclerosis are based on accelerated plaque formation due to: (1) a cholesterol-rich/Western-type diet, (2) manipulation of genes involved in the cholesterol metabolism, and (3) the introduction of additional risk factors for atherosclerosis, such as diabetes.

In this review, we will discuss the animal models that have contributed to the understanding of atherosclerosis and its clinical consequences, and that allow significant improvement in treatment.

Numerous studies have shown that high plasma levels of low-density lipoprotein (LDL) represent one of the most prominent risk factors of atherosclerosis. Indeed, LDL tends to accumulate in the sub-endothelial space of the arterial wall and progressively undergoes oxidative modifications to form oxidized LDL (oxLDL). This induces an inflammatory response characterized by overexpression of chemotactic proteins such as monocyte chemoattractant protein-1 (MCP-1), and adhesion molecules (vascular cell adhesion molecule-1 (VCAM-1), E-selectin and P-selectin) by endothelial cells. [1, 2] Adhesion molecules promote the infiltration of blood-carried monocytes into the inflamed arterial wall. After differentiation into macrophages, these cells engulf oxLDL, transform into foam cells and contribute to plaque development by secreting multiple mediators of the inflammatory process in the vessel wall. [3] The inflammatory response also promotes recruitment of circulating

monocytes and T-cells that stimulate the migration of vascular smooth muscle cells (SMCs) from the tunica media into the sub-endothelial space where they exhibit abnormally high proliferation and secrete extracellular matrix proteins that also contribute to atheroma growth.[1] Advanced human plaques are characterized by a large necrotic core, many lipid laden and activated macrophages, few SMCs, intraplaque neovascularisation and haemorrhages, and a thin fibrous cap that separates the plaque from the blood stream. Rupture of the fibrous cap of such high-risk vulnerable plaques leads to luminal thrombosis, arterial occlusion or embolism in distant vascular beds, resulting in MI, stroke or sudden death. [4] In humans, atherosclerotic plaques can usually be found in the aorta, coronary arteries and in the carotid and cerebral arteries. [5]

In 1908, Ignatowski investigated for the first time plaque formation in the aortic wall of rabbits that were fed a cholesterol-rich diet. [6] Since then many other animal species such as mice, birds, pigs and non-human primates have been used as an experimental model of atherosclerosis. [1, 7]

An ideal animal model resembles human anatomy and pathophysiology, and has the potential to be used in medical and pharmaceutical research to obtain results that can be extrapolated to human medicine. Moreover, it is important that animals used as models are easy to acquire, can be maintained at a reasonable cost, are easy to handle and have well-defined genetic characteristics. A valuable animal model for atherosclerosis research not only shares the crucial aspects of the disease process with humans but also the topography of the lesions. In addition, the animals preferably develop lesions in a spontaneous manner after consumption of a diet similar as in humans. [8] Although several animals develop atherosclerotic plaques after a cholesterol-rich diet, the topography of the lesions is not always similar as compared to humans. Furthermore, it is important to note that in the majority of atherosclerosis models, animals do not spontaneously develop the complications seen in humans such as plaque rupture, MI, stroke and sudden death.

Mouse models of atherosclerosis

Over the past decades, the mouse has become the predominant species to study experimental atherosclerosis because of its rapid reproduction, ease of genetic

manipulation and its ability to monitor atherogenesis in a reasonable time frame.[8-11] However, mice are relatively resistant to the development of atherosclerosis due to their significantly different lipid profile as compared to humans. Therefore, genetic manipulation of their lipid metabolism is mandatory.[8, 12] In mice, most of the cholesterol is transported in high density lipoprotein (HDL) like particles. Accordingly, mice contain only low concentrations of the atherogenic LDL and very low density lipoprotein (VLDL). Mice deficient in the receptor clearing these LDL particles ($LDLr^{-/-}$ mice) develop significantly higher plasma levels of cholesterol. Apolipoprotein E (ApoE) is a glycoprotein synthesized mainly in the liver and the brain and functions as a ligand for receptors that clear chylomicrons and VLDL remnants.[12] Deficiency in this glycoprotein ($ApoE^{-/-}$) leads to increased plasma levels of total cholesterol, mostly in the VLDL and chylomicron fractions,[13] which are quadrupled by a high-fat or Western-type diet.[14] Both mouse models have extensively been used to study the mechanisms underlying the initiation and progression of atherosclerosis. Atherosclerotic lesions in mice develop in regions of the vasculature subjected to low and/or oscillatory shear stress. [9, 10] Predilection sites in the mouse are the aortic root, lesser curvature of the aortic arch and branch points of the brachiocephalic, left carotid and subclavian arteries. However, on a high-cholesterol diet, $ApoE^{-/-}$ mice develop plaques more rapidly and with a more advanced phenotype as compared to $LDLr^{-/-}$ mice [15], making the $ApoE^{-/-}$ model widely used in experimental atherosclerosis studies.

The Apolipoprotein (Apo) E3-Leiden mutation is associated with a genetic form of hyperlipidaemia. Therefore, ApoE3-Leiden transgenic mice can also be used as a model for atherosclerosis, but in comparison with $ApoE^{-/-}$ and $LDLr^{-/-}$ mice, they show rather low levels of total plasma cholesterol and triglycerides when fed a normal diet. Nevertheless, these mice are highly responsive to fat-, sugar-, and cholesterol-containing diets resulting in strongly elevated lipoprotein profiles.[16] Regardless of lesion development, varying from fatty streaks to mild, moderate, and severe plaques, ApoE3-Leiden mice lack the critical events such as plaque rupture, thrombus formation, and/or haemorrhage, which are of major importance in human atherosclerosis. [17, 18]

High plasma levels of lipoprotein (a) [Lp(a)], which is a complex of LDL and a large glycoprotein called Apolipoprotein (a) [Apo(a)], is an independent risk factor for the

development of atherosclerosis in humans.[19, 20] Virtually all species other than primates lack Apo(a), hampering the use of convenient animal models to study its role in atherosclerotic plaque development. Therefore, transgenic mice that express human Apo(a) are used. When fed a Western-type diet, these mice show the presence of macrophage-like cells in combination with the development of fatty-streak lesions at the base of the aorta. [21] In humans, plasma Apo(a) is almost entirely covalently bound to LDL, whereas in mice, Apo(a) circulates as non-lipoprotein associated Apo(a). [21] Therefore, Apo(a) transgenic mice can be used to identify the role of Apo(a) in atherogenesis, independent of human LDL.
The most commonly used mouse models of atherosclerosis are described in detail below and in Figure 1.

Apolipoprotein E deficient (ApoE$^{-/-}$) mice

ApoE is a glycoprotein with a molecular size of approximately 34 kDa. It is synthesized mainly in the liver and brain, and is a structural component of all lipoprotein particles except low-density lipoproteins. It serves as a ligand for cell-surface lipoprotein receptors whose function is to clear chylomicrons and VLDL remnants. It is also synthesized by monocytes and macrophages. [22] Other functions include cholesterol homeostasis, local redistribution of cholesterol within tissues, immunoregulation and dietary absorption and biliary excretion of cholesterol. [23, 24]

In 1992, the first line of ApoE$^{-/-}$ mice was developed almost contemporaneously in two laboratories. [13, 14] The deletion of the ApoE gene was done in mouse embryonic stem cells by homologous recombination. ApoE$^{-/-}$ mice were healthy, had a similar body weight as wild-type mice, and were born at the expected frequency.[14, 25] However, their lipoprotein profile disclosed significant differences with the wild-type mates. The ability of ApoE$^{-/-}$ mice to clear plasma lipoproteins is severely impaired resulting in plasma cholesterol levels of 400-600 mg/dl when fed a normal diet, whereas wild-type mice have levels of 75-110 mg/dl. [26, 27] This drastic change is due to an increase in VLDL-sized particles. The development of significant hypercholesterolaemia, even when fed a normal diet, suggests that in the absence of an environmental stimulus, deficiency of ApoE is sufficient to cause massive changes in lipoprotein metabolism. Furthermore, the lack of ApoE boosts the

sensitivity to dietary fat and cholesterol. After several weeks of feeding a Western-type diet (consisting of 21% fat and 0.15% cholesterol, which is similar to the everyday diet of Western countries), plasma cholesterol levels double in wild-type mice, whereas in ApoE-deficient mice a fourfold increase in total plasma cholesterol is observed. [14] Extensive atherosclerosis is seen in mice on both types of diet by 2 to 3 months of age. [28] On the other hand, heterozygous ApoE-deficient mice do not show an increase in plasma cholesterol levels even when fed a Western-type diet, presuming that a 50% decrease in ApoE is not sufficient to increase plasma lipids. Of note, plasma cholesterol levels in mice are not affected by age or sex of the animal. [26]

The entire spectrum of atherosclerotic lesions is present in ApoE$^{-/-}$ mice. [25] Monocyte attachment to endothelial cells is noticed from 6 weeks of age, and after 8 weeks foam cell lesion development is detectable. After 15 to 20 weeks, intermediate lesions are present containing mostly SMCs as well as fibrous plaques consisting of SMCs, extracellular matrix and a necrotic core covered with a fibrous cap. [26] In more advanced lesions, fibro-fatty nodules are a nidus for calcification and plaques become more calcified with time. [29] When fed a Western-type diet, the time course for lesion formation is tremendously accelerated. [25] Compared to mice fed a low-fat diet, lesions are 3-4 times larger within the same period of time. This response implies a diet-dependent mechanism, i.e. increased fat leads to increased plasma cholesterol, which in turn leads to increased atherosclerosis, which resembles the diet-dependency of atherosclerotic heart disease observed in humans. [14]

ApoE$^{-/-}$ mice tend to develop atherosclerotic plaques at vascular branch points, with predilection for the aortic root, the lesser curvature of the aortic arch, the principal branches of the aorta as well as the pulmonary and carotid arteries. [26] Sequential events of plaque formation in ApoE$^{-/-}$ mice are considerably similar to those in well-established larger animal models of atherosclerosis and in humans. [26] Although this mouse model is used by many research groups, it has some limitations. For instance, ApoE is a multifunctional protein that has an impact on inflammation, oxidation, reverse cholesterol transport by macrophages, and smooth muscle proliferation and migration. These functions might affect atherosclerotic plaque development in ApoE$^{-/-}$ mice, independent of plasma lipid levels. [30] Furthermore, not

LDL, which is characteristic of human atherosclerosis, but VLDL is the most abundant lipoprotein in ApoE$^{-/-}$ mice. [14] However, the major limitation of the 'classical' mouse models of atherosclerosis is the rarity of plaque rupture and thrombosis, [31, 32] whereas these events are fairly common in humans and can lead to MI and stroke. [25] It has been suggested that this might be due to the tiny diameter of the mouse vessels; as the vessel diameter decreases, the surface tension increases exponentially, impeding the likelihood of plaque rupture. [25] However, also other explanations have to be taken into account as discussed below in the section 'mouse models of atherosclerotic plaque rupture'.

A method for the induction of accelerated atherogenesis and plaque rupture is the placement of a perivascular collar or cuff, mainly in ApoE$^{-/-}$ mice. In their study, Sasaki et al., claim that cuff placement around the left carotid artery results in an animal model of plaque rupture. By using the ligation technique to induce neo-intimal hyperplasia, they observed lipid- and collagen-rich lesions accompanied with intraplaque haemorrhage and plaque rupture. Furthermore, a decrease in collagen content, and formation of fibrinogen-positive thrombi were detected, analogous to plaque rupture in humans. [33] Along with this observation, perivascular carotid collar placement also reproduces the induction of rapid and site-controlled atherosclerosis [34], while maintaining the structural integrity of the endothelium. Formed plaques are located primarily in the area proximal to the collar. The advantages of this model over the conventional animal models of mechanically induced atherosclerosis include the closer resemblance to human plaque morphology and endothelial expression pattern. [34]

LDL receptor-deficient (LDLr$^{-/-}$) mice

The LDL receptor is a membrane receptor with a molecular weight of 160 kDa, which mediates the endocytosis of cholesterol-rich LDL and thus maintains the plasma level of LDL. It also facilitates the cellular uptake of apolipoprotein B- and E-containing lipoproteins. LDL receptor deficiency along with mutations in the gene encoding for the LDL receptor count for the phenotypic events described in familial hypercholesterolaemia. [35, 36] Mice with a targeted inactivation of the LDL receptor were created in 1993. [37, 38] Compared with wild-type, LDLr$^{-/-}$ mice display modestly

elevated plasma cholesterol levels and develop no or only mild atherosclerosis when fed a normal diet. [38] In terms of lipoprotein particles, the increase is higher among IDL and LDL sized particles, whereas HDL and triglycerides remain unaffected. [37, 38] It is worth to note that this is different from ApoE$^{-/-}$ mice, in which cholesterol is primarily accumulated in large lipoprotein particles such as chylomicron remnants, VLDL and IDL particles (*vide supra*).[14, 39] The response to high-fat/high cholesterol Western-type diets shows a remarkable change in lipoprotein profile of these mice with a high probability for atherosclerotic lesion development.

The plaques that develop in LDLr$^{-/-}$ mice are generally the same as those seen in ApoE$^{-/-}$ mice. [40] A Western-type diet induces larger and more advanced lesions with a collagen-rich fibrous cap, a necrotic core containing cholesterol clefts and cellular enrichment adjacent to the lumen. [41] The plaque development occurs in a time-dependent manner, initially in the proximal aorta, and spreading toward the distal aorta. Similar to humans, the locations where the blood flow is disturbed are more prone to atherosclerotic lesions. [40] By making LDLr$^{-/-}$ and ApoE$^{-/-}$ mice homozygous for the ApoB-100 allele, total plasma cholesterol levels of approximately 300 mg/dl were obtained on a normal diet. LDLr$^{-/-}$ ApoB$^{100/100}$ mice developed more atherosclerotic lesions than the ApoE$^{-/-}$ ApoB$^{100/100}$ mice, even with a normal diet. [42, 43]

The LDLr$^{-/-}$ mouse model has some advantages in comparison with ApoE$^{-/-}$ mice. Firstly, plasma cholesterol is mostly carried by LDL particles, which generates a more human-like lipid profile. Secondly, the absence of the LDL receptor does not have an impact on inflammation as compared to ApoE deficiency. Thus, atherosclerotic plaque development in this mouse model is based on elevated plasma lipid levels and not caused by other functions linked to the LDL receptor. [8] Thirdly, the LDLr$^{-/-}$ mouse model shares the characteristics observed in human familial hypercholesterolaemia, which is caused by the absence of functional LDL receptors. [44, 45]

ApoE/LDL receptor double-knockout mice

Introduced shortly after ApoE$^{-/-}$ and LDLr$^{-/-}$ mice, ApoE/LDL receptor double knock out mice represent a model that develops more severe hyperlipidaemia and

atherosclerosis than the former ones. [46] It is an animal model with spontaneous atherosclerotic plaque development and it has been reported that even on regular chow diet, the progression of atherosclerosis is usually more marked in ApoE/LDL receptor double knock out mice than in mice deficient for ApoE alone. [47] There is no significant difference in the lipoprotein profile of the double knockouts compared to ApoE$^{-/-}$ mice, they both have high levels of VLDL and LDL [48], except the marked elevations in B48 and B100 apolipoproteins. [49] This mouse model is considered suitable to study the anti-atherosclerotic effects of possible treatments, without the need of an atherogenic diet. [25]

ApoE3-Leiden mice

Although ApoE$^{-/-}$ mice and LDLr$^{-/-}$ mice are the two most frequently used mouse models for atherosclerosis, also ApoE3-Leiden mice are utilized in many studies. Apolipoprotein (Apo)E3-Leiden is associated with a genetic form of hyperlipidaemia and is particularly expressed in a Dutch family. Transgenic mice have been generated using a genomic 27-kilobase DNA construct (containing the ApoE gene, ApoC1 gene and all regulatory elements) isolated from the APOE3-Leiden proband, to study the effect of the ApoE3-Leiden mutation *in vivo.* [17, 50]

Remarkably, although these mice are less susceptible for atherosclerosis than the ApoE deficient mice, they also show dramatically elevated total plasma cholesterol and triglyceride levels when fed a Western-type diet. This is mainly attributed to an increase in VLDL/LDL particles, which demonstrates that ApoE3-Leiden mice have a human-like lipoprotein profile. [51] Another advantage is that ApoE3-Leiden mice have the ability to synthesize functional ApoE. This offers the possibility to study the effect of elevated plasma lipid levels without disturbing inflammatory processes, which is an important limitation of the 'classical' ApoE$^{-/-}$ mouse model. [52]

The ApoE3-Leiden mice develop atherosclerotic lesions in the aorta and large vessels when fed a Western-type diet. Lesions are also observed in the proximal coronary arteries, the aortic root, the aortic arch and its main branch points, the thoracic aorta, the abdominal aorta, the renal artery branch points, the abdominal aorta bifurcation, and the iliac artery bifurcations. It is interesting to note that this strain develops early foam cell lesions on normal chow diet. However, more complex

and advanced lesions are observed after 1, 3 and 6 months of Western-type diet feeding. [17]

ApoE3-Leiden mice are used as a model to elucidate factors involved in the metabolism of ApoE and the aetiology of familial dyslipidaemia in particular. Furthermore, ApoE3-Leiden mice are utilized to study complications of venous bypass grafting, a clinical procedure that bypasses an atherosclerotic obstruction in an artery. Similar to humans, the grafted vein in this model undergoes remodelling, which is a consequence of exposure to higher blood pressure and shear stress but also vessel injury due to surgery. This process results in the formation of intimal hyperplasia and accelerated atherosclerosis, which may lead to obstruction of the graft. [17, 53, 54]

Because similarities were found between lesions in vein grafts and native atherosclerosis, a murine model of vein graft disease has been established. [55] In this model, the thoracic caval vein of a donor mouse is grafted in the carotid artery of a receiver mouse. This procedure has been used in mice that are susceptible to atherosclerosis (ApoE$^{-/-}$ or ApoE3-Leiden mice) so that vein grafts with accelerated atherosclerosis could be studied. [56-58] It has been show that vein grafts in these transgenic mice are morphologically similar to rupture-prone plaques in humans. The lesions in this model have the typical characteristics of late stage atherosclerosis, including the presence of foam cells, a large necrotic core, intraplaque neovascularization, calcification and cholesterol clefts. [59]

PCSK9-AAV mice

Besides the abovementioned models, a new line of mouse model without germline genetic engineering is emerging in the research field of atherosclerosis. The so called pro-protein convertase subtilisin/kexin type 9 (PCSK9) - adeno associated virus (AAV) mice were described independently by two research groups in 2014 as a rapid, versatile and cost-effective animal model for atherosclerosis. [60, 61] PCSK9, a newly identified human subtilase, is a serine protease with plasma concentrations of ≈100 to 200 ng/mL and it is highly expressed in the liver. [62, 63] Several studies have shown that PCSK9 reduces hepatic uptake of LDL by increasing the endosomal and lysosomal degradation of LDL receptors. [64] In brief, after protein

maturation and secretion, circulating PCSK9 binds the LDL receptors on the cell surface and is subsequently co-internalized together with the receptor. This distracts the normal recycling process of the receptor to the plasma membrane and promotes degradation in the lysosome. [63]

Recombinant AAV vectors support long-term transgene expression in many animal models [65-67] and humans. [68] Following single intravenous injection with human D374Y [61] or murine D377Y [60] gain-of-function mutant PCSK9, mice were stably expressing $PCSK9^{DY}$ mRNA in the liver. AAV viral infection does not elicit any adverse effects in the animals and no signs of liver damage or immunologic response were observed following infection. At 30 days after injection, total serum cholesterol in $PCSK9^{DY}$-AAV transgenes was doubled compared to control mice. These differences remained the same even after 1 year post-infection, confirming a chronic effect of a single AAV injection. [61] Western-type diet exacerbated hyperlipidaemia in $PCSK9^{DY}$-AAV mice, leading to plasma cholesterol levels of up to 1165 mg/dl, while chow diet fed mice barely reached 316 mg/dl. The lipoprotein profile of Western-type diet fed $PCSK9^{DY}$-AAV mice showed an equal distribution between VLDL and LDL particles. [61] $PCSK9^{DY}$ transgenic mice develop atherosclerosis in a dose-dependent manner. Hyperlipidaemia provokes the build-up of lesions throughout the vasculature resembling those of $LDLr^{-/-}$ mice, which is exacerbated by HFD feeding. [60, 61] Aortic root lesions show advanced plaque development with foam cells, smooth muscle cells, macrophage infiltration and fibrous tissue, but importantly, lesions progress to the fibro-atheromatous stage. [60, 61] and within the time frame of 15-20 weeks, vascular calcification occurs. [69] When Roche-Molina et al. combined $PCSK9^{DY}$ expression and ApoE deficiency, they revealed an expected synergistic effect: the lesions doubled in size with no significant differences in lipoprotein profile as compared to single mutants on the same diet. [61]

Overall, the induction of hyperlipidaemia and atherosclerosis in animals with different genetic backgrounds, the robust stability after single administration of mutant human PCSK9 and the fact that there are no major biosafety concerns in using AAVs as vectors, makes the PCSK9-AAV model a valuable tool in atherosclerosis research.[61]

Mouse models of atherosclerotic plaque rupture

Despite major advances in cardio- and cerebrovascular research, plaque rupture remains the leading cause of acute events. [70] Therefore, the need for the development of plaque-stabilizing therapies is high. Several research groups have tried to develop suitable models of plaque rupture for the last 15 years but in these models rupture occurs only sporadically, after a long period of time, or depends on mechanical injury .[11, 71, 72] Moreover, the reproducibility is low and events as seen in humans are rarely observed.

As discussed earlier, atherosclerotic plaques in mice develop in specific sites such as the aortic root, the lesser curvature of the aortic arch and the branch points of the brachiocephalic, the left carotid and the subclavian arteries. However, mice show only minor plaque development in the coronary and carotid arteries, which are the main sites of atherosclerotic plaque development in humans. [8-10] To induce plaque rupture in mice, several approaches based on surgical (such as arterial ligation or the positioning of a cuff around an artery) or genetic manipulation have been proposed (Table 1). Although these models have been useful in understanding the concepts of plaque rupture, none of them exhibit the full combination of the characteristics seen in human vulnerable/ruptured plaques. Moreover, plaque rupture with a superimposed occlusive thrombus, the most common complication of human atherosclerosis, is rarely observed. [73] Consequently, clinical events such as MI or ischemic stroke are almost never seen in these models. [9, 70] Furthermore, most of these models do not show 'spontaneous' plaque ruptures. When spontaneous ruptures are observed, they only occur sporadically and after a long period of time. However, recently a model of consistent, spontaneous atherosclerotic plaque ruptures in mice has been described, as discussed below.

Apolipoprotein E-deficient Fibrillin-1 mutant ($ApoE^{-/-}Fbn1^{C1039G+/-}$) mice

The extracellular matrix is a complex network of predominantly elastin and collagen, which is essential to provide structural, adhesive and biochemical signalling support to the vessel wall. In elastic arteries, elastin is the most abundant protein. The elastic fibres comprise the elastin core, which is surrounded by a mantle of fibrillin-rich

microfibrils. [74]The elastic-fibre-associated microfibrils have as the main structural component fibrillin-1, a large glycoprotein of about 350 kDa, whose major role is in binding and sequestering growth factors, such as transforming growth factor-β (TGF-β), as well as providing the scaffold for the deposition and the cross-linking of elastin. [75, 76]

Recently, we reported the effect of an impaired elastin structure of the vessel wall on the progression of atherosclerosis by cross-breeding ApoE$^{-/-}$ mice with mice containing a heterozygous mutation (C1039G$^{+/-}$) in the fibrillin-1 (Fbn1) gene. [76] Mutations in the Fbn1 gene lead to the Marfan syndrome, a genetic disorder characterized by fragmentation of elastic fibres. [77]This results in increased arterial stiffening, elevated pulse pressure and progressive aortic dilatation. [76, 78, 79] Moreover, the mutation leads to the development of highly unstable plaques in ApoE$^{-/-}$ mice, resulting in spontaneous plaque rupture with end-points including MI and sudden death. [76, 80] Importantly, these events do not – or only very occasionally – occur in ApoE$^{-/-}$ mice on a Western-type diet or in ApoE$^{-/-}$Fbn1$^{C1039G+/-}$ mice fed a normal diet. [80, 81] These findings underscore the importance of elastin fragmentation in combination with a Western-type diet as prerequisites for atherosclerotic plaque rupture in mice.

ApoE$^{-/-}$Fbn1$^{C1039G+/-}$ mice have significantly larger plaques with a highly unstable phenotype, characterized by a large necrotic core (occupying about 30% of total plaque area), and a strongly diminished collagen content. Accelerated atherogenesis in these mice is likely the result of enhanced vascular inflammation, leading to increased monocyte attraction, oxidation and accumulation of lipids. [82] Inducible nitric oxide synthase (iNOS), a marker for activated macrophages and inflammation, is significantly more expressed in plaques of ApoE$^{-/-}$Fbn1$^{C1039G+/-}$ mice on either Western-type diet or normal diet as compared to ApoE$^{-/-}$ mice on Western-type diet. Accordingly, inflammatory cytokines tumour necrosis factor-α (TNF-α), interleukin-1β (IL-1β) and interleukin-6 (IL-6) are highly increased. In addition, a higher infiltration of T-cells and their activation marker interferon-γ (IFN-γ) is present, the latter playing an important role in collagen turn-over by inhibiting SMCs to synthesise collagen, required to repair and maintain fibrous cap integrity. [83, 84] Moreover, matrix metalloproteinase (MMP)-2, -9, -12 and -13 expression or activity

is increased in ApoE$^{-/-}$Fbn1$^{C1039G+/-}$ mice. MMP-2 and MMP-9 are implicated in both atherosclerosis and angiogenesis. [85] For example, ApoE$^{-/-}$ mice lacking MMP-2 develop smaller and more stable plaques, whereas macrophages overexpressing active MMP-9 promote neovascularisation, intraplaque haemorrhage [86, 87] and features of plaque rupture in ApoE$^{-/-}$ mice. [87] In the latter case, those features were attributed to elastin degradation, underscoring its role in plaque destabilisation and rupture. MMP-12 and MMP-13 additionally contribute to elastin and (type I) collagen degradation, respectively. Taken together, in ApoE$^{-/-}$Fbn1$^{C1039G+/-}$ mice on Western-type diet enhanced collagen/extracellular matrix breakdown together with decreased synthesis and repair are likely responsible for weakening of the fibrous cap and rendering it more rupture-prone. [84, 85]

Extensive neovascularisation and intraplaque haemorrhages consistently occur in the brachiocephalic and common carotid arteries of ApoE$^{-/-}$Fbn1$^{C1039G+/-}$ mice on Western-type diet. These features are rarely seen in murine atherosclerosis models but are known to highly affect plaque progression and vulnerability in humans. [88] In ApoE$^{-/-}$Fbn1$^{C1039G+/-}$ mice on a Western-type diet, intraplaque neo-vessels, likely arising from adventitial vasa vasorum, clearly sprout out of the media. [89, 90] Neo-vessels are not only present at the base of the plaque but are also frequently observed in its centre, similar to human pathology. [88, 90] Angiogenesis requires extracellular matrix degradation by proteases, including MMPs, to enable endothelial cell migration into the surrounding tissue. [85] In addition, degradation of the extracellular matrix induces release of sequestered angiogenic factors such as vascular endothelial growth factor (VEGF) and TGF-β [85, 86], also observed in ApoE$^{-/-}$ Fbn1$^{C1039G+/-}$ mice on Western-type diet. The extent of neovascularisation in ApoE$^{-/-}$ Fbn1$^{C1039G+/-}$ mice correlates with the degree of elastin fragmentation in the vessel wall. However, degradation of the extracellular matrix alone is not sufficient to induce neovascularisation in atherosclerotic plaques, because microvessels are not present in plaques of ApoE$^{-/-}$Fbn1$^{C1039G+/-}$ mice on a normal diet. This observation indicates that an additional factor is needed to trigger plaque neovascularisation. Hypoxia, a well-known angiogenesis trigger [91], is strongly increased in plaques of brachiocephalic and carotid arteries in ApoE$^{-/-}$Fbn1$^{C1039G+/-}$ mice on Western-type diet. By contrast, hypoxia in the ascending aorta is minor, which likely explains the

absence of neo-vessels at that site. Thus, the highly permeable arterial wall, due to degradation of the extracellular matrix, combined with intraplaque hypoxia seems required for neo-vessel formation in atherosclerotic plaques of ApoE$^{-/-}$Fbn1$^{C1039G+/-}$ mice on Western-type diet. Importantly, those neo-vessels are highly leaky. Moreover, the presence of intraplaque erythrocytes near neo-vessels at the base of the plaque points to intraplaque haemorrhages, substantiating ruptured neo-vessels as source of intraplaque bleeding. [86, 88, 92] Erythrocytes are important sources of free cholesterol, thereby increasing necrotic core size. Hence, neovascularisation, besides supplying plaques with leukocytes and lipoproteins, can promote focal plaque expansion when microvessels rupture or become thrombotic. [88, 91, 92] Taken together, these observations in this mouse model are in line with current concepts of human vulnerable plaques.

In addition to enhanced plaque vulnerability, plaque rupture is consistently present in ApoE$^{-/-}$Fbn1$^{C1039G+/-}$ mice on a Western-type diet, but only very rarely in ApoE$^{-/-}$ mice on a Western-type diet. Moreover, fibrin-rich mural thrombi are present in brachiocephalic, carotid and coronary arteries and ascending aortas. Both intrinsic (i.e. a highly unstable plaque phenotype) and extrinsic factors (i.e. forces acting on the plaque) are elementary for plaque rupture. [93] In general, rupture occurs when the mechanical stress applied on the fibrous cap exceeds its tensile strength. The latter is mainly determined by the collagen content of the plaque, which is significantly decreased in plaques of ApoE$^{-/-}$Fbn1$^{C1039G+/-}$ mice on Western-type diet. [84, 93] Elevated pulse pressure (as a consequence of arterial stiffening) [76] leads to repetitive plaque deformation, increasing the tensile stress on the cap. [79, 94] When applied chronically, this can lead to plaque fatigue, making it prone to rupture. [93, 94] Moreover, due to the progressive aortic dilatation and outward remodelling (as a result of the large plaques), the collagen and elastin fibres of the cap are stretched and become more rigid, increasing the susceptibility to mechanical stress. Aortic dilatation is highly pronounced in the ascending aorta of ApoE$^{-/-}$Fbn1$^{C1039G+/-}$ mice on a Western-type diet, suggesting that this mechanism is responsible for rupture of unstable plaques at this site. In brachiocephalic and carotid arteries, intraplaque neovascularisation and haemorrhage are frequently present, further increasing plaque size and vulnerability to rupture.

In addition, sudden death is observed in ApoE$^{-/-}$Fbn1$^{C1039G+/-}$ mice on a Western-type diet, mainly between 16 and 23 weeks, with 50% mortality after 20 weeks. Moreover, ApoE$^{-/-}$Fbn1$^{C1039G+/-}$ mice on a Western-type diet that died suddenly show a significantly higher frequency of coronary stenosis compared to survivors, suggesting that the presence of coronary artery plaque plays an important role in cardiac death. The majority of ApoE$^{-/-}$Fbn1$^{C1039G+/-}$ mice on Western-type diet show infarcted areas, which compromise cardiac function even more. Although it is not known whether the increased infarcted area is the result of plaque rupture or due to pronounced plaque formation and coronary artery stenosis, these findings are remarkable because coronary artery plaque and spontaneous MIs almost never develop in ApoE$^{-/-}$ mice on a Western-type diet. Also in humans, differences in fibrillin-1 genotype have shown to greatly affect plaque progression and severity of coronary artery disease, underscoring the pathophysiological relevance of fibrillin-1 mutations in cardiovascular disease. [79]

Thus, elastin fragmentation in combination with a Western-type diet leads to plaque destabilisation and rupture in ApoE$^{-/-}$ mice. ApoE$^{-/-}$Fbn1$^{C1039G+/-}$ mice show many features of human end-stage atherosclerosis, such as an enlarged necrotic core, a thin fibrous cap with an important loss of collagen fibres, outward remodelling and the presence of intraplaque microvessels and haemorrhage, resulting in plaque rupture, MI and sudden death. Therefore, ApoE$^{-/-}$Fbn1$^{C1039G+/-}$ mice on a Western-type diet offer the opportunity to investigate the role of key factors involved in plaque destabilisation, including intraplaque neovascularisation, which will provide more insight into the mechanisms of plaque disruption and potential targets for therapeutic interventions. [80, 95-97]

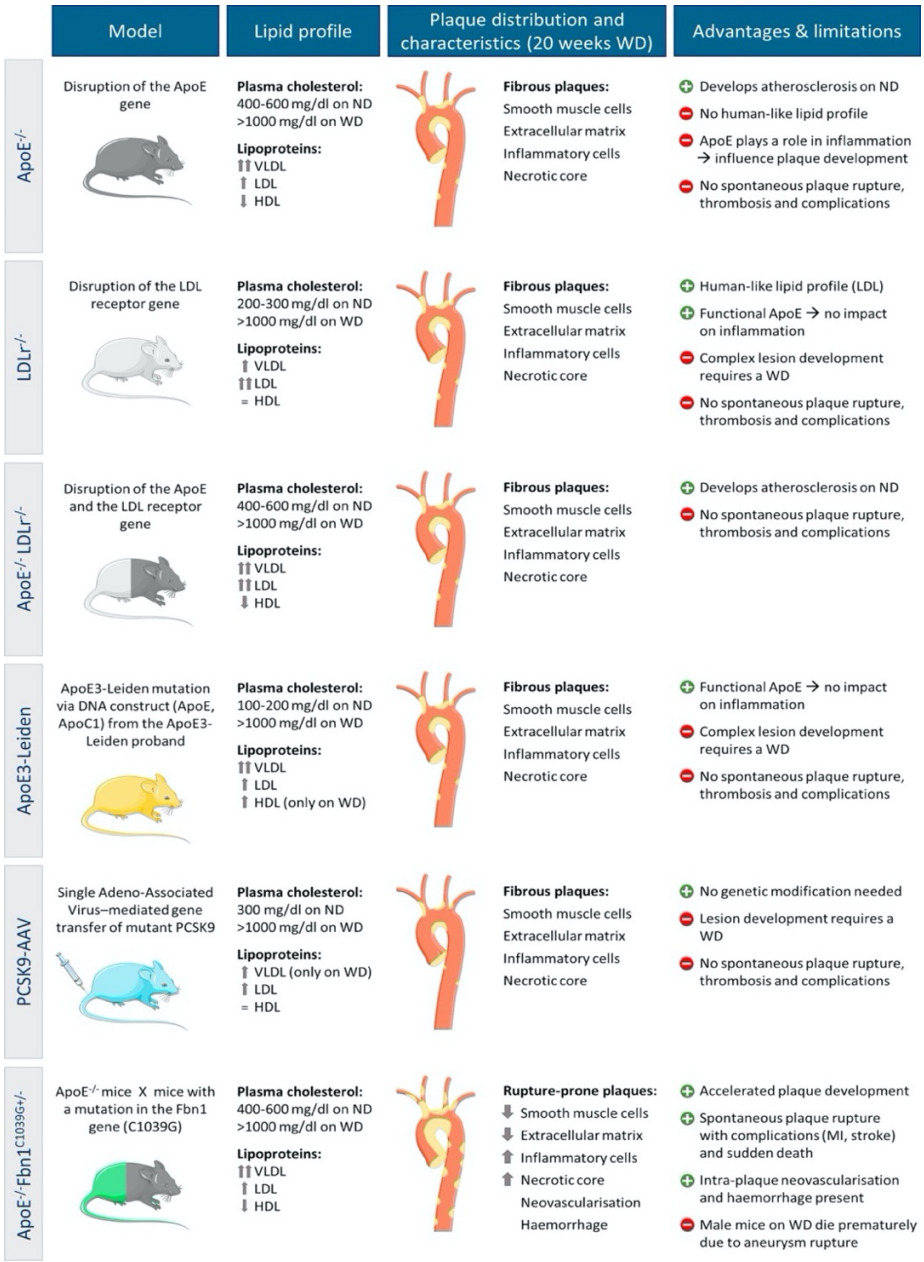

Figure 1. Overview of current mouse models of atherosclerosis. This figure describes the different models with their total plasma cholesterol levels on normal (ND) and Western-type diet (WD), lipoprotein profile, plaque characteristics, advantages and limitations. The distribution of the plaques in the thoracic aorta and the complexity is shown for mice fed a WD for 20 weeks. The composition of the most complex lesions at that time point is displayed (usually found in the aortic root or brachiocephalic artery).

Rabbits

The rabbit has been one of the most frequently used animals in atherosclerosis research because of their easy handling and relatively inexpensive maintenance. [8] However, there has been a reduced trend of using this animal model since 2000, probably due to the availability of ApoE and LDL receptor knock-out mice. [98] Multiple approaches and models have been used to study atherosclerosis and its complication in rabbits, including genetically hypercholesterolaemic rabbits such as Watanabe heritable hyperlipidaemic rabbits (WHHL) [99], New Zeeland White rabbits fed a cholesterol-rich diet [100], and very recently ApoE$^{-/-}$ rabbits. [101]

Rabbits have a lipoprotein metabolism that is similar to humans (except for their hepatic lipase deficiency) and show significant differences with mice. Unlike mice, in which HDL is the predominant plasma lipoprotein, rabbits transport significant amounts of cholesterol via ApoB-containing particles (VLDL and LDL).[102] Consequently, rabbits have been useful to point out the role of elevated plasma cholesterol as a critical factor in the initiation of atherosclerosis. Limitations of rabbit models include a highly abnormal diet required for the development of hypercholesterolaemia, massive inflammation and hepatic toxicity due to the long term high cholesterol feeding.[1]

Watanabe heritable hyperlipidaemic (WHHL) rabbits

WHHL rabbits are a mutant strain that shows spontaneous hypercholesterolaemia and atherosclerosis due to a defect in the LDL receptor.[99] Homozygous WHHL rabbits fed a normal diet are hypercholesterolaemic from birth with LDL as the predominant lipoprotein. They exhibit various types of atherosclerotic lesions ranging from early fatty streaks to advanced lesions in the aorta, coronary arteries and cerebral artery.[100, 103] These rabbits also show an increased risk of MI. The WHHL rabbit was one of the first rabbit models in which the effect of statins to suppress plaque destabilization and to reduce thrombogenicity was investigated. High-fructose and high fat–diet fed WHHL rabbits develop early insulin resistance and glucose tolerance and show aortic lesions with a lipid core and calcifications.

This model has allowed researchers to investigate the effect of insulin resistance on atherosclerosis lesion formation.[104]

New Zealand White (NZW) rabbits

NZW rabbits are commonly used to study atherosclerosis. NZW rabbits that are fed a normal diet have low plasma cholesterol levels (mostly < 50 mg/dl) and consequently do not develop spontaneous atherosclerosis. However, supplementing the diet with 0.3-0.5% cholesterol increases the plasma cholesterol level up to 1000 mg/dl. The plaque composition is determined by the level of dietary cholesterol and the duration of cholesterol feeding. One protocol uses adult rabbits that are fed a cholesterol-rich diet (1.0-1.5% cholesterol) for a short period of time (about 8 weeks). By using such a diet, rabbits develop severe hypercholesterolaemia with plasma cholesterol levels between 1500 and 3000 mg/dl, which are never seen in humans, resulting in atherosclerotic plaques primarily composed of macrophage-derived foam cells. For this reason, the most used protocol lasts 20 to 26 weeks and consists of a diet containing 0.3% cholesterol. On average, cholesterol levels rise to about 800 mg/dl. This protocol develops atherosclerotic plaques in the aortic arch and thoracic aorta, rather than in the abdominal aorta (less pronounced plaque formation) [100, 102], whereas in humans, plaques are commonly found in the abdominal aorta. Coronary atherosclerosis is also observed in cholesterol-fed rabbits but is usually restricted to the left coronary arterial trunks. Depending on the length of the cholesterol feeding, also plaque calcification occurs. However, there is no evidence for spontaneous plaque rupture.

Apolipoprotein E knockout (ApoE$^{-/-}$) rabbits

Recently, ApoE$^{-/-}$ rabbits have been reported as a model to study the relationship between atherosclerosis and human hyperlipidaemia.[101] ApoE$^{-/-}$ rabbits can be generated using genome editing enzymes such as zinc finger nucleases, transcription activator-like effector nucleases (TALENs) or RNA-guided CRISPR-associated protein 9 (Cas9) endonucleases. Because the rabbit lipoprotein profile is similar to humans [105], the ApoE$^{-/-}$ rabbit represents an attractive alternative to the

ApoE$^{-/-}$ mouse. Even on a normal diet, ApoE$^{-/-}$ rabbits show mild hyperlipidaemia with plasma total cholesterol levels around 200 mg/dl. However, when fed a cholesterol-rich diet (0.3% cholesterol and 3% soybean oil for 2 weeks) their plasma total cholesterol levels increase to about 1000 mg/dl (vs. about 170 mg/dl in cholesterol-fed wild-type rabbits). ApoE$^{-/-}$ rabbits develop more pronounced aortic atherosclerosis than wild-type rabbits when fed with a cholesterol diet for 10 weeks.[101] Because both ApoE and the LDL receptor play an important role in mediating cholesterol metabolism, ApoE$^{-/-}$ rabbits together with LDL receptor-deficient WHHL rabbits may be valuable models for the study of human hyperlipidaemia: ApoE$^{-/-}$ rabbits show elevation of remnant lipoproteins, whereas WHHL rabbits have high levels of LDL accompanied by low HDL.[101]

Large animal models (pigs and non-human primates)

Although small animal models have provided insight into the mechanisms that drive atherosclerosis, additional strategies are required to translate these findings into improved prevention and treatment of symptomatic atherosclerosis in humans. Efficient large animal models of atherosclerosis may be useful to deal with these challenges. Indeed, the translation of the knowledge obtained from studies in mice to the development of drugs for human atherosclerosis can benefit from a bridging tool such as porcine models of atherosclerosis. Not only the effects of pharmacological treatments on atherosclerosis can be studied in such models but also clinical imaging end-points can be evaluated as guiding tool for subsequent phase II clinical trials.[106] Gene-editing tools for large animals have made it possible to create gene-modified minipigs that develop atherosclerosis with many similarities to humans in terms of predilection for lesion sites and histopathology. For instance, minipigs with liver-specific expression of human D374Y-PCSK9 show severe hypercholesterolaemia and development of progressive atherosclerotic lesions.[107] Together with existing porcine models of atherosclerosis that are based on spontaneous mutations or severe diabetes, such models may provide new approaches for translational research in atherosclerosis [106]. Non-human primates show hypercholesterolaemia when fed a high fat/high cholesterol diet and develop coronary fibro-fatty atherosclerotic plaques, similar to humans.[8] Yet, working with

monkeys is expensive, highly regulated, and requires very specialized laboratory animal science skills. Therefore, these models are not frequently used. A few years ago, however, also knockout non-human primates have been created, which may reinforce the interest in large animal models with accelerated atherosclerosis.[106, 108]

In conclusion, many efforts have been made to develop animal models that resemble human atherosclerosis as good as possible. However, each of the current animal models has its advantages and limitations, as summarized in Table 2. A great challenge was the development of an animal model of spontaneous (i.e. without mechanical interventions) plaque rupture with human-like endpoints such as MI, stroke and sudden death. These features are present in ApoE$^{-/-}$Fbn1$^{C1039G+/-}$ mice, making it a promising model to evaluate potential plaque stabilizing therapies.

Table 1. Mouse models of atherosclerotic plaque rupture

Strain	mechanism	Duration (weeks)	Plaque disruption	Luminal thrombus	Intraplaque neo-vessels	IPH	Outward remodelling	'Human-like' complications	Comments	Ref.
ApoE$^{-/-}$	'ageing'	60	12%	3%	N.D.	N.D.	N.D.	Coronary thrombosis	Long term experiment Low rate of plaque rupture and thrombosis	109
ApoE$^{-/-}$	Mixed C57BL/6-129SvJ background	30-65	52%	73%	N.D.	N.D.	N.D.	MI ('some cases') sudden death	Long term experiment mixed background	110
ApoE$^{-/-}$	Collar; Ad-p53 in SMC + phenylephrine	15-17	40%	5%	N.D.	35%	N.D.	N.D.	Plaque rupture not spontaneous , complicated manipulation	111
ApoE$^{-/-}$	Active MMP-9 overexpression in Mφ	41	40%	Fibrin deposition (100%)	N.D.	90%	N.D.	Sudden death (20%)	Long term experiment, complicated manipulation	87
ApoE$^{-/-}$	Cuff (+ ligation)	13-14	29-63%	17-42%	N.D.	31-47%	N.D.	N.D.	Plaque rupture not spontaneous	33
ApoE$^{-/-}$; TM$^{Pro/Pro}$	Collar, genetic hypercoagulability	16-17	+	+	N.D.	+	+	N.D.	Plaque rupture not spontaneous	112
ApoE$^{-/-}$	Partial ligation carotid + renal arteries	16	+	50%	N.D.	80%	N.D.	N.D.	Plaque rupture not spontaneous	113
ApoE$^{-/-}$	uPA overexpression in Mφ	43-48	78%	Fibrin deposition (67%)	N.D.	61%	N.D.	N.D.	Long term experiment, complicated manipulation	114
ApoE$^{-/-}$	Tandem stenosis	14-22	32%	+	+	50%	+	N.D.	Plaque rupture not spontaneous	72
ApoE$^{-/-}$ Fbn1$^{C1039G+/-}$	Elastin fragmentation	20-35	50-70%	carotid	+	90%	+	MI, stroke, sudden death	Spontaneous plaque rupture	80

IPH, intraplaque haemorrhage; Ref., reference; +, present; MI, myocardial infarction N.D., not determined; Ad, adenovirus; Mφ, macrophages; uPA, Urokinase-type plasminogen active

Table 2. Most important advantages and limitations of commonly used models of atherosclerosis

	Advantages	Limitations
Mice	• Relatively cheap • Efficient • Easy crossbreeding • Low cost for pharmacological intervention studies	• Differences with human plaques: – Less coronary plaque formation – No intraplaque neovascularisation and haemorrhage – Rare plaque rupture and thrombosis However, these limitations are overcome in ApoE$^{-/-}$Fbn1$^{C1039G+/-}$ mice.
Rabbits	• Allows translation research such as catheterisation of the aorta (coronary arteries are too small) • Relatively cheap • Easy to breed and handle	• Differences in the localisation of the plaques as compared to humans: – Plaques are most pronounced in the aortic arch and descending thoracic aorta (in contrast to the abdominal aorta in humans)
Pigs	• Similarities with human plaques: – Localisation: coronary arteries, abdominal aorta, ileo-femoral – Neovascularisation towards the plaque	• Plaque development mostly ends in the foam cell stage (this can be overcome with the selection of natural mutants, mechanical damage, introduction of other risk factors, genetic engineering with minipigs) • Thrombosis due to plaque rupture is rare (in contrast to humans) • Relatively expensive and more difficult to handle
Non-human primates	• Very similar plaque formation as compared to humans (both micro- and macroscopic) • Plaque formation in the coronary arteries	• Non-human primates are expensive and highly regulated • Specialized training is needed

References

1. Fuster JJ, Castillo AI, Zaragoza C, Ibáñez B, Andrés V. Animal models of atherosclerosis. *Progress in Molecular Biology and Translational Science*. 2012:1-23
2. Tabas I, García-Cardeña G, Owens GK. Recent insights into the cellular biology of atherosclerosis. *J. Cell Biol.* 2015;209:13-22
3. Sakakura K, Nakano M, Otsuka F, Ladich E, Kolodgie FD, Virmani R. Pathophysiology of atherosclerosis plaque progression. *Heart Lung Circ.* 2013;22:399-411
4. Berliner JA, Navab M, Fogelman AM, Frank JS, Demer LL, Edwards PA, Watson AD, Lusis AJ. Atherosclerosis: Basic mechanisms : Oxidation, inflammation, and genetics. *Circulation*. 1995;91:2488-2496
5. Lusis AJ. Atherosclerosis. *Nature*. 2000;407:233-241
6. Konstantinov IE, Jankovic GM. Alexander i. Ignatowski: A pioneer in the study of atherosclerosis. *Tex. Heart Inst. J.* 2013;40:246-249
7. Kapourchali FR, Surendiran G, Chen L, Uitz E, Bahadori B, Moghadasian MH. Animal models of atherosclerosis. *World J. Clin. Cases*. 2014;2:126-132
8. Getz GS, Reardon CA. Animal models of atherosclerosis. *Arterioscler. Thromb. Vasc. Biol.* 2012;32:1104-1115
9. Bond AR, Jackson CL. The fat-fed apolipoprotein e knockout mouse brachiocephalic artery in the study of atherosclerotic plaque rupture. *J. Biomed. Biotechnol.* 2011;2011:1-10
10. VanderLaan PA, Reardon CA, Getz GS. Site specificity of atherosclerosis: Site-selective responses to atherosclerotic modulators. *Arterioscler. Thromb. Vasc. Biol.* 2004;24:12-22
11. Schwartz SM, Galis ZS, Rosenfeld ME, Falk E. Plaque rupture in humans and mice. *Arterioscler. Thromb. Vasc. Biol.* 2007;27:705-713
12. Meir KS, Leitersdorf E. Atherosclerosis in the apolipoprotein e-deficient mouse: A decade of progress. *Arterioscler. Thromb. Vasc. Biol.* 2004;24:1006-1014

13. Piedrahita JA, Zhang SH, Hagaman JR, Oliver PM, Maeda N. Generation of mice carrying a mutant apolipoprotein e gene inactivated by gene targeting in embryonic stem cells. *PNAS*. 1992;89:4471-4475
14. Plump AS, Smith JD, Hayek T, Aalto-Setälä K, Walsh A, Verstuyft JG, Rubin EM, Breslow JL. Severe hypercholesterolemia and atherosclerosis in apolipoprotein e-deficient mice created by homologous recombination in es cells. *Cell*. 1992;71:343-353
15. Silvestre-Roig C, de Winther MP, Weber C, Daemen MJ, Lutgens E, Soehnlein O. Atherosclerotic plaque destabilization. *Circ. Res.* 2014;114:214-226
16. Zadelaar S, Kleemann R, Verschuren L, de Vries-Van der Weij J, van der Hoorn J, Princen HM, Kooistra T. Mouse models for atherosclerosis and pharmaceutical modifiers. *Arterioscler. Thromb. Vasc. Biol.* 2007;27:1706-1721
17. Lutgens E, Daemen M, Kockx M, Doevendans P, Hofker M, Havekes L, Wellens H, de Muinck ED. Atherosclerosis in apoe*3-leiden transgenic mice : From proliferative to atheromatous stage. *Circulation*. 1999;99:276-283
18. Ross R. Cell biology of atherosclerosis. *Annu Rev Physiol*. 1995;57:791-804
19. Breslow JL. Transgenic mouse models of lipoprotein metabolism and atherosclerosis. *Proc. Natl. Acad. Sci. U. S. A.* 1993;90:8314-8318
20. Gencer B, Kronenberg F, Stroes ES, Mach F. Lipoprotein(a): The revenant. *Eur. Heart J.* 2017
21. Lawn RM, Wade DP, Hammer RE, Chiesa G, Verstuyft JG, Rubin EM. Atherogenesis in transgenic mice expressing human apolipoprotein(a). *Nature*. 1992;360:670-672
22. Curtiss LK, Boisvert WA. Apolipoprotein e and atherosclerosis. *Curr. Opin. Lipidol.* 2000;11:243-251
23. Sehayek E, Shefer S, Nguyen LB, Ono JG, Merkel M, Breslow JL. Apolipoprotein e regulates dietary cholesterol absorption and biliary cholesterol excretion: Studies in c57bl/6 apolipoprotein e knockout mice. *PNAS*. 2000;97:3433-3437
24. Mahley R. Apolipoprotein e: Cholesterol transport protein with expanding role in cell biology. *Science*. 1988;240:622-630

25. Jawien J, Nastalek P, Korbut R. Mouse models of experimental atherosclerosis. *J. Physiol. Pharmacol.* 2004;55:503-517
26. Nakashima Y, Plump AS, Raines EW, Breslow JL, Ross R. Apoe-deficient mice develop lesions of all phases of atherosclerosis throughout the arterial tree. *Arterioscler. Thromb. Vasc. Biol.* 1994;14:133-140
27. Plump AS, Breslow JL. Apolipoprotein e and the apolipoprotein e-deficient mouse. *Annu. Rev. Nutr.* 1995;15:495-518
28. Reddick RL, Zhang SH, Maeda N. Atherosclerosis in mice lacking apo e. Evaluation of lesional development and progression [published erratum appears in arterioscler thromb 1994 may;14(5):839]. *Arterioscler. Thromb. Vasc. Biol.* 1994;14:141-147
29. Rattazzi M, Bennett BJ, Bea F, Kirk EA, Ricks JL, Speer M, Schwartz SM, Giachelli CM, Rosenfeld ME. Calcification of advanced atherosclerotic lesions in the innominate arteries of apoe-deficient mice: Potential role of chondrocyte-like cells. *Arterioscler. Thromb. Vasc. Biol.* 2005;25:1420-1425
30. Getz GS, Reardon CA. Apoprotein e as a lipid transport and signaling protein in the blood, liver, and artery wall. *J. Lipid Res.* 2009;50 Suppl:S156-161
31. Smith JD, Breslow JL. The emergence of mouse models of atherosclerosis and their relevance to clinical research. *J. Intern. Med.* 1997;242:99-109
32. Plump AS, Lum PY. Genomics and cardiovascular drug development. *J. Am. Coll. Cardiol.* 2009;53:1089-1100
33. Sasaki T, Kuzuya M, Nakamura K, Cheng XW, Shibata T, Sato K, Iguchi A. A simple method of plaque rupture induction in apolipoprotein e-deficient mice. *Arterioscler. Thromb. Vasc. Biol.* 2006;26:1304-1309
34. von der Thusen JH, van Berkel TJ, Biessen EA. Induction of rapid atherogenesis by perivascular carotid collar placement in apolipoprotein e-deficient and low-density lipoprotein receptor-deficient mice. *Circulation*. 2001;103:1164-1170
35. Marais AD. Familial hypercholesterolaemia. *Clin. Biochem. Rev.* 2004;25:49-68
36. Defesche JC. Low-density lipoprotein receptor--its structure, function, and mutations. *Semin. Vasc. Med.* 2004;4:5-11

37. Ishibashi S, Brown MS, Goldstein JL, Gerard RD, Hammer RE, Herz J. Hypercholesterolemia in low density lipoprotein receptor knockout mice and its reversal by adenovirus-mediated gene delivery. *J. Clin. Invest.* 1993;92:883-893
38. Ishibashi S, Goldstein JL, Brown MS, Herz J, Burns DK. Massive xanthomatosis and atherosclerosis in cholesterol-fed low density lipoprotein receptor-negative mice. *J. Clin. Invest.* 1994;93:1885-1893
39. Zhang SH, Reddick RL, Piedrahita JA, Maeda N. Spontaneous hypercholesterolemia and arterial lesions in mice lacking apolipoprotein e. *Science*. 1992;258:468-471
40. Knowles JW, Maeda N. Genetic modifiers of atherosclerosis in mice. *Arterioscler. Thromb. Vasc. Biol.* 2000;20:2336-2345
41. Hartvigsen K, Binder CJ, Hansen LF, Rafia A, Juliano J, Horkko S, Steinberg D, Palinski W, Witztum JL, Li AC. A diet-induced hypercholesterolemic murine model to study atherogenesis without obesity and metabolic syndrome. *Arterioscler. Thromb. Vasc. Biol.* 2007;27:878-885
42. Véniant MM, Sullivan MA, Kim SK, Ambroziak P, Chu A, Wilson MD, Hellerstein MK, Rudel LL, Walzem RL, Young SG. Defining the atherogenicity of large and small lipoproteins containing apolipoprotein b100. *J. Clin. Invest.* 2000;106:1501-1510
43. Veniant MM, Withycombe S, Young SG. Lipoprotein size and atherosclerosis susceptibility in apoe-/- and ldlr-/- mice. *Arterioscler. Thromb. Vasc. Biol.* 2001;21:1567-1570
44. Hobbs HH, Russell DW, Brown MS, Goldstein JL. The ldl receptor locus in familial hypercholesterolemia: Mutational analysis of a membrane protein. *Annu. Rev. Genet.* 1990;24:133-170
45. Lee YT, Lin HY, Chan YW, Li KH, To OT, Yan BP, Liu T, Li G, Wong WT, Keung W, Tse G. Mouse models of atherosclerosis: A historical perspective and recent advances. *Lipids Health Dis.* 2017;16:12
46. Bonthu S, Heistad DD, Chappell DA, Lamping KG, Faraci FM. Atherosclerosis, vascular remodeling, and impairment of endothelium-dependent relaxation in genetically altered hyperlipidemic mice. *Arterioscler. Thromb. Vasc. Biol.* 1997;17:2333-2340

47. Witting PK, Pettersson K, Ostlund-Lindqvist AM, Westerlund C, Eriksson AW, Stocker R. Inhibition by a coantioxidant of aortic lipoprotein lipid peroxidation and atherosclerosis in apolipoprotein e and low density lipoprotein receptor gene double knockout mice. *FASEB J.* 1999;13:667-675
48. Caligiuri G, Levy B, Pernow J, Thoren P, Hansson GK. Myocardial infarction mediated by endothelin receptor signaling in hypercholesterolemic mice. *Proc. Natl. Acad. Sci. U. S. A.* 1999;96:6920-6924
49. Ishibashi S, Herz J, Maeda N, Goldstein JL, Brown MS. The two-receptor model of lipoprotein clearance: Tests of the hypothesis in "knockout" mice lacking the low density lipoprotein receptor, apolipoprotein e, or both proteins. *Proc. Natl. Acad. Sci. U. S. A.* 1994;91:4431-4435
50. van den Maagdenberg AM, Hofker MH, Krimpenfort PJ, de Bruijn I, van Vlijmen B, van der Boom H, Havekes LM, Frants RR. Transgenic mice carrying the apolipoprotein e3-leiden gene exhibit hyperlipoproteinemia. *J Biol Chem*. 1993;268:10540-10545
51. van Vlijmen BJ, van den Maagdenberg AM, Gijbels MJ, van der Boom H, HogenEsch H, Frants RR, Hofker MH, Havekes LM. Diet-induced hyperlipoproteinemia and atherosclerosis in apolipoprotein e3-leiden transgenic mice. *J Clin Invest*. 1994;93:1403-1410
52. Gijbels MJ, van der Cammen M, van der Laan LJ, Emeis JJ, Havekes LM, Hofker MH, Kraal G. Progression and regression of atherosclerosis in apoe3-leiden transgenic mice: An immunohistochemical study. *Atherosclerosis*. 1999;143:15-25
53. de Vries MR, Simons KH, Jukema JW, Braun J, Quax PHA. Vein graft failure: From pathophysiology to clinical outcomes. *Nat. Rev. Cardiol.* 2016;13:451-470
54. Karper JC, de Vries MR, van den Brand BT, Hoefer IE, Fischer JW, Jukema JW, Niessen HWM, Quax PHA. Toll-like receptor 4 is involved in human and mouse vein graft remodeling, and local gene silencing reduces vein graft disease in hypercholesterolemic apoe*3leiden mice. *Arterioscler. Thromb. Vasc. Biol.* 2011;31:1033-1040
55. Zou Y, Dietrich H, Hu Y, Metzler B, Wick G, Xu Q. Mouse model of venous bypass graft arteriosclerosis. *Am. J. Pathol.* 1998;153:1301-1310

56. Dietrich H, Hu Y, Zou Y, Huemer U, Metzler B, Li C, Mayr M, Xu Q. Rapid development of vein graft atheroma in apoe-deficient mice. *Am. J. Pathol.* 2000;157:659-669

57. Lardenoye JHP, De Vries MR, Grimbergen JM, Havekes LM, Knaapen MW, Kockx MM, van Hinsbergh VW, van Bockel JH, Quax PH. Inhibition of accelerated atherosclerosis in vein grafts by placement of external stent in apoe*3-leiden transgenic mice. *Arterioscler. Thromb. Vasc. Biol.* 2002;22:1433-1438

58. Lardenoye JHP, de Vries MR, Löwik CW, Xu Q, Dhore CR, Cleutjens JP, van Hinsbergh VW, van Bockel JH, Quax PH. Accelerated atherosclerosis and calcification in vein grafts: A study in apoe*3 leiden transgenic mice. *Circ. Res.* 2002;91:577-584

59. Lardenoye JH, Delsing DJ, de Vries MR, Deckers MM, Princen HM, Havekes LM, van Hinsbergh VW, van Bockel JH, Quax PH. Accelerated atherosclerosis by placement of a perivascular cuff and a cholesterol-rich diet in apoe*3leiden transgenic mice. *Circ. Res.* 2000;87:248-253

60. Bjorklund MM, Hollensen AK, Hagensen MK, Dagnaes-Hansen F, Christoffersen C, Mikkelsen JG, Bentzon JF. Induction of atherosclerosis in mice and hamsters without germline genetic engineering. *Circ. Res.* 2014;114:1684-1689

61. Roche-Molina M, Sanz-Rosa D, Cruz FM, Garcia-Prieto J, Lopez S, Abia R, Muriana FJ, Fuster V, Ibanez B, Bernal JA. Induction of sustained hypercholesterolemia by single adeno-associated virus-mediated gene transfer of mutant hpcsk9. *Arterioscler. Thromb. Vasc. Biol.* 2015;35:50-59

62. Denis M, Marcinkiewicz J, Zaid A, Gauthier D, Poirier S, Lazure C, Seidah NG, Prat A. Gene inactivation of proprotein convertase subtilisin/kexin type 9 reduces atherosclerosis in mice. *Circulation*. 2012;125:894-901

63. Akram ON, Bernier A, Petrides F, Wong G, Lambert G. Beyond ldl cholesterol, a new role for pcsk9. *Arterioscler. Thromb. Vasc. Biol.* 2010;30:1279-1281

64. Li J, Tumanut C, Gavigan JA, Huang WJ, Hampton EN, Tumanut R, Suen KF, Trauger JW, Spraggon G, Lesley SA, Liau G, Yowe D, Harris JL.

Secreted pcsk9 promotes ldl receptor degradation independently of proteolytic activity. *Biochem. J.* 2007;406:203-207

65. Cerrone M, Noorman M, Lin X, Chkourko H, Liang FX, van der Nagel R, Hund T, Birchmeier W, Mohler P, van Veen TA, van Rijen HV, Delmar M. Sodium current deficit and arrhythmogenesis in a murine model of plakophilin-2 haploinsufficiency. *Cardiovasc. Res.* 2012;95:460-468
66. Kaspar BK, Roth DM, Lai NC, Drumm JD, Erickson DA, McKirnan MD, Hammond HK. Myocardial gene transfer and long-term expression following intracoronary delivery of adeno-associated virus. *J. Gene Med.* 2005;7:316-324
67. Suhy DA, Kao SC, Mao T, Whiteley L, Denise H, Souberbielle B, Burdick AD, Hayes K, Wright JF, Lavender H, Roelvink P, Kolykhalov A, Brady K, Moschos SA, Hauck B, Zelenaia O, Zhou S, Scribner C, High KA, Renison SH, Corbau R. Safe, long-term hepatic expression of anti-hcv shrna in a nonhuman primate model. *Mol. Ther.* 2012;20:1737-1749
68. Zsebo K, Yaroshinsky A, Rudy JJ, Wagner K, Greenberg B, Jessup M, Hajjar RJ. Long-term effects of aav1/serca2a gene transfer in patients with severe heart failure: Analysis of recurrent cardiovascular events and mortality. *Circ. Res.* 2014;114:101-108
69. Goettsch C, Hutcheson JD, Hagita S, Rogers MA, Creager MD, Pham T, Choi J, Mlynarchik AK, Pieper B, Kjolby M, Aikawa M, Aikawa E. A single injection of gain-of-function mutant pcsk9 adeno-associated virus vector induces cardiovascular calcification in mice with no genetic modification. *Atherosclerosis*. 2016;251:109-118
70. Ylä-Herttuala S, Bentzon JF, Daemen M, Falk E, Garcia-Garcia HM, Herrmann J, Hoefer I, Jukema JW, Krams R, Kwak BR, Marx N, Naruszewicz M, Newby A, Pasterkamp G, Serruys PWJC, Waltenberger J, Weber C, Tokgözoglu L. Stabilisation of atherosclerotic plaques. *Thromb. Haemost.* 2011;106:1-19
71. Ni M, Chen WQ, Zhang Y. Animal models and potential mechanisms of plaque destabilisation and disruption. *Heart*. 2009;95:1393-1398
72. Chen YC, Bui AV, Diesch J, Manasseh R, Hausding C, Rivera J, Haviv I, Agrotis A, Htun NM, Jowett J, Hagemeyer CE, Hannan RD, Bobik A, Peter

K. A novel mouse model of atherosclerotic plaque instability for drug testing and mechanistic/therapeutic discoveries using gene and microrna expression profiling. *Circ. Res.* 2013;113:252-265

73. Bentzon JF, Falk E. Atherosclerotic lesions in mouse and man: Is it the same disease? *Curr. Opin. Lipidol.* 2010;21:434-440
74. Kielty CM, Sherratt MJ, Shuttleworth CA. Elastic fibres. *J. Cell Sci.* 2002;115:2817-2828
75. Judge DP, Dietz HC. Marfan's syndrome. *Lancet*. 2005;366:1965-1976
76. Van Herck JL, De Meyer GRY, Martinet W, Van Hove CE, Foubert K, Theunis MH, Apers S, Bult H, Vrints CJ, Herman AG. Impaired fibrillin-1 function promotes features of plaque instability in apolipoprotein e-deficient mice. *Circulation*. 2009;120:2478-2487
77. Judge DP, Biery NJ, Keene DR, Geubtner J, Myers L, Huso DL, Sakai LY, Dietz HC. Evidence for a critical contribution of haploinsufficiency in the complex pathogenesis of marfan syndrome. *J. Clin. Invest.* 2004;114:172-181
78. Mariko B, Pezet M, Escoubet B, Bouillot S, Andrieu J-P, Starcher B, Quaglino D, Jacob M-P, Huber P, Ramirez F, Faury G. Fibrillin-1 genetic deficiency leads to pathological ageing of arteries in mice. *J. Pathol.* 2011;224:33-44
79. Medley TL, Cole TJ, Gatzka CD, Wang WY, Dart AM, Kingwell BA. Fibrillin-1 genotype is associated with aortic stiffness and disease severity in patients with coronary artery disease. *Circulation*. 2002;105:810-815
80. Van der Donckt C, Van Herck JL, Schrijvers DM, Vanhoutte G, Verhoye M, Blockx I, Van Der Linden A, Bauters D, Lijnen HR, Sluimer JC, Roth L, Van Hove CE, Fransen P, Knaapen MW, Hervent AS, De Keulenaer GW, Bult H, Martinet W, Herman AG, De Meyer GRY. Elastin fragmentation in atherosclerotic mice leads to intraplaque neovascularization, plaque rupture, myocardial infarction, stroke, and sudden death. *Eur. Heart J.* 2015;36:1049-1058
81. Van der Donckt C, Roth L, Vanhoutte G, Blockx I, Bink DI, Ritz K, Pintelon I, Timmermans JP, Bauters D, Martinet W, Daemen MJ, Verhoye M, De Meyer GRY. Fibrillin-1 impairment enhances blood–brain barrier

permeability and xanthoma formation in brains of apolipoprotein e-deficient mice. *Neuroscience*. 2015;295:11-22

82. Fulop T, Larbi A, Fortun A, Robert L, Khalil A. Elastin peptides induced oxidation of ldl by phagocytic cells. *Pathol. Biol. (Paris)*. 2005;53:416-423
83. Koenig W, Khuseyinova N. Biomarkers of atherosclerotic plaque instability and rupture. *Arterioscler. Thromb. Vasc. Biol.* 2007;27:15-26
84. Libby P. Mechanisms of acute coronary syndromes and their implications for therapy. *N. Engl. J. Med.* 2013;368:2004-2013
85. Raffetto JD, Khalil RA. Matrix metalloproteinases and their inhibitors in vascular remodeling and vascular disease. *Biochem. Pharmacol.* 2008;75:346-359
86. de Nooijer R, Verkleij CJ, von der Thüsen JH, Jukema JW, van der Wall EE, van Berkel TJ, Baker AH, Biessen EA. Lesional overexpression of matrix metalloproteinase-9 promotes intraplaque hemorrhage in advanced lesions but not at earlier stages of atherogenesis. *Arterioscler. Thromb. Vasc. Biol.* 2005;26:340-346
87. Gough PJ, Gomez IG, Wille PT, Raines EW. Macrophage expression of active mmp-9 induces acute plaque disruption in apoe-deficient mice. *J. Clin. Invest.* 2006;116:59-69
88. Virmani R, Kolodgie FD, Burke AP, Finn AV, Gold HK, Tulenko TN, Wrenn SP, Narula J. Atherosclerotic plaque progression and vulnerability to rupture: Angiogenesis as a source of intraplaque hemorrhage. *Arterioscler. Thromb. Vasc. Biol.* 2005;25:2054-2061
89. Moulton KS, Olsen BR, Sonn S, Fukai N, Zurakowski D, Zeng X. Loss of collagen xviii enhances neovascularization and vascular permeability in atherosclerosis. *Circulation*. 2004;110:1330-1336
90. Rademakers T, Douma K, Hackeng TM, Post MJ, Sluimer JC, Daemen MJAP, Biessen EAL, Heeneman S, van Zandvoort MAMJ. Plaque-associated vasa vasorum in aged apolipoprotein e-deficient mice exhibit proatherogenic functional features in vivo. *Arterioscler. Thromb. Vasc. Biol.* 2013;33:249-256
91. Sluimer JC, Kolodgie FD, Bijnens APJJ, Maxfield K, Pacheco E, Kutys B, Duimel H, Frederik PM, van Hinsbergh VWM, Virmani R, Daemen MJAP.

Thin-walled microvessels in human coronary atherosclerotic plaques show incomplete endothelial junctions. *J. Am. Coll. Cardiol.* 2009;53:1517-1527

92. Kockx MM, Cromheeke KM, Knaapen MW, Bosmans JM, De Meyer GRY, Herman AG, Bult H. Phagocytosis and macrophage activation associated with hemorrhagic microvessels in human atherosclerosis. *Arterioscler. Thromb. Vasc. Biol.* 2003;23:440-446
93. Slager CJ, Wentzel JJ, Gijsen FJH, Thury A, van der Wal AC, Schaar JA, Serruys PW. The role of shear stress in the destabilization of vulnerable plaques and related therapeutic implications. *Nat. Clin. Pract. Cardiovasc. Med.* 2005;2:456-464
94. Huang Y, Teng Z, Sadat U, He J, Graves MJ, Gillard JH. In vivo mri-based simulation of fatigue process: A possible trigger for human carotid atherosclerotic plaque rupture. *BioMed. Eng. OnLine*. 2013;12:36
95. Roth L, Rombouts M, Schrijvers DM, Martinet W, De Meyer GRY. Cholesterol-independent effects of atorvastatin prevent cardiovascular morbidity and mortality in a mouse model of atherosclerotic plaque rupture. *Vascul. Pharmacol.* 2016;80:50-58
96. Roth L, Rombouts M, Schrijvers DM, Lemmens K, De Keulenaer GW, Martinet W, De Meyer GRY. Chronic intermittent mental stress promotes atherosclerotic plaque vulnerability, myocardial infarction and sudden death in mice. *Atherosclerosis*. 2015;242:288-294
97. Roth L, Van Dam D, Van der Donckt C, Schrijvers DM, Lemmens K, Van Brussel I, De Deyn PP, Martinet W, De Meyer GRY. Impaired gait pattern as a sensitive tool to assess hypoxic brain damage in a novel mouse model of atherosclerotic plaque rupture. *Physiol. Behav.* 2015;139:397-402
98. Fan J, Kitajima S, Watanabe T, Xu J, Zhang J, Liu E, Chen YE. Rabbit models for the study of human atherosclerosis: From pathophysiological mechanisms to translational medicine. *Pharmacol. Ther.* 2015;146:104-119
99. Watanabe Y. Serial inbreeding of rabbits with hereditary hyperlipidemia (whhl-rabbit) *1incidence and development of atherosclerosis and xanthoma. *Atherosclerosis*. 1980;36:261-268

100. Baumgartner C, Brandl J, Münch G, Ungerer M. Rabbit models to study atherosclerosis and its complications – transgenic vascular protein expression in vivo. *Prog. Biophys. Mol. Biol.* 2016;121:131-141
101. Niimi M, Yang D, Kitajima S, Ning B, Wang C, Li S, Liu E, Zhang J, Eugene Chen Y, Fan J. Apoe knockout rabbits: A novel model for the study of human hyperlipidemia. *Atherosclerosis*. 2016;245:187-193
102. Fan J, Watanabe T. Cholesterol-fed and transgenic rabbit models for the study of atherosclerosis. *J. Atheroscler. Thromb.* 2000;7:26-32
103. Atkinson JB, Hoover RL, Berry KK, Swift LL. Cholesterol-fed heterozygous watanabe heritable hyperlipidemic rabbits: A new model for atherosclerosis. *Atherosclerosis*. 1989;78:123-136
104. Ning B, Wang X, Yu Y, Waqar AB, Yu Q, Koike T, Shiomi M, Liu E, Wang Y, Fan J. High-fructose and high-fat diet-induced insulin resistance enhances atherosclerosis in watanabe heritable hyperlipidemic rabbits. *Nutr. Metab. (Lond.)*. 2015;12
105. Brousseau ME, Hoeg JM. Transgenic rabbits as models for atherosclerosis research. *J. Lipid Res.* 1999;40:365-375
106. Shim J, Al-Mashhadi RH, Sorensen CB, Bentzon JF. Large animal models of atherosclerosis--new tools for persistent problems in cardiovascular medicine. *J. Pathol.* 2016;238:257-266
107. Al-Mashhadi RH, Sorensen CB, Kragh PM, Christoffersen C, Mortensen MB, Tolbod LP, Thim T, Du Y, Li J, Liu Y, Moldt B, Schmidt M, Vajta G, Larsen T, Purup S, Bolund L, Nielsen LB, Callesen H, Falk E, Mikkelsen JG, Bentzon JF. Familial hypercholesterolemia and atherosclerosis in cloned minipigs created by DNA transposition of a human pcsk9 gain-of-function mutant. *Sci. Transl. Med.* 2013;5:166ra161
108. Niu Y, Shen B, Cui Y, Chen Y, Wang J, Wang L, Kang Y, Zhao X, Si W, Li W, Xiang Andy P, Zhou J, Guo X, Bi Y, Si C, Hu B, Dong G, Wang H, Zhou Z, Li T, Tan T, Pu X, Wang F, Ji S, Zhou Q, Huang X, Ji W, Sha J. Generation of gene-modified cynomolgus monkey via cas9/rna-mediated gene targeting in one-cell embryos. *Cell*. 2014;156:836-843

109. Calara F, Silvestre M, Casanada F, Yuan N, Napoli C, Palinski W. Spontaneous plaque rupture and secondary thrombosis in apolipoprotein e-deficient and ldl receptor-deficient mice. *J. Pathol.* 2001;195:257-263

110. Williams H. Characteristics of intact and ruptured atherosclerotic plaques in brachiocephalic arteries of apolipoprotein e knockout mice. *Arterioscler. Thromb. Vasc. Biol.* 2002;22:788-792

111. von der Thusen JH, van Vlijmen BJM, Hoeben RC, Kockx MM, Havekes LM, van Berkel TJC, Biessen EAL. Induction of atherosclerotic plaque rupture in apolipoprotein e-/- mice after adenovirus-mediated transfer of p53. *Circulation*. 2002;105:2064-2070

112. Borissoff JI, Otten JJT, Heeneman S, Leenders P, van Oerle R, Soehnlein O, Loubele STBG, Hamulyák K, Hackeng TM, Daemen MJAP, Degen JL, Weiler H, Esmon CT, van Ryn J, Biessen EAL, Spronk HMH, ten Cate H. Genetic and pharmacological modifications of thrombin formation in apolipoprotein e-deficient mice determine atherosclerosis severity and atherothrombosis onset in a neutrophil-dependent manner. *PLoS One*. 2013;8:e55784

113. Jin Sx, Shen Lh, Nie P, Yuan W, Hu Lh, Li Dd, Chen Xj, Zhang Xk, He B. Endogenous renovascular hypertension combined with low shear stress induces plaque rupture in apolipoprotein e-deficient mice. *Arterioscler. Thromb. Vasc. Biol.* 2012;32:2372-2379

114. Hu JH, Du L, Chu T, Otsuka G, Dronadula N, Jaffe M, Gill SE, Parks WC, Dichek DA. Overexpression of urokinase by plaque macrophages causes histological features of plaque rupture and increases vascular matrix metalloproteinase activity in aged apolipoprotein e-null mice. *Circulation*. 2010;121:1637-1644

Chapter 4

Partial inhibition of glycolysis reduces atherogenesis independent of intraplaque neovascularization in mice

Perrotta P*, Van der Veken B*, Van Der Veken P, Pintelon I, Roosens L, Adriaenssens E, Timmerman V, Guns PJ, De Meyer GRY, Martinet W.

Arterioscler Thromb Vasc Biol. 2020; 40:1168-1181

*The first two authors contributed equally to this work

Abstract

Objective: Intraplaque (IP) neovascularization is an important feature of unstable human atherosclerotic plaques. However, its impact on plaque formation and stability is poorly studied. Because proliferating endothelial cells (ECs) generate up to 85% of their ATP from glycolysis, we investigated whether pharmacological inhibition of glycolytic flux by the small molecule 3PO [3-(3-pyridinyl)-1-(4-pyridinyl)-2-propen-1-one] could have beneficial effects on plaque formation and composition.
Approach and results: ApoE$^{-/-}$ mice treated with 3PO (50 µg/g, i.p.; 4x/week, 4 weeks) showed a metabolic switch toward ketone body formation. Treatment of ApoE$^{-/-}$Fbn1$^{C1039G+/-}$ mice with 3PO (50 µg/g, i.p.) either after 4 weeks of western diet (WD) (preventive, twice/week, 10 weeks) or 16 weeks of WD (curative, 4x/week, 4 weeks) inhibited IP neovascularization by 50% and 38%, respectively. Plaque formation was significantly reduced in all 3PO-treated animals. This effect was independent of IP neovascularisation. In vitro experiments showed that 3PO favors an anti-inflammatory M2 macrophage subtype and suppresses an M1 pro-inflammatory phenotype. Moreover, 3PO induced autophagy, which in turn impaired NF-κB signalling and inhibited TNF-α-mediated VCAM-1 and ICAM-1 up-regulation. Consistently, a preventive 3PO regimen reduced endothelial VCAM-1 expression in vivo. Furthermore, 3PO improved cardiac function in ApoE$^{-/-}$Fbn1$^{C1039G+/-}$ mice after 10 weeks of treatment.
Conclusions: Partial inhibition of glycolysis restrained IP angiogenesis without affecting plaque composition. However, less plaques were formed, which was accompanied by downregulation of endothelial adhesion molecules, an event that depends on autophagy induction. Inhibition of coronary plaque formation by 3PO resulted in an overall improved cardiac function.

Keywords: atherosclerosis, intraplaque neovascularization, angiogenesis, glycolysis, 3PO

Graphical abstract

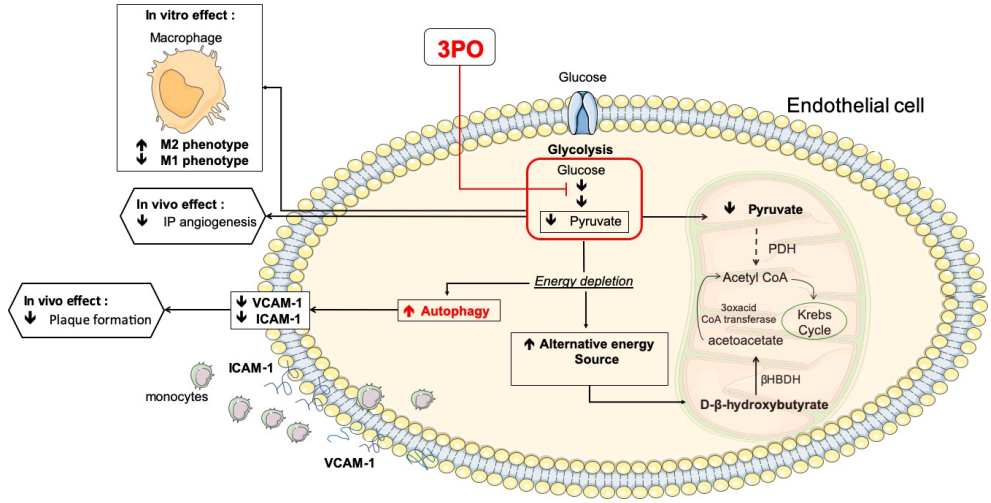

Highlights

- By using a mouse model of advanced atherosclerosis that develops IP neovascularization (ApoE$^{-/-}$Fbn1$^{C1039G+/-}$ mice) we found that partial inhibition of glycolysis impairs neovascularization in plaques
- Partial inhibition of glycolysis restrains atherosclerotic plaque formation independent of IP neovascularization and without affecting plaque composition
- Partial inhibition of glycolysis has a positive impact on cardiac function when administered in a preventive manner
- Partial inhibition of glycolysis increases the number of autophagosomes in endothelial cells
- Partial inhibition of glycolysis reduces endothelial VCAM-1 and ICAM-1 expression in an autophagy-dependent way
- Partial inhibition of glycolysis favors an anti-inflammatory M2 macrophage subtype and suppresses an M1 pro-inflammatory phenotype in vitro.

Introduction

Blood vessels constitute the largest network in our body to ensure a continuous blood flow towards different organs and tissues. However, despite their role in supplying nutrients and oxygenated blood, new vessels that branch off from existing vessels (a process known as neovascularization) could also play a detrimental role in various ischemic and inflammatory diseases including atherosclerosis.[1] Because intraplaque (IP) microvessels are immature and leaky,[2] they facilitate infiltration of lipids, inflammatory mediators and erythrocytes. Consequently, IP neovascularization has been linked to plaque progression.[3, 4] IP neovascularization is initiated in advanced plaques by hypoxia and emerges when the size or inflammatory burden of the plaque exceeds a critical threshold. Clinical trials targeting neovascularization in pathological settings mainly focus on blocking vascular endothelial growth factor (VEGF) signalling.[5] However, these studies have reported moderate success due to drug resistance or adverse effects.[6] Recent evidence indicates that proliferating endothelial cells (ECs) generate up to 85% of their ATP from glycolysis,[7] suggesting that EC metabolism is an attractive alternative target to reduce neovascularization.[8] Pharmacological inhibition of glycolytic flux by intra-peritoneal injection of the small molecule 3PO [3-(3-pyridinyl)-1-(4-pyridinyl)-2-propen-1-one] reduces vessel sprouting in EC spheroids, zebrafish embryos, mouse retina and models of inflammation.[9] 3PO dose dependently reduces glycolysis in ECs, but by no more than 35-40%, thus less than the nonmetabolizable glucose analog 2-deoxy-D-glucose, which reduces glycolysis by approximately 80%.[9] Because 3PO reduces cellular fructose-2,6-bisphosphate levels, it has been proposed that 3PO targets 6-phosphofructo-2-kinase/fructose-2,6-bisphosphatase 3 (PFKFB3).[10]However, more recent findings indicate that 3PO does not bind PFKFB3 and may act through mechanisms that are unrelated to PFKFB3inhibition.[11] Importantly, suppression of glycolysis by 3PO occurs without lowering the energy charge or increasing oxygen consumption, and without abrogating side metabolic pathways such as the pentose phosphate pathway necessary for NADPH production. Although inhibition of glycolysis by 3PO is partial and transient, it is sufficient to reduce neovascularization.[9]

IP neovascularization is a typical feature of advanced human atherosclerotic plaques, but is rarely observed in animal models.[12] Nonetheless, our group has recently reported that apolipoprotein E deficient ($ApoE^{-/-}$) mice, containing a heterozygous mutation (C1039G+/-) in the fibrillin-1 (Fbn1) gene, display substantial IP neovascularization in the brachiocephalic artery and common carotid arteries.[13] Because Fbn1 is the major structural component of extracellular microfibrils in the vessel wall, neovascularization in $ApoE^{-/-}Fbn1^{C1039G+/-}$ mice probably occurs because elastin fragmentation allows microvessel sprouting from the adventitial vasa vasorum through the media into the intimal lesion.[14] Moreover, the high degree of stenosis and presence of activated macrophages in plaques of $ApoE^{-/-}Fbn1^{C1039G+/-}$ mice likely results in IP hypoxia, and triggers the growth of new vessels from the adventitia.[14, 15] In the present study, we explored the possibility of inhibiting IP angiogenesis with 3PO in $ApoE^{-/-}Fbn1^{C1039G+/-}$ mice and studied its potential plaque stabilizing effects.

Material and methods

The authors declare that all supporting data are available within the article (and its online supplementary files).

Mice

Female $ApoE^{-/-}$ mice were fed a western-type diet (WD) (Altromin, C1000 diet supplemented with 20% milkfat and 0.15% cholesterol, #100171), starting at the age of 8 weeks, and treated with glycolysis inhibitor 3PO (50 mg/kg, i.p., 4x/week) or vehicle (DMSO) for 4 weeks. The animals were housed in a temperature-controlled room with a 12-hour light/dark cycle and had free access to water and food [either normal laboratory diet (ssniff, R/M-H) or WD]. To perform a glucose tolerance test, mice were fasted for 16 hours and injected with glucose (1 g/kg, i.p.). Blood glucose levels were determined and plotted in function of time. Insulin action was evaluated in vivo by injection of insulin (Novorapid, 1 U/kg, i.p.). Food and water intake of mice that were individually housed in metabolic cages (Tecniplast, floor area: 200 cm^2) were monitored for 24 hours. Mice in metabolic cages were weighted at the start of

the experiment and after 24 hours in the cage. Fasting and non-fasting blood glucose levels were analyzed with a hand-held glucometer (OneTouch Ultra, range 20-600 mg/dL; Lifescan) by taking a droplet of blood from the tip of the mouse's tail. At the end of the experiment, blood samples were obtained from the retro-orbital plexus of anesthetised mice (sodium pentobarbital 75 mg/kg, i.p.). Subsequently, mice were sacrificed with sodium pentobarbital (250 mg/kg, i.p.). Plasma samples were analyzed with an automated Vista 1500 System (Siemens Healthcare Diagnostics) for liver enzymes, total cholesterol and triglycerides. Insulin and β-hydroxybutyrate were determined with a mouse insulin ELISA kit (80-INSMS-E01, ALPCO) and β-hydroxybutyrate assay kit (ab83390, Abcam), respectively. To assess autophagy induction by 3PO in vivo, GFP-LC3#53 transgenic mice[16] were treated with 3PO (50 mg/kg, i.p., 4x/week) or vehicle (DMSO). After 2 weeks, the autophagic flux inhibitor chloroquine was administered (50 mg/kg, i.p.) and mice were sacrificed 3 hours later using an overdose of sodium pentobarbital (250 mg/kg, i.p.). Liver and heart samples were isolated for immunohistochemical detection of LC3.

For atherosclerosis studies, 3PO (50 mg/kg, i.p.) or solvent (DMSO) was administered to female WD-fed ApoE$^{-/-}$Fbn1$^{C1039G+/-}$ mice, starting either after 4 weeks WD (2x/week, 10 weeks, preventive regimen) or after 16 weeks WD (4x/week, 4 weeks, curative regimen)(Supplemental Figure I). Female mice were chosen because the Fbn1 mutation frequently leads to aortic dissection in male ApoE$^{-/-}$Fbn1$^{C1039G+/-}$ mice, but not in female ApoE$^{-/-}$Fbn1$^{C1039G+/-}$ mice.[13] In addition, ApoE$^{-/-}$ mice on WD were treated with 3PO as described above (preventive regimen) to test the effects of 3PO on plaque size and composition in the absence of IP neovascularization. All animal procedures were conducted according to the guidelines for experimental atherosclerosis studies described in a scientific statement of the American Heart Association and the ATVB Council.[17, 18] Experiments were approved by the ethics committee of the University of Antwerp.

Histology

After euthanasia, the proximal aorta, aortic arch, carotid artery and heart were collected. Tissues were fixed in 4% formalin for 24 hours, dehydrated overnight in 60% isopropanol and subsequently embedded in paraffin. The plaque formation

index in ApoE$^{-/-}$Fbn1$^{C1039G+/-}$ mice was calculated on longitudinal sections of the carotid artery by using the following formula: (∑ total plaque length/∑ total vessel length) x100. Because plaques of ApoE$^{-/-}$ mice are less advanced as compared to ApoE$^{-/-}$Fbn1$^{C1039G+/-}$ mice, the plaque formation index in ApoE$^{-/-}$ mice was measured on longitudinal sections of the aortic arch (instead of the carotid artery). Haematoxylin-eosin (HE) staining was performed on cross-sections of the carotid artery of ApoE$^{-/-}$Fbn1$^{C1039G+/-}$ mice to analyse plaque thickness and percentage necrosis. The plaque thickness was assessed by taking the mean value of 10 random measurements in the respective area. Necrosis was defined as acellular areas filled with necrotic clefts and necrotic debris. Immunohistochemical staining for von Willebrand factor (anti-vWF, PC054, Binding Site) and Ter-119 (anti-Ter-119, 550565, BD Biosciences) were performed to detect plaque ECs and erythrocytes, respectively. Autophagosome formation in liver and heart of 3PO-treated GFP-LC3 mice was measured via LC3 immunostaining using rabbit anti-LC3 antibody (3868S, Cell Signaling). Plaque composition was analysed with Sirius red and anti-α-SMC actin (A2547, Sigma-Aldrich) staining to detect collagen and vascular smooth muscle cells, respectively. Macrophages and macrophage polarization were examined by immunohistochemistry using anti-MAC3 (01781D, Pharmingen) and antibodies against M1/M2 markers (anti-Egr2, PA5-27814, ThermoFisher Scientific; anti-GPR18, PA5-23218, ThermoFisher Scientific; anti-Arg-1, PA5-29645, ThermoFisher Scientific; anti-CD38, MBS129421, MyBioSource). Quantification of immunstains was done from 10 random images per section using ImageJ software. The occurrence of myocardial infarctions (defined as large fibrotic areas) and coronary plaques was analysed on Masson's trichrome staining (transversal sections). Expression of adhesion molecule VCAM-1 was analysed using anti-VCAM-1 (ab134047, Abcam). *En face* Oil Red O staining was performed on the carotid artery and aortic arch of ApoE$^{-/-}$Fbn1$^{C1039G+/-}$ mice.

Echocardiography

Transthoracic echocardiograms were performed on anesthetized mice (isoflurane, 4% for induction and 2.5% for maintenance) at the end of the experiment using a VEVO2100 (VisualSonics), equipped with a 25 MHz transducer. Left ventricular

internal diameter during diastole (LVIDd) and left ventricular internal diameter during systole (LVIDs) were measured and fractional shortening [FS = (LVIDd-LVIDs)/LVIDd*100] was calculated.

Cell culture

Human aortic endothelial cells (HAOECs; Sigma-Aldrich) were cultured in Endothelial Cell Growth Medium (PromoCell) supplemented with 2% fetal bovine serum, 0.4% endothelial cell growth supplement, 0.1 ng/ml epidermal growth factor, 1 ng/ml basic fibroblast growth factor, 90 µg/ml heparin and 1 µg/ml hydrocortisone. To investigate the expression of VCAM-1 and ICAM-1, HAOECs were stimulated with 20 ng/ml human TNF-α. A transcription factor assay kit was used to detect the NF-κB transcription factor DNA binding activity in nuclear extracts according to the manufacturer's instructions (ab133112, Abcam). For siRNA-mediated silencing of the autophagy pathway, HAOECs were seeded into 6-well plates and transfected at 75% confluency with 2.5 ml Opti-MEM Reduced Serum Medium (Thermo Fisher) containing 40 nM ATG7 siRNA (Dharmacon) and 2.5 µl Lipofectamine RNAiMAX (Thermo Fisher) for 6 hours.

Real-time RT-PCR

Total RNA was isolated using an Isolation II RNA mini kit (Bioline) according to the manufacturer's instructions. Reverse transcription was performed with a Sensifast™ cDNA Synthesis Kit (Bioline). Thereafter, Taqman gene expression assay (Applied Biosystems) for CD38 (assay ID: Mm01220906_m1), Gpr18 (assay ID: Mm01224541_m1), Egr2 (assay ID: Mm00456650_m1) and Arg1 (assay ID: Mm00475988_m1) were performed in duplicate on an ABI prism 7300 sequence detector system (Applied Biosystems). The parameters for PCR amplification were 95°C for 10 minutes followed by 40 cycles of 95°C for 15 seconds and 60°C for 1 minute. Relative expression of mRNA was calculated using the comparative threshold cycle method. All data were normalized for quantity of cDNA input by performing measurements on the endogenous reference gene β-actin.

Western Blot analyses

Cells were lysed in an appropriate volume of Laemmli sample buffer (Bio-Rad) containing β-mercaptoethanol (Sigma-Aldrich) and boiled for 5 min. Protein samples were then loaded onto pre-casted Bolt 4-12% Tris-Bis gels (Invitrogen) and after electrophoresis transferred to Immobilon-FL PVDF membranes (Millipore) according to standard procedures. Membranes were blocked for 1 hour with Odyssey blocking buffer (LI-COR Biosciences) diluted 1:5 with PBS. After blocking, membranes were probed overnight at 4°C with primary antibodies diluted in Odyssey blocking buffer, followed by 1 hour incubation with IRDye-labeled secondary antibodies at room temperature. Antibody detection was achieved using an Odyssey SA infrared imaging system (LI-COR Biosciences). The intensity of the protein bands was quantified using Image Studio software. The following primary antibodies were used: anti-β-actin (ab8226, Cell Signaling), anti-mTOR (2972, Cell Signaling), anti-phospho-mTOR (S2448) (2971, Cell Signaling), anti-p70 S6 Kinase (9202, Cell Signaling), anti-phospho-p70 S6 Kinase (Thr389) (9205, Cell Signaling), anti-LC3 (clone 5F10, 0231-100/LC3-5F10, Nanotools), anti-VCAM-1 (ab134047, Abcam), anti-ATG7 (8558S, Cell Signaling), anti-NF-κB (8242, Cell Signaling), anti-phospho-NF-κB (3039, Cell Signaling) and anti-ICAM-1 (ab179707, Abcam). IRDye-labelled secondary antibodies (goat anti-mouse IgG, 926-68070, and goat anti-rabbit IgG, 926-32211) were purchased from LI-COR Biosciences.

Transmission electron microscopy

Tissue samples were fixed in 2.5% glutaraldehyde, 0.1M sodium cacodylate and 0.05% $CaCl_2$ (pH 7.4) and further processed for transmission electron microscopy as described previously,[19] with a minor modification (extra staining with 1% tannic acid in veronal acetate for 1 hour after OsO4 postfixation). A FEI Tecnai microscope was used to examine ultrathin sections at 80-120 kV. Autophagic vacuoles were quantified on 5 different images taken at random per section.

Statistics

All data are expressed as mean ± SEM. Statistical analyses were performed using SPSS software (version 25, SPSS Inc.). Statistical tests are specified in the figure and table legends. When parametric statistics (ANOVA, Student's t-test) were used, a test of normality (Shapiro-Wilk test) and a test for equal variances (Levene's test) were performed. In every case, the data passed normality and equal variance tests. If not, non-parametric statistics (Mann-Whitney U test, Kruskal-Wallis test) were used. A Chi-square test was used to determine whether there was an association between categorical variables (i.e., whether the variables are independent or related). A Fisher's exact test was used when sample sizes were small (i.e. when one of the four cells of a 2x2 table had less than five observations) to test whether two categorical variables were associated with each other or not. A Mann-Whitney U test was used to compare differences between two independent groups when the dependent variable was either ordinal or continuous, but not normally distributed. A Kruskal-Wallis test was used as an alternative for a one-way ANOVA if the assumptions of the latter were violated (i.e. data not normally distributed and/or unequal variances). Differences were considered significant at $p<0.05$.

Results

3PO is not toxic, but causes a metabolic switch in mice

To evaluate whether glycolysis inhibitor 3-(3-pyridinyl)-1-(4-pyridinyl)-2-propen-1-one (3PO) affects general metabolism, female ApoE$^{-/-}$ mice were fed a western-type diet and treated with 3PO (50 mg/kg, i.p., 4x/week) or vehicle for 4 weeks. Plasma analysis did not reveal changes in the level of liver enzymes (GTT, ALT, ALP), fasting and non-fasting blood glucose, insulin or total cholesterol (Table 1). Moreover, according to a glucose and insulin tolerance test, glucose absorption and insulin receptor sensitivity were not different in 3PO-treated mice as compared to vehicle-treated controls (Supplemental Figure II). Experiments in metabolic cages showed that water intake was not altered, though food consumption significantly decreased in 3PO-treated mice (P=0.0002, Table 1). Also body weight tended to decrease, though this effect was not statistically significant (P=0.1241). Levels of plasma

triglycerides clearly decreased (*P*=0.0086), whereas those of ketone body β-hydroxybutyrate increased (*P*=0.0443, Table 1). Because starvation is a well-known trigger of autophagy induction, we evaluated whether reduced food intake after 3PO treatment stimulates autophagy in liver and heart, which are one of the most sensitive organs to starvation-induced autophagy.[16] Unlike complete food withdrawal that strongly evoked autophagy, autophagosome staining was negative in liver and heart of 3PO treated GFP-LC3 mice (supplemental Figure III).

Table 1. Metabolic parameters of ApoE$^{-/-}$ mice treated for 4 weeks with 3PO or vehicle (DMSO)

Metabolic parameters	Control	3PO
Liver enzymes		
- γ-glutamyltransferase (U/L)	11 ± 1	9 ± 1
- Alanine transaminase (U/L)	34 ± 6	29 ± 6
- Alkaline phosphatase (U/L)	174 ± 10	130 ± 20
Fasting blood glucose (mg/dL)	85 ± 3	81 ± 4
Non-fasting blood glucose (mg/dL)	186 ± 5	171 ± 10
Insulin (ng/ml)	0.2 ± 0.1	0.2 ± 0.1
Total cholesterol (mg/dL)	599 ± 1	563 ± 20
Food intake (g/day)	2.6 ± 0.1	1.7 ± 0.1***
Water intake (ml/day)	4.1 ± 0.3	3.4 ± 0.5
Body weight (g)	20.3 ± 0.4	19.4 ± 0.3
Triglycerides (mg/dL)	93 ± 7	65 ± 7**
β-hydroxybutyrate (μM)	8 ± 1	12 ± 1*

3PO was administered at 50 mg/kg (i.p.; 4x/week) for 4 weeks. Data shown as mean ± SEM. **P*<0.05, ***P*<0.01, ****P*<0.001 versus control (unpaired Student *t* test, n=10-12).

3PO inhibits neovascularization in plaques of ApoE$^{-/-}$Fbn1$^{C1039G+/-}$ mice

3PO (50 mg/kg, i.p.) or vehicle was administered to ApoE$^{-/-}$ Fbn1$^{C1039G+/-}$ mice starting either after 4 weeks western-type diet (WD; 2x/week, 10 weeks, preventive regimen) or after 16 weeks WD (4x/week, 4 weeks, curative regimen). As shown by anti-VWF staining of plaques in the carotid arteries of ApoE$^{-/-}$Fbn1$^{C1039G+/-}$ mice, 3PO reduced the number of mice with IP neovascularization with almost 40% (curative regimen) and 50% (preventive regimen) (Figure 1A). Moreover, the number of microvessels per plaque significantly decreased (Figure 1A). IP microvessels were not observed in the proximal aorta. An anti-Ter-119 staining showed that microvessels were leaky and released erythrocytes into the plaque (Figure 1B). The number of IP haemorrhages was reduced after treatment with 3PO in the preventive setting (control= 2.25 [0.0-7.0]/; 3PO= 0.00 [0.0-3.0]/mm^2; *P*=0.03). A decrease in the number of IP haemorrhages was also observed in a curative 3PO regimen, though this effect was not significant (control= 9.57 [0.0-25.53]; 3PO= 0.0 [0.0-23.09]/mm^2; *P*=0.46).

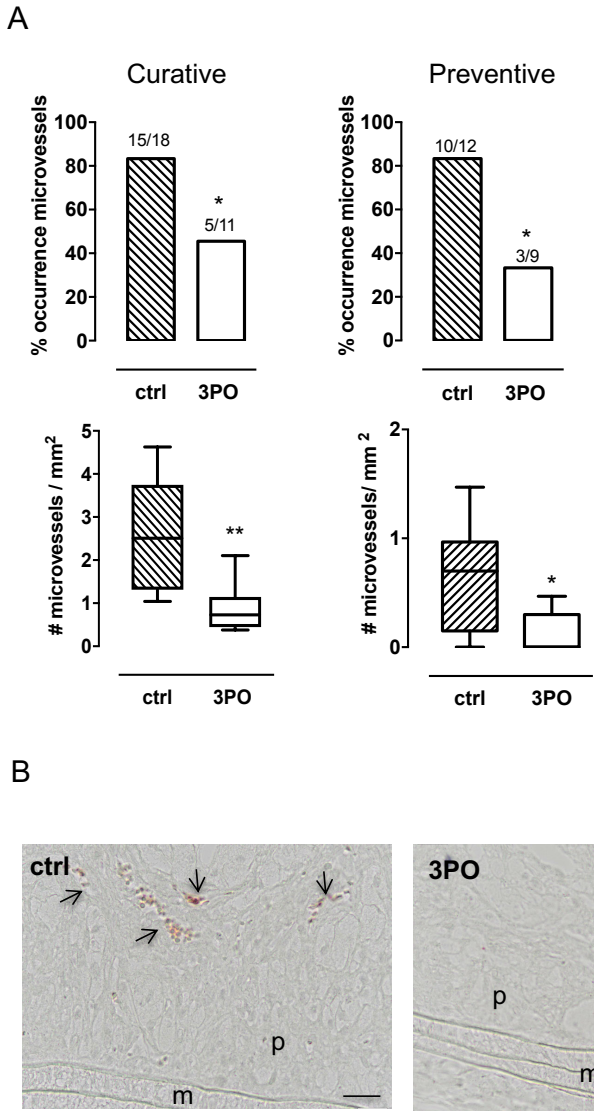

Figure 1. 3PO inhibits intraplaque neovascularization in the carotid artery of ApoE$^{-/-}$ Fbn1$^{C1039G+/-}$ mice. (A) Differences in the occurrence (number of mice) and the number of intraplaque microvessels of control (ctrl) and 3PO-treated mice that underwent a curative or preventive 3PO regimen. **P*<0.05, ***P*<0.01 versus ctrl (Chi-square (upper panels) or Mann-Whitney U test (lower panels); control: n=8-10, 3PO: n=9-13). (B) Anti-Ter-119 staining of atherosclerotic plaques in the carotid artery of control (ctrl) and 3PO-treated mice (curative regimen). Microvessels are marked by arrows. M=media, P=plaque. Scale bar = 50 µm.

3PO inhibits atherosclerotic plaque formation independent of IP neovascularization and without affecting plaque composition

An analysis of total cholesterol did not reveal significant differences between 3PO-treated ApoE$^{-/-}$Fbn1$^{C1039G+/-}$ mice and untreated controls (curative regimen: 507 ± 58 vs 602 ± 58 mg/dl; preventive regimen: 454 ± 24 vs 527 ± 33 mg/dl). 3PO did not change plaque thickness and plaque necrosis (Table 2, Supplemental Figure IV). Moreover, the smooth muscle cell and macrophage content of plaques as well as the percentage of total plaque collagen was not different between control and 3PO-treated animals (Table 2, Supplemental Figure IV). Nonetheless, plaque formation was reduced in both the curative regimen and preventive regimen as illustrated by the plaque formation index (Figure 2A) and *en face* oil-red O stainings (Figure 2B). Importantly, ApoE$^{-/-}$Fbn1$^{C1039G+/-}$ mice that contained plaques without obvious IP neovascularization revealed similar inhibition of plaque formation (Figure 2A), suggesting that 3PO may control atherosclerotic plaque formation independent of IP microvessel growth. In line with this finding, 3PO was able to inhibit plaque formation in the aortic arch of regular ApoE$^{-/-}$ mice that do not develop IP neovascularization (control= 53.9 ± 4.8 %; 3PO=38.6 ± 5.2 %, *P*=0.04).

Table 2. Thickness and composition of atherosclerotic plaques in the carotid artery of ApoE$^{-/-}$Fbn1$^{C1039G+/-}$ mice

	Curative		*Preventive*	
	Control	3PO	Control	3PO
Plaque thickness (µm)	316 ± 13	312 ± 27	314 ± 27	262 ± 12
Necrosis (%)	13 ± 1	14 ± 3	7 ± 1	7 ± 2
Smooth muscle cells (%)	8 ± 1	9± 1	7 ± 2	6 ± 1
Macrophages (%)	7 ± 1	5 ± 1	12 ± 4	8 ± 2
Collagen (%)	26 ± 2	25 ± 2	16 ± 1	15 ± 4

Data shown as mean ± SEM, n=10-16; Curative=4 weeks treatment (weeks 16-20 on western-type diet), preventive=10 weeks treatment (weeks 4-14 on western-type diet). Unpaired Student *t* test: not significant.

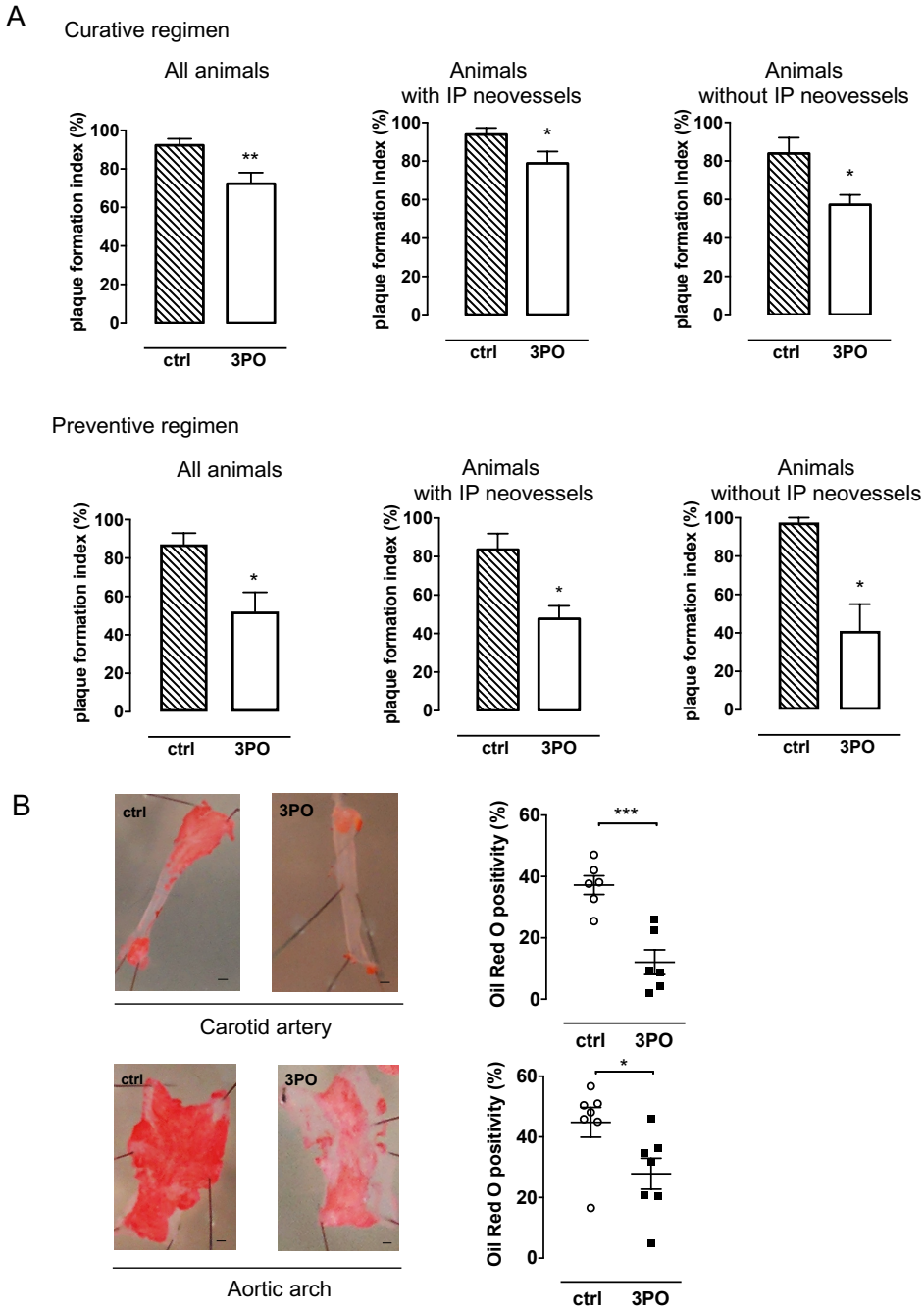

Figure 2. 3PO inhibits atherosclerotic plaque formation in ApoE$^{-/-}$Fbn1$^{C1039G+/-}$ mice. (A) Plaque formation index of the right carotid artery as a measure of plaque occurrence in control (ctrl) and 3PO-treated mice that underwent a curative or preventive 3PO regimen. Plaque

formation index is shown for all animals (left panel) of the control (crtl) group (n=12) and 3PO-treated group (n=9), for mice with intraplaque microvessels (middle panel; 10/12 control mice and 3/9 treated mice) or for mice without intraplaque microvessels (right; 2/12 controls and 6/9 treated mice). *P<0.05, **P<0.01 versus ctrl (Mann-Whitney U test). (B) En face Oil Red O staining of the carotid artery and aortic arch of control (n=6-7) and 3PO-treated vessels (n=6-7). Scale bar = 1.5 mm. *P<0.05, ***P<0.001 versus ctrl (Independent samples t-test).

3PO has a positive impact on cardiac function when administered in a preventive manner

Unlike standard ApoE$^{-/-}$ mice or ApoE$^{-/-}$Fbn1$^{C1039G+/-}$ mice on normal laboratory diet, ApoE$^{-/-}$Fbn1$^{C1039G+/-}$ mice on western-type diet develop (sometimes highly stenotic) coronary artery plaques, which negatively affect the heart.[13] Therefore, cardiac function and structure were assessed in ApoE$^{-/-}$Fbn1$^{C1039G+/-}$ mice after 3PO treatment via echocardiography and histology, respectively. In the curative setting, measurements of the left ventricular internal diameter during diastole (LVIDd) (control= 4.6 ± 0.2 µm; 3PO= 4.5 ± 0.2 µm) and the left ventricular internal diameter during systole (LVIDs) (control= 3.5 ± 0.2 µm; 3PO= 3.2 ± 0.3 µm) did not show significant differences between control and treated animals. The fractional shortening (FS) was also similar between both groups (control= 23.1 ± 3.0; 3PO= 29.3 ± 3.7 µm). However, the ratio heart weight/body weight was significantly different between 3PO-treated animals and controls (control= 9.8 ± 0.8 %; 3PO= 6.9 ± 0.3 %, P=0.0081). The preventive regimen resulted in significantly smaller LVIDs and LVIDd with an increased FS (Supplemental Figure VA-D). Analysis of fibrotic areas on heart sections did not show a decrease in the occurrence of myocardial infraction (Fisher's exact test, curative= ctrl 2/15 vs 3PO 2/12; P=1.00; preventive= ctrl 2/10 vs 3PO 0/9; P=0.47). The number of mice with coronary plaque formation tended to decrease in the curative setting (Fisher's exact test, ctrl 12/14 mice vs 3PO 7/12 mice; P=0.19). It was not significant in the preventive setting, even though a 50% decrease in the occurrence of coronary plaque formation was observed in animals after 10 weeks of treatment (Fisher's exact test, ctrl 6/10 mice vs 3PO 3/9 mice, P=0.36). Further analysis of coronary arteries (in preventive regimen) showed

that perivascular fibrosis decreased after treatment with 3PO (supplemental Figure VE).

3PO increases the number of autophagosomes in EC

3PO is a glycolysis inhibitor that leads to moderate ATP depletion.[9] To investigate whether this metabolic stress condition triggers autophagy, human aortic endothelial cells were stimulated in vitro with 3PO for 16 hours. Levels of the autophagosomal marker protein LC3-II increased in a concentration-dependent manner (Figure 3A), and stimulated formation of autophagic vesicles as shown by transmission electron microscopy (Figure 3B). In contrast to the well-known autophagy inducer everolimus that stimulates autophagy via mTOR inhibition, the phosphorylation status of mTOR or its downstream substrate p70S6K was not affected by 3PO (Figure 3C).

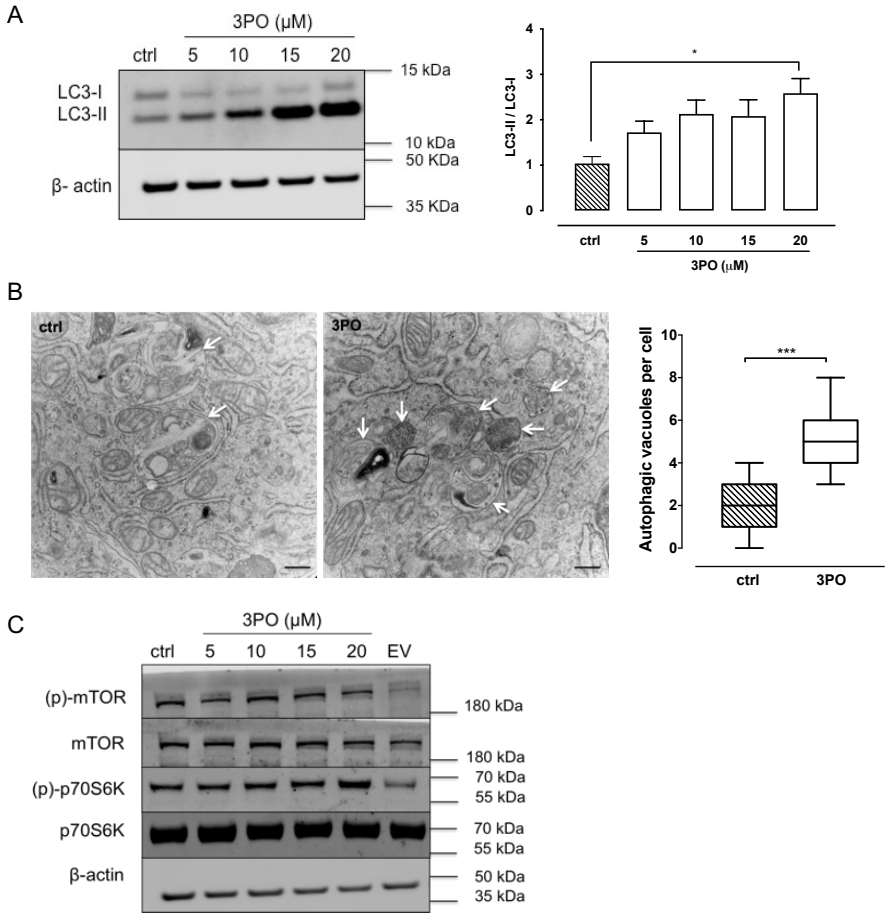

Figure 3. 3PO stimulates autophagosome formation in endothelial cells independent of mTOR. (A) Human aortic endothelial cells (HAOECs) were stimulated with 3PO (5-20 μM) for 16 hours followed by western blot analysis for the autophagosomal marker protein LC3. Protein levels of LC3-I and LC3-II were quantified relative to the reference protein β-actin. **P*<0.05 versus untreated control cells (ctrl) (1-way ANOVA, followed by Dunnett test, n=3). (B) Detection and quantification of autophagic vacuoles (arrows) in 3PO-treated HAOECs (20 μM 3PO, 16 hours) using transmission electron microscopy. Scale bar = 500 nm. ****P*<0.001 (Mann-Whitney U test; n=3). (C) Evaluation of the phosphorylation status of mTOR and its downstream target p70S6K in 3PO-treated HAOECs via western blotting. Everolimus (EV, 10 μM) was used as a positive control.

3PO reduces endothelial VCAM-1 expression in an autophagy-dependent way

One of the early steps in plaque formation is up-regulation of adhesion molecules such as VCAM-1 followed by monocyte infiltration.[20, 21] Because 3PO inhibits plaque formation, we investigated whether VCAM-1 expression could be inhibited by 3PO. To this end, human aortic endothelial cells were stimulated with TNF-α in the presence or absence of 3PO. TNF-α treated cells clearly upregulated VCAM-1 and ICAM-1 protein expression, yet upregulation of both proteins was significantly impaired in the presence of 3PO (Figure 4). Moreover, NF-κB signalling was blunted by 3PO, given the significantly lower levels of phosphorylated NF-κB and a reduced DNA binding activity of NF-κB in 3PO-treated cells (Supplemental Figure VI). Silencing of the essential autophagy gene ATG7 promoted VCAM-1 and ICAM-1 expression and could neither be enhanced by TNF-α nor inhibited by 3PO (Figure 4). $ApoE^{-/-}Fbn1^{C1039G+/-}$ and $ApoE^{-/-}$ mice treated with 3PO (preventive regimen) revealed a decreased expression of VCAM-1 at the luminal EC surface of the plaque (Figure 4).

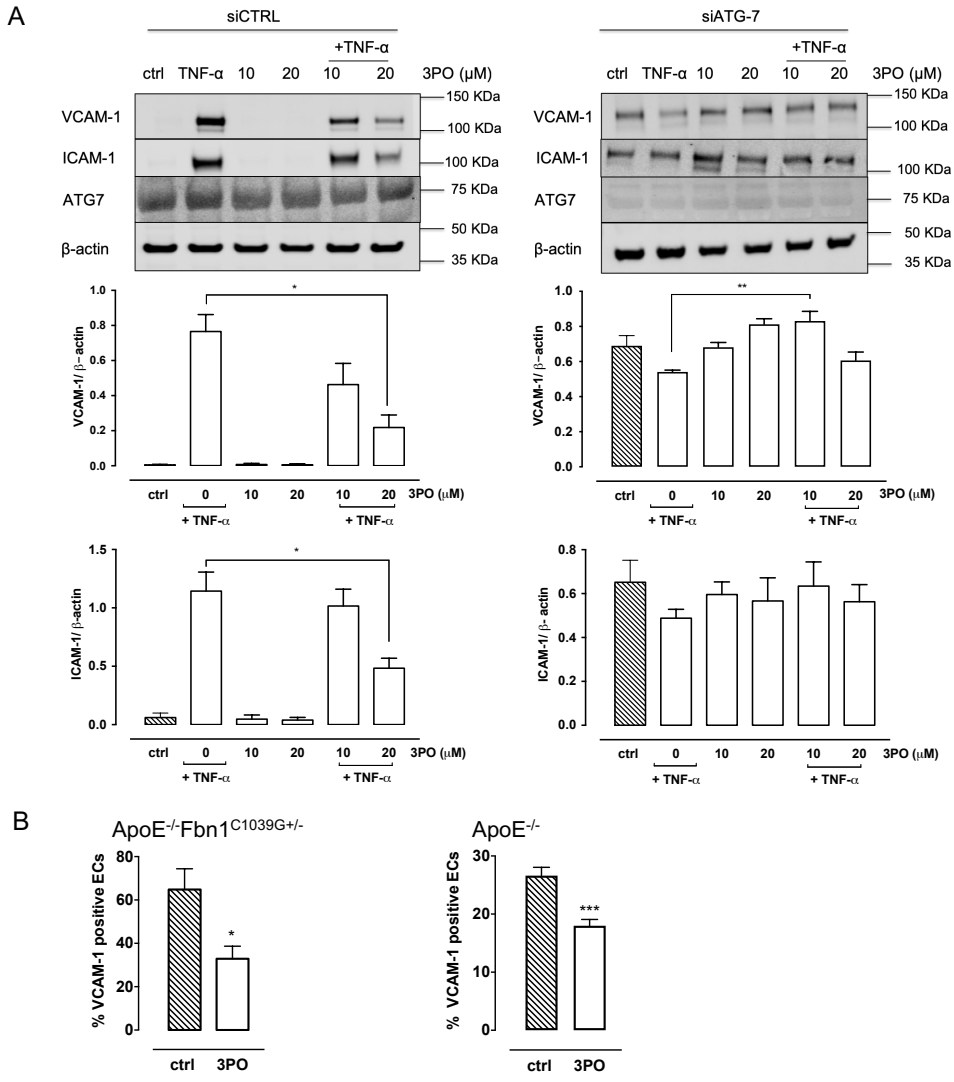

Figure 4. 3PO impairs TNF-α mediated upregulation of VCAM-1 and ICAM-1 in endothelial cells via autophagy. (A) qPCR and western blot analysis of VCAM-1, ICAM-1 and ATG7 expression, either in wild type (siCTRL-treated) human aortic endothelial cells (HAOECs; left panels) or siATG7-treated HAOECs (right panels), and exposed to hTNF-α (20 ng/ml) in the presence or absence of 3PO (10-20 μM) for 24 hours. β-actin was used as a reference gene. **P*<0.05, ***P*<0.01 (1-way ANOVA followed by Dunnett test, n=3). (B) Quantification of VCAM-1 positive endothelial cells in the carotid artery of ApoE$^{-/-}$Fbn1$^{C1039G+/-}$ and the aortic arch of ApoE$^{-/-}$ mice treated with 3PO or solvent (ctrl) for 10 weeks (preventive regimen). **P*<0.05, ****P*<0.001 versus ctrl (unpaired Student *t* test, n=7-12).

3PO promotes an M2 macrophage subtype in vitro

Because 3PO regulates inflammation and may affect macrophage polarization,[22] gene expression of M1 and M2 exclusive genes[23] was analysed *in vitro* by real-time PCR in 3PO-treated mouse macrophages. 3PO did not change gene expression of M1 genes CD38 and Gpr18, but significantly upregulated expression of M2 genes Egr2 and Arg1 in a concentration-dependent manner (Figure 5). Furthermore, stimulation of an M1 phenotype by IFN-γ/LPS was inhibited by 3PO (Figure 5). Because of aspecific and unreliable antibody staining, the abovementioned M1/M2 markers failed to translate to macrophages in plaques of vehicle- or 3PO-treated carotid arteries and confirms recent statements in literature that valid *in vivo* M1/M2 surface markers remain to be discovered.[24]

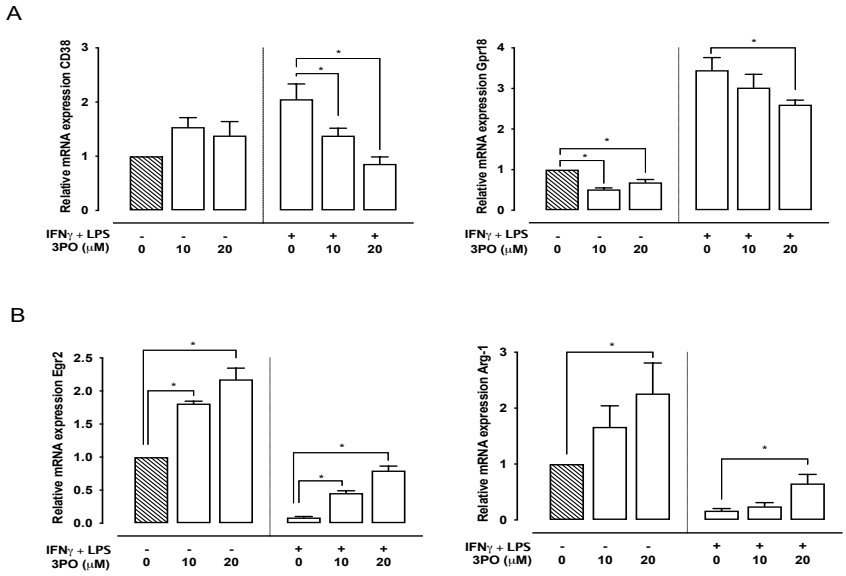

Figure 5. 3PO promotes a macrophage M2 phenotype. Bone marrow derived macrophages from ApoE$^{-/-}$ mice were treated in vitro with 3PO (10-20 μM) and/or a mixture of IFN-γ (20 ng/ml) and LPS (100 ng/ml) for 24 hours. Subsequently, mRNA expression of M1 exclusive genes CD38 and Gpr18 (A) or the M2 specific genes Erg2 and Arg-1 (B) was analyzed by real time PCR. **P*<0.05 (Kruskal-Wallis followed by Mann-Whitney U test, n=4).

Discussion

There is an obvious association between IP neovascularization and plaque vulnerability in advanced human plaques.[25] However, the causality and impact of IP neovascularization on plaque destabilization is poorly studied. In oncology, research is far more ahead on this topic and several anti-angiogenic strategies have been tested in an experimental set-up.[26] To date, blocking VEGF was the primary strategy for reducing neovascularization.[27, 28] Unfortunately, limited efficacy and adverse effects have been downsizing its success, even when multiple blockers were used simultaneously.[5, 29] Therefore, a fundamentally different approach is required to re-boost anti-angiogenic therapies. Given that ECs rely on glycolysis for up to 85% of their energy demand,[7] targeting EC metabolism may represent an attractive new strategy to inhibit neovascularization.[8, 30] Transient and partial inhibition of glycolysis in proliferating ECs by the small molecule 3PO inhibits pathological angiogenesis without interfering with the metabolism of healthy cells.[9] In line with this statement, experimental evidence from the present study indicates that treatment of $ApoE^{-/-}$ mice with 3PO for 4 weeks caused neither substantial adverse effects nor changes in general metabolism. Reduced food intake was observed, yet circulating liver enzymes, blood glucose, insulin and total cholesterol were not affected. Also a glucose and insulin tolerance test was perfectly normal. However, 3PO caused a decrease in the level of circulating triglycerides and a significant rise in β-hydroxybutyrate levels, indicating a metabolic switch from glucose to fatty acid-derived ketones in order to provide sufficient energy. Lack of major side effects was also reported recently by Beldman et al.[31] after treatment of atherosclerotic $ApoE^{-/-}$ mice for 6 weeks with 3PO (25 mg/kg, i.p., 3x/week).

Once safe administration of 3PO was evident, we next investigated the effect of 3PO on the formation of IP microvessels in a mouse model of advanced atherosclerosis (i.e. $ApoE^{-/-}$ mice with a heterozygous mutation in the fibrillin-1 gene [$Fbn1^{C1039G+/-}$], yielding large plaques with a highly unstable phenotype and extensive IP neovascularization).[13] Analysis of IP neovascularization in the carotid artery revealed a significant decrease in the occurrence and the amount of microvessels in $ApoE^{-/-}Fbn1^{C1039G+/-}$ mice treated with 3PO. These results are in line with the effect of 3PO in cancer tissue, where 3PO inhibits vascular sprouting in pathological

angiogenesis.[7] Because inhibition of angiogenesis in malignant tissue can affect tumor growth,[32] it was interesting to investigate the impact of 3PO on plaque size and vulnerability. After 4 weeks of treatment, we could not observe a difference in plaque composition between control and treated animals. These results fed the presumption that even though 4 weeks of treatment is enough to inhibit IP neovascularization, it may have been too short to have any impact on plaque size or composition. Therefore, we decided to repeat the experiment in a preventive manner with 3PO being administered over a longer period of time. Given that i.p. injections are very stressful for ApoE$^{-/-}$Fbn1$^{C1039G+/-}$ mice, they were injected with 3PO for a maximum of 10 weeks.[33] The preventive treatment regimen confirmed the results that we obtained after the curative treatment regimen with an even larger decrease in IP neovascularization. Nonetheless, we could not observe a difference in parameters defining plaque vulnerability such as changes in macrophages, smooth muscle cells and total collagen. Because IP microvessels are considered a potential entry site for erythrocytes, lipids and inflammatory mediators in the plaque,[34, 35] it was highly unexpected that, after 10 weeks of treatment, plaque composition was similar between control and treated animals.

Importantly, although the plaque size and composition remained unchanged, the occurrence of plaques as measured by the plaque formation index was significantly reduced in 3PO-treated animals. After 10 weeks of treatment, a 35% reduction in plaque formation was observed in the carotid artery. Given that neovascularization occurs after a certain degree of hypoxia, plaque progression is already in an advanced state. A decrease in the plaque formation index demonstrates that EC metabolism plays an important role in the early stages of plaque development, apart from angiogenesis. Indeed, a 3PO-mediated reduction in plaque development was also observed in regular ApoE$^{-/-}$ mice, which develop plaques without IP neovascularization. When ECs undergo inflammatory activation, the upregulation of adhesion molecules such as VCAM-1 represents an important trigger in early lesion development, as they attract and encourage monocytes to enter the lesion.[36] In the present study, we provide in vitro and in vivo evidence that 3PO interferes with the upregulation of VCAM-1 and ICAM-1. In vitro experiments with ECs, pre-activated with TNF-α and treated with 3PO, revealed impaired NF-κB signalling and reduced VCAM-1 (and ICAM-1) expression levels. Moreover, a preventive 3PO regimen was

able to reduce VCAM-1 expression in the endothelium in vivo. A study performed in cancer research consolidates these results as 3PO reduced the expression of adhesion molecules concomitant with tumour vessel normalization due to an altered EC pro-inflammatory signature.[37] Nonetheless, the question remains why changes in VCAM-1 expression in 3PO-treated mice do not alter plaque composition. Our data seem to suggest that 3PO only impairs initiation of plaque development, but not plaque progression. Indeed, one may speculate that once early plaques have formed, downregulation of VCAM-1 expression in ECs by 3PO does not significantly affect further leukocyte recruitment and plaque progression. Histological data from human plaques indicate that in early lesions VCAM-1 and ICAM-1 are predominantly expressed by the endothelium, whereas in more advanced lesions, the majority of VCAM-1 expression is found in subsets of intimal VSMCs and macrophages.[38] These findings may explain why downregulation of adhesion molecules by 3PO in ECs mainly affects the initial stage of atherosclerosis development, but not further steps of plaque progression.

Interestingly, the metabolic stress caused by 3PO stimulated autophagosome formation in ECs and led to induction of autophagy. Similar observations were previously reported in cancer cells.[39] Our results indicate that downregulation of endothelial VCAM-1 (and ICAM-1) expression by 3PO depends on autophagy induction. Expression of the adhesion molecules was not downregulated by 3PO in TNF-α-treated ECs in which expression of the essential autophagy gene ATG7 was silenced. On the contrary, VCAM-1 (and ICAM-1) expression was upregulated in ATG7-deficient ECs, suggesting that autophagy suppresses expression of these adhesion molecules. Previously, we reported similar data with the biguanide metformin. The latter compound attenuates expression of the endothelial cell adhesion molecules ICAM-1 and VCAM-1 as well as formation of atherosclerotic plaques via autophagy induction.[40] Downregulation of ATG7 gene expression prevented TNF-α induced upregulation of VCAM-1 expression and monocyte adhesion to ECs. Both metformin and 3PO govern the expression of cell adhesion molecules in ECs by inhibiting NF-κB activation. Our findings support previous data showing that endothelial autophagy is atheroprotective and limits atherosclerotic plaque formation by preventing endothelial apoptosis, senescence and inflammation.[41-43]

Apart from the atheroprotective effects on ECs, several lines of evidence indicate that 3PO also negatively influences inflammation.[22, 31, 44-46] In the present study, we could demonstrate that 3PO favors an anti-inflammatory M2 macrophage subtype and suppresses an M1 pro-inflammatory phenotype *in vitro*. This finding is consistent with previous reports showing a strong linear correlation between glycolytic flux and proinflammatory activation of macrophages (as measured by TNF-α production)[22] and 3PO-mediated suppression of T cell activation.[44] Moreover, inhibition of glycolysis by 3PO has profound effects on cell viability of M1 macrophages.[22]

Given the importance of neovascularization in the ischemic myocardium after an acute myocardial infarction, we analysed cardiac function and morphology.[47] The inhibition of angiogenesis by targeting cell metabolism is still in a preclinical stage, thus literature regarding this topic is still lacking. After a curative treatment regimen, no significant differences were observed in cardiac function. However, after 10 weeks of treatment (preventive regimen), we observed an improved cardiac morphology and function (smaller LVIDs and LVIDd with increased fractional shortening). Moreover, even though only a small non-significant reduction was observed in the occurrence of myocardial infarctions, the occurrence of coronary plaques was decreased by 50% in treated animals. These findings are consistent with the overall effect of 3PO on plaque formation, in this case coronary plaques. As such, it is conceivable that the overall improved cardiac function is a result of less coronary plaque formation. To further explain the improved cardiac function after 3PO treatment (preventive regimen), we also documented the level of perivascular fibrosis of coronary arteries. This parameter was significantly reduced by 3PO. Because coronary perivascular fibrosis can be caused by an impaired coronary blood flow,[48] a lower degree of stenosis in the coronary arteries of 3PO treated mice probably contributes to this finding. Similar observations were recently made in the same mouse model using lipid lowering therapy.[49] Apart from improved cardiac function through less coronary plaque formation and coronary perivascular fibrosis, it is important to note that autophagy induction has beneficial effects on the heart.[50]Because 3PO promotes autophagy, it is plausible to assume that autophagy induction by 3PO also contributes to improved cardiac function. However, given the lack of autophagosome formation in 3PO-treated GFP-LC3 mice, we consider this hypothesis unlikely, though cannot completely rule out this possibility.

In conclusion, we were able to inhibit IP neovascularization with 3PO. However, the reduction in IP microvessels did not exert a significant effect on plaque composition. Surprisingly, 3PO reduced the formation of plaques, not in size but in frequency. Less plaques were formed in the carotid artery indicating that 3PO already has an effect in the early onset of atherosclerosis by downregulating endothelial cell adhesion molecules. In addition, fewer coronary plaques were formed, which resulted in overall improved cardiac function. Interestingly, inhibition of key steps in glycolysis with small molecules has recently provided a novel area of cancer research and has been proven effective in slowing the proliferation of cancer cells, with PFK158 as a first-in-human and first-in class PFKFB3 inhibitor in a phase I clinical trial (NCT02044861). Compared to cancer, the endothelial cell metabolism in atherosclerosis is largely unexplored, though is an emerging target that may offer attractive therapeutic avenues to counteract plaque progression.[8, 51, 52]

Acknowledgements

The authors would like to thank Dr. Bart Peeters, Sofie De Moudt, Anne-Elise Van Hoydonck, Hermine Fret and Rita Van den Bossche for technical help. The authors are grateful to Dr. Bronwen Martin for critical reading of the manuscript.

Sources of Funding

This work was supported by the University of Antwerp [DOCPRO-BOF], the Hercules Foundation [grant number AUHA/13/03] and the Horizon 2020 program of the European Union – Marie Sklodowska Curie actions – ITN – MOGLYNET [grant number 675527].

Supplemental Material

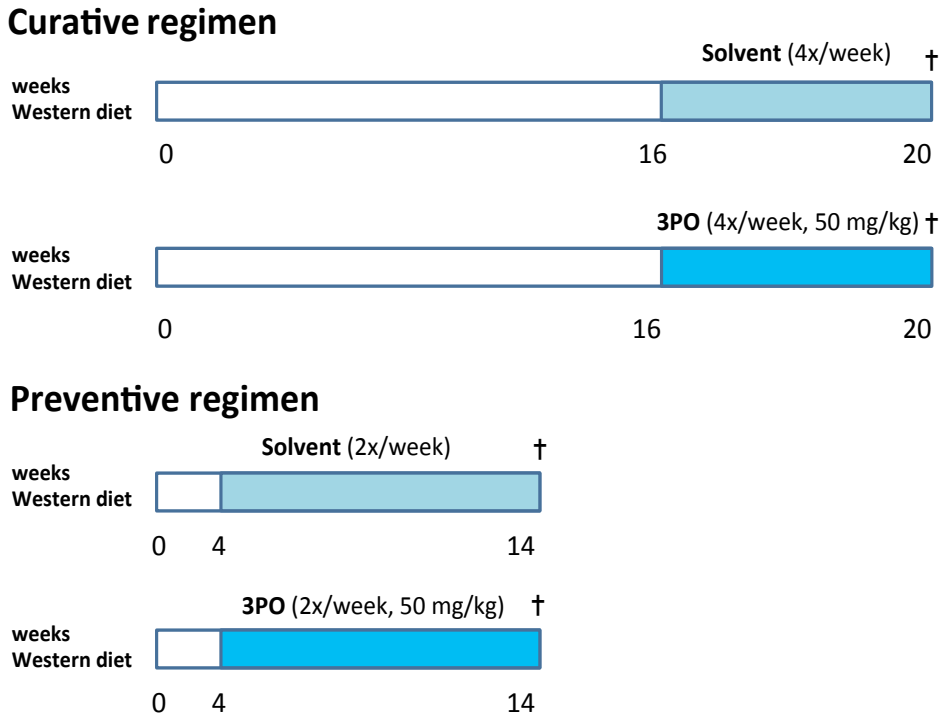

Figure I. Schematic overview of 3PO treatment regimens applied in ApoE$^{-/-}$Fbn1$^{C1039G+/-}$ mice. Mice were fed a western diet and received i.p. injections of 3PO (50 mg/kg) after 4 weeks of diet (preventive regimen, 2x/week) or after 16 weeks of diet (curative treatment regimen, 4x/week). The preventive regimen was also applied to ApoE$^{-/-}$ mice.

A

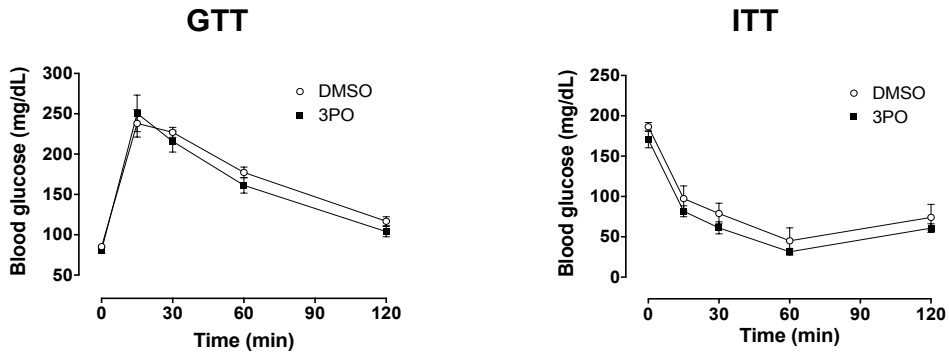

Figure II. Glucose clearance in 3PO- or vehicle-treated ApoE$^{-/-}$ mice after intraperitoneal injection with glucose or insulin. A glucose tolerance test (GTT) and insulin tolerance test (ITT) were performed in female ApoE$^{-/-}$ mice after 4 weeks of treatment with 3PO (50 mg/kg, i.p.; 4x/week) or vehicle. Blood glucose was measured at different time points after injection of glucose (1 g/kg, i.p.) or insulin (1 U/kg, i.p.). Two-way ANOVA: GTT, Time: P<0.001, 3PO: P=0.181, Interaction: P=0.708; ITT, Time: P<0.001, 3PO: P=0.083, Interaction: P=0.992

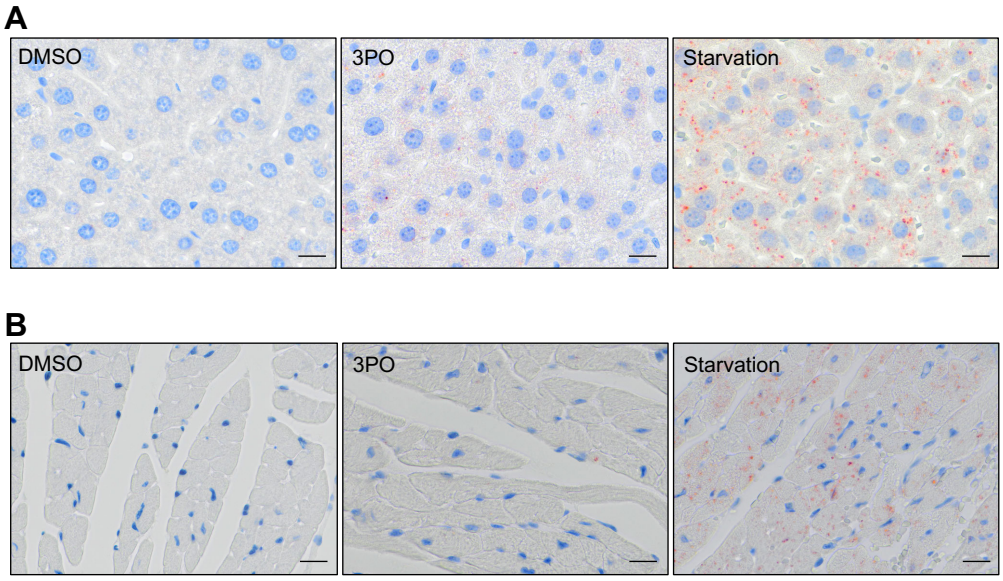

Figure III. Immunohistochemical analysis of autophagy induction in liver and heart of GFP-LC3 transgenic mice after treatment with 3PO or after starvation. GFP-LC3 mice were treated with 3PO (50 mg/kg, i.p., 4x/week) or vehicle (DMSO) for 2 weeks, or underwent nutrient deprivation (starvation) for 24 hours. Autophagic flux inhibitor chloroquine was administered (50 mg/kg, i.p.) 3 hours before the sacrification of mice. Liver (A) and heart samples (B) were isolated for immunohistochemical detection of autophagosomes using LC3 antibodies. Scale bar = 20 μm.

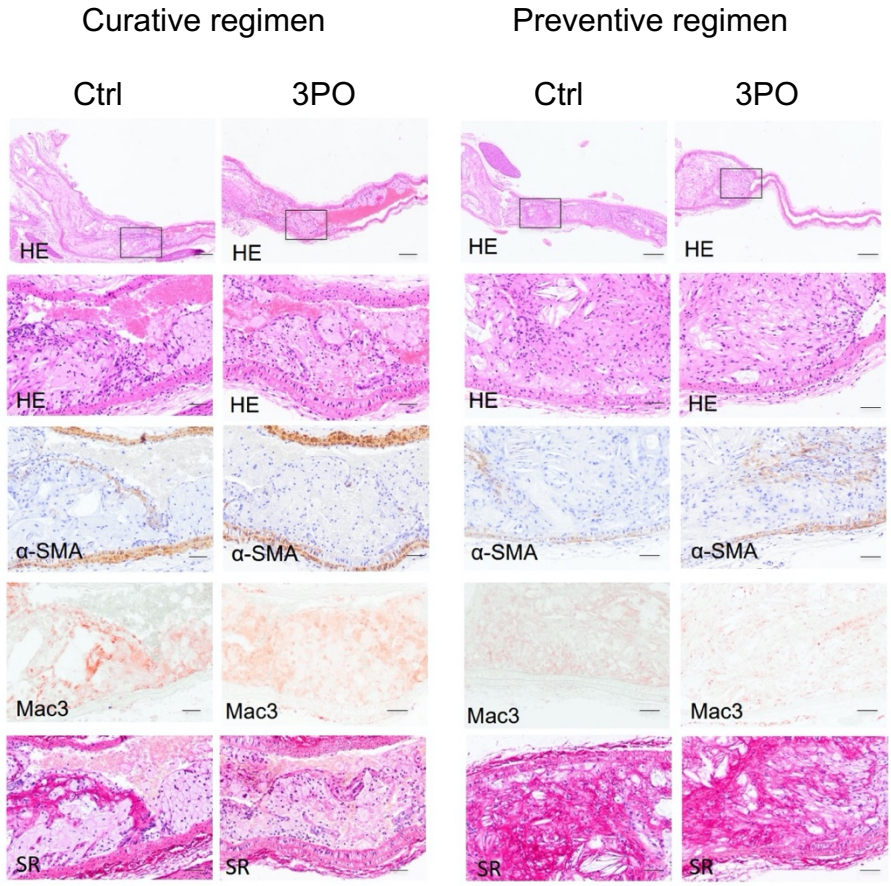

Figure IV. Histological analysis of atherosclerotic plaques in the right carotid artery of ApoE$^{-/-}$Fbn1$^{C1039G+/-}$ mice after a curative or preventive treatment regimen with 3PO. The plaque formation index and plaque thickness were measured on (HE)-stained longitudinal sections. Macrophages and smooth muscle cells were detected via immunohistochemistry using Mac-3 and α-SMC actin (α-SMA) antibodies, respectively. Collagen deposition was analysed after staining with Sirius red (SR). Representative images for each staining are shown. For quantification of the different stainings, see Table 2. Scale bar = 500 µm (first row) or 50 µm (other rows).

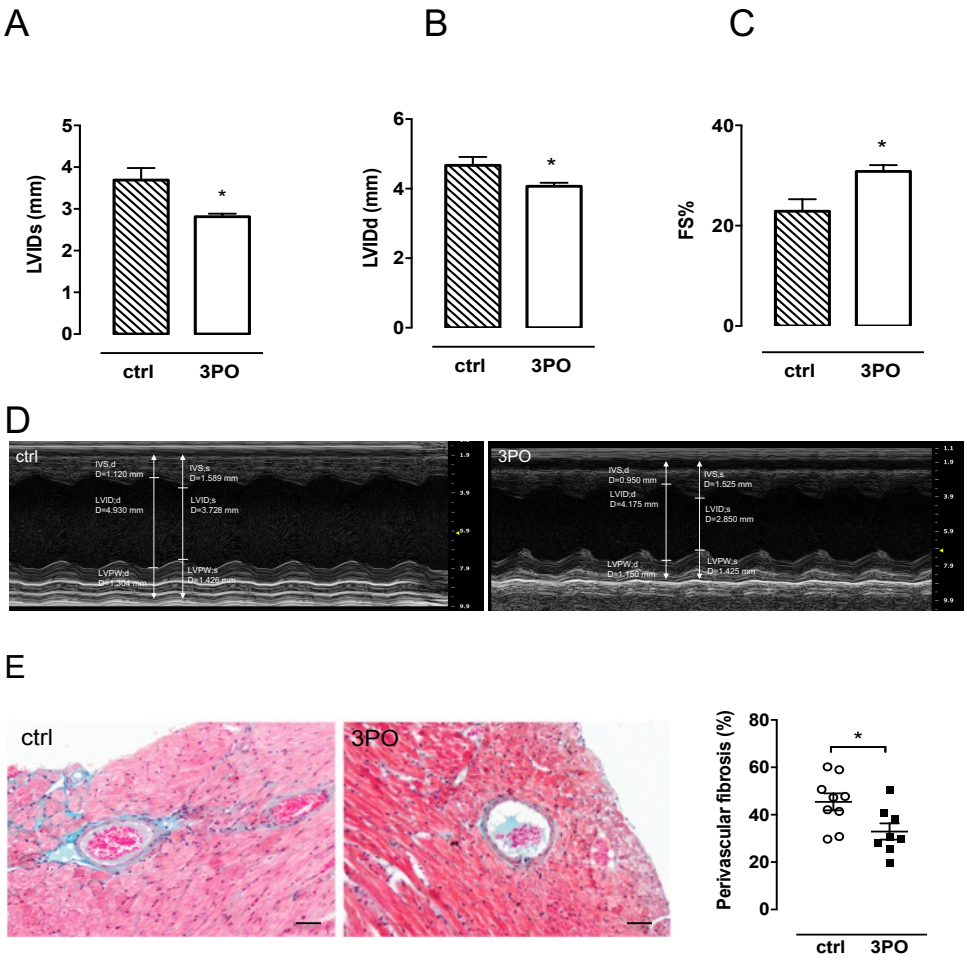

Figure V. 3PO improves the cardiac morphology and function in atherosclerotic ApoE$^{-/-}$Fbn1$^{C1039G+/-}$ mice. Measurements of left ventricular internal diameter (LVID) during systole (A) and diastole (B) in control mice versus treated mice (preventive regimen). Panel (C) represents the fractional shortening (FS) as a measure of cardiac function. **P*<0.05 (Independent samples t-test; n=12-15). (D) Representative echocardiographic images of short axis view in M-mode tracing the LV at the level of papillary muscle in control mice (left panel) and 3PO-treated mice (right panel). LVID = Left ventricle internal diameter. LVPW = Left ventricle posterior wall. IVS = interventricular septal thickness. -d = in diastole, -s = in systole. (E) Histological analysis of perivascular fibrosis around coronary arteries via Masson's trichrome staining in ApoE$^{-/-}$Fbn1$^{C1039G+/-}$ mice. Scale bar = 50 µm. **P*<0.05 (unpaired Student's t-test; control: n=9, 3PO: n=8).

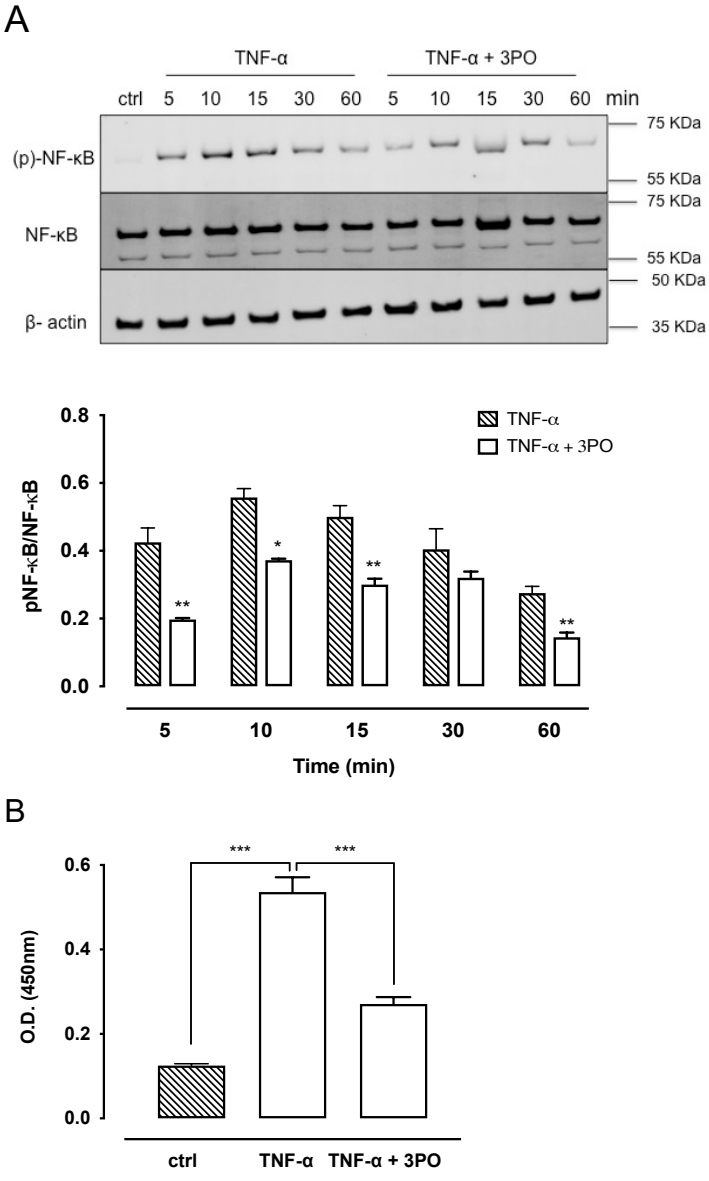

Figure VI. 3PO inhibits TNF-α-mediated NF-κB activation in endothelial cells. Human aortic endothelial cells were treated with hTNF-α (20 ng/ml) for 5, 10, 15, 30, 60 minutes in the presence or absence of 3PO (20 μM). (A) Western blot analysis of NF-κB phosphorylation (pNF-κB) and total NF-κB. Bars represent the ratio of pNF-κB over total NF-κB normalized to the loading control β-actin. **P*<0.05, ***P*<0.01 (unpaired Student's t-test; n=3). (B) DNA binding activity of NF-κB as measured by ELISA. ****P*<0.001(one-way ANOVA, followed by Bonferroni multiple comparisons test, n=3).

References

1. Carmeliet P. Angiogenesis in health and disease. *Nat Med*. 2003;9:653-660
2. Sedding DG, Boyle EC, Demandt JAF, Sluimer JC, Dutzmann J, Haverich A, Bauersachs J. Vasa vasorum angiogenesis: Key player in the initiation and progression of atherosclerosis and potential target for the treatment of cardiovascular disease. *Front Immunol*. 2018;9:706
3. Sluimer JC, Kolodgie FD, Bijnens AP, Maxfield K, Pacheco E, Kutys B, Duimel H, Frederik PM, van Hinsbergh VW, Virmani R, Daemen MJ. Thin-walled microvessels in human coronary atherosclerotic plaques show incomplete endothelial junctions relevance of compromised structural integrity for intraplaque microvascular leakage. *J Am Coll Cardiol*. 2009;53:1517-1527
4. Virmani R, Kolodgie FD, Burke AP, Finn AV, Gold HK, Tulenko TN, Wrenn SP, Narula J. Atherosclerotic plaque progression and vulnerability to rupture: Angiogenesis as a source of intraplaque hemorrhage. *Arterioscler Thromb Vasc Biol*. 2005;25:2054-2061
5. Vasudev NS, Reynolds AR. Anti-angiogenic therapy for cancer: Current progress, unresolved questions and future directions. *Angiogenesis*. 2014;17:471-494
6. Camare C, Pucelle M, Negre-Salvayre A, Salvayre R. Angiogenesis in the atherosclerotic plaque. *Redox Biol*. 2017;12:18-34
7. De Bock K, Georgiadou M, Schoors S, Kuchnio A, Wong BW, Cantelmo AR, Quaegebeur A, Ghesquiere B, Cauwenberghs S, Eelen G, Phng LK, Betz I, Tembuyser B, Brepoels K, Welti J, Geudens I, Segura I, Cruys B, Bifari F, Decimo I, Blanco R, Wyns S, Vangindertael J, Rocha S, Collins RT, Munck S, Daelemans D, Imamura H, Devlieger R, Rider M, Van Veldhoven PP, Schuit F, Bartrons R, Hofkens J, Fraisl P, Telang S, Deberardinis RJ, Schoonjans L, Vinckier S, Chesney J, Gerhardt H, Dewerchin M, Carmeliet P. Role of pfkfb3-driven glycolysis in vessel sprouting. *Cell*. 2013;154:651-663

8. Pircher A, Treps L, Bodrug N, Carmeliet P. Endothelial cell metabolism: A novel player in atherosclerosis? Basic principles and therapeutic opportunities. *Atherosclerosis*. 2016;253:247-257
9. Schoors S, De Bock K, Cantelmo AR, Georgiadou M, Ghesquiere B, Cauwenberghs S, Kuchnio A, Wong BW, Quaegebeur A, Goveia J, Bifari F, Wang X, Blanco R, Tembuyser B, Cornelissen I, Bouche A, Vinckier S, Diaz-Moralli S, Gerhardt H, Telang S, Cascante M, Chesney J, Dewerchin M, Carmeliet P. Partial and transient reduction of glycolysis by pfkfb3 blockade reduces pathological angiogenesis. *Cell Metab*. 2014;19:37-48
10. Clem B, Telang S, Clem A, Yalcin A, Meier J, Simmons A, Rasku MA, Arumugam S, Dean WL, Eaton J, Lane A, Trent JO, Chesney J. Small-molecule inhibition of 6-phosphofructo-2-kinase activity suppresses glycolytic flux and tumor growth. *Mol Cancer Ther*. 2008;7:110-120
11. Boyd S, Brookfield JL, Critchlow SE, Cumming IA, Curtis NJ, Debreczeni J, Degorce SL, Donald C, Evans NJ, Groombridge S, Hopcroft P, Jones NP, Kettle JG, Lamont S, Lewis HJ, MacFaull P, McLoughlin SB, Rigoreau LJ, Smith JM, St-Gallay S, Stock JK, Turnbull AP, Wheatley ER, Winter J, Wingfield J. Structure-based design of potent and selective inhibitors of the metabolic kinase pfkfb3. *J Med Chem*. 2015;58:3611-3625
12. Emini Veseli B, Perrotta P, De Meyer GRA, Roth L, Van der Donckt C, Martinet W, De Meyer GRY. Animal models of atherosclerosis. *Eur J Pharmacol*. 2017;816:3-13
13. Van der Donckt C, Van Herck JL, Schrijvers DM, Vanhoutte G, Verhoye M, Blockx I, Van Der Linden A, Bauters D, Lijnen HR, Sluimer JC, Roth L, Van Hove CE, Fransen P, Knaapen MW, Hervent AS, De Keulenaer GW, Bult H, Martinet W, Herman AG, De Meyer GRY. Elastin fragmentation in atherosclerotic mice leads to intraplaque neovascularization, plaque rupture, myocardial infarction, stroke, and sudden death. *Eur Heart J*. 2015;36:1049-1058
14. Van Herck JL, De Meyer GRY, Martinet W, Van Hove CE, Foubert K, Theunis MH, Apers S, Bult H, Vrints CJ, Herman AG. Impaired fibrillin-1 function promotes features of plaque instability in apolipoprotein e-deficient mice. *Circulation*. 2009;120:2478-2487

15. Chistiakov DA, Melnichenko AA, Myasoedova VA, Grechko AV, Orekhov AN. Role of lipids and intraplaque hypoxia in the formation of neovascularization in atherosclerosis. *Ann Med*. 2017;49:661-677
16. Mizushima N, Yamamoto A, Matsui M, Yoshimori T, Ohsumi Y. In vivo analysis of autophagy in response to nutrient starvation using transgenic mice expressing a fluorescent autophagosome marker. *Mol Biol Cell*. 2004;15:1101-1111
17. Daugherty A, Tall AR, Daemen M, Falk E, Fisher EA, Garcia-Cardena G, Lusis AJ, Owens AP, 3rd, Rosenfeld ME, Virmani R, American Heart Association Council on Arteriosclerosis T, Vascular B, Council on Basic Cardiovascular S. Recommendation on design, execution, and reporting of animal atherosclerosis studies: A scientific statement from the american heart association. *Arterioscler Thromb Vasc Biol*. 2017;37:e131-e157
18. Robinet P, Milewicz DM, Cassis LA, Leeper NJ, Lu HS, Smith JD. Consideration of sex differences in design and reporting of experimental arterial pathology studies-statement from atvb council. *Arterioscler Thromb Vasc Biol*. 2018;38:292-303
19. Martinet W, Timmermans JP, De Meyer GRY. Methods to assess autophagy in situ--transmission electron microscopy versus immunohistochemistry. *Methods Enzymol*. 2014;543:89-114
20. Blankenberg S, Barbaux S, Tiret L. Adhesion molecules and atherosclerosis. *Atherosclerosis*. 2003;170:191-203
21. Gimbrone MA, Jr., Garcia-Cardena G. Endothelial cell dysfunction and the pathobiology of atherosclerosis. *Circ Res*. 2016;118:620-636
22. Tawakol A, Singh P, Mojena M, Pimentel-Santillana M, Emami H, MacNabb M, Rudd JH, Narula J, Enriquez JA, Traves PG, Fernandez-Velasco M, Bartrons R, Martin-Sanz P, Fayad ZA, Tejedor A, Bosca L. Hif-1alpha and pfkfb3 mediate a tight relationship between proinflammatory activation and anerobic metabolism in atherosclerotic macrophages. *Arterioscler Thromb Vasc Biol*. 2015;35:1463-1471
23. Jablonski KA, Amici SA, Webb LM, Ruiz-Rosado Jde D, Popovich PG, Partida-Sanchez S, Guerau-de-Arellano M. Novel markers to delineate murine m1 and m2 macrophages. *PLoS One*. 2015;10:e0145342

24. Orecchioni M, Ghosheh Y, Pramod AB, Ley K. Macrophage polarization: Different gene signatures in m1(lps+) vs. Classically and m2(lps-) vs. Alternatively activated macrophages. *Front Immunol*. 2019;10:1084
25. de Vries MR, Quax PH. Plaque angiogenesis and its relation to inflammation and atherosclerotic plaque destabilization. *Curr Opin Lipidol*. 2016;27:499-506
26. Rajabi M, Mousa SA. The role of angiogenesis in cancer treatment. *Biomedicines*. 2017;5
27. Van der Veken B, De Meyer GRY, Martinet W. Intraplaque neovascularization as a novel therapeutic target in advanced atherosclerosis. *Expert Opin Ther Targets*. 2016;20:1247-1257
28. Carmeliet P. Vegf as a key mediator of angiogenesis in cancer. *Oncology*. 2005;69 Suppl 3:4-10
29. Moreo A, Vallerio P, Ricotta R, Stucchi M, Pozzi M, Musca F, Meani P, Maloberti A, Facchetti R, Di Bella S, Giganti MO, Sartore-Bianchi A, Siena S, Mancia G, Giannattasio C. Effects of cancer therapy targeting vascular endothelial growth factor receptor on central blood pressure and cardiovascular system. *Am J Hypertens*. 2016;29:158-162
30. Ali L, Schnitzler JG, Kroon J. Metabolism: The road to inflammation and atherosclerosis. *Curr Opin Lipidol*. 2018;29:474-480
31. Beldman TJ, Malinova TS, Desclos E, Grootemaat AE, Misiak ALS, van der Velden S, van Roomen C, Beckers L, van Veen HA, Krawczyk PM, Hoebe RA, Sluimer JC, Neele AE, de Winther MPJ, van der Wel NN, Lutgens E, Mulder WJM, Huveneers S, Kluza E. Nanoparticle-aided characterization of arterial endothelial architecture during atherosclerosis progression and metabolic therapy. *ACS Nano*. 2019;13:13759-13774
32. Bielenberg DR, Zetter BR. The contribution of angiogenesis to the process of metastasis. *Cancer J*. 2015;21:267-273
33. Roth L, Rombouts M, Schrijvers DM, Lemmens K, De Keulenaer GW, Martinet W, De Meyer GRY. Chronic intermittent mental stress promotes atherosclerotic plaque vulnerability, myocardial infarction and sudden death in mice. *Atherosclerosis*. 2015;242:288-294

34. Michel JB, Virmani R, Arbustini E, Pasterkamp G. Intraplaque haemorrhages as the trigger of plaque vulnerability. *Eur Heart J*. 2011;32:1977-1985, 1985a, 1985b, 1985c
35. Kolodgie FD, Gold HK, Burke AP, Fowler DR, Kruth HS, Weber DK, Farb A, Guerrero LJ, Hayase M, Kutys R, Narula J, Finn AV, Virmani R. Intraplaque hemorrhage and progression of coronary atheroma. *N Engl J Med*. 2003;349:2316-2325
36. Davies MJ, Gordon JL, Gearing AJ, Pigott R, Woolf N, Katz D, Kyriakopoulos A. The expression of the adhesion molecules icam-1, vcam-1, pecam, and e-selectin in human atherosclerosis. *J Pathol*. 1993;171:223-229
37. Cantelmo AR, Conradi LC, Brajic A, Goveia J, Kalucka J, Pircher A, Chaturvedi P, Hol J, Thienpont B, Teuwen LA, Schoors S, Boeckx B, Vriens J, Kuchnio A, Veys K, Cruys B, Finotto L, Treps L, Stav-Noraas TE, Bifari F, Stapor P, Decimo I, Kampen K, De Bock K, Haraldsen G, Schoonjans L, Rabelink T, Eelen G, Ghesquiere B, Rehman J, Lambrechts D, Malik AB, Dewerchin M, Carmeliet P. Inhibition of the glycolytic activator pfkfb3 in endothelium induces tumor vessel normalization, impairs metastasis, and improves chemotherapy. *Cancer Cell*. 2016;30:968-985
38. O'Brien KD, Allen MD, McDonald TO, Chait A, Harlan JM, Fishbein D, McCarty J, Ferguson M, Hudkins K, Benjamin CD, et al. Vascular cell adhesion molecule-1 is expressed in human coronary atherosclerotic plaques. Implications for the mode of progression of advanced coronary atherosclerosis. *J Clin Invest*. 1993;92:945-951
39. Klarer AC, O'Neal J, Imbert-Fernandez Y, Clem A, Ellis SR, Clark J, Clem B, Chesney J, Telang S. Inhibition of 6-phosphofructo-2-kinase (pfkfb3) induces autophagy as a survival mechanism. *Cancer Metab*. 2014;2:2
40. Michiels CF, Apers S, De Meyer GRY, Martinet W. Metformin attenuates expression of endothelial cell adhesion molecules and formation of atherosclerotic plaques via autophagy induction. *Annals of Clinical & Experimental Metabolism*. 2016:1(1): 1001
41. Vion AC, Kheloufi M, Hammoutene A, Poisson J, Lasselin J, Devue C, Pic I, Dupont N, Busse J, Stark K, Lafaurie-Janvore J, Barakat AI, Loyer X,

Souyri M, Viollet B, Julia P, Tedgui A, Codogno P, Boulanger CM, Rautou PE. Autophagy is required for endothelial cell alignment and atheroprotection under physiological blood flow. *Proc Natl Acad Sci U S A*. 2017;114:E8675-E8684

42. Salminen A, Kaarniranta K. Glycolysis links p53 function with nf-kappab signaling: Impact on cancer and aging process. *J Cell Physiol*. 2010;224:1-6
43. Zhang R, Li R, Liu Y, Li L, Tang Y. The glycolytic enzyme pfkfb3 controls tnf-alpha-induced endothelial proinflammatory responses. *Inflammation*. 2019;42:146-155
44. Telang S, Clem BF, Klarer AC, Clem AL, Trent JO, Bucala R, Chesney J. Small molecule inhibition of 6-phosphofructo-2-kinase suppresses t cell activation. *J Transl Med*. 2012;10:95
45. Bosca L, Gonzalez-Ramos S, Prieto P, Fernandez-Velasco M, Mojena M, Martin-Sanz P, Alemany S. Metabolic signatures linked to macrophage polarization: From glucose metabolism to oxidative phosphorylation. *Biochem Soc Trans*. 2015;43:740-744
46. McGarry T, Biniecka M, Gao W, Cluxton D, Canavan M, Wade S, Wade S, Gallagher L, Orr C, Veale DJ, Fearon U. Resolution of tlr2-induced inflammation through manipulation of metabolic pathways in rheumatoid arthritis. *Sci Rep*. 2017;7:43165
47. Khurana R, Simons M, Martin JF, Zachary IC. Role of angiogenesis in cardiovascular disease: A critical appraisal. *Circulation*. 2005;112:1813-1824
48. Dai Z, Aoki T, Fukumoto Y, Shimokawa H. Coronary perivascular fibrosis is associated with impairment of coronary blood flow in patients with non-ischemic heart failure. *J Cardiol*. 2012;60:416-421
49. Roth L, Rombouts M, Schrijvers DM, Martinet W, De Meyer GRY. Cholesterol-independent effects of atorvastatin prevent cardiovascular morbidity and mortality in a mouse model of atherosclerotic plaque rupture. *Vascul Pharmacol*. 2016;80:50-58
50. Abdellatif M, Sedej S, Carmona-Gutierrez D, Madeo F, Kroemer G. Autophagy in cardiovascular aging. *Circ Res*. 2018;123:803-824

51. Theodorou K, Boon RA. Endothelial cell metabolism in atherosclerosis. *Front Cell Dev Biol*. 2018;6:82

52. Perrotta P, Emini Veseli B, Van der Veken B, Roth L, Martinet W, De Meyer GRY. Pharmacological strategies to inhibit intraplaque angiogenesis in atherosclerosis. *Vascul Pharmacol*. 2019;112:72-78

Chapter 5

Small molecule 3PO inhibits glycolysis but does not bind to 6-phosphofructo-2-kinase/fructose-2,6-bisphosphatase-3 (PFKFB3)

Emini Veseli B*, **Perrotta P***, Van Wielendaele P, Lambeir A, Abdali A, Bellosta B, Monaco G, Bultynck G, Martinet W, De Meyer GRY.

FEBS Letters 2020 Jul 3. DOI: 10.1002/1873-3468.13878

* The first two authors contributed equally to this work

Abstract

6-phosphofructo-2-kinase/fructose-2,6-bisphosphatase isoform 3 (PFKFB3) is a key enzyme of the glycolytic pathway and it plays an essential role in angiogenesis. 3-(3-pyridinyl)-1-(4-pyridinyl)-2-propen-1-one (3PO) is frequently used as a glycolysis inhibitor and is thought to inhibit PFKFB3. However, this latter effect of 3PO has never been investigated in detail and was the aim of the present study. To demonstrate binding of 3PO to PFKFB3, we used isothermal titration calorimetry. However, 3PO did not bind to PFKFB3, even up to 750 μM, in contrast to 3 μM of AZ67, which is a potent and specific PFKFB3 inhibitor. Instead, 3PO accumulated lactic acid inside the cells, leading to a decrease in the intracellular pH and an inhibition of enzymatic reactions of the glycolytic pathway.

Keywords: glycolysis, PFKFB3, 3PO, intracellular pH, isothermal titration calorimetry

Introduction

Glycolysis is an essential bioenergetic pathway in endothelial cells (ECs) generating up to 85% of total cellular ATP. A key regulating enzyme in the glycolytic pathway is 6-phosphofructo-2-kinase/fructose-2,6-bisphosphatase (PFKFB), which is involved in both synthesis and degradation of fructose-2,6-bisphosphate. Among the four known PFKFB isoforms, only PFKFB3 reveals a kinase to phosphatase ratio of about 740:1, which favors the formation of intracellular fructose-2,6-bisphosphate (Fru-2,6-P_2) and enhanced glycolysis.[1, 2] Interestingly, expression of PFKFB3 is upregulated in response to hypoxia and inflammatory stimuli. [3, 4]. Because silencing or inactivation of PFKFB3 reduces glycolysis and impairs vessel sprouting [5], PFKFB3 has become an attractive therapeutic target in preventing pathological angiogenesis. 3-(3-pyridinyl)-1-(4-pyridinyl)-2-propen-1-one (3PO) has been reported as a novel compound that reduces glycolytic flux through competitive inhibition of PFKFB3. [6] It causes a rapid reduction in Fru-2,6-P_2 levels and inhibits tumorigenic growth *in vivo.* It also diminishes ^{18}F-2-DG uptake within xenografts [6] and inhibits EC proliferation and migration, resulting in reduced vessel sprouting in EC spheroids, zebrafish embryos, and the postnatal mouse retina. Notably, all these effects of 3PO are attributable to only partial and transient inhibition of glycolysis. [7]

Although 3PO and the more potent analogue PFK15 are considered to act as PFKFB3 inhibitors [8-12], thorough experimental evidence is currently lacking. Moreover, recent data indicate that 3PO is inactive in a PFKFB3 kinase assay (IC_{50} >100 μM) and no crystal structure is available confirming binding of 3PO to PFKFB3 kinase. [13] It should be noted that 3PO does not inhibit the enzymatic activity of other enzymes involved in the glycolytic pathway such as hexokinase, glucose-6-phosphate dehydrogenase, transketolase, phosphofructokinase, pyruvate kinase and lactate dehydrogenase.[7] In the present study, we demonstrate that the anti-glycolytic activity of 3PO relies on its ability to interfere with intracellular milieu acidification, rather than on a direct binding to PFKFB3.

Materials and methods

Glycolysis measurements

Glycolysis was measured *in vitro* using a Glycolysis Cell-Based Assay Kit (Cayman Chemical) following the manufacturer's instructions. Briefly, human umbilical vein endothelial cells (HUVECs) were seeded in a 96-well culture plate at a density of 15,000 cells/well and incubated overnight at 37°C in M199 culture medium, supplemented with 0.25% heat-inactivated fetal calf serum (FCS), 1% non-essential amino-acids (NEAA), and antibiotics. Thereafter, cells were treated with 3PO (Sigma; 2-100 µM) for 24 h and assayed to determine the L-lactate concentration in the culture medium. A neutral red viability assay was performed as described [14] to test cell viability.

Glycolytic flux was also assessed in HUVECs by measuring the extracellular acidification rate (ECAR) using a Seahorse XFp Analyzer (Agilent Technologies) and following manufacturer recommended protocol. ECAR values were expressed in units of mpH/min, which follow the changes in pH in the media surrounding the cells, an acidification mostly due to glycolytic proton efflux [15]. Assays were performed prior to experiments to determine optimal cell seeding density, viability, and optimal concentrations of each compound. Briefly, 10,000 HUVECs/well were plated into XF8 polystyrene cell culture plates. After 16 h of incubation at 37°C, cells were treated with 3PO (0, 20 or 40 µM) for 5 h. Prior to performing a glycolysis stress test, growth medium in the wells of XF cell plates was exchanged with the appropriate Seahorse assay medium (Agilent Technologies, 103335-100). Baseline rates were measured three times prior to any injection. Firstly, glucose (Sigma Aldrich, G8270; 10 mM final concentration) was injected into the medium to provide a measure of glycolytic rate. Subsequently, oligomycin, a mitochondrial ATP synthase inhibitor (Sigma Aldrich, 75351; 2 µM final concentration) was injected, blocking oxidative phosphorylation and giving an estimate of glycolytic capacity. Finally, 2-DG (Sigma Aldrich, D8375; 50 mM final concentration) was injected, which is a glucose analog that inhibits glycolysis, providing an estimate of non-glycolytic acidification. All compounds were prepared in assay medium and adjusted to pH 7.4. Glycolytic

capacity was calculated as the difference between ECAR following the injection of 2 μM oligomycin and the basal ECAR reading. [16]

Intracellular lactate measurements

Intracellular lactate levels were measured *in vitro* using an L-Lactate Assay Kit (Cayman Chemical) according to the manufacturer's protocol. HUVECs were plated into a cell culture plate until 80% confluency in M199 growth medium supplemented with 20% FCS, 1% non-essential amino-acids, and antibiotics. Next, HUVECs were treated with 3PO (20 μM) or vehicle (DMSO) for 24 h. A cell count was performed with an automated cell counter (Countess® II FL, Life Technologies). After deproteinization with 0.25 M metaphosphoric acid, potassium carbonate (5 M) was added to the cell pellet to neutralize the acid. Following centrifugation (10,000 x g for 5 min) at 4˚C, the supernatant was used for assaying. Lactate fluorescent substrate was used as a fluorophore while fluorescence (λ_{ex}=540 nm; λ_{em}=595 nm) was measured and normalized to the cell number. 2-Cyano-3-(4-hydroxyphenyl)-2-propenoic acid (CHC), a classical inhibitor of monocarboxylate transporters, was used as a reference compound.

Intracellular pH assay

Intracellular pH changes were measured with a Fluorometric Intracellular pH assay kit (Sigma-Aldrich, MAK150) following the manufacturer's protocol. In brief, HUVECs were plated overnight in M199 growth medium supplemented with 20% FCS, 1% non-essential aminoacids, and antibiotics in a 96-well culture plate. Subsequently, the fluorescent pH indicator BCFL-AM was added for 30 min. 3PO (20μM) was diluted in Hank's Buffer (HBSS) containing 20 mM HEPES and added to the cells. Fluorescence (λ_{ex}=490 nm; λ_{em}=535 nm) was measured 5 h after addition of 3PO. 2-Cyano-3-(4-hydroxyphenyl)-2-propenoic acid (CHC), a well-known inhibitor of monocarboxylate transporters, was used as a reference compound.

In vitro angiogenesis assay

Inhibition of endothelial tube formation by 3PO was monitored using an *in vitro* angiogenesis assay kit (Millipore) following the manufacturer's instructions. Briefly, HUVECs were cultured in M199 medium supplemented with 20% FCS, 1% non-essential amino-acids, and antibiotics. After addition of 3PO (0-20 μM) for 16 h, changes in tube formation and formation of cellular networks were evaluated. Capillary tube branching points were counted in 5 random fields per concentration.

Endothelial cell migration assay

Murine immortalized heart ECs (H5V) were cultured on 12-well plates in DMEM medium supplemented with 10% FCS and antibiotics. After reaching confluence, H5V were starved overnight in DMEM containing 0.5% FCS. Each well was marked below the plate surface by drawing a vertical line. Five different scratches intercepting the marked line were done in each well using a 200 μL sterile tip. Pictures of scratches were taken before and after 18 hours incubation with DMEM (with 2.5% FCS) with or without 3PO (20 μM) and with or without vascular endothelial growth factor (VEGF, 10 ng/mL). Next, the mean closure of five different scratches was analyzed using ImageJ software. EC migration was expressed as the percentage of scratch closure after 18 h versus the initial area by using the following formula: % closure = [(scratched area at 0 h – scratched area at 18 h)/scratched area at 0 h] ×100.

Aortic sprouting

An aortic ring assay was performed as previously described. [17] In brief, murine thoracic aortas were dissected, cleaned under sterile conditions, transferred to 10 cm culture dishes, and cut into 0.5 mm thick rings with a sterile scalpel. After overnight starvation in serum-free Opti-MEM at 37°C, ring segments were transferred into wells of a 96-well plate coated with 50 μL of a freshly prepared collagen type I solution (1 mg/mL). The aortic rings remained in Opti-MEM (supplemented with 2.5% FCS and antibiotics) in the presence or absence of 3PO

and/or VEGF (50 ng/mL) (R&D Systems). Medium was replaced every 2 days. On day 6, rings were fixed with 4% paraformaldehyde, stained with von Willebrand factor antibody (anti-vWF, PC054, Binding Site) and DAPI prior to fluorescence microscopy imaging. The number of sprouts was counted for each ring and sprout numbers per ring were averaged for each group and graphed.

Isothermal Titration Calorimetry (ITC)

Binding of 3PO and AZ PFKFB3 67 (further abbreviated as AZ67, Tocris, used as control) to PFKFB3 was analyzed by calorimetry using a MicroCal Peaq-ITC isothermal titration calorimeter (non-automated version, Malvern Preanalytical). Prior to ITC analysis, recombinant human PFKFB3 from *E. coli* (Flemish Institute for Biotechnology (VIB), Protein Service Facility, University of Ghent, Belgium) was dialyzed against 2 L buffer (40 mM Tris, 500 mM NaCl, 5 mM $MgCl_2$, 2 mM DTT at pH 7.4) for 2 h at 4 °C under constant stirring, followed by switching to a novel 2 L buffer vial and overnight dialysis. For this purpose, Slide-A-Lyzer Dialysis G2 cassettes (Thermo Scientific) were used. The concentration of the sample after dialysis was determined through UV-absorbance at 280 nm using a Spectramax Plus 384 (Molecular Devices). A small portion of the second dialysis buffer volume was kept for matching the ligand solutions (AZ67 or 3PO). All buffers were prepared in ultrapure water (18.2 MΩ.cm), equilibrated to room temperature and degassed for 15 min in an ultrasonication bath before use. All titrations were performed with the same PFKFB3 sample, diluted to a working concentration of 3 µM, and with the same titration conditions (except for the ligand concentration) in order to allow mutual comparison between the different runs.

The reference cell of the Peaq-ITC was filled with degassed ultrapure water. The PFKFB3 solution was put in the sample cell after a 2 min pre-equilibration with assay buffer (same recipe as dialysis buffer). The ligand solution was administered in the injection syringe. Titration conditions were as follows: one initial injection of 0.4 µL was followed by 14 injections of 2.5 µL. The initial spacing was set to 180 s, while the remaining spacing was set to 150 s. The sample cell was continuously stirred at 750 rpm. Temperature was set to 37 °C before loading and kept constant during the

complete run. The DP (differential power between the reference and sample cells to maintain a zero temperature difference between the cells) was set to 5.
To determine the dilution heats for each PFKFB3-ligand concentration combination, control titrations were performed consisting of injection of ligand into the buffer-filled cell (thus in the absence of PFKFB3, without binding). Thermograms were analyzed using the Microcal Peaq-ITC Analysis software, using the 'one set of sites' binding model, by including the corresponding control titration. In order to visually compare the different titrations with completely different molar ratios, the data were transformed to generated heat (ΔH) per injection.

Statistics

All data are expressed as mean ± SEM. Statistical analyses were performed using SPSS software (version 25). Statistical tests are specified in the figure legends. N indicates the number of times an experiment has been repeated. Differences were considered significant at $P<0.05$.

Results

3PO inhibits glycolysis in endothelial cells

Lactate measurements in the culture medium of human umbilical vein endothelial cells (HUVECs) as well as Seahorse ECAR measurements showed that 3PO inhibits glycolysis in a concentration-dependent manner (Figure 1A-B). The extracellular acidification rate diminished by more than 50% after treatment with 20 μM 3PO (Figure 1B). Viability of HUVECs was not affected when cells were treated with 3PO up to 20 μM (Figure 1C). However, cytotoxic effects were noticed after exposure to higher 3PO concentrations (40 and 100 μM).

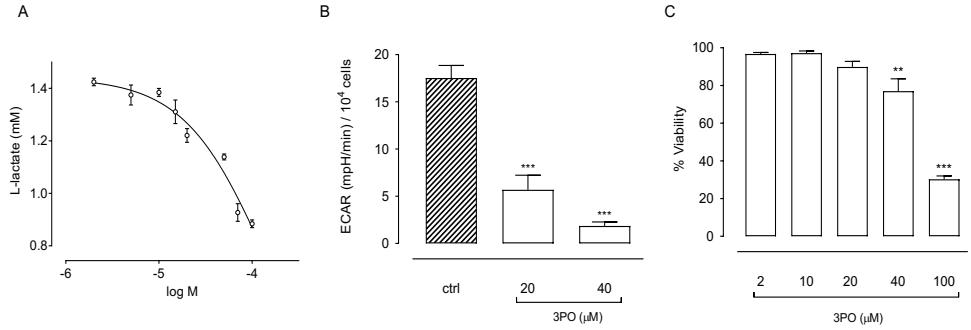

Figure 1. **3PO inhibits glycolysis *in vitro***. (A) Human umbilical vein endothelial cells (HUVECs) were cultured and treated with 3PO (2 – 100 μM) for 24 h. Extracellular lactatewas measured to evaluate glycolysis. (B) Glycolytic flux was assessed by measuring the extracellular acidification rate (ECAR) using a Seahorse XFp Analyzer. Cultured HUVECs were treated without or with 3PO (20 or 40 μM) for 5 h. (C) 3PO (2, 10, 20 μM) did not show cytotoxic effects up to 24 h treatment compared to vehicle (DMSO), whereas concentrations starting from 40 μM 3PO onward decreased cell viability. ***P*<0.01, ****P*<0.001 (one-way analysis of variance (ANOVA) followed by Dunnett test, n=3).

3PO inhibits capillary tube formation, EC migration, and formation of aortic sprouts

To confirm whether glycolysis inhibition by 3PO in ECs affects neoangiogenesis, an *in vitro* matrigel assay with HUVECs was performed. This assay is based on the ability of ECs to form cord and mesh structures when seeded on a growth factor-enriched matrix. 3PO fully inhibited cord formation at 20 μM. At lower concentrations (5-10 μM), mesh structures consisting of EC chords were visible but their numbers were reduced in a concentration-dependent manner. A healthy network of chord structures was formed in the absence of 3PO (Figure 2A). Branch point counting demonstrated an inverse correlation between the amount of branch points and the concentration of 3PO (Figure 2B). Apart from inhibition of capillary tube formation, 3PO inhibited EC migration after scratching EC monolayers (Figure 3) and prevented aortic sprouting (Figure 4) both under basal conditions and after stimulation with VEGF.

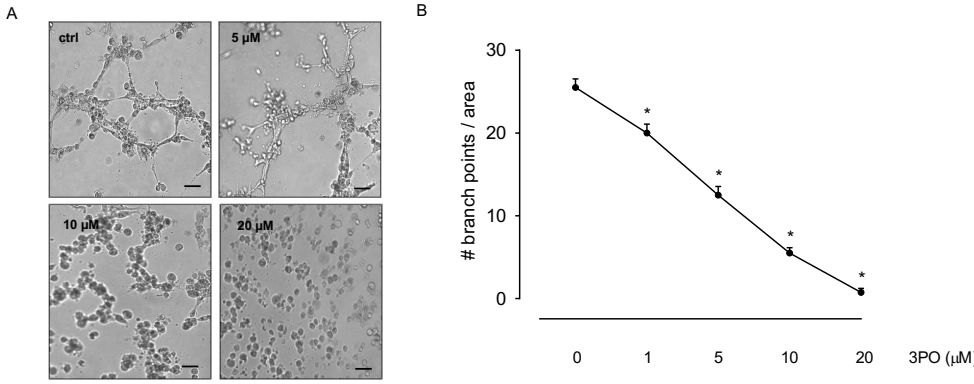

Figure 2. 3PO inhibits endothelial cell tube formation. (A) Representative images of an *in vitro* angiogenesis assay. Human umbilical vein endothelial cells (HUVECs) were seeded on ECMatrix in the presence or absence of 3PO (5, 10, 20 µM) for 16 h. Images of tube formation and branching were taken and quantified. Scale bar = 100 µm. (B) The progression of angiogenesis was quantified by counting the amount of capillary tube branch points at different concentrations. *P<0.05 vs. control (Mann-Whitney U test, n=4).

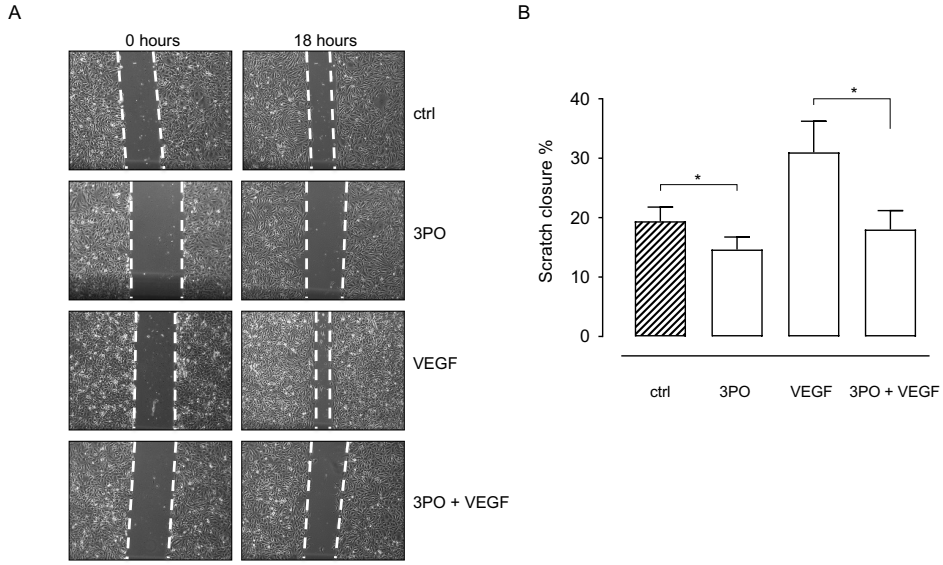

Figure 3. 3PO inhibits endothelial cell migration. (A) Representative images of a scratch assay. Murine immortalized heart endothelial cells (H5V) were starved, subsequently wounded and treated with DMEM (2.5% FCS) with or without 20 µM 3PO, and with or without

10 ng/mL VEGF for 18 h. (B) The wound area was measured at 0 and 18 h, and migration was quantified. Factorial ANOVA, n=5-7; effect of 3PO: P=0.020; effect of VEGF: P=0.046; interaction: P=0.255.

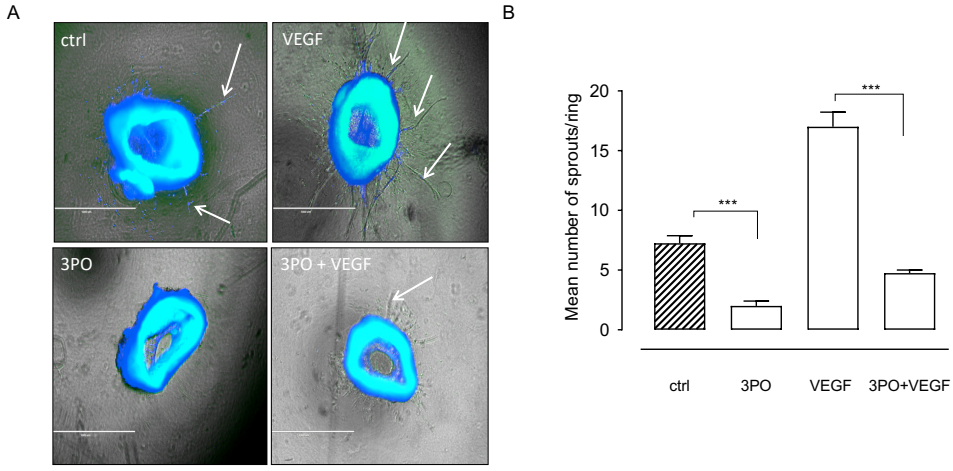

Figure 4. 3PO inhibits aortic sprouting. (A) Aortic rings from ApoE$^{-/-}$ mice were embedded in collagen type I and treated with Opti-MEM (supplemented with 2.5% FCS) in the presence or absence of 20 µM 3PO and/or VEGF (50 ng/mL) 2.5% (vol/vol) FBS or VEGF 50 ng/mL. At day 6, rings were fixed and stained to delineate ECs. Images of ring sprouting were obtained and quantified. Scale bar = 1 mm. (B) Sprouts were quantified, n=4 mice. ****P*<0.001 Factorial ANOVA, effect of 3PO: P<0.001, effect of VEGF: P<0.001, interaction: P<0.001.

3PO does not bind PFKFB3

Isothermal titration calorimetry measurements did not show any binding of 3PO towards recombinant PFKFB3. Even usage of 750 µM 3PO as final concentration did not yield any binding indication. In contrast, AZ67, which is a potent and specific PFKFB3 inhibitor [13] that was used as a positive control clearly showed binding towards recombinant PFKFB3 (Figure 5).

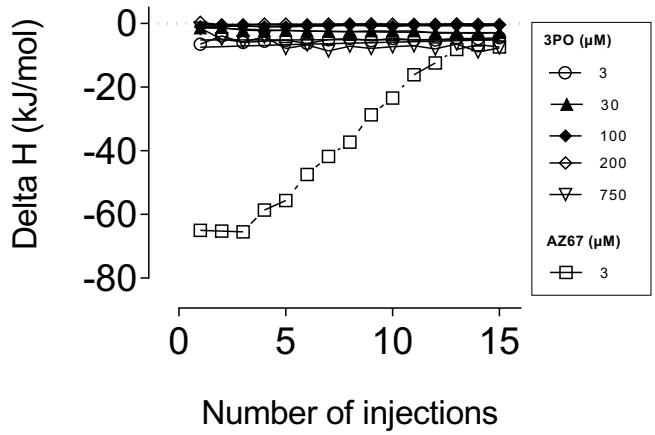

Figure 5. 3PO does not bind to PFKFB3. Binding of 3PO to PFKFB3 was analyzed via calorimetry using a MicroCal ITC isothermal titration calorimeter. Discharged or absorbed heat during the eventual interaction between the PFKFB3 protein and 3PO was measured (Delta H). PFKFB3 inhibitor AZ PFKFB3 67 (3 µM) was used as a positive control. Indicated concentrations are the concentrations in the injection syringe of the Peaq-ITC.

3PO induces intracellular lactate accumulation and decreases the intracellular pH

Disruption of the intracellular pH (pHi) has been shown to play an important role in regulating angiogenesis [18] and glycolysis. [18, 19] Therefore, we studied the effect of 3PO treatment on the pHi in ECs. 3PO (20 µM) induced intracellular acidification, as shown by a significant decrease in pHi in HUVECs (Figure 6A). Given that lactate is an important regulator of pH [20], we measured intracellular lactate levels in HUVECs after treatment with 3PO and showed that it increased the lactate concentration intracellularly (Figure 6B). CHC, a well-known inhibitor of monocarboxylate transporters [21], was used as a reference compound.

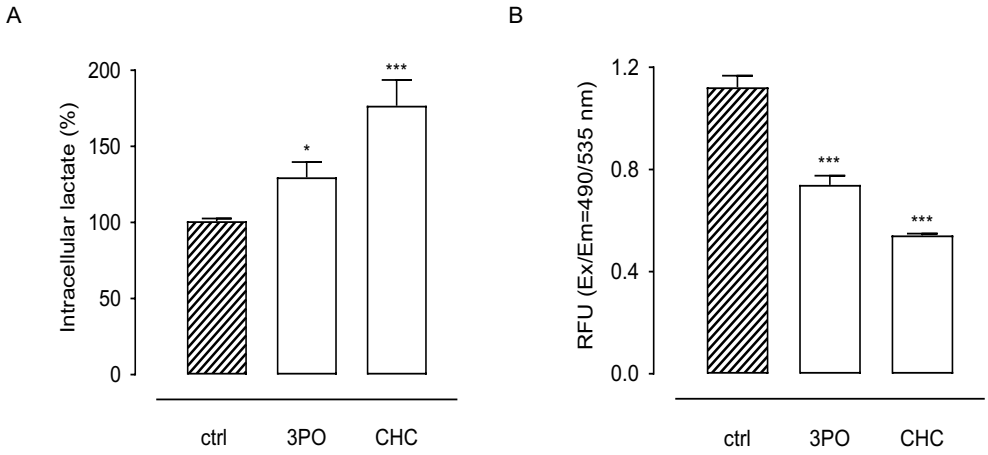

Figure 6. 3PO interferes with intracellular pH. (A) 3PO induces intracellular lactate accumulation. Human umbilical vein endothelial cells (HUVECs) were treated with 3PO (20 μM) for 24 h. Lactate fluorescent substrate was added and fluorescence was measured, n=4-9. **P*<0.05, ****P*<0.001 vs. control (one-way ANOVA followed by Dunnett test). (B) 3PO decreases the intracellular pH. HUVECs were treated with 3PO (20 μM) for 5 h. Fluorescent pH indicator BCFL-AM was added and fluorescence was measured. CHC (2-Cyano-3-(4-hydroxyphenyl)-2-propenoic acid; 2 mM) was used as a positive control, n=6-20. ****P*<0.001 vs. control (one-way ANOVA followed by Dunnett test).

Discussion

The rate of glycolysis in ECs is much higher than in any other healthy cell type. Accordingly, the majority of ATP produced in these cells is through the anaerobic glycolytic pathway. These findings highlight glycolysis inhibition as a promising anti-angiogenic strategy. Using computational techniques, 3PO was identified as a small-molecule inhibitor of PFKFB3. [6] Follow-up experiments indicate that 3PO reduces Fru-2,6-P_2 levels and glycolytic flux [6]. Since then, administration of 3PO has been considered as an attractive therapeutic strategy in cancer research, acute lung injury, lung fibrosis, and atherosclerosis. [22-25] The ability of 3PO to inhibit glycolysis was confirmed in the present study. Indeed, by using Seahorse technology, we could demonstrate that 3PO inhibits glycolysis in a concentration-dependent manner in HUVECs, resulting in an up to 50% reduction in glycolytic rate. Moreover, 3PO inhibits capillary tube formation, migration of ECs, and formation of aortic sprouts, which are all processes that heavily depend on glycolysis. However, an enzyme binding assay via isothermal titration calorimetry did not reveal binding of 3PO to PFKFB3, not even when titrating with up to 750 µM final concentration, which is more than 35 times higher than the 20 µM 3PO used in the *in cellulo* experiments. This raises considerable doubts as to whether 3PO does work via PFKFB3 inhibition. Importantly, 3PO does not inhibit the enzymatic activity of other enzymes involved in the glycolytic pathway, such as hexokinase, glucose 6-phosphate dehydrogenase, transketolase, glyceraldehyde 3-phosphate dehydrogenase, pyruvate kinase, and lactate dehydrogenase. The question remains which mechanism is responsible for the inhibition of glycolysis by 3PO. The present study shows that the inhibitory effect of 3PO on glycolysis relies on the ability of this compound to cause an imbalance in intracellular pH by accumulating lactic acid inside the cell. It is known that some glycolytic enzymes including lactate dehydrogenase and phosphofructokinase-1 (PFK-1) are very pH-sensitive. A change of less than one pH unit, even a few tenths, may reduce the activity of PFK-1 by more than 10-fold. [18, 19, 26-28] Moreover, PFKFB3, also known as phosphofructokinase-2 (PFK-2), has been shown to be allosterically regulated by hydrogen ion concentrations. [29] On the other hand, lactate is an important regulator of pH [20], hence the intracellular increase of this metabolite leads to intracellular milieu acidification, thus indirectly affecting the rate of glycolysis.

Manipulating intracellular acidification has been considered to have therapeutic utility in tumors. One of the strategies include the inhibition of monocarboxylate transporters (MCTs). Among different acid extruders present in the cell membrane, monocarboxylate transporters 1 and 4 are responsible for bumping out lactate and hydrogen ions. More specifically, a multitude of studies have documented that MCT1 or MCT4 inhibition conferred antiangiogenic effects and block tumor growth. [30-32] In this light, we do not rule out the possibility that 3PO acts as an inhibitor of one or more MCT transporters.

Altogether, our study indicates that the inhibitory effect of 3PO on PFKFB3 enzymatic activity, glycolysis, and angiogenesis is not mediated through direct binding to the PFKFB3 protein, as already suggested previously. [6] This is the first study to report these findings, as no previous studies have investigated the thermodynamic profile and biomolecular interactions of 3PO and PFKFB3. Intracellular acidification and lactate accumulation are followed by a chain reaction starting with MCT1/4 inhibition, pHi decrease, influence of pH dependent rate-limiting enzymes, and glycolysis suppression. This backward chain reaction supports our hypothesis of 3PO targeting MCT 1 and 4. The identification of this target may have an important impact on angiogenesis research and on the development of specific anti-angiogenic treatments, which has implications for a variety of pathologies.

Acknowledgements

This work was supported by the University of Antwerp (BOF, grant number 29068 and 40183). Besa Emini Veseli, Paola Perrotta, and Anahita Abdali are PhD fellows of the Horizon 2020 program of the European Union - Marie Skłodowska-Curie Actions, Innovative Training Networks (ITN), Call: H2020-MSCA-ITN-2015, NUMBER — 675527 — MOGLYNET. The authors are grateful to Dr. Bronwen Martin for critical reading of the manuscript.

References

1. Yalcin A, Telang S, Clem B, Chesney J. Regulation of glucose metabolism by 6-phosphofructo-2-kinase/fructose-2,6-bisphosphatases in cancer. *Experimental and molecular pathology*. 2009;86:174-179

2. Sakakibara R, Kato M, Okamura N, Nakagawa T, Komada Y, Tominaga N, Shimojo M, Fukasawa M. Characterization of a human placental fructose-6-phosphate, 2-kinase/fructose-2,6-bisphosphatase. *Journal of biochemistry*. 1997;122:122-128

3. Minchenko O, Opentanova I, Caro J. Hypoxic regulation of the 6-phosphofructo-2-kinase/fructose-2,6-bisphosphatase gene family (pfkfb-1-4) expression in vivo. *FEBS letters*. 2003;554:264-270

4. Obach M, Navarro-Sabate A, Caro J, Kong X, Duran J, Gomez M, Perales JC, Ventura F, Rosa JL, Bartrons R. 6-phosphofructo-2-kinase (pfkfb3) gene promoter contains hypoxia-inducible factor-1 binding sites necessary for transactivation in response to hypoxia. *The Journal of biological chemistry*. 2004;279:53562-53570

5. De Bock K, Georgiadou M, Schoors S, Kuchnio A, Wong BW, Cantelmo AR, Quaegebeur A, Ghesquiere B, Cauwenberghs S, Eelen G, Phng LK, Betz I, Tembuyser B, Brepoels K, Welti J, Geudens I, Segura I, Cruys B, Bifari F, Decimo I, Blanco R, Wyns S, Vangindertael J, Rocha S, Collins RT, Munck S, Daelemans D, Imamura H, Devlieger R, Rider M, Van Veldhoven PP, Schuit F, Bartrons R, Hofkens J, Fraisl P, Telang S, Deberardinis RJ, Schoonjans L, Vinckier S, Chesney J, Gerhardt H, Dewerchin M, Carmeliet P. Role of pfkfb3-driven glycolysis in vessel sprouting. *Cell*. 2013;154:651-663

6. Clem B, Telang S, Clem A, Yalcin A, Meier J, Simmons A, Rasku MA, Arumugam S, Dean WL, Eaton J, Lane A, Trent JO, Chesney J. Small-molecule inhibition of 6-phosphofructo-2-kinase activity suppresses glycolytic flux and tumor growth. *Molecular cancer therapeutics*. 2008;7:110-120

7. Schoors S, De Bock K, Cantelmo AR, Georgiadou M, Ghesquiere B, Cauwenberghs S, Kuchnio A, Wong BW, Quaegebeur A, Goveia J, Bifari F, Wang X, Blanco R, Tembuyser B, Cornelissen I, Bouche A, Vinckier S, Diaz-Moralli S, Gerhardt H, Telang S, Cascante M, Chesney J, Dewerchin M, Carmeliet P. Partial and transient reduction of glycolysis by pfkfb3 blockade reduces pathological angiogenesis. *Cell metabolism*. 2014;19:37-48

8. Rao TN, Hansen N, Hilfiker J, Rai S, Majewska JM, Lekovic D, Gezer D, Andina N, Galli S, Cassel T, Geier F, Delezie J, Nienhold R, Hao-Shen H, Beisel C, Di Palma S, Dimeloe S, Trebicka J, Wolf D, Gassmann M, Fan TW, Lane AN, Handschin C, Dirnhofer S, Kroger N, Hess C, Radimerski T, Koschmieder S, Cokic VP, Skoda RC. Jak2-mutant hematopoietic cells display metabolic alterations that can be targeted to treat myeloproliferative neoplasms. *Blood*. 2019;134:1832-1846

9. Cao Y, Zhang X, Wang L, Yang Q, Ma Q, Xu J, Wang J, Kovacs L, Ayon RJ, Liu Z, Zhang M, Zhou Y, Zeng X, Xu Y, Wang Y, Fulton DJ, Weintraub NL, Lucas R, Dong Z, Yuan JX, Sullivan JC, Meadows L, Barman SA, Wu C, Quan J, Hong M, Su Y, Huo Y. Pfkfb3-mediated endothelial glycolysis promotes pulmonary hypertension. *Proceedings of the National Academy of Sciences of the United States of America*. 2019;116:13394-13403

10. Houddane A, Bultot L, Novellasdemunt L, Johanns M, Gueuning MA, Vertommen D, Coulie PG, Bartrons R, Hue L, Rider MH. Role of akt/pkb and pfkfb isoenzymes in the control of glycolysis, cell proliferation and protein synthesis in mitogen-stimulated thymocytes. *Cellular signalling*. 2017;34:23-37

11. Pisarsky L, Bill R, Fagiani E, Dimeloe S, Goosen RW, Hagmann J, Hess C, Christofori G. Targeting metabolic symbiosis to overcome resistance to anti-angiogenic therapy. *Cell reports*. 2016;15:1161-1174

12. Finucane OM, Sugrue J, Rubio-Araiz A, Guillot-Sestier MV, Lynch MA. The nlrp3 inflammasome modulates glycolysis by increasing pfkfb3 in an il-1beta-dependent manner in macrophages. *Scientific reports*. 2019;9:4034

13. Boyd S, Brookfield JL, Critchlow SE, Cumming IA, Curtis NJ, Debreczeni J, Degorce SL, Donald C, Evans NJ, Groombridge S, Hopcroft P, Jones NP, Kettle JG, Lamont S, Lewis HJ, MacFaull P, McLoughlin SB, Rigoreau LJ, Smith JM, St-Gallay S, Stock JK, Turnbull AP, Wheatley ER, Winter J, Wingfield J. Structure-based design of potent and selective inhibitors of the metabolic kinase pfkfb3. *Journal of medicinal chemistry*. 2015;58:3611-3625

14. Repetto G, del Peso A, Zurita JL. Neutral red uptake assay for the estimation of cell viability/cytotoxicity. *Nature protocols*. 2008;3:1125-1131

15. Zhang J, Nuebel E, Wisidagama DR, Setoguchi K, Hong JS, Van Horn CM, Imam SS, Vergnes L, Malone CS, Koehler CM, Teitell MA. Measuring energy metabolism in cultured cells, including human pluripotent stem cells and differentiated cells. *Nature protocols*. 2012;7:1068-1085

16. Divakaruni AS, Paradyse A, Ferrick DA, Murphy AN, Jastroch M. Analysis and interpretation of microplate-based oxygen consumption and ph data. *Methods in enzymology*. 2014;547:309-354

17. Baker M, Robinson SD, Lechertier T, Barber PR, Tavora B, D'Amico G, Jones DT, Vojnovic B, Hodivala-Dilke K. Use of the mouse aortic ring assay to study angiogenesis. *Nat Protoc*. 2011;7:89-104

18. White KA, Grillo-Hill BK, Barber DL. Cancer cell behaviors mediated by dysregulated ph dynamics at a glance. *Journal of cell science*. 2017;130:663-669

19. Quach CH, Jung KH, Lee JH, Park JW, Moon SH, Cho YS, Choe YS, Lee KH. Mild alkalization acutely triggers the warburg effect by enhancing hexokinase activity via voltage-dependent anion channel binding. *PloS one*. 2016;11:e0159529

20. Huber V, Camisaschi C, Berzi A, Ferro S, Lugini L, Triulzi T, Tuccitto A, Tagliabue E, Castelli C, Rivoltini L. Cancer acidity: An ultimate frontier of tumor immune escape and a novel target of immunomodulation. *Seminars in cancer biology*. 2017;43:74-89

21. Sonveaux P, Vegran F, Schroeder T, Wergin MC, Verrax J, Rabbani ZN, De Saedeleer CJ, Kennedy KM, Diepart C, Jordan BF, Kelley MJ, Gallez B, Wahl ML, Feron O, Dewhirst MW. Targeting lactate-fueled respiration selectively kills hypoxic tumor cells in mice. *The Journal of clinical investigation*. 2008;118:3930-3942

22. Conradi LC, Brajic A, Cantelmo AR, Bouche A, Kalucka J, Pircher A, Bruning U, Teuwen LA, Vinckier S, Ghesquiere B, Dewerchin M, Carmeliet P. Tumor vessel disintegration by maximum tolerable pfkfb3 blockade. *Angiogenesis*. 2017;20:599-613

23. Gong Y, Lan H, Yu Z, Wang M, Wang S, Chen Y, Rao H, Li J, Sheng Z, Shao J. Blockage of glycolysis by targeting pfkfb3 alleviates sepsis-related acute lung injury via suppressing inflammation and apoptosis of alveolar epithelial cells. *Biochemical and biophysical research communications*. 2017;491:522-529

24. Xie N, Tan Z, Banerjee S, Cui H, Ge J, Liu RM, Bernard K, Thannickal VJ, Liu G. Glycolytic reprogramming in myofibroblast differentiation and lung fibrosis. *American journal of respiratory and critical care medicine*. 2015;192:1462-1474

25. Perrotta P, Van der Veken B, Van Der Veken P, Pintelon I, Roosens L, Adriaenssens E, Timmerman V, Guns PJ, De Meyer GRY, Martinet W. Partial inhibition of glycolysis reduces atherogenesis independent of intraplaque neovascularization in mice. *Arteriosclerosis, thrombosis, and vascular biology*. 2020:ATVBAHA119313692

26. Andres V, Carreras J, Cusso R. Regulation of muscle phosphofructokinase by physiological concentrations of bisphosphorylated hexoses: Effect of alkalinization. *Biochemical and biophysical research communications*. 1990;172:328-334

27. Kamp G, Schmidt H, Stypa H, Feiden S, Mahling C, Wegener G. Regulatory properties of 6-phosphofructokinase and control of glycolysis in boar spermatozoa. *Reproduction*. 2007;133:29-40

28. Trivedi B, Danforth WH. Effect of ph on the kinetics of frog muscle phosphofructokinase. *The Journal of biological chemistry*. 1966;241:4110-4112

29. Putney LK, Barber DL. Expression profile of genes regulated by activity of the na-h exchanger nhe1. *BMC genomics*. 2004;5:46

30. Hong CS, Graham NA, Gu W, Espindola Camacho C, Mah V, Maresh EL, Alavi M, Bagryanova L, Krotee PAL, Gardner BK, Behbahan IS, Horvath S, Chia D, Mellinghoff IK, Hurvitz SA, Dubinett SM, Critchlow SE, Kurdistani SK, Goodglick L, Braas D, Graeber TG, Christofk HR. Mct1 modulates cancer cell pyruvate export and growth of tumors that co-express mct1 and mct4. *Cell reports*. 2016;14:1590-1601

31. Sonveaux P, Copetti T, De Saedeleer CJ, Vegran F, Verrax J, Kennedy KM, Moon EJ, Dhup S, Danhier P, Frerart F, Gallez B, Ribeiro A, Michiels C, Dewhirst MW, Feron O. Targeting the lactate transporter mct1 in endothelial cells inhibits lactate-induced hif-1 activation and tumor angiogenesis. *PloS one*. 2012;7:e33418

32. Voss DM, Spina R, Carter DL, Lim KS, Jeffery CJ, Bar EE. Disruption of the monocarboxylate transporter-4-basigin interaction inhibits the hypoxic response, proliferation, and tumor progression. *Scientific reports*. 2017;7:4292

Chapter 6

PFKFB3 gene deletion in endothelial cells inhibits intraplaque angiogenesis and lesion formation in a murine model of venous bypass grafting

Perrotta P, de Vries MR, De Meyer GRY, Quax P and Martinet W

Submitted for publication

Abstract

Objective: Vein grafting is a frequently used surgical intervention for cardiac revascularization. However, vein grafts display regions with intraplaque (IP) angiogenesis, which promotes atherogenesis and formation of unstable plaques. Graft neovessels are mainly composed of endothelial cells (ECs) that largely depend on glycolysis for migration and proliferation. In the present study, we aimed to investigate whether loss of the glycolytic flux enzyme phosphofructokinase-2/fructose-2,6-bisphosphatase 3 (PFKFB3) in ECs inhibits IP angiogenesis and as such prevents unstable plaque formation.

***Approach and results*:** Apolipoprotein E deficient ($ApoE^{-/-}$) mice were backcrossed to a previously generated $PFKFB3^{fl/fl}$ $Cdh5^{iCre}$ mouse strain. Animals were injected with either corn oil ($ApoE^{-/-}PFKFB3^{fl/fl}$) or tamoxifen ($ApoE^{-/-}PFKFB3^{ECKO}$), and were fed a western type diet for 4 weeks prior to vein grafting. Hereafter, mice received ~~a~~ western diet for an additional 28 days and were then sacrificed for graft assessment. Size and thickness of vein graft lesions were reduced respectively by 35% and 32% in $ApoE^{-/-}PFKFB3^{ECKO}$ mice as compared to controls, whereas stenosis diminished by 23%. Moreover, vein graft lesions in $ApoE^{-/-}PFKFB3^{ECKO}$ mice showed a significant reduction in macrophage infiltration (29%), number of neovessels (62%) and hemorrhages (86%). EC-specific PFKFB3 deletion did not show obvious adverse effects or changes in general metabolism.

To investigate the effect of an EC-specific deletion of PFKFB3 on native atherosclerosis, $ApoE^{-/-}PFKFB3^{fl/fl}$ and $ApoE^{-/-}PFKFB3^{ECKO}$ were fed a western type diet for 12 weeks without the vein graft procedure. At the end of the experiment, brachiocephalic arteries were collected and analyzed. PFKFB3 EC-specific deletion also decreased plaque area and thickness of native lesions in atherosclerotic $ApoE^{-/-}$ mice.

***Conclusions*:** EC-specific PFKFB3 gene deletion leads to a significant reduction in lesion size, IP angiogenesis and hemorrhagic complications in vein grafts. This study also shows that inhibition of endothelial glycolysis is a promising therapeutic strategy to slow down plaque progression in the context of accelerated atherosclerosis following vein graft surgical intervention.

Graphic abstract

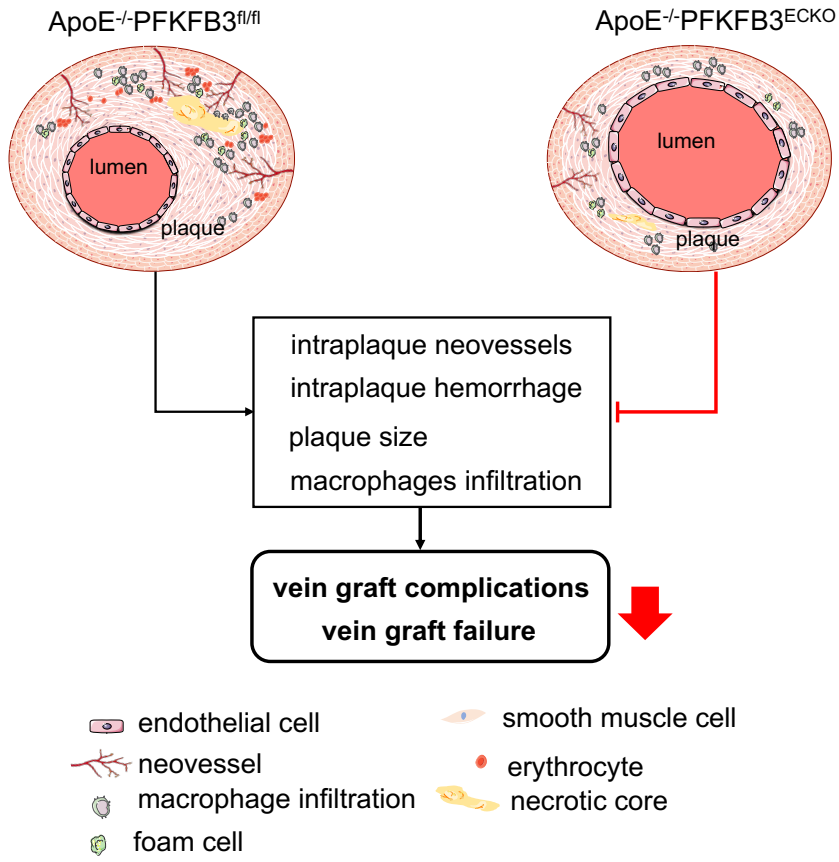

Highlights

- PFKFB3 deletion in endothelial cells reduces intraplaque angiogenesis in a mouse model of venous bypass grafting.
- PFKFB3 deletion in endothelial cells reduces lesion size and macrophage infiltration in mouse vein grafts.
- PFKFB3 deletion in endothelial cells reduces hemorrhagic complications in mouse vein graft lesions.
- PFKFB3 deletion in endothelial cells does not affect general metabolism of adult mice.

Introduction

Atherosclerosis is a chronic inflammatory disease of the arterial wall and is one of the most important causes of cardiovascular disease including severe conditions such as coronary artery disease, myocardial infarction, heart failure and stroke. Vein bypass grafting is a surgical procedure that uses large saphenous veins to bypass occluded atherosclerotic arteries, thereby allowing revascularization of an ischemic region of the heart or limbs.[1] Unfortunately, at least 40% of patients suffer from bypass failure within eight years after the procedure due to negative vascular remodeling and intimal hyperplasia.[1-4] Furthermore, vein grafts often present accelerated atherosclerosis with formation of unstable plaques and increased risk of rupture.[5-7]

New capillaries can form inside vein grafts to fulfill an increased demand of oxygen and nourishment of the vessel wall. This event, which is further promoted by inflammatory conditions, leads to intraplaque (IP) angiogenesis and contributes to plaque instability in the vein graft.[8] Indeed, apolipoprotein E deficient ($ApoE^{-/-}$) mice undergoing a vein graft interposition of the carotid artery develop unstable plaques with extensive IP neovessels that are often dysfunctional or immature and contribute to lesion destabilization by enhancing leukocyte recruitment and accumulation of cholesterol and platelets.[9, 10]

Angiogenesis is an energy-intensive process that requires extensive metabolic functioning of endothelial cells (ECs) to support sprouting, migration and proliferation.[11] Recent studies have shown that ECs in neovessels generate more than 85% of their ATP by glycolysis.[12, 13] One of the rate-limiting checkpoints of glycolytic flux is the conversion of fructose-6-phosphate to fructose-1,6-bisphosphate by 6-phosphofructo-1-kinase. Phosphofructokinase-2/fructose-2,6-bisphosphatase (PFKFB) enzymes synthesize fructose-2,6-bisphosphate, an allosteric activator of 6-phosphofructo-1-kinase and the most potent stimulator of glycolysis. Of all PFKFB iso-enzymes, PFKFB3 appears the major producer of intracellular fructose-2,6-bisphosphate in ECs. PFKFB3 is upregulated in ECs under inflammatory conditions and its pharmacological inhibition or gene silencing reduces pathological angiogenesis in response to injury and inflammation.[14 15, 16] Previous findings have shown that inhibition of PFKFB3 leads to reduced EC migration and

proliferation in vitro. Additionally, sprout number and length of EC spheroids significantly decrease after knocking out PFKFB3.[17]

We have recently reported that the partial glycolysis inhibitor 3PO (3-(3-pyridinyl)-1-(4-pyridinyl)-2-propen-1-one) reduces IP angiogenesis and plaque formation.[18] However, the specific role of endothelial PFKFB3 in the context of IP neovascularization and lesion progression remains to be investigated. Therefore, in the present study we used a vein graft procedure in EC-specific conditional PFKFB3 knockout mice on an $ApoE^{-/-}$ background to test whether endothelial PFKFB3 is an important driver of IP angiogenesis and atherosclerotic lesion progression.

Methods

All primary data that support the findings of this study are available from the corresponding author upon reasonable request.

Animals

EC-specific conditional PFKFB3 knockout mice ($PFKFB3^{fl/fl}$) were generated by crossbreeding $PFKFB3^{fl/fl}$ mice with VE-cadherin (PAC)-Cre^{ERT2} mice ($Cdh5^{iCre}$).[17] Resulting mice were crossbred with $ApoE^{-/-}$ mice to generate an $ApoE^{-/-}PFKFB3^{fl/fl}Cdh5^{iCre}$ strain. All mice were on C57BL/6N background. $ApoE^{-/-}PFKFB3^{fl/fl}Cdh5^{iCre}$ mice (male, 6 weeks old) were injected with tamoxifen (0.1g/kg body weight) for 5 consecutive days to induce PFKFB3 deletion in ECs, termed $ApoE^{-/-}PFKFB3^{ECKO}$. $ApoE^{-/-}PFKFB3^{fl/fl}Cdh5^{iCre}$ control mice, further referred to as $ApoE^{-/-}PFKFB3^{fl/fl}$ mice, were injected with corn-oil using the same protocol. All animal procedures were conducted according to the guidelines from Directive 2010/63/EU of the European Parliament on the protection of animals used for scientific purposes. Experiments were approved by the ethics committee of the University of Antwerp.

Vein graft surgery

ApoE-/-PFKFB3ECKO and ApoE-/-PFKFB3fl/fl mice were fed a western-type diet (Altromin, C1000 diet supplemented with 20% milkfat and 0.15% cholesterol, #100171) for 4 weeks (Supplemental Figure I). Next, vein graft surgery was performed as described.[5, 7] Briefly, thoracal caval veins from donor ApoE-/-PFKFB3ECKO or ApoE-/-PFKFB3fl/fl mice were harvested. In the first group, ApoE-/-PFKFB3fl/fl recipient mice received the caval veins from ApoE-/-PFKFB3fl/fl donor mice; in the second group, ApoE-/-PFKFB3ECKO mice received the caval veins from ApoE-/-PFKFB3ECKO mice. For each experiment, the right carotid artery of recipient mice was dissected and cut in the middle. On both the proximal and distal artery end, a nylon cuff was sleeved and fixated with hemostatic clamps. The artery was everted around the cuffs and ligated with 8.0 sutures. Next, the caval veins were positioned over both cuffs, and ligated. Before surgery, mice were anesthetized with midazolam (5 mg/kg body weight, i.p., Roche), medetomidine (0.5 mg/kg body weight, i.p., Orion) and Fentanyl (0.05 mg/kg body weight, i.p., Janssen). After the procedure, mice were antagonized with atipamezole (2.5 mg/kg body weight, i.p., Orion) and fluminazenil (0.5 mg/kg body weight, i.p., Fresenius Kabi). Buprenorphine (0.1 mg/kg body weight, i.p., MSD Animal Health) was given after surgery to relieve pain. Animals were sacrificed under the aforementioned anesthesia 28 days after the graft procedure, followed by 2 minutes of in vivo perfusion-fixation.

Native Atherosclerosis study

In another series of experiments, atherosclerotic plaques in the brachiocephalic arteries of $ApoE^{-/-}$ $PFKFB3^{fl/fl}$ and $ApoE^{-/-}$ $PFKFB3^{ECKO}$ mice (8 weeks old) were examined after feeding western-type diet (WD) for 12 weeks (Supplemental Figure IB).

Histology

After euthanasia, vein graft segments were collected, fixed in 4% paraformaldehyde (PFA) for 24 hours, dehydrated overnight in 60% isopropanol and subsequently

embedded in paraffin. Cross sections of vein graft segments were stained with hematoxylin and eosin to evaluate lumen and lesion area, plaque thickness and percentage of vein stenosis. Neovessels were detected inside vein graft lesions via standard immunohistochemistry using anti-CD31 antibody (endothelial cells; ab124432, Abcam). Anti-TER-119 (550565, BD Biosciences) was used to determine plaque hemorrhages and anti-α-smooth muscle actin (α-SMA) (A2547, Sigma-Aldrich) was used to determine vascular smooth muscle cell (VSMC) coverage of neovessels. Anti-MAC3 (550292, Pharmingen), a Masson's Trichrome stain and anti-vascular cell adhesion molecule-1 (VCAM) (ab134047, Abcam) were used to stain macrophages, collagen and VCAM positive ECs, respectively.

Metabolic parameters

To determine whether ApoE$^{-/-}$PFKFB3^{ECKO} mice exhibit an alteration in glucose metabolism and to characterize the metabolic phenotype, a glucose tolerance test (GTT) and insulin tolerance test (ITT) were done.

To perform GTT, mice were fasted for 16 hours, injected with a single dose of glucose (1 g/kg body weight, i.p.) and then glucose levels in peripheral blood (from tail) were determined after fixed time intervals (0-30-60-120 minutes) using hand-held glucometer (OneTouch Ultra, range 20-600 mg/dL; Lifescan). For ITT, a single insulin dose was injected (Novorapid, 1 U/kg body weight, i.p.) in mice and blood glucose levels were monitored as in GTT. Liver enzymes, total cholesterol and triglycerides, were analyzed with an automated Vista 1500 System (Siemens Healthcare Diagnostics). Insulin and β-hydroxybutyrate in plasma samples were determined with a mouse insulin ELISA kit (80-INSMS-E01, ALPCO) and β-hydroxybutyrate assay kit (ab83390, Abcam), respectively.

Aortic sprouting

An aortic ring assay was performed as previously described.[19] In brief, murine thoracic aortas were dissected, cleaned under sterile conditions, transferred to 10 cm culture dishes, and cut into 0.5 mm thick rings with a sterile scalpel. After overnight starvation in serum-free Opti-MEM at 37°C, ring segments were transferred into wells of a 96-well plate coated with 50 µL of a freshly prepared collagen type I solution (1 mg/mL). The aortic rings remained in Opti-MEM (supplemented with 2.5% fetal bovine serum and antibiotics) in the presence or absence of vascular endothelial growth factor (40 ng/mL, R&D Systems). Medium was

replaced every 2 days. On day 6, rings were fixed with 4% paraformaldehyde and stained with von Willebrand factor antibody (PC054, Binding Site), that was added overnight prior to fluorescence microscopy imaging. The number of sprouts was counted for each ring and sprout numbers per ring were averaged for each group and graphed.

Mouse lung EC isolation

Primary mouse ECs were isolated as previously described.[20] Briefly, 4 lungs were harvested, finely minced with scissors and digested with 1.5 mg/ml collagenase Type I (Sigma-Aldrich #C0130) at 37°C for 45 min (under gentle agitation). The digested cell suspension was filtered on a 70 µM sterile cell strainer, and spun at 400g for 10 min. The pellet was resuspended in 2 ml of 0.1% bovine serum albumin and 50 µl magnetic dynabeads (ThermoFisher #11035) precoated overnight with anti-mouse CD31 (BD Pharmingen #553370) for EC-positive selection. After 20 min at room temperature under slow rotation, the bead-bound cells were recovered with a magnetic separator and washed five times with DMEM containing 10% fetal bovine serum. Cells were finally resuspended in 10 ml of complete DMEM medium (DMEM containing 20% fetal bovine serum, endothelial cell growth supplement and antibiotics) and seeded onto gelatin-precoated 10 cm plates.

Western blot analyses

Cells were lysed in an appropriate volume of Laemmli sample buffer (Bio-Rad) containing β-mercaptoethanol (Sigma-Aldrich) and boiled for 5 min. Protein samples were then loaded onto pre-casted Bolt 4-12% Tris-Bis gels (Invitrogen) and after electrophoresis transferred to Immobilon-FL PVDF membranes (Millipore) according to standard procedures. Membranes were blocked for 1 hour with Odyssey blocking buffer (LI-COR Biosciences) diluted 1:5 with PBS. After blocking, membranes were probed overnight at 4°C with primary antibodies diluted in Odyssey blocking buffer, followed by 1 hour incubation with IRDye-labeled secondary antibodies at room temperature. Antibody detection was achieved using an Odyssey SA infrared imaging system (LI-COR Biosciences). The intensity of the protein bands was quantified using Image Studio software. The following primary antibodies were used: anti-β-actin (ab8226, Abcam) and anti-PFKFB3 (ab181861, Abcam). IRDye-labelled secondary antibodies (goat anti-mouse IgG, 926-68070, and goat anti-rabbit IgG, 926-32211) were purchased from LI-COR Biosciences.

Statistics

All data are expressed as mean ± SEM. Statistical analyses were performed using Graph Prism software (version 8). Statistical tests are specified in the figure legends. Differences were considered significant at $P<0.05$.

Results

ECs of ApoE$^{-/-}$PFKFB3^{ECKO} mice are PFKFB3 deficient

To assess the efficiency of PFKFB3 deletion after tamoxifen injection, lung ECs from ApoE$^{-/-}$PFKFB3$^{fl/fl}$ and ApoE$^{-/-}$PFKFB3^{ECKO} mice were isolated and examined by western blotting. PFKFB3 protein levels were reduced by more than 80% in ApoE$^{-/-}$PFKFB3^{ECKO} mice (Supplemental Figure II A). Similar findings were observed after co-staining of thoracic aorta segments with anti-PFKFB3 and anti-von Willebrand factor antibodies (Supplemental Figure II B).

ECs of ApoE$^{-/-}$PFKFB3^{ECKO} mice show impaired sprouting in an ex vivo mouse aortic ring assay

Previous findings have shown that inhibition of PFKFB3 leads to a reduction of EC migration and proliferation in vitro.[17] In line with these results, we found that vascular endothelial growth factor-induced sprouting in aortic rings of ApoE$^{-/-}$PFKFB3^{ECKO} mice was 65% less as compared to ApoE$^{-/-}$PFKFB3$^{fl/fl}$ control mice (Supplemental Figure III). This observation indicates a direct effect of endothelial PFKFB3 on angiogenesis.

PFKFB3 deficiency in ECs does not cause metabolic changes in adult mice

To evaluate whether EC-specific PFKFB3 gene deletion affects general metabolism, we analyzed plasma samples of ApoE$^{-/-}$PFKFB3$^{fl/fl}$ and ApoE$^{-/-}$PFKFB3^{ECKO} mice after 4 weeks western-type diet. No differences were observed in liver enzymes (γ-glutamyltransferase, alanine transaminase, alkaline phosphatase) and insulin (Table 1), indicating that PFKFB3 deletion in ECs has no obvious systemic side effects.

Moreover, there were no differences in glucose and insulin tolerance tests after 12 weeks western-type diet (Supplemental Figure IV), indicating that glucose absorption and insulin receptor sensitivity is normal in both strains. Also, body weight and cholesterol levels were not different between both groups of mice (Table 1). ApoE$^{-/-}$PFKFB3^{ECKO} mice displayed a trend toward reduced levels of plasma triglycerides as compared to controls, though this effect was not statistically significant (P=0.3698). In addition, levels of the ketone-body β-hydroxybutyrate were not changed in ApoE$^{-/-}$PFKFB3^{ECKO} mice as compared to ApoE$^{-/-}$PFKFB3$^{fl/fl}$ mice (Table 1). These observations suggest that endothelial PFKFB3 deletion does not induce a metabolic switch from glucose to fatty acid–derived ketones and does not cause major side effects in ApoE$^{-/-}$ mice.

Table 1. Metabolic parameters of ApoE$^{-/-}$PFKFB3$^{fl/fl}$ and ApoE$^{-/-}$PFKFB3^{ECKO} mice

Metabolic parameters	ApoE$^{-/-}$PFKFB3$^{fl/fl}$	ApoE$^{-/-}$PFKFB3^{ECKO}
Liver enzymes		
- γ-glutamyltransferase (U/L) - Alanine transaminase (U/L) - Alkaline phosphatase (U/L)	5.5 ± 0.6 39 ± 11 132 ± 13	5 ± 0.4 34 ± 6 154 ± 13
Fasting blood glucose (mg/dL)	116 ± 4	100 ± 8
Non-fasting blood glucose (mg/dL)	152 ± 9	138 ± 10
Insulin (ng/ml)	0.2 ± 0.1	0.2 ± 0.1
Total cholesterol (mg/dL)	306 ± 2	317 ± 1
Body weight (g)	20 ± 0.4	19 ± 0.3
Triglycerides (mg/dL)	79 ± 23	57 ± 6
β-hydroxybutyrate (μM)	1.9 ± 0.2	2.0 ± 0.1

Data between ApoE$^{-/-}$PFKFB3^{ECKO} and ApoE$^{-/-}$PFKFB3$^{fl/fl}$ mice are not significantly different (Independent Sample t-test, n=8-11).

PFKFB3 deficiency in ECs inhibits neovascularization in vein graft lesions

Both ApoE$^{-/-}$PFKFB3$^{fl/fl}$ and ApoE$^{-/-}$PFKFB3^{ECKO} mice displayed an intact endothelium 28 days after vein graft surgery (black arrows Figure 1A-B; Figure 2A-B). Circular oriented VSMCs were seen in ApoE$^{-/-}$PFKFB3$^{fl/fl}$ and ApoE$^{-/-}$PFKFB3^{ECKO} vein graft lesions, close to the lumen, suggesting a cap-like organization (white arrows, Figure 1A-B). Foam cells, a small necrotic core and cholesterol crystals were found particularly in vein grafts of ApoE$^{-/-}$PFKFB3$^{fl/fl}$ mice near the luminal side (asterisks, Figure 1A-B). Furthermore, neovessels were found through the vein graft wall, predominantly in ApoE$^{-/-}$PFKFB3$^{fl/fl}$ mice. The newly formed vessels were often leaky as extravasated erythrocytes were found near and outside these microvessels (Figure 1 A-B).

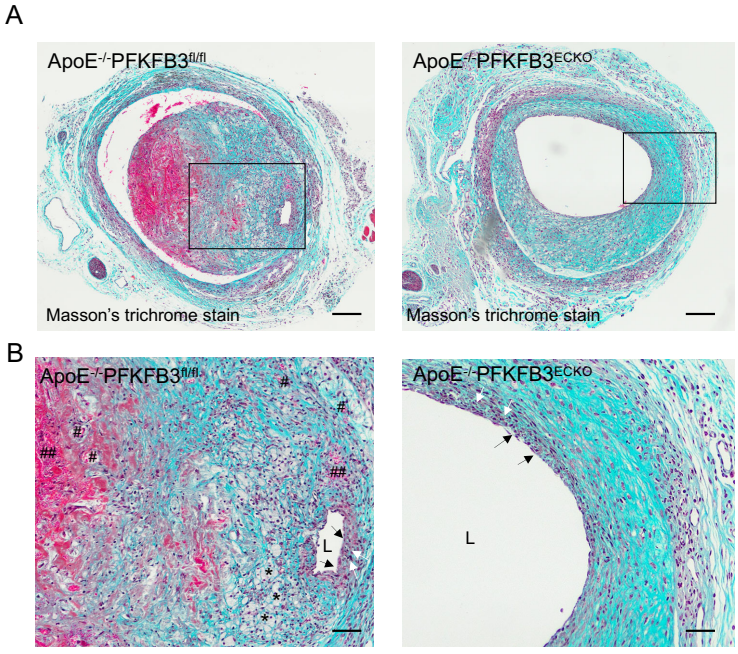

Figure 1. PFKFB3 deletion in endothelial cells evokes a more stable vein graft lesion phenotype. (A) Masson's Trichrome staining of representative vein grafts. Scale bar = 200 µm. (B) Boxed area of panel A showing an almost intact endothelium exposed to the lumen (L) (black arrows), a fibrous cap with numerous vascular smooth muscle cells (white arrows),

small foam cells (asterisks), an area with extravasate erythrocytes (##) and neovascularization (#). Scale bar = 100 μm.

As shown by a CD31 staining, the number of microvessels per lesion was reduced by 62% in ApoE$^{-/-}$PFKFB3^{ECKO} vs ApoE$^{-/-}$PFKFB3$^{fl/fl}$ mice (Figure 2A-2B, 2E). IP microvessels, were further characterized with α-SMA staining to detect the presence of a VSMC layer around the microvessels (Figure 2C-D). VSMC coverage was observed in vein grafts from both ApoE$^{-/-}$PFKFB3^{ECKO} and ApoE$^{-/-}$PFKFB3$^{fl/fl}$ mice (Figure 2F). There was not statistically difference between the two groups (p=0.05), although a trend of higher VSMC coverage in ApoE$^{-/-}$PFKFB3^{ECKO} mice was observed. The organization of the microvessel network was further assessed by immunofluorescence confocal microscopy (Figure 3). Staining of graft lesions with CD31 antibody revealed IP microvessels that were often covered by VSMCs as demonstrated by α-SMA staining (Figure 3). These findings suggest that IP microvessels are able to reach a significant level of structural and multicellular complexity. Anti-TER-119 staining showed more erythrocyte infiltration into the lesions of ApoE-/-PFKFB3$^{fl/fl}$ mice as compared to lesions of ApoE$^{-/-}$PFKFB3^{ECKO} mice (Figure 4A-C), suggesting increased IP vessel leakage in ApoE-/-PFKFB3$^{fl/fl}$ mice. A possible mechanism behind this effect may be due to tightening EC junctions following PFKFB3 deletion as recently demonstrated. [15]

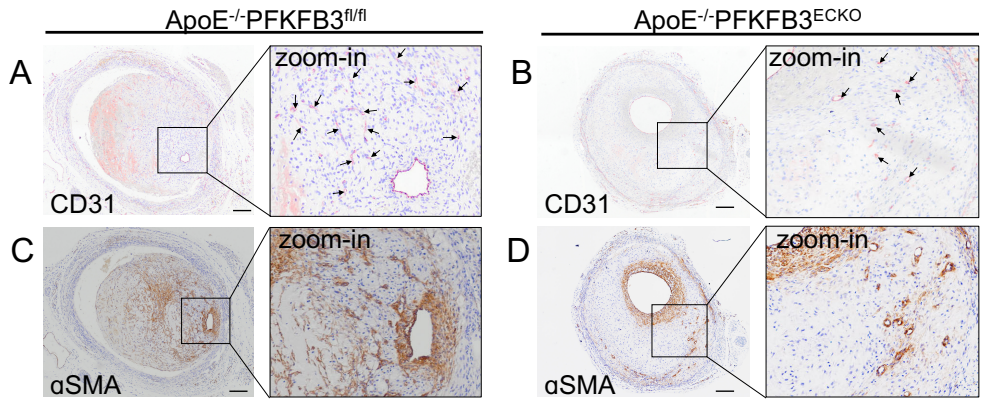

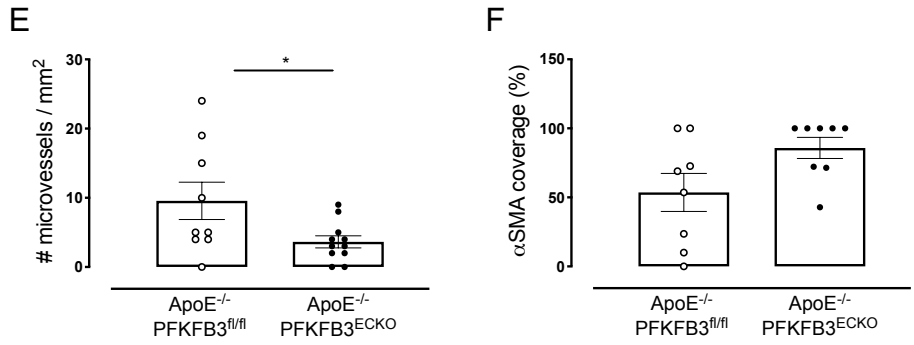

Figure 2. **PFKFB3 deficiency in endothelial cells inhibits intraplaque neovascularization in vein graft lesions but does not alter αSMA coverage of microvessels.** (A-B) Representative vein graft lesions stained with CD31 antibody. (C-D) Representative vein graft lesions stained with anti-αSMA. (E) Quantification of microvessels in vein grafts of ApoE$^{-/-}$ PFKFB3$^{fl/fl}$ and ApoE$^{-/-}$PFKFB3^{ECKO} mice. (F) Quantification of α-SMA coverage of microvessels in vein grafts of ApoE$^{-/-}$PFKFB3$^{fl/fl}$ and ApoE$^{-/-}$PFKFB3^{ECKO} mice. (Independent samples t test; n=8-11). Microvessels are marked by arrows. Scale bar= 200 μm

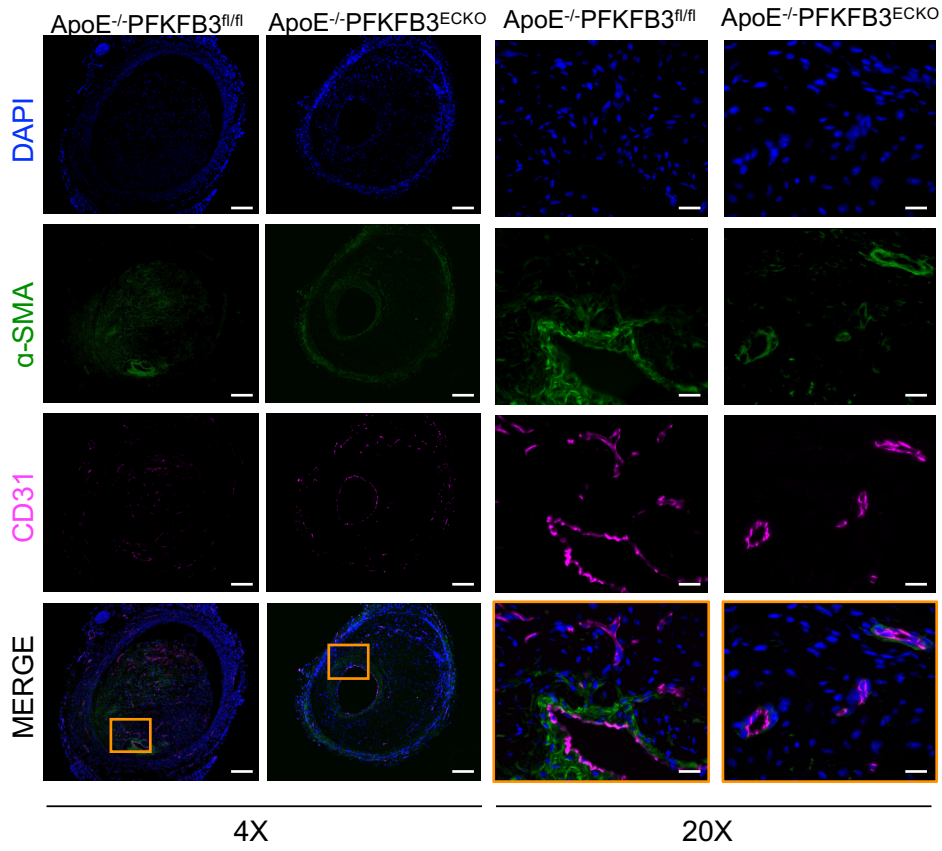

Figure 3. Examples of atherosclerotic lesions in vein grafts of ApoE$^{-/-}$PFKFB3$^{fl/fl}$ and ApoE$^{-/-}$PFKFB3^{ECKO} mice stained with anti-CD31, α-SMA and DAPI. An overlay of the three stainings is also shown as well as a magnification (20x) of the boxed areas showing mature and immature vessels. Scale bar = 500 μm (4x) or 100 μm (20x).

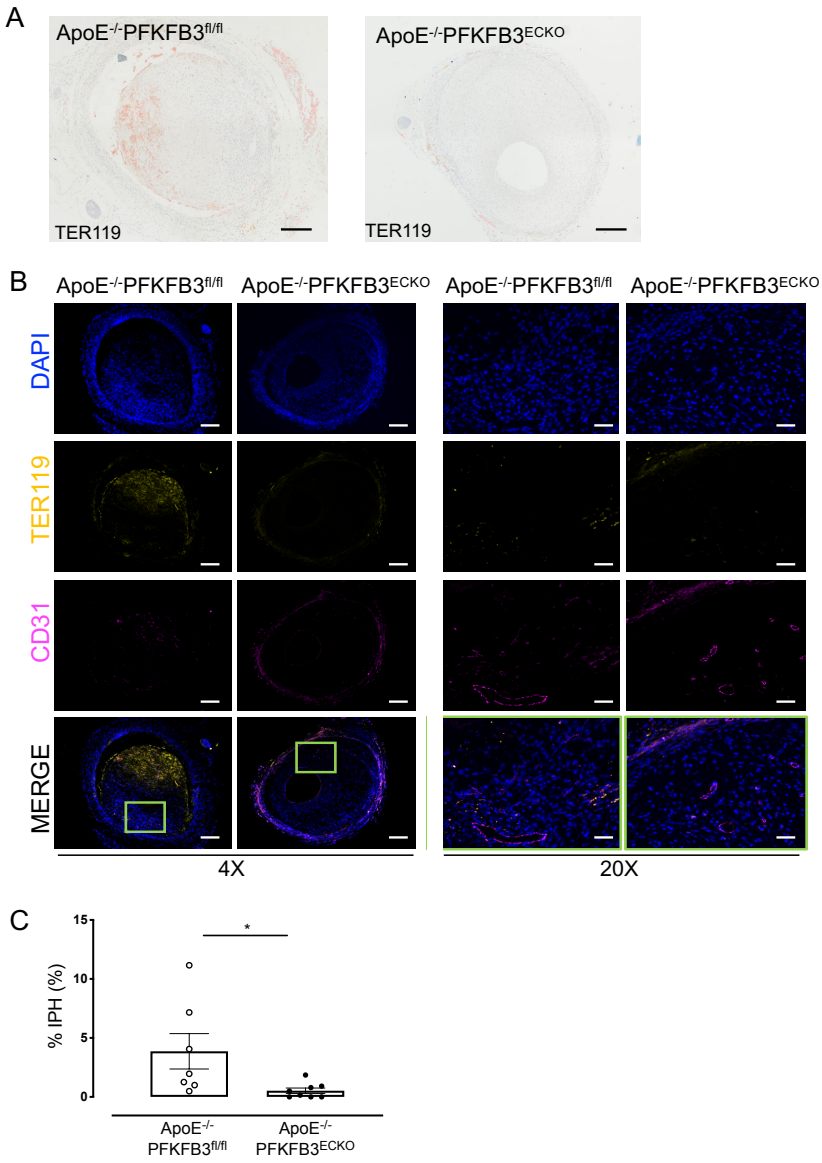

Figure 4. PFKFB3 deficiency in endothelial cells reduces intraplaque hemorrhages (IPH) in vein graft lesions. (A) Representative vein graft lesions stained with anti-TER-119. Scale bar= 200 μm. (B) Examples of atherosclerotic lesions in vein grafts of ApoE$^{-/-}$PFKFB3$^{fl/fl}$ and ApoE$^{-/-}$PFKFB3^{ECKO} mice stained with anti-CD31, anti-TER-119 and DAPI. An overlay of the three stainings is also shown as well as a magnification (20x) of the boxed areas showing erythrocyte extravasation. Scale bar = 500 μm (4x) or 100 μm (20x). (C) Quantification of IPH. *P<0.05 versus ApoE$^{-/-}$PFKFB3$^{fl/fl}$ (Independent samples t-test; n=6-8).

PFKFB3 deficiency in ECs reduces lesion size of vein grafts

Twenty-eight days after vein graft surgery, the lesion area in the graft was decreased by 36% in ApoE$^{-/-}$PFKFB3^{ECKO} mice as compared to ApoE$^{-/-}$PFKFB3$^{fl/fl}$ mice (Figure 5A-B), suggesting a significant role of endothelial PFKFB3 in lesion formation and/or progression. Vein graft stenosis was reduced by 23% and lesion thickness was reduced by 33% in vein grafts of ApoE$^{-/-}$PFKFB3^{ECKO} mice (Figure 5C-D).

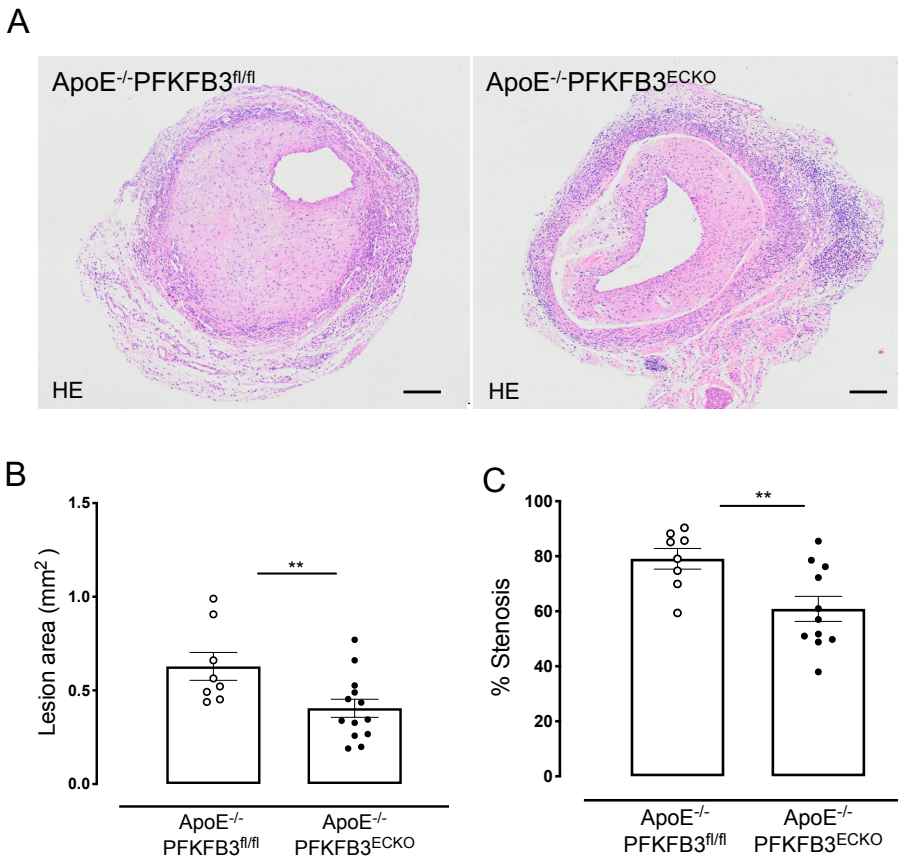

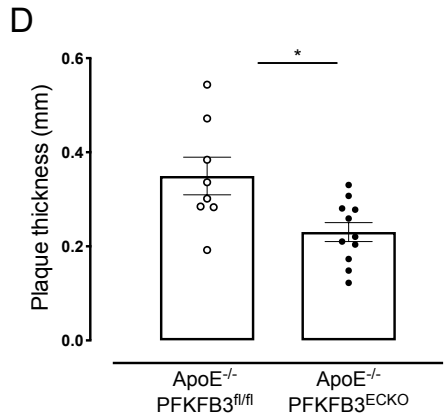

Figure 5. **PFKFB3 deficiency in endothelial cells reduces the area, percentage stenosis and thickness of vein graft lesions.** Scale bar= 200 µm. (A) Representative cross sections of H&E-stained vein grafts from ApoE-/-PFKFB3fl/fl and ApoE-/-PFKFB3ECKO mice. Scale bar= 200 µm. (B-D) Quantification of lesion area, percentage stenosis and thickness of vein graft lesions. *P<0.05, **P<0.01 versus ApoE-/-PFKFB3fl/fl (Independent samples t-test; n=8-11).

PFKFB3 deficiency in ECs decreases macrophage infiltration

Macrophage accumulation was mainly observed underneath the luminal EC or around the endothelium of microvessels in vein graft lesions of ApoE$^{-/-}$PFKFB3^{ECKO} mice. In vein graft lesions of ApoE$^{-/-}$PFKFB3$^{fl/fl}$ mice, macrophages appeared much more diffuse in the vascular wall (Figure 6A). Quantification of the macrophage infiltration showed a significant decrease in ApoE$^{-/-}$PFKFB3^{ECKO} mice (Figure 6B). Analysis of VCAM-1 expression at the luminal side of the vein graft did not reveal significant differences in ApoE$^{-/-}$PFKFB3^{ECKO} mice as compared to ApoE$^{-/-}$PFKFB3$^{fl/fl}$ mice (Figure 7 A-C).

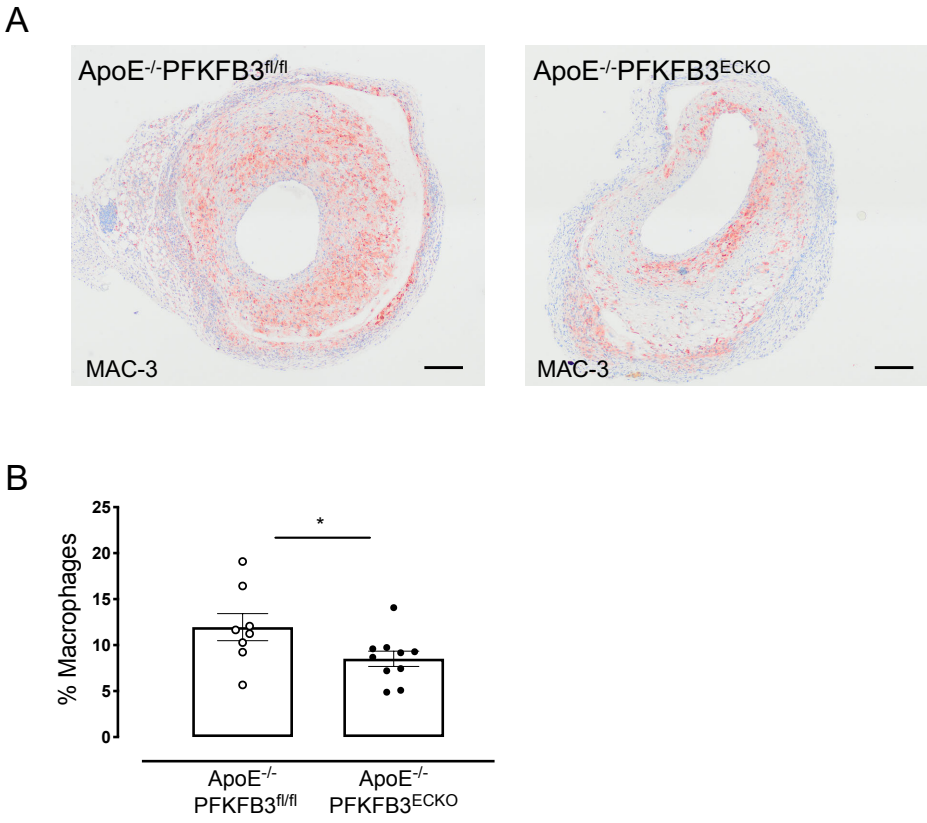

Figure 6. PFKFB3 deficiency in endothelial cells reduces macrophage infiltration in vein graft lesions. (A) Immunohistochemical detection of macrophages in representative vein graft lesions of ApoE$^{-/-}$PFKFB3$^{fl/fl}$ and ApoE$^{-/-}$PFKFB3^{ECKO} mice using MAC3 antibody. Scale bar = 200 μm. (B) Quantification of macrophages in vein graft lesions of ApoE$^{-/-}$PFKFB3$^{fl/fl}$ and ApoE$^{-/-}$PFKFB3^{ECKO} mice. *P<0.05 versus ApoE$^{-/-}$PFKFB3$^{fl/fl}$ mice (Independent samples t-test; n=8-10).

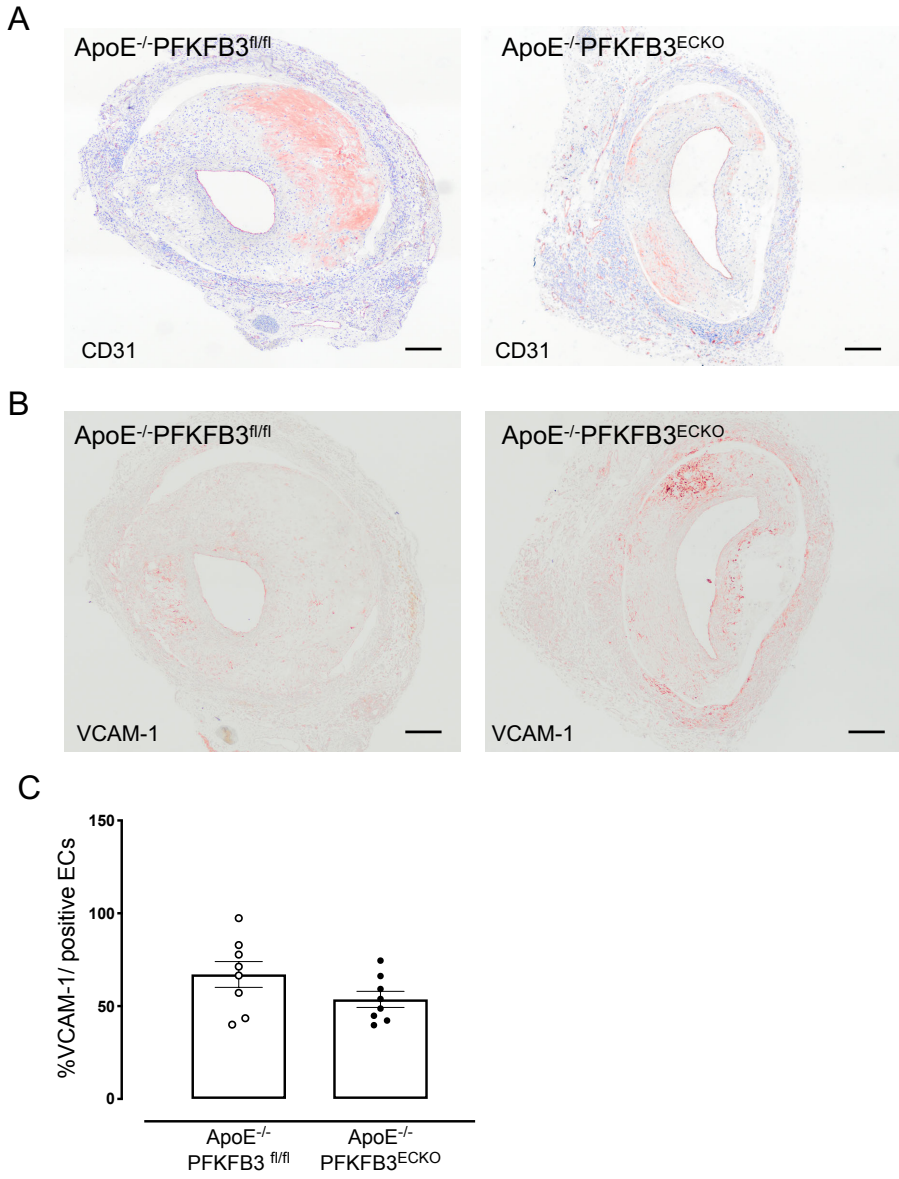

Figure 7. PFKFB3 deficiency in endothelial cells does not influence vascular cell adhesion molecule-1 (VCAM-1) expression in vein graft lesions. (A-B) Immunohistochemical detection of endothelial cells in representative vein graft lesions of ApoE$^{-/-}$PFKFB3$^{fl/fl}$ and ApoE$^{-/-}$PFKFB3^{ECKO} mice using CD31 and VCAM-1 antibody. Scale bar = 200 µm. (C) Quantification of VCAM-1 positive endothelial cells in vein graft lesions of ApoE$^{-/-}$PFKFB3$^{fl/fl}$ and ApoE$^{-/-}$PFKFB3^{ECKO} mice (Independent samples t test, n=8).

PFKFB3 deficiency in ECs has a positive impact on plaque formation in native atherosclerosis

An analysis of total cholesterol did not reveal significant differences between ApoE$^{-/-}$PFKFB3$^{fl/fl}$ and ApoE$^{-/-}$PFKFB3^{ECKO} mice after 12 weeks WD (ApoE$^{-/-}$PFKFB3$^{fl/fl}$ = 574±26 mmol/l vs ApoE$^{-/-}$PFKFB3^{ECKO} = 520±51 mmol/l; P=0.36). Nonetheless, plaque thickness (Figure 6A-B) and percentage stenosis was reduced in ApoE$^{-/-}$PFKFB3^{ECKO} mice as compared to ApoE$^{-/-}$PFKFB3$^{fl/fl}$ mice (Figure 8).

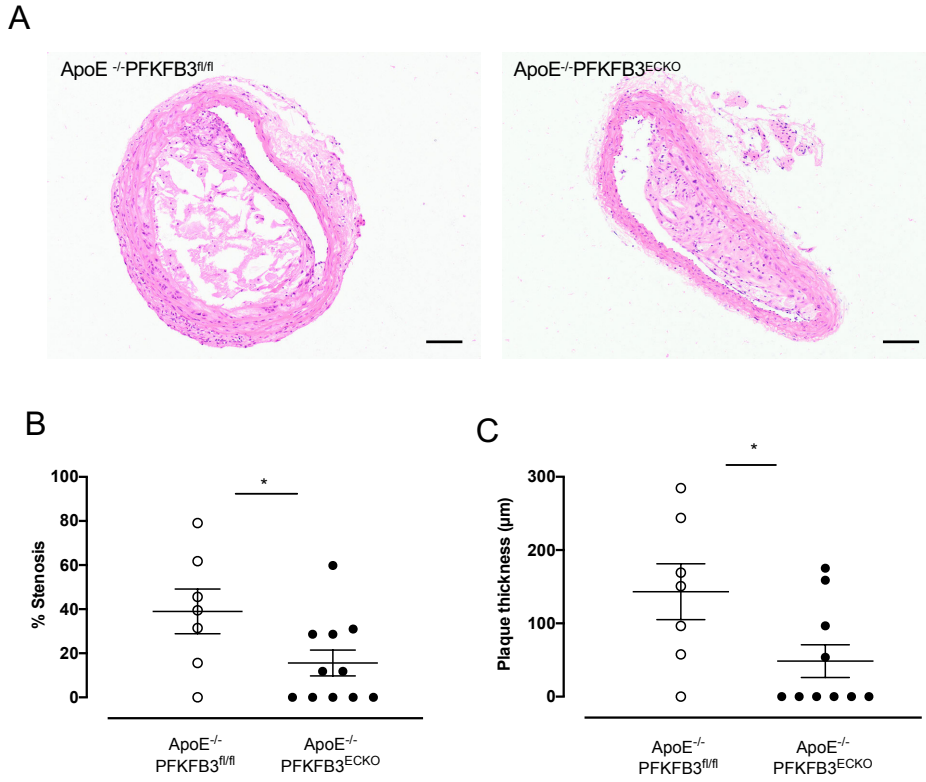

Figure 8. PFKFB3 deficiency in endothelial cells decreases plaque thickness and percentage of stenosis in ApoE$^{-/-}$ mice. Scale bar= 100 µm. (A) Representative plaque lesions of ApoE$^{-/-}$PFKFB3$^{fl/fl}$ and ApoE$^{-/-}$PFKFB3^{ECKO} mice fed a western diet for 12 weeks. (B) Quantification of stenosis and plaque thickness. *P<0.05 versus ApoE$^{-/-}$PFKFB3$^{fl/fl}$ (Independent samples t-test; n=7-11).

Discussion

IP angiogenesis is frequently observed inside human vein graft lesions and is recognized as a contributing factor of plaque vulnerability.[3, 6, 9, 10, 21]

In the present study, we crossed EC-specific PFKFB3 knockout mice with ApoE$^{-/-}$ mice to investigate the role of EC glycolysis modulation in vein graft IP angiogenesis. To our knowledge, this is the first study using a conditional EC-specific PFKFB3 knockout mouse in the context of advanced atherosclerosis.

First of all, we did not observe adverse effects or changes in general metabolism after PFKFB3 deletion in ECs. Circulating liver enzymes, blood glucose, insulin and total cholesterol were not affected. Also glucose and insulin tolerance tests were similar in ApoE$^{-/-}$PFKFB3$^{fl/fl}$ versus ApoE$^{-/-}$PFKFB3^{ECKO} mice. Ketone-body β-hydroxybutyrate was not changed in both groups. These findings suggest that PFKFB3 deletion in ECs does not lead to severe side effects or to a major metabolic switch in ApoE$^{-/-}$ mice.

Next, and in line with previous studies, we found that PFKFB3 deletion impaired vessel sprouting from aortic rings. Along these lines ApoE$^{-/-}$PFKFB3^{ECKO} mice showed a significantly reduced number of microvessels in vein graft lesions.

Moreover, IP microvessels in ApoE$^{-/-}$PFKFB3^{ECKO} showed less leakage of erythrocytes inside the graft lesion. These findings are consistent with recent in vitro and in vivo observations showing that PFKFB3 inhibition reduces VE-cadherin endocytosis and promotes normalization of the endothelial barrier.[15]

We also observed a reduction in plaque size in vein grafts of ApoE$^{-/-}$PFKFB3^{ECKO} mice, which suggests that PFKFB3 may play a direct role in plaque progression. Interestingly, EC-specific deletion of PFKFB3 also promoted an atheroprotective effect in ApoE$^{-/-}$ mice, which normally develop plaques without IP neovessels. These results suggest that PFKFB3 in ECs may affect early onset of atherosclerosis. Although this study was not designed to investigate the impact of EC-specific PFKFB3 deletion on atherogenesis, our findings are in agreement with the general concept that glycolysis inhibition prevents endothelial activation, recruitment of monocytes and vascular inflammation. Such compelling possibility

corresponds with data from in vitro studies showing that PFKFB3 is linked to pro-inflammatory signalling of ECs in response to blood flow shear stress. Indeed, turbulent blood flow in atheroprone regions leads to inhibition of Krüppel-like Factor 2 activity, which correlates with PFKFB3 upregulation, increased EC glycolysis and inflammatory activation.[22] The importance of PFKFB3 in plaque progression has also been suggested by a recent study showing a positive correlation between PFKFB3 expression and an unstable plaque phenotype in both carotid and coronary plaques in humans. [23] Furthermore, administration of the PFKFB3 inhibitor PFK158 in mice led to a reduction in advanced plaques with a vulnerable phenotype and an increase in plaque stability.[23]

Most interestingly, we detected a reduction in the percentage of macrophage infiltration in vein graft lesions of ApoE$^{-/-}$PFKFB3^{ECKO} mice. This finding is in agreement with the presence of crosstalk between EC metabolism and macrophages in pathological conditions as previously reported.[24, 25] For example, in tumor settings a metabolic competition for glucose between EC and macrophages reduces EC hyperactivation and prevent abnormal vessel leakage. [26] PFKFB3 inhibition also abolishes the inflammatory response caused by lipoprotein(a) with concomitant attenuation of transendothelial monocyte migration in atherosclerotic plaques.[27] It is therefore possible that the observed reduction in macrophage infiltration in vivo is in part due to an improved restoration of EC junctions after PFKFB3 deletion.

The reduction of IP angiogenesis in ApoE$^{-/-}$PFKFB3^{ECKO} mice, as described in this study, is in line with previous findings in our group showing decreased IP angiogenesis following administration of the glycolysis inhibitor 3PO in a mouse model of advanced atherosclerosis.[18] Moreover, 3PO significantly reduced initiation of plaque formation in a preventive study design.

Altogether, our findings indicate that endothelial PFKFB3 plays a critical role in IP angiogenesis and lesion progression, and that PFKFB3 inhibition is a promising approach to prevent plaque development and to reduce the complications of vein bypass grafting.

Acknowledgments

a) Acknowledgments: The authors would like to thank Dr. Laurence Roosens, Anne-Elise Van Hoydonck, Hermine Fret, Rita Van den Bossche and Mandy Vermont for technical help. VE-cadherin (PAC)-Cre^{ERT2} mice were a kind gift of Prof. Peter Carmeliet (KULeuven, Belgium). The authors are grateful to Dr. Bronwen Martin for critical reading of the manuscript.

b) Sources of Funding: This work was supported by the University of Antwerp [DOCPRO-BOF] and the Horizon 2020 program of the European Union – Marie Sklodowska Curie actions – ITN – MOGLYNET [grant number 675527].

c) Disclosures: None

Data availability

All primary data that support the findings of this study are available from the corresponding author upon reasonable request.

Supplemental material

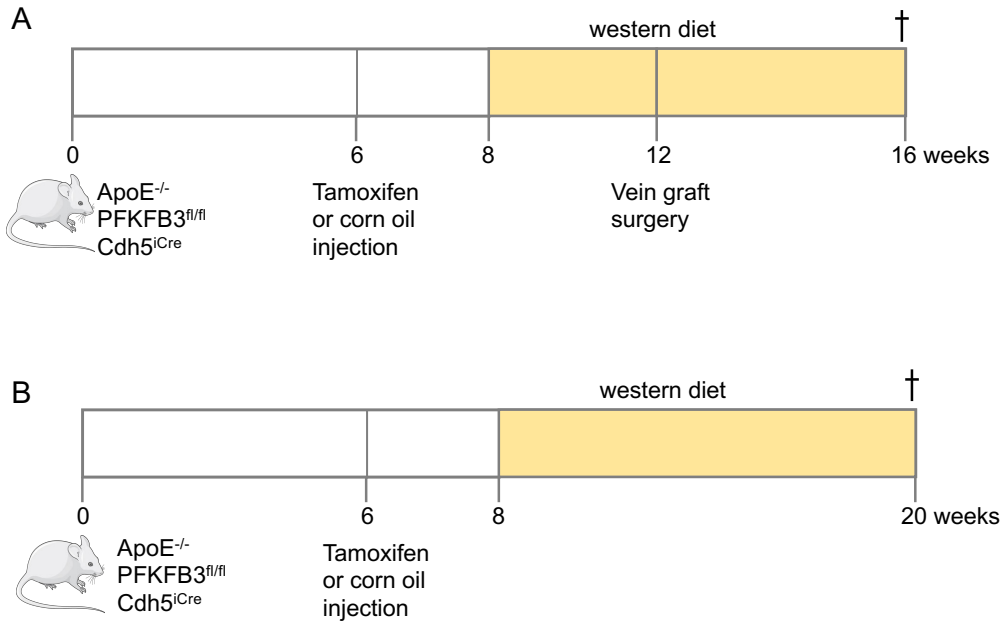

Figure I. Schematic overview of the experimental design. ApoE$^{-/-}$PFKFB3$^{fl/fl}$Cdh5^{iCre} mice (6 weeks old) were injected with tamoxifen (0.1 g/kg body weight) for 5 consecutive days to induce PFKFB3 deletion in ECs. Control mice were injected with corn-oil using the same protocol. After 2 weeks, mice were fed a western-type diet. Four weeks later, vein graft surgeries were performed. Mice were sacrificed 4 weeks after surgery. (B) atherosclerotic plaque study: ApoE$^{-/-}$PFKFB3$^{fl/fl}$Cdh5^{iCre} (6 weeks old) were injected with tamoxifen (0.1 g/kg body weight) for 5 consecutive days to induce PFKFB3 deletion in ECs . Control mice were injected with corn-oil using the same protocol. After 2 weeks, mice were fed a western-type diet. Twelve weeks later, mice were sacrificed.

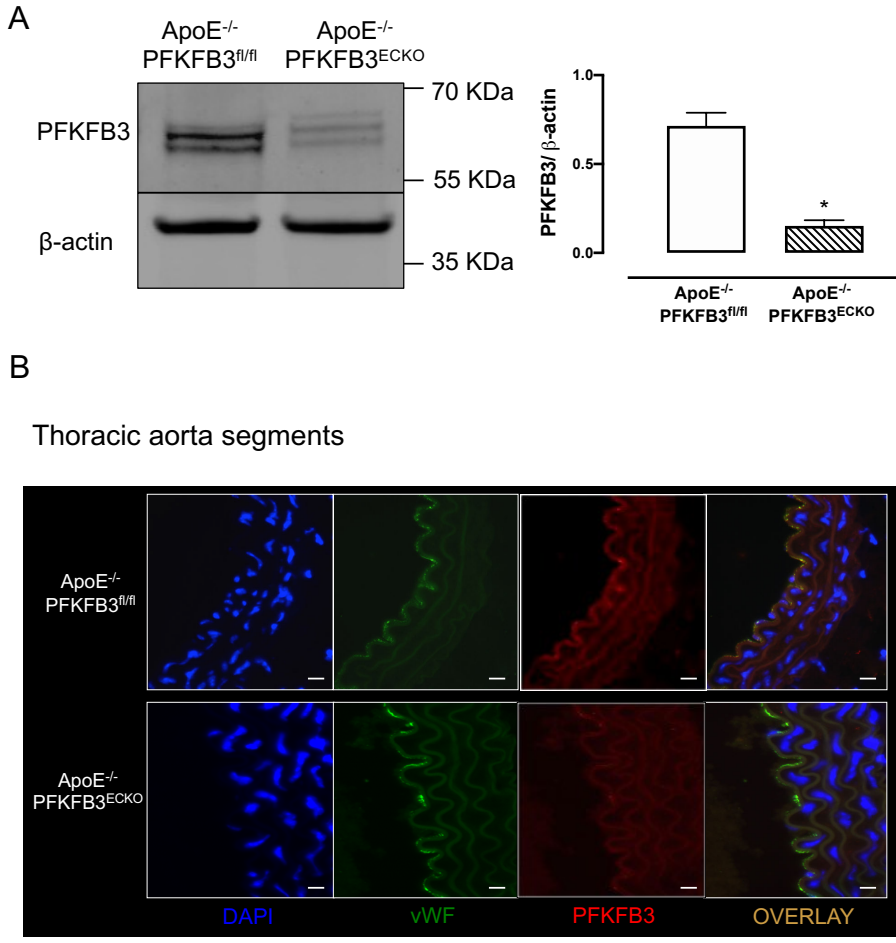

Figure II. Validation of PFKFB3 gene deletion in endothelial cells. (A) Representative western blot showing protein levels of PFKFB3 and β-actin. Bars represent relative protein quantification of PFKFB3 normalized to the reference protein β-actin. *P<0.05 versus ApoE$^{-/-}$PFKFB3$^{fl/fl}$ (Independent samples t-test; n=3). (B) Representative thoracic aorta segments of ApoE$^{-/-}$PFKFB3$^{fl/fl}$ and ApoE$^{-/-}$PFKFB3^{ECKO} stained with antibodies against PFKFB3 or von Willebrand Factor (endothelial cell marker). Nuclei were stained with DAPI.

A

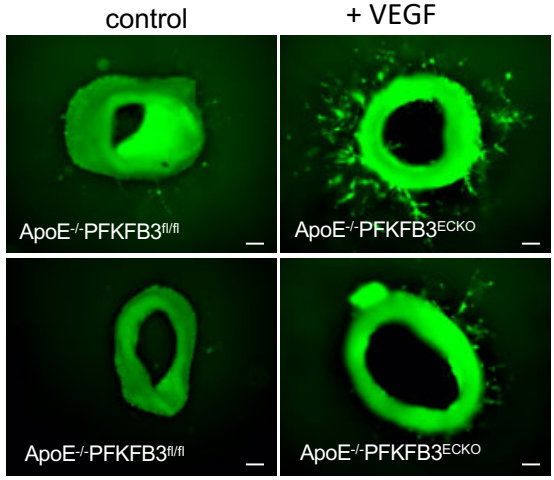

B

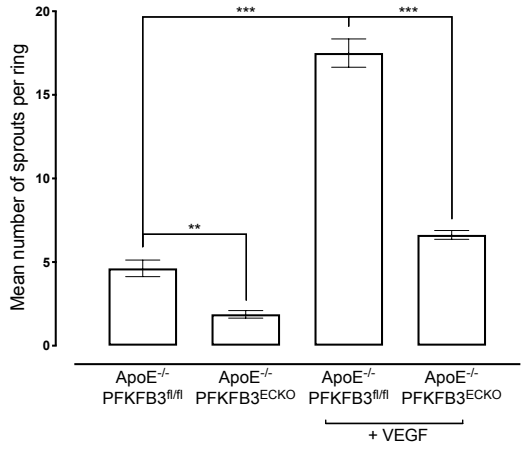

Figure III. PFKFB3 deficiency in endothelial cells inhibits aortic sprouting. (A) Aortic rings from ApoE$^{-/-}$PFKFB3$^{fl/fl}$ and ApoE$^{-/-}$PFKFB3^{ECKO} were embedded in collagen type I and treated with Opti-MEM supplemented with 2.5% FBS (control) in the presence or absence of VEGF (50 ng/mL). At day 6, rings were fixed and stained to delineate ECs. Images of ring sprouting were obtained and quantified. (B) Sprouts were quantified, n=4 mice. ***P<0.0001 One way ANOVA, effect of PFKFB3^{ECKO}: **P<0.005, effect of VEGF: ***P<0.0001, interaction: ***P<0.0001.

A

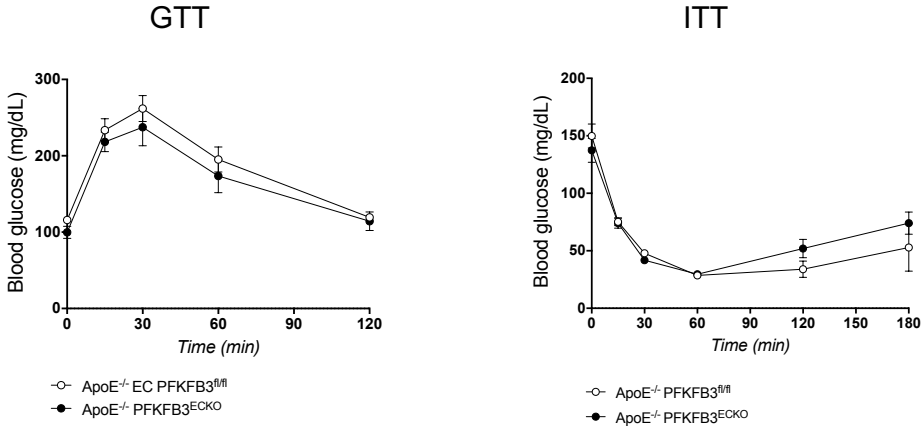

Figure IV. Glucose clearance in ApoE$^{-/-}$PFKFB3$^{fl/fl}$ and ApoE$^{-/-}$PFKFB3^{ECKO} mice after intraperitoneal injection with glucose or insulin. A glucose tolerance test (GTT) and insulin tolerance test (ITT) was performed after 12 weeks of western diet. Blood glucose was measured at different time points after injection of glucose (1 g/kg, i.p.) or insulin (1 U/kg, i.p.).

References

1. Virmani R, Atkinson JB, Forman MB. Aortocoronary saphenous vein bypass grafts. *Cardiovasc Clin*. 1988;18:41-62
2. de Vries MR, Quax PHA. Inflammation in vein graft disease. *Front Cardiovasc Med*. 2018;5:3
3. de Vries MR, Simons KH, Jukema JW, Braun J, Quax PH. Vein graft failure: From pathophysiology to clinical outcomes. *Nat Rev Cardiol*. 2016;13:451-470
4. Yahagi K, Kolodgie FD, Otsuka F, Finn AV, Davis HR, Joner M, Virmani R. Pathophysiology of native coronary, vein graft, and in-stent atherosclerosis. *Nat Rev Cardiol*. 2016;13:79-98
5. de Vries MR, Niessen HW, Lowik CW, Hamming JF, Jukema JW, Quax PH. Plaque rupture complications in murine atherosclerotic vein grafts can be prevented by timp-1 overexpression. *PLoS One*. 2012;7:e47134
6. Janiec M, Nazari Shafti TZ, Dimberg A, Lagerqvist B, Lindblom RPF. Graft failure and recurrence of symptoms after coronary artery bypass grafting. *Scand Cardiovasc J*. 2018;52:113-119
7. de Vries MR, Parma L, Peters HAB, Schepers A, Hamming JF, Jukema JW, Goumans M, Guo L, Finn AV, Virmani R, Ozaki CK, Quax PHA. Blockade of vascular endothelial growth factor receptor 2 inhibits intraplaque haemorrhage by normalization of plaque neovessels. *J Intern Med*. 2019;285:59-74
8. Aarup A, Pedersen TX, Junker N, Christoffersen C, Bartels ED, Madsen M, Nielsen CH, Nielsen LB. Hypoxia-inducible factor-1alpha expression in macrophages promotes development of atherosclerosis. *Arterioscler Thromb Vasc Biol*. 2016;36:1782-1790
9. Parma L, Baganha F, Quax PHA, de Vries MR. Plaque angiogenesis and intraplaque hemorrhage in atherosclerosis. *Eur J Pharmacol*. 2017;816:107-115
10. de Vries MR, Quax PH. Plaque angiogenesis and its relation to inflammation and atherosclerotic plaque destabilization. *Curr Opin Lipidol*. 2016;27:499-506

11. Carmeliet P. Angiogenesis in health and disease. *Nat Med*. 2003;9:653-660
12. Cantelmo AR, Brajic A, Carmeliet P. Endothelial metabolism driving angiogenesis: Emerging concepts and principles. *Cancer J*. 2015;21:244-249
13. Eelen G, de Zeeuw P, Treps L, Harjes U, Wong BW, Carmeliet P. Endothelial cell metabolism. *Physiol Rev*. 2018;98:3-58
14. Tawakol A, Singh P, Mojena M, Pimentel-Santillana M, Emami H, MacNabb M, Rudd JH, Narula J, Enriquez JA, Traves PG, Fernandez-Velasco M, Bartrons R, Martin-Sanz P, Fayad ZA, Tejedor A, Bosca L. Hif-1alpha and pfkfb3 mediate a tight relationship between proinflammatory activation and anerobic metabolism in atherosclerotic macrophages. *Arterioscler Thromb Vasc Biol*. 2015;35:1463-1471
15. Cantelmo AR, Conradi LC, Brajic A, Goveia J, Kalucka J, Pircher A, Chaturvedi P, Hol J, Thienpont B, Teuwen LA, Schoors S, Boeckx B, Vriens J, Kuchnio A, Veys K, Cruys B, Finotto L, Treps L, Stav-Noraas TE, Bifari F, Stapor P, Decimo I, Kampen K, De Bock K, Haraldsen G, Schoonjans L, Rabelink T, Eelen G, Ghesquiere B, Rehman J, Lambrechts D, Malik AB, Dewerchin M, Carmeliet P. Inhibition of the glycolytic activator pfkfb3 in endothelium induces tumor vessel normalization, impairs metastasis, and improves chemotherapy. *Cancer Cell*. 2016;30:968-985
16. Schoors S, De Bock K, Cantelmo AR, Georgiadou M, Ghesquiere B, Cauwenberghs S, Kuchnio A, Wong BW, Quaegebeur A, Goveia J, Bifari F, Wang X, Blanco R, Tembuyser B, Cornelissen I, Bouche A, Vinckier S, Diaz-Moralli S, Gerhardt H, Telang S, Cascante M, Chesney J, Dewerchin M, Carmeliet P. Partial and transient reduction of glycolysis by pfkfb3 blockade reduces pathological angiogenesis. *Cell Metab*. 2014;19:37-48
17. De Bock K, Georgiadou M, Schoors S, Kuchnio A, Wong BW, Cantelmo AR, Quaegebeur A, Ghesquiere B, Cauwenberghs S, Eelen G, Phng LK, Betz I, Tembuyser B, Brepoels K, Welti J, Geudens I, Segura I, Cruys B, Bifari F, Decimo I, Blanco R, Wyns S, Vangindertael J, Rocha S, Collins RT, Munck S, Daelemans D, Imamura H, Devlieger R, Rider M, Van Veldhoven PP, Schuit F, Bartrons R, Hofkens J, Fraisl P, Telang S, Deberardinis RJ, Schoonjans L, Vinckier S, Chesney J, Gerhardt H, Dewerchin M, Carmeliet

P. Role of pfkfb3-driven glycolysis in vessel sprouting. *Cell*. 2013;154:651-663

18. Perrotta P, Van der Veken B, Van Der Veken P, Pintelon I, Roosens L, Adriaenssens E, Timmerman V, Guns PJ, De Meyer GRY, Martinet W. Partial inhibition of glycolysis reduces atherogenesis independent of intraplaque neovascularization in mice. *Arterioscler Thromb Vasc Biol*. 2020:ATVBAHA119313692
19. Landskroner-Eiger S, Qiu C, Perrotta P, Siragusa M, Lee MY, Ulrich V, Luciano AK, Zhuang ZW, Corti F, Simons M, Montgomery RL, Wu D, Yu J, Sessa WC. Endothelial mir-17 approximately 92 cluster negatively regulates arteriogenesis via mirna-19 repression of wnt signaling. *Proc Natl Acad Sci U S A*. 2015;112:12812-12817
20. Corti F, Wang Y, Rhodes JM, Atri D, Archer-Hartmann S, Zhang J, Zhuang ZW, Chen D, Wang T, Wang Z, Azadi P, Simons M. N-terminal syndecan-2 domain selectively enhances 6-o heparan sulfate chains sulfation and promotes vegfa165-dependent neovascularization. *Nat Commun*. 2019;10:1562
21. Parma L, Peters HAB, Baganha F, Sluimer JC, de Vries MR, Quax PHA. Prolonged hyperoxygenation treatment improves vein graft patency and decreases macrophage content in atherosclerotic lesions in apoe3*leiden mice. *Cells*. 2020;9
22. Doddaballapur A, Michalik KM, Manavski Y, Lucas T, Houtkooper RH, You X, Chen W, Zeiher AM, Potente M, Dimmeler S, Boon RA. Laminar shear stress inhibits endothelial cell metabolism via klf2-mediated repression of pfkfb3. *Arterioscler Thromb Vasc Biol*. 2015;35:137-145
23. Poels K, Schnitzler JG, Waissi F, Levels JHM, Stroes ESG, Daemen M, Lutgens E, Pennekamp AM, De Kleijn DPV, Seijkens TTP, Kroon J. Inhibition of pfkfb3 hampers the progression of atherosclerosis and promotes plaque stability. *Front Cell Dev Biol*. 2020;8:581641
24. Baer C, Squadrito ML, Iruela-Arispe ML, De Palma M. Reciprocal interactions between endothelial cells and macrophages in angiogenic vascular niches. *Exp Cell Res*. 2013;319:1626-1634

25. Kalucka J, Bierhansl L, Wielockx B, Carmeliet P, Eelen G. Interaction of endothelial cells with macrophages-linking molecular and metabolic signaling. *Pflugers Arch*. 2017;469:473-483
26. Wenes M, Shang M, Di Matteo M, Goveia J, Martin-Perez R, Serneels J, Prenen H, Ghesquiere B, Carmeliet P, Mazzone M. Macrophage metabolism controls tumor blood vessel morphogenesis and metastasis. *Cell Metab*. 2016;24:701-715
27. Schnitzler JG, Hoogeveen RM, Ali L, Prange KHM, Waissi F, van Weeghel M, Bachmann JC, Versloot M, Borrelli MJ, Yeang C, De Kleijn DPV, Houtkooper RH, Koschinsky ML, de Winther MPJ, Groen AK, Witztum JL, Tsimikas S, Stroes ESG, Kroon J. Atherogenic lipoprotein(a) increases vascular glycolysis, thereby facilitating inflammation and leukocyte extravasation. *Circ Res*. 2020;126:1346-1359
28. Emini Veseli B, Perrotta P, Van Wielendaele P, Lambeir AM, Abdali A, Bellosta S, Monaco G, Bultynck G, Martinet W, De Meyer GRY. Small molecule 3po inhibits glycolysis but does not bind to 6-phosphofructo-2-kinase/fructose-2,6-bisphosphatase-3 (pfkfb3). *FEBS Lett*. 2020

Chapter 7

[^{18}F]ZCDD083: a PFKFB3 targeted PET tracer for imaging the atherosclerotic plaque

De Dominicis C, **Perrotta P**, Dall'Angelo S, Wyffels L, Staelens S, De Meyer GRY, Matteo Zanda M.

ACS Medicinal Chemistry Letters.2020;11:933-939

Abstract

An emerging target for diagnosis and therapy of atherosclerosis is PFKFB3, a glycolysis-related enzyme up-regulated in inflammatory conditions and angiogenesis. A tosylated precursor of the phenoxindazole PFKFB3 inhibitor [^{18}F]ZCDD083 was synthesised, radiolabelled in 17 ±5% radiochemical yield and >99% radiochemical purity and formulated for *in vivo* PET imaging. *In vivo* stability analysis showed no significant metabolite formation. Biodistribution studies showed high blood pool activity and slow hepatobiliary clearance. Significant activity was detected in the lung (2 h pi: 11.0 ±1.5 %ID/g), while at 6h pi no pulmonary background was observed. *Ex vivo* autoradiography at 6 h pi showed significant high uptake of [^{18}F]ZCDD083 in arch region and brachiocephalic artery of atherosclerotic mice, and no uptake in control mice. This is consistent with plaques distribution seen by lipid staining along with PFKFB3 expression seen by immunofluorescent staining. *In vivo* PET scans showed higher aortic region uptake of [^{18}F]ZCDD083 in atherosclerotic ApoE$^{-/-}$Fbn1$^{C1039G+/-}$ than control mice (0.78 ± 0.05 vs 0.44 ± 0.09 %ID/g). [^{18}F]ZCDD083 was detected in aortic arch and brachiocephalic artery of ApoE$^{-/-}$ (with moderate atherosclerosis) and ApoE$^{-/-}$Fbn1$^{C1039G+/-}$ (with severe, advanced atherosclerosis) mice, suggesting that it may represent a promising tracer for the non-invasive detection of atherosclerotic plaques

Introduction

Atherosclerosis is a pathological process characterized by progressive accumulation of lipids, inflammatory cells and connective tissue in the arterial wall.[1] This process, leading to the formation of the so-called “atherosclerotic plaques”, is predominantly asymptomatic. However, the progression of the disease can cause progressive stenosis of arterial lumen, which can eventually result in ischemic heart pain. Acute clinical events, such as myocardial infarction, stroke and unstable angina, are mainly associated with instability of plaques and formation of occlusive thrombi.[2] According to World Health Organization (WHO), cardiovascular diseases are the first cause of death worldwide and indeed atherosclerosis is a condition associated with the majority of these diseases.[3,4]

The progression of atherosclerotic plaques is initially asymptomatic, characterized by the slow growth of “silent” stable plaques. The development of fibrous plaques in coronary arteries may lead to stable angina, whereas plaque rupture is associated with unstable angina, acute myocardial infarction (MI), and sudden cardiac death. Similarly, rupture of carotid artery plaque is associated with cerebral ischemic events.[5] The risk of thrombotic complications of atherosclerosis is mostly related to the instability of an atheroma rather than the size of the plaque.

Currently, cardiovascular medicine aims principally to identify atherosclerotic plaques prone to rupture, improve the risk stratification, monitor the disease progression, assess new anti-atherosclerotic therapies and promptly evaluate the efficacy of therapeutic treatment. PET imaging is non-invasive and has a great potential in this context. Indeed, new targets and radiotracers are currently being investigated for imaging unstable atherosclerotic plaque.[6,7]

We have studied PFKFB3 enzyme as a new target to be used for the in vivo assessment of atherosclerotic plaques.[8,9] PFKFB3 is a glycolysis-related enzyme upregulated in inflammatory and hypoxic conditions.[10,11] Several studies have shown a tight correlation between PFKFB3 and angiogenesis, which is a feature of vulnerable atherosclerotic plaques.[12,13,14,15] Here we described the development of a specific PET radiotracer targeting PFKFB3 - the ^{18}F-radiolabelled phenoxindazole ZCDD083 – based on the structure of the potent PFKFB3 inhibitor AZ68 (IC_{50}= 4nM).[16]

Results

Fragment 2 (Scheme 1) was obtained from N-Boc-proline and O-Bn-4-aminophenol which were coupled to afford compound 1 which was debenzylated over Pd.

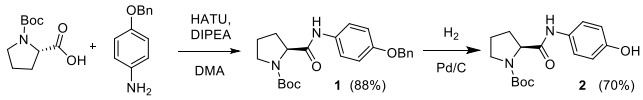

Scheme 1. Synthesis of fragment 2.

Fragment 4 (Scheme 2) was synthesized by NIS-promoted iodination of (2-amino) phenyl-acetonitrile, followed by indazole ring formation via Sandmeyer reaction and intramolecular ring closure of the diazonium salt formed from 3.

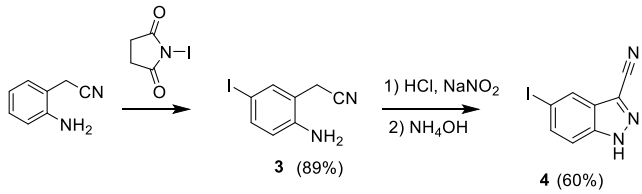

Scheme 2. Synthesis of fragment 4.

The radiofluorination precursor 7 (Scheme 3) was synthesized next. Commercial 2-methyl-1,3-propanediol was then treated with tosyl chloride to give the mono tosylated derivative 5, which was reacted with the indazole 4 via Mitsunobu reaction to give compound 6. Ullmann-type coupling with phenol 4 afforded the target tosylated precursor 7.

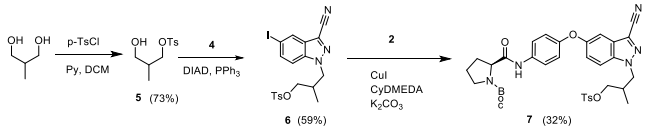

Scheme 3. Synthesis of radiofluorination precursor 7.

The ‘cold’ (e.g. non-radioactive) tracer ZCDD083 (Scheme 4) was prepared from the indazole tosylate 6, which was treated with TBAF to give the fluorinated compound 8. The latter was subjected to the Ullmann coupling affording 9, which was N-Boc-deprotected to afford the target molecule.

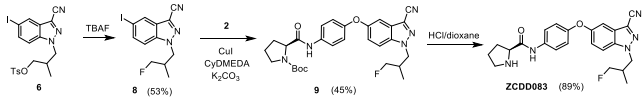

Scheme 4. Synthesis of 'cold' ZCDD083.

Radiosynthesis of [^{18}F]ZCDD083

Starting from the tosylated precursor 7, [^{18}F]ZCDD083 was prepared in a two-step synthesis (Scheme 5) using standard ^{18}F-fluoride chemistry, producing first the protected tracer 10 which was then treated with HCl in order to remove the N-Boc-protection.

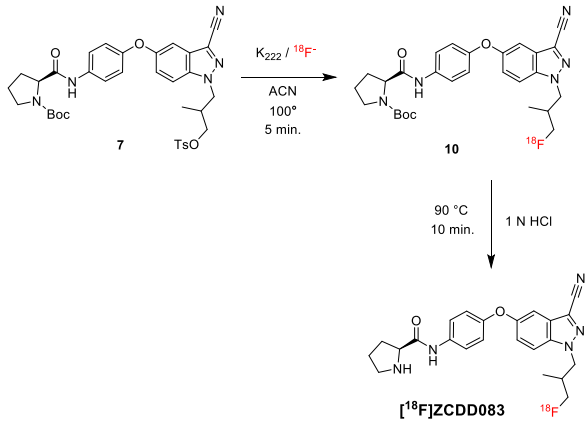

Scheme 5. Radiosynthesis of [^{18}F]ZCDD083.

[^{18}F]ZCDD083 was obtained with a 17 ±5% radiochemical yield (decay-corrected to EOB) and the activity was in the range of 4.7-7.2 GBq (n = 7). The average time taken for synthesis, purification and formulation was 65 minutes. [^{18}F]ZCDD083 was obtained with radiochemical purity >99%, chemical purity >95% and specific activity >130 GBq/μmol (Figure 1).

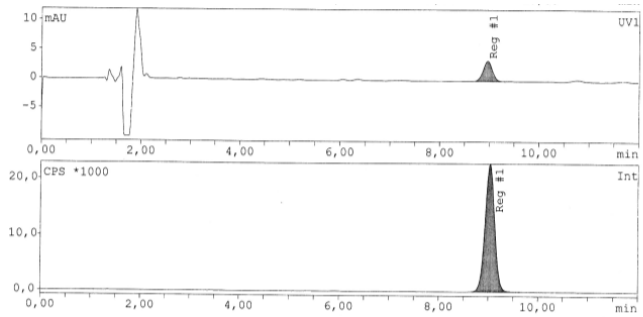

Figure 1. Chemical and radiochemical purity assessed by analytical RP-HPLC. No impurities were detected in the UV (top) and radioactive (bottom) spectra. Column: Phenomenex Luna C18 column (5 µm, 100 Å, 250 × 4.6 mm). Mobile phase: solvent A = H_2O + 0.1% TFA, solvent B = CH_3CN + 0.1% TFA; Isocratic method 40% B.

In vivo stability and ex vivo biodistribution

The radio-HPLC analysis showed no significant metabolite formation within 6 h. The eluate from HPLC was collected in fractions and the radioactivity in each fraction was measured in a γ-counter. At 6 h pi, 78.9% ±1.2 of [^{18}F]ZCDD083 was intact.

The measurement of radioactivity by γ-counter showed a high overall accumulation of [^{18}F]ZCDD083 in tissues and organs within 2 h pi, as shown in Figure 2. More specifically, high blood radioactivity was observed (7.2 ±2.2 %ID/g at 15 min pi, 5.5±1.6 %ID/g at 1 h pi, and 2.1±0.4 %ID/g at 2 h pi), revealing a slow clearance of [^{18}F]ZCDD083 from blood pool. Also, high pulmonary uptake was found (34.7 ± 6.0 %ID/g at 15 min) with a slow washout from lungs (11.0 ± 1.5 %ID/g at 2 h. On the contrary, at 6 h pi the radioactivity in lungs and blood was significantly lower (5.5±3.9 %ID/g and 1.5±1.1 %ID/g respectively).

Instead, at the late time point [^{18}F]ZCDD083 had mostly accumulated in the excretory organs (i.e. 25.5 ± 3.8 %ID/g in small intestine and 47.9 ± 6.4 %ID/g in large intestine). Level of uptake in the liver and the intestines were significantly higher compared to the kidneys. Therefore, it can be concluded that [^{18}F]ZCDD083 is predominantly cleared via the hepatobiliary system into the intestines and that the renal clearance is less significant.

Ex vivo biodistribution evaluation at 6 h pi was carried out also in atherosclerotic ApoE$^{-/-}$ mice. A similar [^{18}F]ZCDD083 biodistribution profile was observed in atherosclerotic ApoE$^{-/-}$ and control C57BL/6J mice. Pharmacokinetic studies in ApoE$^{-/-}$ atherosclerotic mice confirmed a prolonged plasma half-life of [^{18}F]ZCDD083 (1.4 ±0.2 %ID/g in blood).

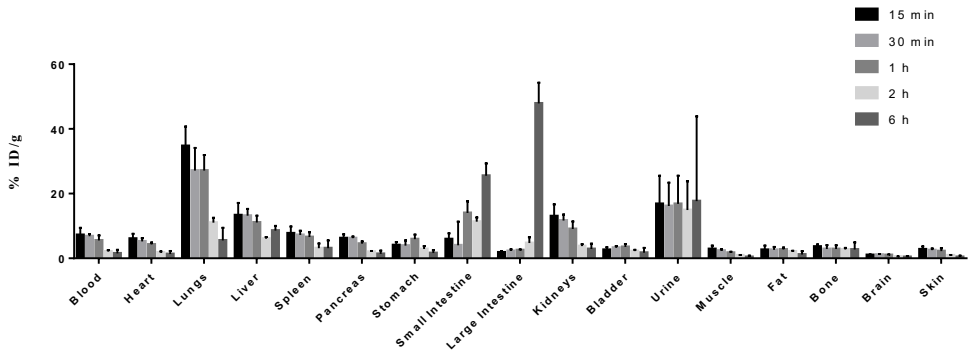

Figure 2. Ex vivo biodistribution of [18F]ZCDD083. Slow blood clearance and high tracer uptake in the lungs were observed at earlier time points within 2 h pi.At 6 h pi [18F]ZCDD083 was mostly accumulated in the intestines.

Residual high radioactivity accumulation was observed in lungs (8.6 ± 1.9 %ID/g), whereas the maximal uptake was found in small and large intestine (40.6 ± 45.8 %ID/g and 35.6 ± 2.3 %ID/g respectively).

PET/CT imaging studies

[^{18}F]ZCDD083 PET imaging scans were performed using two different disease models (ApoE$^{-/-}$ and ApoE$^{-/-}$Fbn1$^{C1039G+/-}$) and aged-matched wild type C57BL/6J mice as controls.

Spherical ROI$_s$ were drawn manually over each aortic arch and ascending aorta using the axial view of CT images. The [^{18}F]ZCDD083 signal was then quantified as SUV_{mean} values. Tracer uptake was significantly different in ApoE$^{-/-}$Fbn1$^{C1039G+/-}$ (SUV 0.78 ± 0.05), ApoE$^{-/-}$ (SUV 0.55 ± 0.06) and C57BL/6J mice (SUV 0.44 ± 0.09), as shown in Figures 3 and 4.

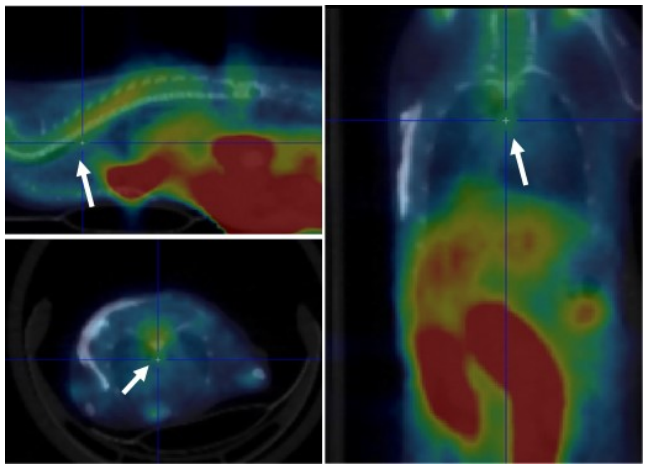

Figure 3. Representative axial, sagittal and coronal views of PET/CT images of ApoE$^{-/-}$ Fbn1$^{C1039G+/-}$acquired at 6 h after injection of [^{18}F]ZCDD083. Radioactive signal in aorta (white arrows) was observed.

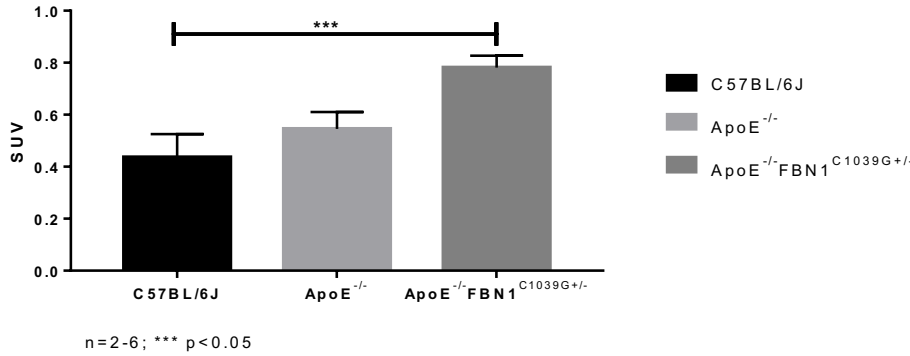

Figure 4. Comparison of SUV measurements in C57BL/6J (n = 6), ApoE$^{-/-}$ (n = 6) and ApoE$^{-/-}$Fbn1 $^{C1039G+/-}$ mice (n = 2). All values are given as mean ± SD. One-way ANOVA was performed to test for difference between groups. One ApoE$^{-/-}$Fbn1$^{C1039G+/-}$ mouse was excluded from the analysis because of a PET image acquisition technicality. (***p = 0.0006, one-way ANOVA followed by Brown-Forsythe test).

Autoradiography and Oil red O staining

At the end of the PET imaging scans, three mice of C57BL/6J, ApoE$^{-/-}$ and ApoE$^{-/-}$ Fbn1$^{C1039G+/-}$ were sacrificed and the aorta was harvested for Red Oil O staining and autoradiography (ARG). The ex vivo distribution of atherosclerotic plaques within the aorta was assessed by Red Oil O staining, whereas the accumulation of [^{18}F]ZCDD083 was assessed by autoradiography of the in vivo injected [^{18}F]ZCDD083. Oil This aforementioned Red O staining and ex vivo autoradiography were performed on the same aortic specimens in order to visually compare fat-stained areas and tracer distribution within the aorta (Figure 5).

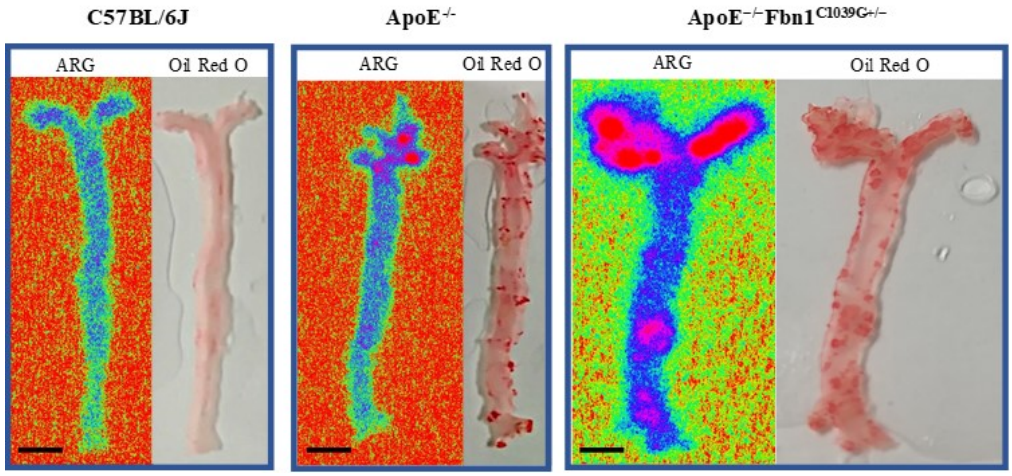

Figure 5. [^{18}F]ZCDD083 aortic uptake vs plaque distribution. Ex vivo autoradiography (left) and fat staining using Oil-red O (right) of longitudinally opened aortas at 6h post injection of [^{18}F]ZCDD083 in C57BL/6J control mice compared to atherosclerotic mice (ApoE$^{-/-}$ and ApoE$^{-/-}$Fbn1$^{C1039G+/-}$). [^{18}F]ZCDD083 uptake colocalises with atherosclerotic plaques. Scale bar = 1 cm.

Aortas from C57BL/6J control mice did not show focal lipid stained areas and radioactivity signal. Conversely, atherosclerotic plaques were found in ApoE$^{-/-}$ mice, especially in the aortic arch, proximal aorta and brachiocephalic aorta. The Oil Red O staining showed also a low plaque load in the thoracic descending aorta of the ApoE$^{-/-}$ strain. The ARG of the same specimen showed that the tracer accumulation within the aorta matched exactly with the distribution of atherosclerotic lesions. More specifically, the radioactivity was accumulated mostly in the aortic arch and in the branches. In these regions the [^{18}F]ZCDD083 uptake was significantly higher in ApoE$^{-/-}$ (0.022 ± 0.004 %ID/μL) than control mice (0.011 ± 0.003 %ID/μL) ($p = 0.0378$, unpaired t test).

The correlation between plaques and tracer uptake was also consistent using ApoE$^{-/-}$Fbn1$^{C1039G+/-}$ mice with higher plaque load than the ApoE$^{-/-}$ strain . The comparison of corresponding en face lipid staining and autoradiographic signals demonstrated a high correlation of fat-stained areas and radioactivity distribution. ApoE$^{-/-}$Fbn1$^{C1039G+/-}$ mice showed more extended atherosclerotic lesions in the arch

region, brachiocephalic artery along with thoracic descending aorta. [^{18}F]ZCDD083 was, indeed, detected in the same areas along the aorta.

Histology and immunohistochemistry

Aortic specimens of C57BL/6J and ApoE$^{-/-}$ (n = 3/ each group) were used for further histological analysis after PET imaging studies. Longitudinal sections of aortic arch and right common carotid artery as well as cross sections of brachiocephalic aorta and proximal aorta were stained with hematoxylin and eosin (H&E) to visualize atherosclerotic plaques and lesion morphology. Aortas of healthy mice did not show atherosclerosis, whereas ApoE$^{-/-}$ mice showed fibrous/atheromatous plaques and some small calcifications. The H&E staining confirmed atherosclerotic disease especially in brachiocephalic artery, proximal aorta and aortic arch.
The immunohistochemistry of ApoE$^{-/-}$ aortic arch sections, revealed that the enzyme target PFKFB3 is overexpressed inside atherosclerotic plaques (Figure 6).

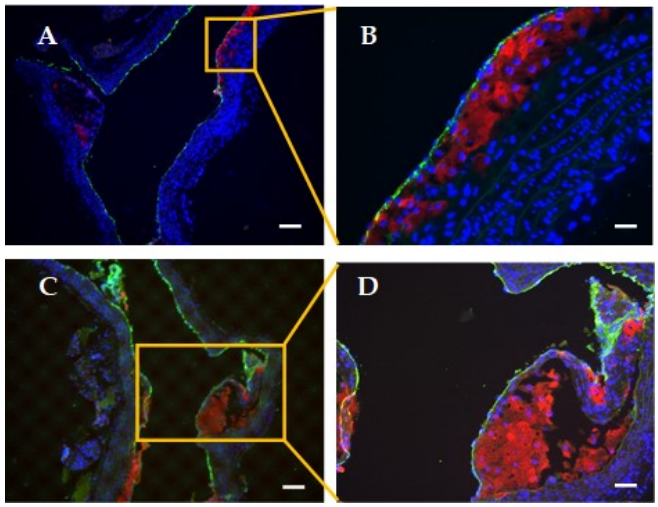

Figure 6. Immunohistochemistry of the aorta from ApoE$^{-/-}$ mice. Two longitudinal sections of the aortic arch are shown (A, C) as well as a high-power magnification (B, D). Endothelial cells are stained using von Willebrand factor (green). Nuclei (blue) are counter-stained with DAPI. Positive staining areas for PFKFB3 (red) are observed inside atherosclerotic plaques. Scale bar = 100 μm (A, C); 20 μm (B); 50μm (D).

The comparison among brachiocephalic arteries of atherosclerotic and control mice showed that PFKFB3 was highly expressed within atherosclerotic plaques, whereas in normal vessels PFKFB3 is present just in a basal level along the arterial wall (Figure 7).

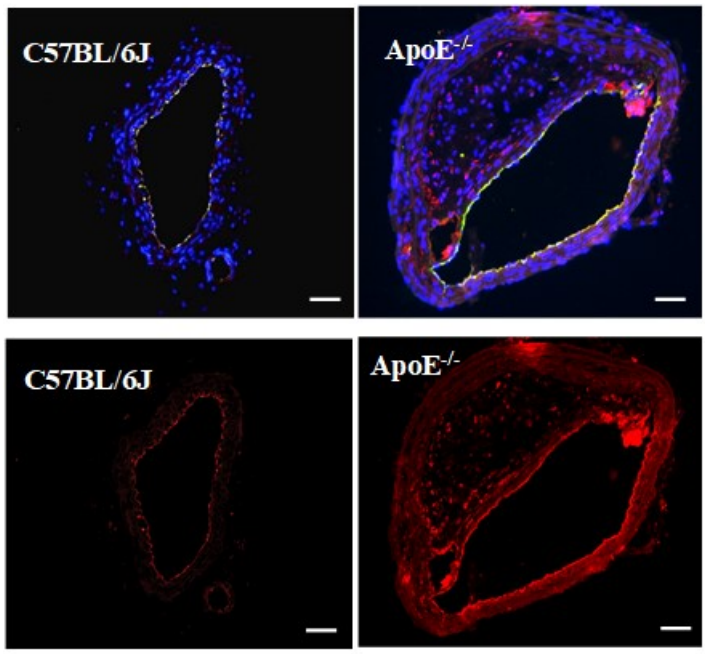

Figure 7. Immunohistochemistry of murine brachiocephalic arteries. Upper panels: immunofluorescent staining for von Willebrand factor to detect endothelial cells (green) and PFKFB3 (red). Counter-staining with DAPI to detect nuclei (blue). Lower panels = PFKFB3 staining (red). ApoE$^{-/-}$ mice exhibit high expression level of PFKFB3 enzyme in contrast to C57BL/6J controls. Scale bar = 50 µm.

Discussion

Atherosclerosis is responsible for the majority of acute cardiovascular events. Specifically, rupture of atherosclerotic plaques and consequent thrombosis remains the largest underlying cause of cardio- and cerebrovascular death. Despite extraordinary advances in the understanding of the pathophysiology of atherosclerosis, both the diagnosis and treatment of the disease still present limitations. Currently, the main challenge in cardiovascular medicine is to identify patients who are at risk of coronary plaque rupture and subsequent heart attack or stroke originating from carotid plaque depoistions.[17] Among the cardiovascular imaging modalities used, coronary angiography has a wide clinical application but provides information only on vessel stenosis. Other imaging techniques, such as intravascular ultrasound (IVUS), optical coherence tomography (OCT) and near-infrared spectroscopy (NIRS), can provide only a limited plaque characterization but, unfortunately, they are invasive and thus not useful for patient diagnosis and follow up.[18,19,20] Therefore, new non-invasive approaches to detect potentially unstable plaque are urgently needed.

In this context, positron emission tomography (PET) imaging has great potential, since - compared to other molecular imaging modalities - it shows higher sensitivity allowing better visualization of biological and biochemical processes involved in the development of atherosclerotic plaques.[21] Among the PET radiotracers currently available, only ^{18}F-FDG has been approved for clinical use. In particular, clinical studies showed that ^{18}F-FDG is useful to assess carotid artery stenosis in asymptomatic patients.[22,23] However, carotid artery imaging using ^{18}F-FDG PET is challenging due to (1) the low spatial resolution of PET (≈ 4 mm in human PET and 1,2 mm in rodent PET), (2) cardiac motion and (3) myocardial spill over.[24] To address the latter limitation, new imaging targets and radiotracers having lower unspecific myocardial uptake are currently under investigation.[25]

The results above validate PFKFB3 enzyme as an imaging target of atherosclerosis in two mouse models.[26,27] Firstly, we observed an increased target engagement in cross sections of diseased aortas of atherosclerotic mice compared to those of healthy mice. Secondly, longitudinal sections of aortic arch specimens of ApoE$^{-/-}$ mice showed higher expression level of PFKFB3 enzyme within atherosclerotic

plaques compared to normal vessel wall. Hence, all these results demonstrated the appropriateness and the specificity of the target PFKFB3 for the detection of atherosclerotic plaques.

Once we demonstrated the relevance of PFKFB3 enzyme as an imaging target, we used the new ^{18}F-radiolabeled PFKFB3-targeted ligand, [^{18}F]ZCDD083, which could be obtained in high radiochemical yields, activity concentrations and quality parameters. [^{18}F]ZCDD083 demonstrated high in vivo metabolic stability and long circulation time in the blood. The slow clearance from the blood may be explained by the high hydrophobicity of [^{18}F]ZCDD083. Indeed, a $LogD_{7.4}$ of 3.6 was reported for the parent compound AZ68.[16] The correlation of high hydrophobicity with high binding to plasma proteins and prolonged circulation time in the blood is well known.[28] High binding to plasma proteins is documented for the compound AZ26[16] (chemically similar to AZ68) and might be valid also for our tracer [^{18}F]ZCDD083. This may likely explain the slow tracer clearance. Also, the excretion route is usually related to lipophilicity, as lipophilic compounds are generally cleared via the hepatobiliary system. This is in accordance with our ex vivo biodistribution results which showed a predominant excretion from the liver to the intestines. We also noticed a high uptake in the lung. However, it is not clear whether this high uptake in the lung is due to nonspecific binding (due to the high [^{18}F]ZCDD083 lipophilicity) or somehow correlated with PFKFB3 tissue distribution. In 2003, Minchenko et al. studied the in vivo expression of the PFKFB enzyme family and its response to hypoxia, disclosing that lungs exhibit high basal level of PFKFB3 mRNA.[29] Moreover, the proteome analysis reported in the Human Protein Atlas shows that lung, stomach and placenta have the highest PFKFB3 expression among all tissues considered.[30]

Our PET imaging studies showed significantly increased signals in the aorta of ApoE$^{-/-}$ (+25%) and ApoE$^{-/-}$Fbn1$^{C1039G+/-}$ (+79%) compared to C57BL/6J mice. This is in accordance with the higher plaque burden in ApoE$^{-/-}$Fbn1$^{C1039G+/-}$ mice compared to ApoE$^{-/-}$ mice . Moreover, these results were supported by aortic autoradiography which showed a 2-fold increased uptake in the aortic arch of ApoE$^{-/-}$ compared to WT mice. The autoradiographic signal in ApoE$^{-/-}$Fbn1$^{C1039G+/-}$ was considerably higher too. The increment in uptake is clearly correlated with the increment in plaque load, as confirmed by histological evaluation. Indeed, the highest uptake was found

in ApoE$^{-/-}$Fbn1$^{C1039G+/-}$ at an advanced stage of the disease and high level of plaques in the aortic arch along with the thoracic aorta.

Unfortunately, despite the higher uptake, the [^{18}F]ZCDD083 signal in these small sized atherosclerotic plaques was affected by partial volume effect and due to the limited spatial resolution of PET[31] no “hotspots” could be detected in the in vivo imaging studies. Indeed, the vessel wall in mouse aorta is usually 30-80 µm, whereas the resolution in PET imaging is ~1,2 mm.[18]

The specificity of the tracer accumulation at the target structure (i.e. atherosclerotic plaque) was demonstrated by the combination of ex vivo autoradiography with en face Oil Red O staining of the same aortic specimens. Indeed, we observed co-localization of [^{18}F]ZCDD083 signal with plaque distribution along the aorta. These cross studies, involving C57BL/6J, ApoE$^{-/-}$ and ApoE$^{-/-}$Fbn1$^{C1039G+/-}$ demonstrated high sensitivity of [^{18}F]ZCDD083 to detect atherosclerotic plaques, whereas little signal was detected in normal vessel or outside atherosclerotic lesions. These stained areas exhibited a higher tracer accumulation. Hence, the [^{18}F]ZCDD083 uptake was clearly correlated with plaque distribution as well as with the progression of the disease.

Conclusion

In summary, we efficiently radiosynthesized a novel PET tracer, [^{18}F]ZCDD083 targeting the PFKFB3enzyme. Using in vivo and ex vivo studies, we characterized and validated [^{18}F]ZCDD083, demonstrating its ability to detect atherosclerotic plaques. This tracer may represent a promising tool for the non-invasive diagnosis and follow-up of atherosclerotic plaques prone to rupture, which in turn could help improving risk stratification and evaluation of the efficacy of anti-atherosclerotic therapies.

Currently, cardiovascular medicine aims principally to identify atherosclerotic plaques prone to rupture, improve the risk stratification, monitor the disease progression, assess new anti-atherosclerotic therapies and promptly evaluate the efficacy of therapeutic treatment. PET imaging is non-invasive and has a great potential in this context. Indeed, new targets and radiotracers are currently being investigated for imaging unstable atherosclerotic plaque.[6,7]

We have studied PFKFB3 enzyme as a new target to be used for the in vivo assessment of atherosclerotic plaques.[8,9] PFKFB3 is a glycolysis-related enzyme upregulated in inflammatory and hypoxic conditions.[10,11] Several studies have shown a tight correlation between PFKFB3 and angiogenesis, which is a feature of vulnerable atherosclerotic plaques.[12,13,14,15] Here we described the development of a specific PET radiotracer targeting PFKFB3 - the 18F-radiolabelled phenoxindazole ZCDD083 – based on the structure of the potent PFKFB3 inhibitor AZ68 (IC50= 4nM).[16]

Supporting Information

The Supporting Information is available on the ACS Publications website.

Author Contributions

CDD performed and co-designed all the experiments, contributed to writing the manuscript. SDA, and LW designed and performed radiochemistry experiments, corrected the manuscript. SS designed in vivo experiments and corrected the manuscript. GDM, and PP designed biology experiments and corrected the manuscript. MZ designed the experiments and wrote the manuscript.

Funding Sources

Acknowledgment

We thank the European Union's Horizon 2020 research and innovation programme under the Marie Skłodowska-Curie ITN-European Joint Doctorate MOGLYNET (grant agreement No. 675527).

Abbreviations

CCR2, CC chemokine receptor 2; CCL2, CC chemokine ligand 2; CCR5, CC chemokine receptor 5; TLC, thin layer chromatography.

References

1. Lusis, A. J. Atherosclerosis. *Nature* 407, 233–241 (2000).
2. Ross, R. Atherosclerosis — An Inflammatory Disease. *N. Engl. J. Med.* 340, 115–126 (1999).
3. Cardiovascular diseases (CVDs). Available at: https://www.who.int/news-room/fact-sheets/detail/cardiovascular-diseases-(cvds). (Accessed: 1st May 2019)
4. Roth, G. A. *et al.* Global, Regional, and National Burden of Cardiovascular Diseases for 10 Causes, 1990 to 2015. *J. Am. Coll. Cardiol.* 70, 1–25 (2017).
5. Spagnoli, L. G., Bonanno, E., Sangiorgi, G. & Mauriello, A. Role of Inflammation in Atherosclerosis. *J. Nucl. Med.* 48, 1800–1815 (2007).
6. Tawakol, A. & Finn, A. V. Imaging Inflammatory Changes in Atherosclerosis. *JACC Cardiovasc. Imaging* 4, 1119–1122 (2011).
7. Rudd James H.F., Hyafil Fabien & Fayad Zahi A. Inflammation Imaging in Atherosclerosis. *Arterioscler. Thromb. Vasc. Biol.* 29, 1009–1016 (2009).
8. Van Schaftingen, E., Jett, M. F., Hue, L. & Hers, H. G. Control of liver 6-phosphofructokinase by fructose 2,6-bisphosphate and other effectors. *Proc. Natl. Acad. Sci. U. S. A.* 78, 3483–3486 (1981).
9. Okar, D. A. & Lange, A. J. Fructose-2,6-bisphosphate and control of carbohydrate metabolism in eukaryotes. *BioFactors* 10, 1–14 (1999).
10. Pober, J. S. & Sessa, W. C. Evolving functions of endothelial cells in inflammation. *Nat. Rev. Immunol.* 7, 803–815 (2007).
11. Zhang, R., Li, R., Liu, Y., Li, L. & Tang, Y. The Glycolytic Enzyme PFKFB3 Controls TNF-α-Induced Endothelial Proinflammatory Responses. *Inflammation* 42, 146–155 (2019).
12. Tawakol, A. *et al.* HIF-1α and PFKFB3 mediate a tight relationship between pro-inflammatory activation and anaerobic metabolism in atherosclerotic macrophages. *Arterioscler. Thromb. Vasc. Biol.* 35, 1463–1471 (2015).
13. Parathath, S., Yang, Y., Mick, S. & Fisher, E. A. Hypoxia in murine atherosclerotic plaques and its adverse effects on macrophages. *Trends Cardiovasc. Med.* 23, 80–84 (2013).

14. Sluimer, J. C. & Daemen, M. J. Novel concepts in atherogenesis: angiogenesis and hypoxia in atherosclerosis. *J. Pathol.* 218, 7–29 (2009).
15. Perrotta, P. *et al.* Pharmacological strategies to inhibit intraplaque angiogenesis in atherosclerosis. *Vascul. Pharmacol.* 112, 72–78 (2019).
16. Boyd, S. *et al.* Structure-Based Design of Potent and Selective Inhibitors of the Metabolic Kinase PFKFB3. *J. Med. Chem.* 58, 3611–3625 (2015).
17. Qureshi, W. T., Rana, J. S., Yeboah, J., bin Nasir, U. & Al-Mallah, M. H. Risk Stratification for Primary Prevention of Coronary Artery Disease: Roles of C-Reactive Protein and Coronary Artery Calcium. *Curr. Cardiol. Rep.* 17, 110 (2015).
18. Vigne, J. *et al.* Current and Emerging Preclinical Approaches for Imaging-Based Characterization of Atherosclerosis. *Mol. Imaging Biol.* 20, 869–887 (2018).
19. Rathod, K. S., Hamshere, S. M., Jones, D. A. & Mathur, A. Intravascular Ultrasound Versus Optical Coherence Tomography for Coronary Artery Imaging – Apples and Oranges? *Interv. Cardiol. Rev.* 10, 8–15 (2015).
20. de Boer, S. P. M. *et al.* Determinants of high cardiovascular risk in relation to plaque-composition of a non-culprit coronary segment visualized by near-infrared spectroscopy in patients undergoing percutaneous coronary intervention. *Eur. Heart J.* 35, 282–289 (2014).
21. Hammad, B., Evans, N. R., Rudd, J. H. F. & Tawakol, A. Molecular imaging of atherosclerosis with integrated PET imaging. *J. Nucl. Cardiol.* 24, 938–943 (2017).
22. Skagen, K. *et al.* Carotid Plaque Inflammation Assessed with 18F-FDG PET/CT is Higher in Symptomatic Compared with Asymptomatic Patients. *Int. J. Stroke* 10, 730–736 (2015).
23. Tawakol, A. *et al.* In Vivo 18F-Fluorodeoxyglucose Positron Emission Tomography Imaging Provides a Noninvasive Measure of Carotid Plaque Inflammation in Patients. *J. Am. Coll. Cardiol.* 48, 1818–1824 (2006).
24. Joshi, N. V. *et al.* 18F-fluoride positron emission tomography for identification of ruptured and high-risk coronary atherosclerotic plaques: a prospective clinical trial. *The Lancet* 383, 705–713 (2014).

25. Rudd, J. H. F. *et al.* Imaging Atherosclerotic Plaque Inflammation by Fluorodeoxyglucose With Positron Emission Tomography. *J. Am. Coll. Cardiol.* 55, 2527–2535 (2010).
26. Emini Veseli, B. *et al.* Animal models of atherosclerosis. *Eur. J. Pharmacol.* doi:10.1016/j.ejphar.2017.05.010
27. Van der Donckt, C. *et al.* Elastin fragmentation in atherosclerotic mice leads to intraplaque neovascularization, plaque rupture, myocardial infarction, stroke, and sudden death. *Eur. Heart J.* 36, 1049–1058 (2015).
28. Gee, A. D., Bongarzone, S. & Wilson, A. A. Small Molecules as Radiopharmaceutical Vectors. in *Radiopharmaceutical Chemistry* (eds. Lewis, J. S., Windhorst, A. D. & Zeglis, B. M.) 119–136 (Springer International Publishing, 2019). doi:10.1007/978-3-319-98947-1_7
29. Minchenko, O., Opentanova, I. & Caro, J. Hypoxic regulation of the 6-phosphofructo-2-kinase/fructose-2,6-bisphosphatase gene family (PFKFB-1–4) expression in vivo. *FEBS Lett.* 554, 264–270 (2003).
30. Tissue expression of PFKFB3 - Summary - The Human Protein Atlas. Available at: https://www.proteinatlas.org/ENSG00000170525-PFKFB3/tissue. (Accessed: 2nd April 2019)
31. Position paper of the Cardiovascular Committee of the European Association of Nuclear Medicine (EANM) on PET imaging of atherosclerosis | SpringerLink. Available at: https://link.springer.com/article/10.1007%2Fs00259-015-3259-3. (Accessed: 5th February 2019)

Chapter 8

Three-dimensional imaging of intraplaque neovascularization in a mouse model of advanced atherosclerosis

Perrotta P, Pintelon I, de Vries M.R, Quax P.H.A, Timmermans J, De Meyer G.R.Y, Martinet W.

*Journal of Vascular Research.*2020 Jul 1;1-7.

Abstract

Multiple lines of evidence suggest that intraplaque (IP) neovascularization promotes atherosclerotic plaque growth, destabilization and rupture. However, pharmacological inhibition of IP neo-vascularization remains largely unexplored due to the limited number of animal models that develop IP neovessels and the lack of reliable methods for visualizing IP angiogenesis. Here, we applied 3D confocal microscopy with an optimized tissue-clearing process, termed iDISCO (immunolabeling-enabled 3D Imaging of Solvent Cleared Organs) to visualize IP neovessels in ApoE$^{-/-}$ mice carrying a heterozygous mutation (C1039+/-) in the fibrillin-1 gene. Unlike regular ApoE$^{-/-}$ mice, this mouse model is characterized by the presence of advanced plaques with evident IP neovascularization. Plaques were stained with antibodies against endothelial marker CD31 for 3 days, followed by incubation with fluorescently labelled secondary antibodies. Subsequent tissue clearing with dichloromethane (DCM)/methanol, DCM and dibenzyl ether allowed easy visualization and 3D reconstruction of the IP vascular network while plaque morphology remained intact.

Introduction

Atherosclerosis is a progressive inflammatory disease that leads to plaque formation at specific sites of the arterial tree [1]. Formation of atherosclerotic plaques typically starts with the deposition of lipids in the intima, followed by endothelial activation and infiltration of macrophages and other inflammatory cells into the subendothelial layer. The first grossly visible vascular lesions, called fatty streaks, transform into more advanced lesions by the migration and proliferation of vascular smooth muscle cells (VSMCs), activation of macrophages and the accumulation of lipid-rich necrotic debris. These plaques typically have a thick fibrous cap consisting of VSMCs and extracellular matrix that encloses a lipid-rich necrotic core [2, 3]. Over time, plaques can become increasingly complex with calcification, ulceration at the luminal surface, and the presence of small neovessels that grow into the lesion from the media of the blood vessel wall. Several stimuli inside the plaque such as hypoxia and high oxidative stress trigger the formation of such intraplaque (IP) neovessels [4]. Growing evidence suggests that IP neovessels are leaky and promote the entry of several plaque components including red blood cells, lipids and inflammatory cells [5], which may accelerate the progression and destabilization of developing plaques [6, 7]. Along these lines, blocking IP angiogenesis has been proposed as a novel approach for decreasing plaque instability and for limiting cardiovascular risk [8, 9]. Apolipoprotein E-deficient ($ApoE^{-/-}$) mice containing a heterozygous mutation (C1039G+/-) in the fibrillin-1 (Fbn1) gene represent a unique mouse model of advanced atherosclerosis with human-like plaque characteristics such as IP neovascularization [10, 11]. Unlike other experimental models of atherosclerosis, $ApoE^{-/-}Fbn1^{C1039G+/-}$ mice show fragmentation of elastic fibers, which facilitates neovessel sprouting from the adventitial vasa vasorum into the plaque [12], similarly to what occurs in human plaques. Conventional immunohistochemistry is currently the gold standard for analysis of plaque composition, yet it does not allow an accurate visualization and quantification of such neovessels inside the complex structure of the plaque. In the present study, we optimized an optical ex vivo clearing method for the visualization of IP angiogenesis in $ApoE^{-/-}Fbn1^{C1039G+/-}$ mice, termed immunolabeling-enabled three-dimensional imaging of solvent–cleared organs (iDISCO)

Materials and Methods

Mice

Female ApoE$^{-/-}$Fbn1$^{C1039G+/-}$ mice were fed a western-type diet (WD) (Altromin, C1000 diet supplemented with 20% milkfat and 0.15% cholesterol, #100171) starting at 8 weeks of age. After 20 weeks on the WD, mice were euthanized with an overdose of sodium pentobarbital (250 mg/kg i.p.) and perfused with 20 mL of 4% paraformaldehyde (PFA) in phosphate-buffered saline (PBS). Carotid arteries were dissected and incubated in 4% PFA in PBS overnight. Standard ApoE$^{-/-}$ mice that did not contain the C1039+/- mutation (but fed WD for 20 weeks) were used as negative controls since they develop plaques without IP neovascularization. All animal procedures were conducted according to the guidelines from Directive 2010/63/EU of the European Parliament on the protection of animals used for scientific purposes. Experiments were approved by the ethics committee of the University of Antwerp.

Immunostaining and iDISCO clearing

Tissue samples were incubated in permeabilization solution (1x PBS, 0.2% Triton X-100, 0.3M glycine, 20% DMSO) overnight. Samples were then washed for 1 hour in 1x PBS/0.2% Tween-20 and incubated in blocking buffer (1xPBS, 0.2% Triton X-100, 10% DMSO, 3% donkey serum) for 8 hours, followed by incubation with primary rat anti-mouse CD31 antibody (Abcam, ab56299; 10 µg/ml) in permeabilization buffer (1x PBS, 0.2% Triton X-100, 0.3M glycine, 20% DMSO) for 72 hours. Finally, samples were washed 3 times in 1xPBS, 0.2% Triton X-100 followed by incubation with goat anti-rat Alexa fluor 546 (Thermo Fisher, A11081; 1:500 dilution) for 48 hours. For nuclear labelling, samples were incubated with DAPI (Sigma-Aldrich, 5 µg/ml) for 30 minutes. Next, immunolabeled samples were dehydrated in a methanol gradient (in PBS) by incubating tissue specimens in 20% methanol (30 min), 50% methanol (30 min), 70% methanol (30 min), and 100% methanol (overnight).

Subsequently, samples were incubated for 2 hours in 66% dichloromethane (DCM)/34% methanol, then washed twice for 15 min in 100% DCM.

Finally, samples were incubated in dibenzyl ether (DBE) until transparency was achieved (approximately 3 hours)

Confocal imaging and histology

Cleared samples were imaged on an inverted Leica TCS SP8 confocal laser scanning microscope, using a 20x/0.75 HC PL Apo objective lens. Samples were positioned in a glass bottom Petri dish and submerged in DBE. DAPI was visualized using a 405 nm diode laser and the Alexa Fluor 546 fluorescence was imaged with the 546 nm wavelength of a white light laser. For each sample, an image stack (z step size ~ 5 µm) with 1024x1024 pixel resolution was captured. Three-dimensional renderings were obtained using Leica LAS X 3D visualisation software. The Imaris image analysis software enabled the specific selection and measurement of the IP blood vessels, by applying a new surface rendering based on the intensity of the fluorescent signal. Following the imaging, samples were embedded in paraffin, cut into 5 µm sections and stained with hematoxylin and eosin (H&E). H&E stains were imaged using an Olympus BX43 microscope.

Results and Discussion

We previously reported that the heterozygous mutation C1039G+/- in the fibrillin-1 (Fbn1) gene leads to advanced unstable atherosclerotic plaques in $ApoE^{-/-}$ mice, a standard mouse model of atherosclerosis [10, 11]. Fbn1 is an extracellular matrix glycoprotein secreted by fibroblasts and incorporated into microfibrils. These fibrillin-rich microfibrils are associated with cross-linked elastin to form mature elastic fibers. Mutations in the Fbn1 gene result in impaired microfibrillar assembly and deposition, followed by fragmentation of elastic fibers. This loss of structural integrity of the vessel wall leads to progressive dilatation and arterial stiffening, resembling vascular ageing [11]. Fragmentation of the elastic fibers gives rise to elastin-derived peptides, which attract monocytes, enhancing the inflammatory reaction in the vessel wall. Moreover, extensive neovascularization is observed in the brachiocephalic and common carotid arteries of $ApoE^{-/-}Fbn1^{C1039G+/-}$ mice fed the WD [12]. These features are rarely seen in murine atherosclerosis models, but are frequently observed in

advanced human plaques. IP neovessels in ApoE$^{-/-}$Fbn1$^{C1039G+/-}$ mice on the WD likely arise from the adventitial vasa vasorum and sprout out of the media into the plaque [9]. Although the exact role of IP neovessels is not exactly understood, it is important to note that such structures are immature and leaky. Indeed, besides being an entry point for leukocytes and lipoproteins, IP neovessels appear to be a source of erythrocytes and platelets inside the plaque, thereby promoting macrophage activation and plaque destabilization.

Imaging of IP neovascularization is possible in human plaques using microvascular imaging and contrast-enhanced ultrasonography [13-16], though this approach is not feasible (or at least unlikely) in mouse plaques due to the extremely small size of the IP neovessels. Hitherto, immunohistochemical analysis of paraffin-embedded sections remains the only method for evaluating IP angiogenesis in mouse plaques. Figure 1 shows representative (immuno)histochemical stains of IP neovessels in plaques of ApoE$^{-/-}$Fbn1$^{C1039G+/-}$ mice. Because both contrast-enhanced ultrasonography and histological analysis of plaques are 2D imaging techniques, they have limitations regarding the interpretation of the “architecture” of microvessel circuits in the atherosclerotic plaque. In recent years, a technique called ‘tissue clearing’ has re-emerged, offering an alternative approach for tissue sectioning. Nowadays numerous protocols allow optical clearing and detailed 3D imaging of intact organs [17-22].

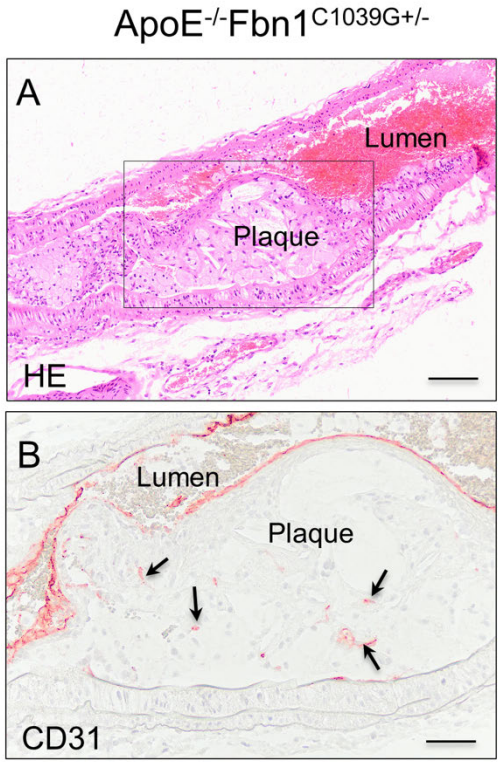

Figure 1. Standard (immuno)histochemical analyses of intraplaque neovascularization in carotid artery plaques from ApoE$^{-/-}$Fbn1$^{C1039G+/-}$ mice that were fed a western diet for 20 weeks. (a) Representative low power micrograph of an H&E stained, paraffin-embedded longitudinal section of carotid plaque. Scale bar = 100µm. (b) Detail of plaque with intraplaque microvessel stain for CD31 (boxed area in panel a) Scale bar = 50 µm.

Immunolabeling-enabled three-dimensional imaging of solvent-cleared organs (iDISCO) combines immunolabeling of large tissue samples for volume imaging with 3DISCO (3D imaging of solvent-cleared organs) [23]. iDISCO is an optical clearing method that makes biological samples more transparent ('cleared') (Figure 2) and has been successfully used to image three-dimensional structures, including intact mouse organs such as brain, kidney, intestine, eye and even whole embryos [21-25]. Recently, Becher et al. [26] applied iDISCO technology for 3D profiling of atherosclerotic plaques and arterial remodeling after carotid artery ligation. We

optimized iDISCO for mouse atherosclerotic tissue using endothelial cell (EC)-specific CD31 antibodies and we show here for the first time a 3D reconstruction of IP neovascularization in carotid plaques of ApoE$^{-/-}$Fbn1$^{C1039G+/-}$ mice. From our experience, the following modifications to the iDISCO protocol were essential for obtaining good visualization of neovessels in carotid plaques: (i) high CD31 antibody concentrations (10 µg/ml) were required for best imaging results, (ii) an overnight incubation step in permeabilizing solution for good tissue penetration of the primary antibody, though we recommend a 72 hour incubation, and (iii) a simple clearing protocol with a mixture of 66% dichloromethane (DCM) and 34% methanol (MeOH), followed by incubation in pure DCM and dibenzyl ether was sufficient to visualize the IP vascular network, in contrast to previously published protocols that are more labor-intensive[17].

Cleared samples of total organs are typically visualized using light sheet microscopy, allowing rapid 3D imaging of these large samples [17-20]. Less thick, cleared specimens can also be imaged by confocal microscopy and hence benefit from the higher resolution that can be obtained [22]. Imaging of cleared segments of the carotid arteries by confocal microscopy resulted in visualization of the delicate IP neovascularization in carotid plaques of ApoE$^{-/-}$Fbn1 $^{C1039G+/-}$ mice and confirmed the labeling of IP neovessels and the complete clearing of the carotid artery segments.

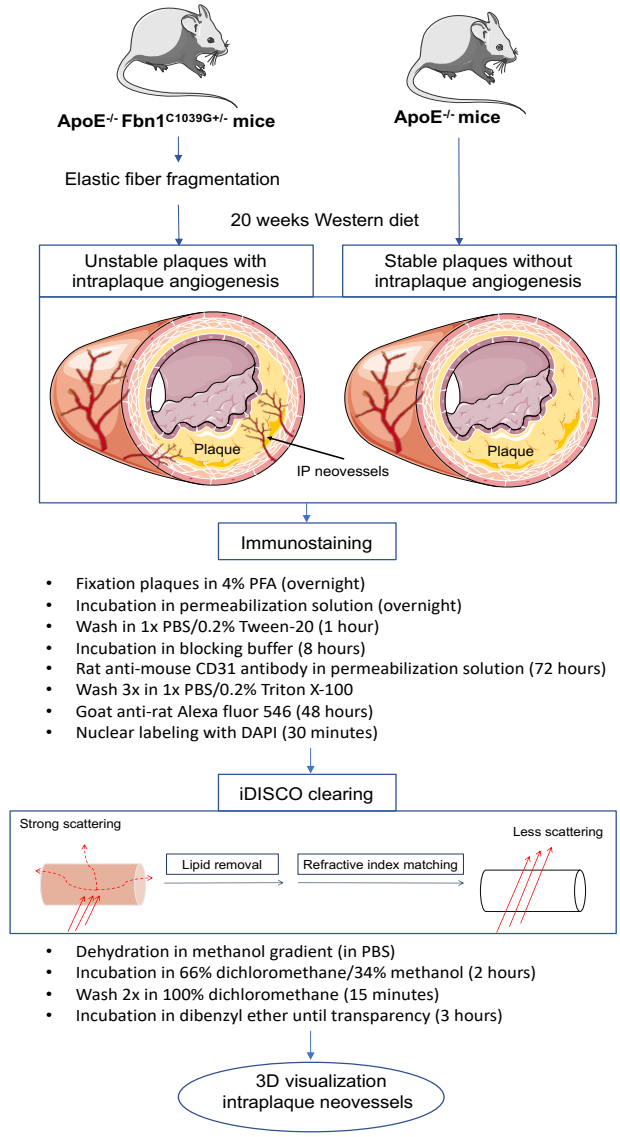

Figure 2. Schematic overview of the different steps required for immunostaining and tissue clearing. Solvent-based tissue clearing is a three-step process. Firstly, the tissue is dehydrated and lipids are removed by sequential incubation in a methanol gradient (20, 50, 70, 100% methanol in distilled water). Secondly, the tissue is transferred to a high refractive index solution where additional lipid solvation and clearing occurs (66% dichloromethane/34% methanol). Finally, the lipid-free tissue sample is placed in a high refractive index matching solution (dibenzyl ether) for further clearing.

Three-dimensional reconstruction (online supplementary video 1) and a z-stack (online supplementary video 2) show the high degree of tortuosity and irregularities in the structure of IP neovessels from ApoE$^{-/-}$Fbn1 $^{C1039G+/-}$ mice, which is not obvious in single plane images of 2D sections (Figure 3). To evaluate the specificity of endothelial CD31 staining in IP angiogenesis, we also applied this technique to regular ApoE$^{-/-}$ mice that develop plaques after being fed the WD, albeit without IP neovascularization. The recorded z-stack shows that CD31 staining did not occur in carotid plaques of ApoE$^{-/-}$ mice (online supplementary video 3), although it was clearly present at the luminal EC layer and in the adventitia (Figure 4).

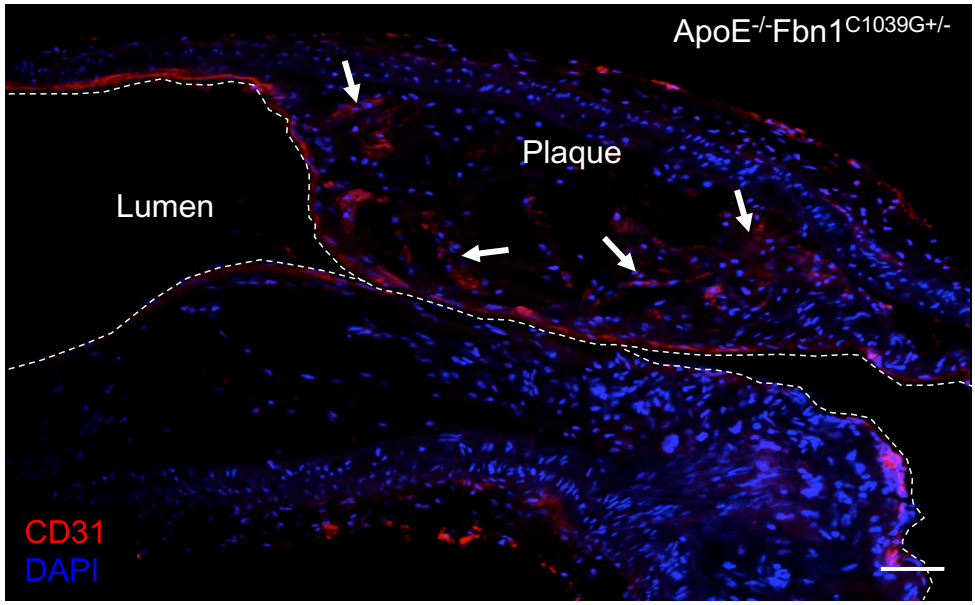

Figure 3. Representative 2D visualization of intraplaque neovascularization in a single z-stack slide of a carotid artery plaque from ApoE$^{-/-}$Fbn1$^{C1039G+/-}$ mice after CD31 immunohistochemical staining and iDISCO clearing. Multiple red-stained CD31 positive endothelial cells are detectable inside the plaque (arrows). Scale bar = 50 µm.

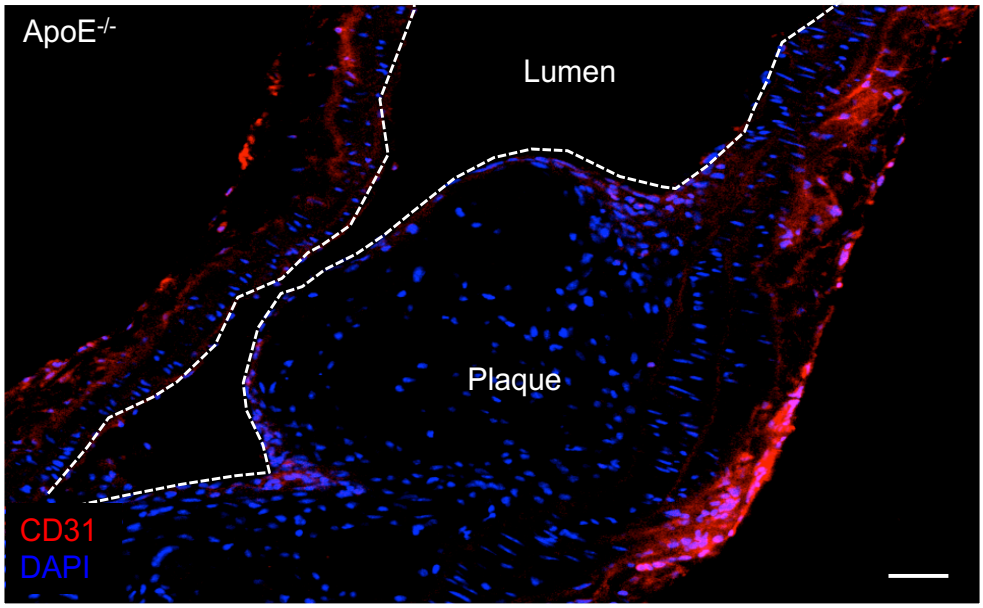

Figure 4. Intraplaque neovascularization is absent in plaques of ApoE$^{-/-}$ mice. A single representative z-stack slide of a plaque in the brachiocephalic artery is shown. CD31 positive cells (red) are not present inside the plaque, but clearly detectable in the intima. Scale bar = 50 µm.

Further analyses of the obtained images demonstrated that the applied technique is not only limited to the visualization of the 3D distribution of the IP neovascularisation (Figure 5A). Using 3D analysis software, neovessels entering the plaque can be selectively depicted in the 3D rendering and quantitative measurements can be obtained (white area in Figure 5B). The total of volume of IP vessels as shown in Figure 5B was calculated to be 0.068 mm^3 and can be used to compare IP angiogenesis between different plaques. Clearing procedures such as 3DISCO lead to substantial shrinkage and might affect tissue morphology [22, 27]. However, the shorter clearing procedure that was used for the carotid segments definitely protected the tissue from the effects of the clearing process, as the structure of the plaque was not altered after clearing. This was confirmed by applying our standard 2D histological techniques on the cleared tissues after imaging, allowing us to examine the structure and composition of the plaque (Figure 6). Moreover,

fluorescent labeling of the tissue was preserved after the clearing process and paraffin embedding (data not shown) allowing re-examination of H&E-stained sections of the paraffin embedded tissue by fluorescence microscopy, if needed.

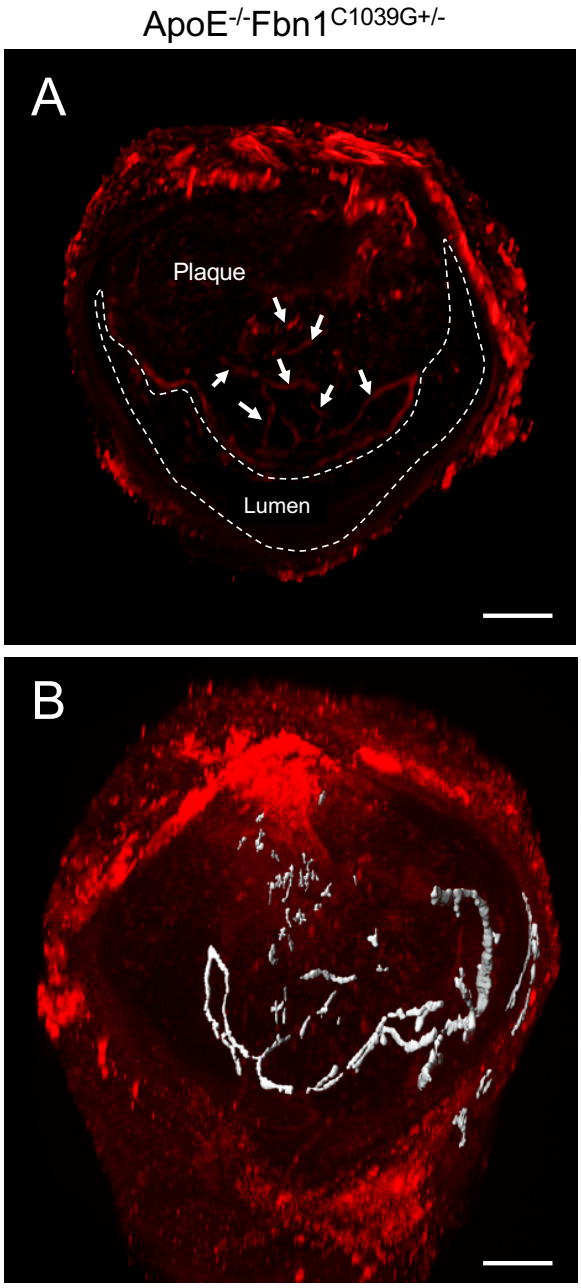

Figure 5. Representative 3D reconstruction of a carotid artery segment (50 z-stack slides) from ApoE$^{-/-}$Fbn1$^{C1039G+/-}$ mice after CD31 immunohistochemical staining and iDISCO clearing. (a) Multiple red-stained CD31 positive endothelial cells are detectable inside the plaque that is bulging the lumen. The 3D reconstruction clearly illustrates the complex distribution of the neovascularisation inside the plaque (white arrows). (b) Using 3D analysis software, neovessels entering the plaque can selectively be depicted (grey) in the 3D image and quantitative measurements such as the total of volume of the IP vessels can be obtained. Scale bar = 80 µm

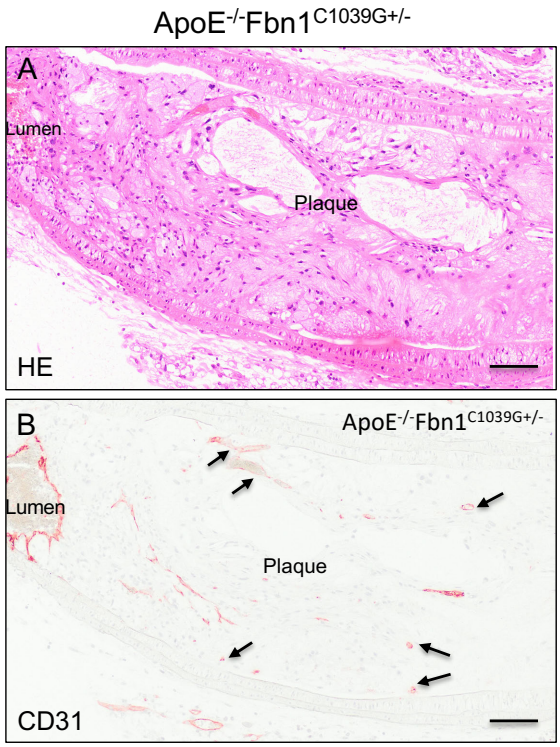

Figure 6. (a-b) Hematoxylin & eosin staining and CD31 immunohistochemical staining of a carotid artery plaque from a representative ApoE$^{-/-}$Fbn1$^{C1039G+/-}$ mouse after iDISCO clearing, showing that the morphology of the plaque and the structure of the neovessels (arrows) were not affected by the clearing procedure. Scale bar = 100 µm.

Clearing and 3D imaging of human artery segments was not performed in this study and might present certain challenges and constraints. Considering the thickness and

composition of human plaques, we expect that the described iDISCO procedure for mouse tissue will need to be adapted, and will become more complex with longer incubation times for dehydration and clearing. Because of their size, 3D imaging of human plaques will require dedicated light sheet microscopy. In addition to the clearing procedure limitations that have already been described by Ali Ertürk et al. [27], such as that this protocol can only be used on fixed tissues and that samples cannot be stored for prolonged periods, the toxicity of the organic solutions used in our protocol might be an extra limitation. Nevertheless, our protocol is straightforward and reproducible which makes it an effective method for visualizing and analyzing neovessels inside atherosclerotic plaques.

In conclusion, this is the first report to apply iDISCO technology to atherosclerotic blood vessels and it provides a simple, inexpensive and effective method for visualizing and reconstructing, in three dimensions, the presence of IP neovessels inside these lesions. This could be a useful new tool for studies aimed at determining whether there is a causal relationship between the presence of neovessel structures and atherogenesis or between angiogenic stimuli and plaque angiogenesis.

Online supplemental material

Video 1. Representative 3D reconstruction of a carotid artery segment (50 z-stack slides) in ApoE$^{-/-}$Fbn1$^{C1039G+/-}$ mice stained with the endothelial marker CD31. For a general overview of the different parts of the vessel, we refer to a single frame of this video in Figure 5A.

Video 2. Video showing all confocal planes from a z-stack taken from a carotid artery segment of a representative ApoE$^{-/-}$Fbn1$^{C1039G+/-}$ mouse. DAPI (blue) was used to stain the nuclei and CD31 (red) visualizes the endothelial cells.

Video 3. Video showing all confocal planes from a z-stack taken from a brachiocephalic artery segment of a representative ApoE$^{-/-}$ mouse, confirming that there is no CD31 (red) staining present inside the plaque. Nuclei are stained with DAPI (blue).

Acknowledgement

The authors would like to thank Rita Van den Bossche, Mandy Vermont, Dominique De Rijck and Gleison D.P. Bossolani for technical help. The authors are grateful to Dr. Bronwen Martin for critical reading of the manuscript.

Statement of Ethics

All animal procedures were conducted according to the guidelines from Directive 2010/63/EU of the European Parliament on the protection of animals used for scientific purposes. Experiments were approved by the ethics committee of the University of Antwerp.

Disclosure Statement

The authors have no conflicts of interest to declare.

Funding Sources

This work was supported by the University of Antwerp (DOCPRO-BOF) and the Horizon 2020 program of the European Union – Marie Sklodowska Curie actions – ITN – MOGLYNET [grant number 675527]. The Leica SP 8 (Hercules grant AUHA.15.12) confocal microscope was funded by the Hercules Foundation of the Flemish Government.

Author Contributions

Paola Perrotta, Isabel Pintelon and Wim Martinet: study conception and design
Paola Perrotta, Isabel Pintelon and Margreet R. De Vries: acquisition of data
All authors contributed to the analysis and interpretation of data. All authors also helped drafting the manuscript and approved the final version of the manuscript.

References

1. Ross R. Atherosclerosis is an inflammatory disease. *Am Heart J*. 1999;138:S419-420
2. Moreno PR, Sanz J, Fuster V. Promoting mechanisms of vascular health: Circulating progenitor cells, angiogenesis, and reverse cholesterol transport. *J Am Coll Cardiol*. 2009;53:2315-2323
3. Bentzon JF, Otsuka F, Virmani R, Falk E. Mechanisms of plaque formation and rupture. *Circ Res*. 2014;114:1852-1866
4. Moreno PR, Purushothaman KR, Sirol M, Levy AP, Fuster V. Neovascularization in human atherosclerosis. *Circulation*. 2006;113:2245-2252
5. de Vries MR, Quax PH. Plaque angiogenesis and its relation to inflammation and atherosclerotic plaque destabilization. *Curr Opin Lipidol*. 2016;27:499-506
6. Stary HC, Chandler AB, Dinsmore RE, Fuster V, Glagov S, Insull W, Jr., Rosenfeld ME, Schwartz CJ, Wagner WD, Wissler RW. A definition of advanced types of atherosclerotic lesions and a histological classification of atherosclerosis. A report from the committee on vascular lesions of the council on arteriosclerosis, american heart association. *Circulation*. 1995;92:1355-1374
7. Nakamura J, Nakamura T, Deyama J, Fujioka D, Kawabata K, Obata JE, Watanabe K, Watanabe Y, Kugiyama K. Assessment of carotid plaque neovascularization using quantitative analysis of contrast-enhanced ultrasound imaging is useful for risk stratification in patients with coronary artery disease. *Int J Cardiol*. 2015;195:113-119
8. Parma L, Baganha F, Quax PHA, de Vries MR. Plaque angiogenesis and intraplaque hemorrhage in atherosclerosis. *Eur J Pharmacol*. 2017;816:107-115
9. Perrotta P, Emini Veseli B, Van der Veken B, Roth L, Martinet W, De Meyer GRY. Pharmacological strategies to inhibit intraplaque angiogenesis in atherosclerosis. *Vascul Pharmacol*. 2019;112:72-78

10. Van Herck JL, De Meyer GR, Martinet W, Van Hove CE, Foubert K, Theunis MH, Apers S, Bult H, Vrints CJ, Herman AG. Impaired fibrillin-1 function promotes features of plaque instability in apolipoprotein e-deficient mice. *Circulation*. 2009;120:2478-2487
11. Van der Donckt C, Van Herck JL, Schrijvers DM, Vanhoutte G, Verhoye M, Blockx I, Van Der Linden A, Bauters D, Lijnen HR, Sluimer JC, Roth L, Van Hove CE, Fransen P, Knaapen MW, Hervent AS, De Keulenaer GW, Bult H, Martinet W, Herman AG, De Meyer GR. Elastin fragmentation in atherosclerotic mice leads to intraplaque neovascularization, plaque rupture, myocardial infarction, stroke, and sudden death. *Eur Heart J*. 2015;36:1049-1058
12. Emini Veseli B, Perrotta P, De Meyer GRA, Roth L, Van der Donckt C, Martinet W, De Meyer GRY. Animal models of atherosclerosis. *Eur J Pharmacol*. 2017;816:3-13
13. Coli S, Magnoni M, Sangiorgi G, Marrocco-Trischitta MM, Melisurgo G, Mauriello A, Spagnoli L, Chiesa R, Cianflone D, Maseri A. Contrast-enhanced ultrasound imaging of intraplaque neovascularization in carotid arteries: Correlation with histology and plaque echogenicity. *J Am Coll Cardiol*. 2008;52:223-230
14. Cattaneo M, Staub D, Porretta AP, Gallino JM, Santini P, Limoni C, Wyttenbach R, Gallino A. Contrast-enhanced ultrasound imaging of intraplaque neovascularization and its correlation to plaque echogenicity in human carotid arteries atherosclerosis. *Int J Cardiol*. 2016;223:917-922
15. Oura K, Kato T, Ohba H, Terayama Y. Evaluation of intraplaque neovascularization using superb microvascular imaging and contrast-enhanced ultrasonography. *J Stroke Cerebrovasc Dis*. 2018;27:2348-2353
16. Andrews JPM, Fayad ZA, Dweck MR. New methods to image unstable atherosclerotic plaques. *Atherosclerosis*. 2018;272:118-128
17. Richardson DS, Lichtman JW. Clarifying tissue clearing. *Cell*. 2015;162:246-257
18. Richardson DS, Lichtman JW. Snapshot: Tissue clearing. *Cell*. 2017;171:496-496 e491

19. Ariel P. A beginner's guide to tissue clearing. *Int J Biochem Cell Biol*. 2017;84:35-39
20. Orlich M, Kiefer F. A qualitative comparison of ten tissue clearing techniques. *Histol Histopathol*. 2018;33:181-199
21. Vogt N. Transparency in large tissue samples. *Nat Methods*. 2015;12:11
22. Bossolani GDP, Pintelon I, Detrez JD, Buckinx R, Thys S, Zanoni JN, De Vos WH, Timmermans JP. Comparative analysis reveals ce3d as optimal clearing method for in toto imaging of the mouse intestine. *Neurogastroenterol Motil*. 2019;31:e13560
23. Renier N, Wu Z, Simon DJ, Yang J, Ariel P, Tessier-Lavigne M. Idisco: A simple, rapid method to immunolabel large tissue samples for volume imaging. *Cell*. 2014;159:896-910
24. Henning Y, Osadnik C, Malkemper EP. Eyeci: Optical clearing and imaging of immunolabeled mouse eyes using light-sheet fluorescence microscopy. *Exp Eye Res*. 2019;180:137-145
25. Walter A, van der Spek L, Hardy E, Bemelmans AP, Rouach N, Rancillac A. Structural and functional connections between the median and the ventrolateral preoptic nucleus. *Brain Struct Funct*. 2019
26. Becher T, Riascos-Bernal DF, Kramer DJ, Almonte V, Chi J, Tong T, Oliveira-Paula GH, Koleilat I, Chen W, Cohen P, Sibinga NE. Three-dimensional imaging provides detailed atherosclerotic plaque morphology and reveals angiogenesis after carotid artery ligation. *Circ Res*. 2020
27. Erturk A, Becker K, Jahrling N, Mauch CP, Hojer CD, Egen JG, Hellal F, Bradke F, Sheng M, Dodt HU. Three-dimensional imaging of solvent-cleared organs using 3disco. *Nat Protoc*. 2012;7:1983-1995

Chapter 9

General summary and future perspectives

Summary

In recent years, endothelial cells (ECs) metabolism has attracted renewed attention which has unveiled an unexpected complexity of regulatory mechanisms and a plethora of potential novel targets for vascular-related diseases.[1, 2] Despite the fact that ECs have readily available oxygen in the blood, they mainly generate ATP via anaerobic glycolysis rather than Krebs cycle. Thus, by relying on anaerobic rather than aerobic metabolism, ECs are able to sprout in low oxygen conditions such as the tumor environment.[1, 3] Among the different enzymes involved in the control of glycolytic flux, PFKFB3 (6-Phosphofructo-2-Kinase/Fructose-2,6-Biphosphatase 3) has been shown to play a critical role for the proliferation and migration of ECs. [4, 5] Intraplaque (IP) neovascularization, has been identified as a contributing factor of atherosclerotic plaque vulnerability in human atherosclerosis. In this context, regulation of EC metabolism may represent a novel target to inhibit IP angiogenesis and to promote plaque stability. The experimental work of this thesis focuses on PFKFB3 as a modulator of EC glycolysis and its effect on atherosclerosis progression and intraplaque angiogenesis.

In **chapter 2,** a review of potential pharmacological strategies to inhibit IP angiogenesis is presented. Such strategies include: (1) inhibition of vascular endothelial growth factor signaling, (2) inhibition of glycolytic flux, and (3) inhibition of fatty acid oxidation. Overall targeting IP neovascularization might be suitable therapeutic approach to promote plaque stabilization in combination with lipid-lowering treatment.

In **chapter 3,** a comprehensive review of all animal models of atherosclerosis is presented. The chapter also includes a description of the two main models that have been used in this thesis, namely apolipoprotein E-deficient Fibrillin-1 mutant mice ($ApoE^{-/-}Fbn1^{C1039G+/-}$) and vein grafts in $ApoE^{-/-}$ mice. These two animal models develop unstable atherosclerotic plaques with IP angiogenesis, and thus are suitable to study the role of glycolysis during IP neovascularization and plaque progression.

In **chapter 4,** a pharmacological study with partial glycolysis inhibitor 3PO [3-(3-pyridinyl)-1-(4-pyridinyl)-2-propen-1-one] in the context of advanced atherosclerotic plaques in $ApoE^{-/-}Fbn1^{C1039G+/-}$ mice is described. 3PO treatment restrains IP

angiogenesis and plaque frequency, however it does not affect plaque size and composition. In addition, a 3PO-mediated reduction in plaque formation is observed in regular ApoE$^{-/-}$ mice that develop plaques without IP neovascularization. Overall, these data suggest that vessel wall metabolism may play a role in the early stages of atherosclerosis. In vitro and in vivo data show that 3PO prevent upregulation of VCAM-1 and ICAM-1 in ECs, two key adhesion molecules involved in early-stage plaque development. Mechanistically, 3PO inhibits TNFα-NF-κB signalling pathway in ECs, which led to suppression of VCAM-1 expression both in vitro and in vivo. Furthermore, downregulation of endothelial VCAM-1 (and ICAM-1) expression depends on 3PO-inducted autophagy. Expression of the adhesion molecules is not downregulated by 3PO in TNF-α-treated ECs in which expression of the essential autophagy gene ATG7 was silenced. On the contrary, VCAM-1 (and ICAM-1) expression is upregulated in ATG7-deficient ECs, suggesting that autophagy suppresses expression of these adhesion molecules. These findings support previous data showing that endothelial autophagy is atheroprotective and limits atherosclerotic plaque formation by preventing endothelial apoptosis, senescence and inflammation.[6]

In **chapter 5,** the mechanism behind glycolysis inhibition by 3PO is investigated. 3PO is considered a PFKFB3 competitive inhibitor however conclusive affinity assays are still lacking**.** The study presented in chapter 5 shows data from isothermal titration calorimetry indicating that 3PO does not bind to PFKFB3, up to 750 μM. Conversely, AZ PFKFB3 67 at 3 μM concentration shows strong and potent PFKFB3 inhibition. This study also confirms that 3PO inhibits glycolysis in ECs and demonstrates that the inhibitory effect of 3PO on glycolysis relies on its capacity to cause an imbalance in intracellular pH through the accumulation of lactic acid inside the cell. This finding is not surprising as other glycolytic enzymes such as lactate dehydrogenase and phosphofructokinase-1 (PFK-1) are also extremely sensitive to pH. A change of less than one pH unit, even a few tenths, reduces the activity of PFK-1 by more than 10-fold. Moreover, PFKFB3, also known as phosphofructokinase-2 (PFK-2), has been shown to be allosterically regulated by hydrogen ion concentrations. On the other hand, lactate is a modulator of intracellular pH, hence the accumulation of this metabolite leads to intracellular milieu acidification and affect indirectly the glycolysis rate

In **Chapter 6,** a genetic approach to study the role of endothelial PFKFB3 in IP angiogenesis and plaque development is described. ApoE$^{-/-}$ mice were crossbreed with PFKFB3$^{fl/fl}$ Cdh5^{iCre} mice (containing a tamoxifen-inducible EC-specific Cre) to generate an ApoE$^{-/-}$ PFKFB3^{ECKO} mouse strain. A vein graft model is then used to study the effect of an EC-specific deletion of PFKFB3 in advanced plaques with IP neovascularization. Analysis of IP neovascularization in vein graft lesions of ApoE$^{-/-}$ PFKFB3^{ECKO} mice show a significant decrease in the amount of microvessels, which is in line with the effects obtained with glycolysis inhibitor 3PO. However, in contrast with 3PO, a decrease in vein graft lesion area and percentage of stenosis in ApoE$^{-/-}$ PFKFB3^{ECKO} mice is observed. One possible explanation for such differences is the use of 3PO as therapeutic agent (administration after 4 or 16 weeks of western diet), while PFKFB3 is deleted ahead of the western diet regimen. Furthermore, 3PO is not an EC-specific agent and may also interfere with the metabolism of other cell types involved in plaque development. The reduction in IP angiogenesis observed in vein graft lesions was accompanied by a reduction in leakage of these microvessels. These findings are in line with in vitro and in vivo observations showing that PFKFB3 inhibition in ECs reduces VE-cadherin endocytosis and promotes normalization of the endothelial barrier in the settings of cancer biology.[7] Together with a decreased number of microvessels, reduction of macrophage infiltration in lesions of ApoE$^{-/-}$ PFKFB3^{ECKO} mice is also observed, suggesting a link between EC metabolism and macrophage infiltration. In agreement with previous findings, it is possible that such reduced lesion infiltration *in vivo*, is in part due to an improved restoration of EC cell-cell junction after PFKFB3 deletion.[7] Interestingly, EC-specific PFKFB3 deletion inhibits plaque development in ApoE$^{-/-}$ mice, a native atherosclerosis animal model that does not develop features of advanced lesions such as IP microvessels. Altogether, these findings show the potential value of targeting EC glycolysis and in particular PFKFB3 as a therapeutic strategy to counteract plaque development in vein grafts and native atherosclerosis.

In **chapter 7,** a study performed in collaboration with the University of Aberdeen is presented. Here the development of a PFKFB3-targeted PET radiotracer, [^{18}F]ZCDD083 (^{18}F-radiolabelled phenoxindazole compound, ZCDD083), for imaging the atherosclerotic plaque in vivo is described. ZCDD083 is a close structural mimic of the potent PFKFB3 inhibitor AZ68 (IC50 = 4 nM), whose

radiofluorination is deemed to be chemically viable and unlikely to affect the binding to PFKFB3. The specificity of the tracer for atherosclerotic plaques is demonstrated by the combination of ex vivo autoradiography with en face Oil Red O staining of the same aortic specimens. Indeed, co-localisation of the $^{[18}$F]ZCDD083 signal with plaque distribution along the aorta is observed. These cross studies in C57BL/6J, ApoE$^{-/-}$ and ApoE$^{-/-}$Fbn1$^{C1039G+/-}$ mice demonstrates high sensitivity of $^{[18F]}$ZCDD083 to detect atherosclerotic plaques, whereas little signal is detected in normal vessels or outside atherosclerotic lesions. This tracer is a promising non-invasive diagnostic tool to detect rupture-prone atherosclerotic plaques, which in turn could help improving risk stratification and evaluation of the efficacy of anti-atherosclerotic therapies.

In **chapter 8,** a novel imaging method for a three dimensional reconstruction of the IP vessel network in a mouse model of advanced atherosclerosis that spontaneously develops IP angiogenesis is presented. This method based on immunolabeling-enabled 3D Imaging of Solvent Cleared Organs (iDISCO) and confocal microscopy, may represent a useful tool for studies aimed at determining whether there is a causal relationship between the presence of IP neovessel structures and atherogenesis or between angiogenic stimuli and plaque angiogenesis.

General discussion and future perspective

Glycolytic flux in ECs is 200-fold higher than glucose oxidation, fatty acid oxidation, and glutamine oxidation, resulting in the generation of >85% of the total cellular ATP content.[1] The glycolytic activity of ECs is often as high as in cancer cells. Recent studies have shown that the proangiogenic response to growth factors such as VEGF (vascular endothelial growth factor) or FGF (fibroblast endothelial growth factor) relies on metabolic changes such as increased glycolytic flux and fatty acid oxidation (FAO) in endothelial cells (ECs).[3, 5, 9]

In the context of atherosclerosis, there has been growing interest on the role of EC metabolism and how it affects both plaque formation and intraplaque (IP) angiogenesis.[2] For example, recent results have shown that laminar shear stress *in vitro* reduces glucose uptake by ECs, via an upregulation of the transcription factor

Krüppel-like factor 2 (KLF2). This mechanism allows to maintain a quiescent metabolic phenotype in ECs and may promote an atheroprotective effect.[10] Another link between ECs metabolism and atherosclerosis has been identified in the glycolytic enzyme PFKFB3, which is upregulated in atheroprone regions of arterial vessels (usually exposed to turbulent blood flow) and in carotid plaques of patients with elevated levels of lipoprotein(a).[8, 10] However, to date there are no published studies on the role of EC metabolism in animal model of atherosclerosis.

ECs are also capable of switching from a quiescent state to a highly proliferative and migratory state when angiogenesis needs to take place. Studies on the metabolic requirements for ECs to undergo an angiogenic switch are slowly emerging. Our increasing understanding of EC-metabolism regulation in the context of IP angiogenesis may unveil novel pharmacological targets to promote plaque stability. Interestingly, neovascular networks are often found inside advanced or vulnerable atherosclerotic plaques and recent evidence suggests that 50% of patients with acute coronary syndrome present one or more lesions with IP angiogenesis. This is five times more frequently than in lesions from patients with stable coronary artery disease.[11] The experimental data generated in this thesis with the use of animal models that recapitulate advanced human atherosclerosis, strongly suggest a critical role of EC metabolism in the formation and progression of atherosclerosis in addition to IP angiogenesis.

This thesis includes a number of pharmacological and genetic preclinical studies that describe the effect of glycolysis inhibition in the activated vessel wall and endothelium in the context of atherosclerosis. In particular, the work of this thesis focuses on PFKFB3, nevertheless, other metabolic enzymes have also been recently identified in the control of EC glycolytic flux and angiogenesis. Indeed, a recent study has shown that deletion of hexokinase 2 (HK2) in ECs leads to decreased glycolysis, which impaired EC proliferation, migration and angiogenesis in vivo.[9] Finally, endothelial fatty acid oxidation (FAO) has been shown to play a rather unexpected role in vessel sprouting. A recent study proved that EC-specific deletion of carnitine palmitoyltransferase 1a (CPT1a), which imports fatty acids (FAs) into mitochondria and thereby rate-limits FAO flux, decreased EC proliferation and caused sprouting reduction both in vitro and in vivo.[12] The role of these EC metabolic

pathways in the context of atherosclerotic plaque formation and progression has not been investigate thus far.

Overall, the results presented in this thesis strongly argues that glycolysis inhibition in ECs may promotes beneficial effects such as a reduction in plaque formation, plaque progression and IP angiogenesis. Given the strong evidence that decreased IP vascularization makes plaques less vulnerable, glycolysis inhibition may represent a novel strategy to reduce the risk of plaque rupture and frequency of adverse cardiovascular events.[13-15]

The work of this thesis also presents new compelling data that will be expanded in future studies. For example, in vein graft lesions of ApoE$^{-/-}$ PFKFB3^{ECKO} mice, a marked reduction in IP neovascularization is associated with reduced plaque growth (See Chapter 6), however whether these events are causally linked require additional investigation. Interestingly, mice treated with glycolysis inhibitor 3PO do not display changes in progression of established plaques however the number of plaques is reduced. Histological data from human plaques indicate that in early lesions VCAM-1 and ICAM-1 are predominantly expressed by the endothelium, whereas in more advanced lesions, the majority of VCAM-1 expression is found in subsets of intimal VSMCs and macrophages. These findings may explain why downregulation of adhesion molecules by 3PO in ECs mainly affects plaque formation, but not further steps of plaque progression. Interestingly, the metabolic stress caused by 3PO stimulated autophagosome formation in ECs and led to induction of autophagy. Similar observations were previously reported in cancer cells.[16]

Statins are competitive inhibitors of 3-hydroxy-3-methylglutaryl coenzyme A (HMG-CoA) reductase, the enzyme that catalyses the rate limiting step in cholesterol synthesis and they are one the most widely prescribed drugs. Statins are used to slow down atherosclerosis progression and to reduce cardiovascular risk. Apart from their cholesterol lowering action, they also have anti-inflammatory properties and improve endothelial function by increasing the expression of endothelial progenitor cells involved in vascular repair as well as the expression of endothelial nitric oxide synthase.[17] More recently, the class of PCSK9 Inhibitors (e.g. alirocumab, evolocumab) that inactivate liver *proprotein convertase subtilisin kexin* 9 achieve

even lower circulating LDL-C levels, and have been approved as first-line drugs to reduce the risk of cardiovascular events in patients that cannot tolerate statins.[18] Statins and PCSK9 inhibitors act on hyperlipidaemia, which is a well-established risk factor for plaque progression, rupture and adverse cardiovascular events. Drugs that specifically target EC metabolism may offer a novel approach to inhibit the development of atherosclerosis lesions by targeting the underlying mechanisms of endothelial disfunction. Furthermore, a combination therapy for both ECs and lipid metabolism in established atherosclerosis may result in reduced cardiovascular complications due to vulnerable plaques and leads to an overall improved survival.

Development of new diagnostic and imaging tools in atherosclerosis has been active area of research in the last few decades.[19] Indeed, studying the complex mechanisms behind the progression of atherosclerosis has been made hard by the difficulty of following the morphological changes in a patient over time. Moreover, there are a limited number of non-invasive image modalities that allow to collect information on the composition of atherosclerotic plaques. For example, intravascular ultrasound (IVUS), optical coherence tomography (OCT) and near-infrared spectroscopy (NIRS), can provide a limited plaque characterization but they are invasive and thus not ideal in early-diagnosis or follow-up.[20]

To date Positron emission tomography (PET) is a non-invasive nuclear imaging method which can detect and quantify the pathophysiological processes associated with atherogenesis and subsequent risk of plaque destabilization. However, there is a need for a better PET tracer for routine clinical imaging. Numerous pathways and targets have been studied but currently there is only one approved tracer for clinical use (18F-FDG) .[21] However, carotid artery imaging using 18F-FDG PET often shows unspecific myocardial uptake.[22, 23] A new PFKFB3-targeted PET radiotracer ([^{18}F]ZCDD083) has been presented in this thesis with several advantages which include a higher in vivo metabolic stability and specific uptake in atherosclerotic plaques. This new radiotracer may represent a better tool for the evaluation of plaque morphology and identification of vulnerable plaques.

The majority of the studies aimed at identifying pathological pathways of human atherosclerosis plaques have been done using two dimensional cross-sections of autoptic or surgical samples. However, a more detailed study of atherosclerotic lesions with particular regard to the morphological features that make a plaque

vulnerable such as the presence of intraplaque neovessels, could be obtained through the three-dimensional reconstruction of human atherosclerotic plaques. For the first time in this thesis, is presented a preclinical study in which using innovative clearing techniques it is possible to reconstruct the small vessels inside the atherosclerotic plaque three-dimensionally. Additional studies with human samples are still required but this method may provide the missing tool to characterize and understand the complexity of intraplaque neovessel network in human atherosclerotic plaque.

The studies and experimental results described in this thesis contribute to a better understanding of EC metabolism in the context of atherosclerosis and intraplaque angiogenesis. This work also suggests a strong link between EC metabolism, intraplaque angiogenesis and plaque stability which potentially unveil a completely, novel therapeutic approach to enhance plaque stability.

References

1. Rohlenova K, Veys K, Miranda-Santos I, De Bock K, Carmeliet P. Endothelial cell metabolism in health and disease. *Trends Cell Biol*. 2018;28:224-236

2. Pircher A, Treps L, Bodrug N, Carmeliet P. Endothelial cell metabolism: A novel player in atherosclerosis? Basic principles and therapeutic opportunities. *Atherosclerosis*. 2016;253:247-257

3. Cantelmo AR, Brajic A, Carmeliet P. Endothelial metabolism driving angiogenesis: Emerging concepts and principles. *Cancer J*. 2015;21:244-249

4. Schoors S, De Bock K, Cantelmo AR, Georgiadou M, Ghesquiere B, Cauwenberghs S, Kuchnio A, Wong BW, Quaegebeur A, Goveia J, Bifari F, Wang X, Blanco R, Tembuyser B, Cornelissen I, Bouche A, Vinckier S, Diaz-Moralli S, Gerhardt H, Telang S, Cascante M, Chesney J, Dewerchin M, Carmeliet P. Partial and transient reduction of glycolysis by pfkfb3 blockade reduces pathological angiogenesis. *Cell Metab*. 2014;19:37-48

5. Cruys B, Wong BW, Kuchnio A, Verdegem D, Cantelmo AR, Conradi LC, Vandekeere S, Bouche A, Cornelissen I, Vinckier S, Merks RM, Dejana E, Gerhardt H, Dewerchin M, Bentley K, Carmeliet P. Glycolytic regulation of cell rearrangement in angiogenesis. *Nat Commun*. 2016;7:12240

6. Vion AC, Kheloufi M, Hammoutene A, Poisson J, Lasselin J, Devue C, Pic I, Dupont N, Busse J, Stark K, Lafaurie-Janvore J, Barakat AI, Loyer X, Souyri M, Viollet B, Julia P, Tedgui A, Codogno P, Boulanger CM, Rautou PE. Autophagy is required for endothelial cell alignment and atheroprotection under physiological blood flow. *Proc Natl Acad Sci U S A*. 2017;114:E8675-E8684

7. Cantelmo AR, Conradi LC, Brajic A, Goveia J, Kalucka J, Pircher A, Chaturvedi P, Hol J, Thienpont B, Teuwen LA, Schoors S, Boeckx B, Vriens J, Kuchnio A, Veys K, Cruys B, Finotto L, Treps L, Stav-Noraas TE, Bifari F,

Stapor P, Decimo I, Kampen K, De Bock K, Haraldsen G, Schoonjans L, Rabelink T, Eelen G, Ghesquiere B, Rehman J, Lambrechts D, Malik AB, Dewerchin M, Carmeliet P. Inhibition of the glycolytic activator pfkfb3 in endothelium induces tumor vessel normalization, impairs metastasis, and improves chemotherapy. *Cancer Cell*. 2016;30:968-985

8. Schnitzler JG, Hoogeveen RM, Ali L, Prange KHM, Waissi F, van Weeghel M, Bachmann JC, Versloot M, Borrelli MJ, Yeang C, De Kleijn DPV, Houtkooper RH, Koschinsky ML, de Winther MPJ, Groen AK, Witztum JL, Tsimikas S, Stroes ESG, Kroon J. Atherogenic lipoprotein(a) increases vascular glycolysis, thereby facilitating inflammation and leukocyte extravasation. *Circ Res*. 2020;126:1346-1359

9. Yu P, Wilhelm K, Dubrac A, Tung JK, Alves TC, Fang JS, Xie Y, Zhu J, Chen Z, De Smet F, Zhang J, Jin SW, Sun L, Sun H, Kibbey RG, Hirschi KK, Hay N, Carmeliet P, Chittenden TW, Eichmann A, Potente M, Simons M. Fgf-dependent metabolic control of vascular development. *Nature*. 2017;545:224-228

10. Doddaballapur A, Michalik KM, Manavski Y, Lucas T, Houtkooper RH, You X, Chen W, Zeiher AM, Potente M, Dimmeler S, Boon RA. Laminar shear stress inhibits endothelial cell metabolism via klf2-mediated repression of pfkfb3. *Arterioscler Thromb Vasc Biol*. 2015;35:137-145

11. Herrmann J, Lerman LO, Mukhopadhyay D, Napoli C, Lerman A. Angiogenesis in atherogenesis. *Arterioscler Thromb Vasc Biol*. 2006;26:1948-1957

12. Schoors S, Bruning U, Missiaen R, Queiroz KC, Borgers G, Elia I, Zecchin A, Cantelmo AR, Christen S, Goveia J, Heggermont W, Godde L, Vinckier S, Van Veldhoven PP, Eelen G, Schoonjans L, Gerhardt H, Dewerchin M, Baes M, De Bock K, Ghesquiere B, Lunt SY, Fendt SM, Carmeliet P. Fatty acid carbon is essential for dntp synthesis in endothelial cells. *Nature*. 2015;520:192-197

13. de Vries MR, Quax PH. Plaque angiogenesis and its relation to inflammation and atherosclerotic plaque destabilization. *Curr Opin Lipidol*. 2016;27:499-506

14. Camare C, Pucelle M, Negre-Salvayre A, Salvayre R. Angiogenesis in the atherosclerotic plaque. *Redox Biol*. 2017;12:18-34

15. Virmani R, Kolodgie FD, Burke AP, Finn AV, Gold HK, Tulenko TN, Wrenn SP, Narula J. Atherosclerotic plaque progression and vulnerability to rupture: Angiogenesis as a source of intraplaque hemorrhage. *Arterioscler Thromb Vasc Biol*. 2005;25:2054-2061

16. Aarup A, Pedersen TX, Junker N, Christoffersen C, Bartels ED, Madsen M, Nielsen CH, Nielsen LB. Hypoxia-inducible factor-1alpha expression in macrophages promotes development of atherosclerosis. *Arterioscler Thromb Vasc Biol*. 2016;36:1782-1790

17. Oesterle A, Laufs U, Liao JK. Pleiotropic effects of statins on the cardiovascular system. *Circ Res*. 2017;120:229-243

18. Wang Y, Liu ZP. Pcsk9 inhibitors: Novel therapeutic strategies for lowering ldlcholesterol. *Mini Rev Med Chem*. 2019;19:165-176

19. Mushenkova NV, Summerhill VI, Zhang D, Romanenko EB, Grechko AV, Orekhov AN. Current advances in the diagnostic imaging of atherosclerosis: Insights into the pathophysiology of vulnerable plaque. *Int J Mol Sci*. 2020;21

20. Tarkin JM, Dweck MR, Evans NR, Takx RA, Brown AJ, Tawakol A, Fayad ZA, Rudd JH. Imaging atherosclerosis. *Circ Res*. 2016;118:750-769

21. Evans NR, Tarkin JM, Chowdhury MM, Warburton EA, Rudd JH. Pet imaging of atherosclerotic disease: Advancing plaque assessment from anatomy to pathophysiology. *Curr Atheroscler Rep*. 2016;18:30

22. Joshi NV, Vesey AT, Williams MC, Shah AS, Calvert PA, Craighead FH, Yeoh SE, Wallace W, Salter D, Fletcher AM, van Beek EJ, Flapan AD, Uren NG, Behan MW, Cruden NL, Mills NL, Fox KA, Rudd JH, Dweck MR, Newby DE. 18f-fluoride positron emission tomography for identification of ruptured

and high-risk coronary atherosclerotic plaques: A prospective clinical trial. *Lancet*. 2014;383:705-713

23. Rudd JH, Narula J, Strauss HW, Virmani R, Machac J, Klimas M, Tahara N, Fuster V, Warburton EA, Fayad ZA, Tawakol AA. Imaging atherosclerotic plaque inflammation by fluorodeoxyglucose with positron emission tomography: Ready for prime time? *J Am Coll Cardiol*. 2010;55:2527-2535

Nederlandse samenvatting

In de afgelopen jaren heeft het metabolisme van endotheelcellen (EC's) veel aandacht getrokken en een onverwachte complexiteit van de reguleringsmechanismen blootgelegd, waardoor nieuwe mogelijke doelwitten zijn ontstaan voor een overvloed aan vaatziekten. Ondanks het feit dat EC's gemakkelijk zuurstof vanuit het bloed kunnen opnemen, is het verrassend dat ze ATP vooral via glycolyse genereren in plaats van via de Krebs-cyclus. Door te vertrouwen op het anaërobe in plaats van het aërobe metabolisme zijn EC's dus in staat om te ontkiemen in zuurstofarme omstandigheden zoals het tumormilieu. Van de verschillende enzymen die betrokken zijn bij de controle van glycolytische flux is aangetoond dat PFKFB3 (6-Phosphofructo-2-Kinase/Fructose-2,6-Bifosfatase 3) een cruciale rol speelt bij de proliferatie en migratie van EC's. In dit proefschrift hebben we vooral aandacht besteed aan PFKFB3 als modulator van het EC metabolisme en hebben we de rol ervan bestudeerd in verschillende aspecten van atherosclerose, zoals plaquevorming en plaqueprogressie. We hebben ook onderzocht of PFKFB3 remming implicaties heeft op intraplaque (IP) neovascularisatie, hetgeen beschouwd wordt als een factor die bijdraagt aan de kwetsbaarheid van humane plaques. In deze context kan regulering van het EC metabolisme een nieuw doelwit vormen om IP angiogenese te remmen en de stabiliteit van de plaque te bevorderen.

In **hoofdstuk 2** hebben we potentiële farmacologische strategieën besproken om IP angiogenese te remmen, waaronder (1) remming van vasculaire endotheelgroeifactor signalering, (2) remming van glycolytische flux en (3) remming van vetzuuroxidatie. Op de lange termijn concludeerden we dat IP neovascularisatie van toepassing zou kunnen zijn als therapeutisch doelwit om plaquestabilisatie te induceren bovenop een lipidenverlagende behandeling.

In **hoofdstuk 3** hebben we een uitgebreid overzicht gegeven van alle diermodellen van atherosclerose. Het hoofdstuk bevat ook een beschrijving van de twee belangrijkste modellen die in dit proefschrift zijn gebruikt, namelijk apolipoproteïne E-deficiënte Fibrilline-1 mutant muizen ($ApoE^{-/-}Fbn1^{C1039G+/-}$) en adertransplantaties in $ApoE^{-/-}$ muizen. Deze twee diermodellen ontwikkelen onstabiele atherosclerotische plaques met IP angiogenese, en zijn dus geschikt om de rol van glycolyse tijdens IP neovascularisatie en plaque progressie te bestuderen.

In **hoofdstuk 4** beschrijven we een farmacologische studie met de partiële glycolyse remmer 3PO [3-(3-pyridinyl)-1-(4-pyridinyl)-2-propen-1-één] in de context van geavanceerde atherosclerotische plaques van $ApoE^{-/-}Fbn1^{C1039G+/-}$ muizen. We vonden dat 3PO behandeling IP angiogenese en plaquevorming reduceert. Verrassend genoeg had 3PO geen invloed op de grootte en samenstelling van de plaque. Bovendien werd een 3PO-gemedieerde vermindering van de plaquevorming waargenomen bij gewone $ApoE^{-/-}$ muizen die plaques ontwikkelen zonder IP neovascularisatie. Over het geheel genomen suggereren deze gegevens dat het vaatwandmetabolisme een rol kan spelen in de vroege stadia van atherosclerose. We hebben ook in vitro en in vivo bewijs geleverd dat 3PO interfereert met de opregulatie van VCAM-1 en ICAM-1 in EC's. VCAM-1 en ICAM-1 zijn twee belangrijke adhesiemoleculen die betrokken zijn bij de ontwikkeling van plaque in een vroeg stadium. Mechanistisch gezien vonden we dat 3PO de TNFα-NF-κB signaalweg in EC's remt. Dit leidt tot onderdrukking van VCAM-1 expressie zowel in vitro als in vivo. Onze studie roept echter ook enkele aanvullende vragen op, zoals waarom veranderingen in VCAM-1 expressie in 3PO behandelde muizen de plaquevorming niet veranderen, maar alleen de (vroege) plaquevorming. Men kan speculeren dat wanneer vroege plaques eenmaal gevormd zijn, downregulering van VCAM-1 expressie in EC's door 3PO geen significante invloed heeft op verdere leukocytenrecrutering en plaqueprogressie. Histologische gegevens van menselijke plaques geven aan dat in vroege lesies VCAM-1 en ICAM-1 voornamelijk tot expressie komen door het endotheel, terwijl in meer gevorderde lesies de meerderheid van de VCAM-1 expressie wordt gevonden in subsets van intimale gladde spiercellen en macrofagen. Deze bevindingen kunnen verklaren waarom downregulering van adhesiemoleculen door 3PO in EC's voornamelijk de initiële fase van de ontwikkeling van atherosclerose beïnvloedt, maar niet verdere stappen van plaque progressie. Interessant is dat de metabole stress veroorzaakt door 3PO de vorming van autofagosomen in EC's stimuleerde en leidde tot inductie van autofagie. Soortgelijke waarnemingen werden eerder gemeld in kankercellen. Onze resultaten geven aan dat downregulering van endotheliale VCAM-1 (en ICAM-1) expressie door 3PO afhankelijk is van autofagie-inductie. De expressie van deze adhesiemoleculen werd niet verminderd door 3PO in TNF-α-behandelde EC's waarin expressie van het essentiële autofagie gen ATG7 werd stilgelegd.

Integendeel, de expressie van VCAM-1 (en ICAM-1) werd opgereguleerd in ATG7-deficiënte EC's, wat suggereert dat autofagie de expressie van deze adhesiemoleculen onderdrukt. Onze bevindingen ondersteunen eerdere gegevens die aantonen dat endotheliale autofagie atheroprotectief is en de vorming van atherosclerotische plaque beperkt door het voorkomen van endotheliale apoptose, senescentie en ontsteking.

In **hoofdstuk 5** hebben we geprobeerd aan te geven of remming van glycolyse door 3PO gerelateerd is aan een directe remming van het PFKFB3-enzym zoals eerder gesuggereerd in de literatuur. Omdat overtuigende affiniteitstests om dit probleem aan te pakken nog steeds ontbreken, presenteerden we een studie met isotherme titratie calorimetrie die suggereert dat 3PO niet bindt aan PFKFB3, tot 750 µM, in tegenstelling tot 3 µM van AZ PFKFB3 67, dat een krachtige en specifieke PFKFB3 remmer is. We hebben echter bevestigd dat 3PO de glycolyse in de EC's remt en we hebben aangetoond dat het remmende effect van 3PO op de glycolyse berust op het vermogen om een onevenwicht in de intracellulaire pH te veroorzaken door de accumulatie van melkzuur in de cel. Dit is niet verwonderlijk omdat glycolytische enzymen, waaronder lactaatdehydrogenase en phosphofructokinase-1 (PFK-1), zeer pH-gevoelig zijn. Een verandering van minder dan één pH-eenheid, zelfs een paar tienden, kan de activiteit van PFK-1 meer dan 10-voudig verminderen. Bovendien is aangetoond dat PFKFB3, ook wel bekend als phosphofructokinase-2 (PFK-2), door waterstofionenconcentraties allosterisch wordt gereguleerd. Aan de andere kant is lactaat een belangrijke regulator van de pH, vandaar dat de intracellulaire toename van deze metaboliet leidt tot intracellulaire verzuring van het milieu, waardoor indirect de snelheid van de glycolyse wordt beïnvloed.

In **hoofdstuk 6** hebben we met behulp van een genetische benadering de rol van endotheliaal PFKFB3 in IP-angiogenese en plaque-ontwikkeling bestudeerd. We kruisten ApoE$^{-/-}$ muizen met PFKFB3$^{fl/fl}$ Cdh5^{iCre} muizen (die een tamoxifen-induceerbare EC-specifieke Cre bevatten) om een ApoE$^{-/-}$ PFKFB3^{ECKO} muizenstam te genereren. Een adertransplantaatmodel werd gebruikt om het effect van een EC-specifieke verwijdering van PFKFB3 in geavanceerde plaques met IP-neovascularisatie te bestuderen. Analyse van IP neovascularisatie in adertransplantatieletsels van ApoE$^{-/-}$ PFKFB3^{ECKO}-muizen toonde een significante afname van het aantal microvaten, wat in lijn is met de effecten verkregen met 3PO.

Echter, in tegenstelling tot 3PO, zagen we een afname in het gebied van de adertransplantatie en het percentage vernauwingen in ApoE$^{-/-}$ PFKFB3^{ECKO} muizen. Een mogelijke verklaring voor deze verschillen is het feit dat 3PO als therapeutisch middel werd toegediend (na 4 of 16 weken westerse voeding), terwijl bij adertransplantaties PFKFB3 werd verwijderd in de EC's vóór de ontwikkeling van de ziekte. Bovendien zou 3PO kunnen interfereren met het metabolisme van andere celtypes die betrokken zijn bij de ontwikkeling van plaque. De vermindering van de IP-angiogenese die wordt waargenomen bij adertransplantaties gaat gepaard met een vermindering van de lekkage van deze microvaatjes. Deze bevindingen zijn in lijn met in vitro waarnemingen en tumorangiogenesemodellen die aantonen dat PFKFB3-remming in EC's VE-cadherine endocytose vermindert en normalisering van de endotheliale barrière bevordert. Aanvullend onderzoek is nodig om te begrijpen of de rijping van IP-vaten wordt beïnvloed door PFKFB3-deletie. Samen met een reductie van microvaten hebben we ook minder macrofaag infiltratie in lesies van ApoE$^{-/-}$ PFKFB3^{ECKO} muizen gedetecteerd, wat suggereert dat er een verband bestaat tussen het EC metabolisme en macrofaag infiltratie. Deze laatste bevinding is ook anders dan de farmacologische remming van glycolyse. Desalniettemin, in lijn met eerdere bevindingen, speculeren we dat het effect dat in vivo is waargenomen na EC-specifieke PFKFB3 deletie, te wijten is aan het herstel van de celverbinding met minder monocyten die de lesie binnendringen, wat plaques stabieler maakt. Interessant is dat EC-specifieke PFKFB3 deletie de ontwikkeling van plaques remt in ApoE$^{-/-}$ muizen, een natief atherosclerose diermodel dat geen kenmerken van geavanceerde lesies zoals IP-microscopische cellen ontwikkelt. Al met al tonen deze bevindingen de potentiële waarde aan van de modulatie van EC-glycolyse, en in het bijzonder PFKFB3, als een therapeutische strategie om de ontwikkeling van plaque tegen te gaan in adertransplantaties en native atherosclerose.

In **hoofdstuk 7** presenteerden we een studie die werd uitgevoerd in samenwerking met de Universiteit van Aberdeen. Hier beschreven we de ontwikkeling van een PFKFB3-gerichte PET-radiotracer, [18F] ZCDD083 (18F-radiolabelde fenoxindazoolverbinding, ZCDD083), voor beeldvorming van de atherosclerotische plaque in vivo. ZCDD083 is een nauwe structurele nabootsing van de krachtige PFKFB3-remmer AZ68 (IC50 = 4 nM), waarvan de radiofluorisatie wordt geacht

chemisch levensvatbaar te zijn en waarvan het onwaarschijnlijk is dat het de binding met PFKFB3 beïnvloedt. De specificiteit van de tracer voor atherosclerotische plaques wordt aangetoond door de combinatie van ex vivo autoradiografie met en face Oil Red O kleuring van dezelfde aortaspecimens. Inderdaad, we hebben co-lokalisatie van het [18F]ZCDD083 signaal met plaqueverdeling langs de aorta waargenomen. Deze kruisstudies in C57BL/6J, ApoE$^{-/-}$ en ApoE$^{-/-}$Fbn1$^{C1039G+/-}$ muizen toonden een hoge gevoeligheid van [18F]ZCDD083 aan om atherosclerotische plaques te detecteren, terwijl weinig signaal werd gedetecteerd in normale vaten of buiten atherosclerotische lesies. Deze tracer is een veelbelovend niet-invasief diagnostisch hulpmiddel om ruptuurgevoelige atherosclerotische plaques op te sporen, wat op zijn beurt kan helpen bij het verbeteren van de risicostratificatie en de evaluatie van de werkzaamheid van anti-atherosclerotische therapieën.

In **hoofdstuk 8** presenteerden we een nieuwe beeldvormingsmethode voor een driedimensionale reconstructie van het IP-vaatnetwerk in een muismodel van geavanceerde atherosclerose dat spontaan IP-angiogenese ontwikkelt. Deze methode is een nuttig instrument voor studies die erop gericht zijn te bepalen of er een causaal verband bestaat tussen de aanwezigheid van IP neovatstructuren en atherogenese of tussen angiogene stimuli en plaque angiogenese.

Recente studies hebben onthuld dat glycolyse en vetzuuroxidatie (FAO) in EC's het uitlopen van vaten parallel aan gevestigde groeifactoren zoals VEGF (vasculaire endotheliale groeifactor) of FGF (fibroblast endotheliale groeifactor) aandrijven. Met name EC's vertonen een hoge glycolytische activiteit en het is aangetoond dat het niveau van de glycolyse in actieve EC's vergelijkbaar is met dat van tumorcellen en veel hoger is dan dat van andere gezonde cellen. Bovendien is de glycolytische flux in EC's >200 maal zo hoog als glucose-oxidatie, vetzuuroxidatie en glutamine-oxidatie, waardoor >85% van het totale cellulaire ATP-gehalte wordt gegenereerd.

Dit proefschrift bevat een aantal farmacologische en genetische preklinische studies die het effect van glycolyse-inhibitie in de geactiveerde vaatwand en endotheel in de context van atherosclerose beschrijven. In het algemeen vinden we dat glycolyse remming in EC’s geassocieerd wordt met gunstige effecten zoals een vermindering

van de plaquevorming, plaque progressie en IP angiogenese. Gezien het sterke bewijs dat verminderde IP-vascularisatie plaques minder kwetsbaar maakt, kan glycolyse-inhibitie een nieuwe strategie zijn om het risico op plaquebreuk en de frequentie van ongunstige cardiovasculaire gebeurtenissen te verminderen.
In dit proefschrift hebben we diermodellen geanalyseerd die de kenmerken van menselijke atherosclerose en plaque progressie recapituleren. De experimentele data verkregen uit deze modellen suggereren een kritische rol van het EC metabolisme in de vorming en progressie van atherosclerose naast IP vascularisatie. Toch zijn er nog open vragen. Zo zagen we bijvoorbeeld bij adertransplantaties van ApoE$^{-/-}$ PFKFB3^{ECKO} muizen een duidelijke afname in IP neovascularisatie geassocieerd met verminderde plaque groei, maar of deze gebeurtenissen oorzakelijk verbonden zijn blijft onduidelijk.

We hebben ons gefocuseerd op PFKFB3 als doelwit voor glycolyse-inhibitie. Het is aangetoond dat dit enzym onder atheroprone turbulente stroming en in halsslagaders van patiënten met verhoogde niveaus van lipoproteïne(a) (die verhoogde glycolyse en EC activering veroorzaken) opgereguleerd is. Onlangs werden echter andere metabolische enzymen geïdentificeerd in de controle van de EC glycolytische flux en angiogenese. Een recente studie heeft inderdaad aangetoond dat verwijdering van hexokinase 2 (HK2) in EC's leidt tot verminderde glycolyse, wat de EC proliferatie, migratie en angiogenese in vivo belemmert. Tot slot is aangetoond dat oxidatie van endotheelvetzuren (FAO) een tamelijk onverwachte rol speelt bij het uitlopen van vaten. Een recente studie heeft inderdaad aangetoond dat de EC-specifieke verwijdering van carnitine palmitoyltransferase 1a (CPT1a), die vetzuren (FA's) invoert in mitochondriën en daardoor de FAO-flux beperkt, de EC-proliferatie vermindert en een vermindering van neoangiogenese veroorzaakt, zowel in vitro als in vivo. Al deze factoren die betrokken zijn bij de EC-metabole pathways moeten worden onderzocht in de context van atherosclerotische plaquevorming en -groei om de rol van het EC-metabolisme in de verschillende stadia van de ziekte beter te kunnen ontleden.

Statines zijn competitieve remmers van 3-hydroxy-3-methylglutaryl coenzyme A (HMG-CoA) reductase, het enzym dat de snelheidsbeperkende stap in de

cholesterolsynthese katalyseert en ze zijn een van de meest voorgeschreven medicijnen. Statines worden gebruikt om de progressie van atherosclerose te vertragen en het cardiovasculaire risico te verminderen. Naast hun cholesterolverlagende werking hebben ze ook ontstekingsremmende eigenschappen en verbeteren ze de endotheliale functie door de expressie van endotheliale progenitorcellen die betrokken zijn bij vasculair herstel en de expressie van endotheliale stikstofoxide synthase te verhogen.11 Meer recentelijk heeft de klasse van PCSK9 Inhibitors (bijv. alirocumab, evolocumab) die leverproteïneconvertase subtilisine kexine 9 inactiveren een nog lager circulerend LDL-C-gehalte bereikt en is goedgekeurd als eerstelijnsmedicijn om het risico van cardiovasculaire aandoeningen bij patiënten die geen statines kunnen verdragen te verminderen.12 Statines en PCSK9-remmers werken in op hyperlipidemie, wat een bewezen risicofactor is voor plaque progressie, ruptuur en ongunstige cardiovasculaire aandoeningen. Geneesmiddelen die specifiek gericht zijn op het EG-metabolisme kunnen een nieuwe aanpak bieden om de ontwikkeling van atherosclerotische lesies te remmen door zich te richten op de onderliggende mechanismen van endotheliale disfunctie. Bovendien kan een combinatie van manipulatie van de ECs en het lipidenmetabolisme in gevestigde atherosclerose leiden tot minder cardiovasculaire complicaties als gevolg van kwetsbare plaques en tot een algemene verbetering van de overlevingskansen.

Statines zijn competitieve remmers van 3-hydroxy-3-methylglutaryl coenzyme A (HMG-CoA) reductase, het enzym dat de snelheidsbeperkende stap in de cholesterolsynthese katalyseert en ze zijn één van de meest voorgeschreven geneesmiddelen. Statines worden gebruikt om de progressie van atherosclerose te vertragen en het cardiovasculaire risico te verminderen. Naast hun cholesterolverlagende werking hebben ze ook ontstekingsremmende eigenschappen en verbeteren ze de endotheliale functie door de expressie van endotheliale progenitorcellen die betrokken zijn bij vasculair herstel en de expressie van endotheliale stikstofoxide synthase te verhogen. Meer recentelijk heeft de klasse van PCSK9 Inhibitors (bijv. alirocumab, evolocumab) die leverproteïneconvertase subtilisine kexine 9 inactiveren een nog lager circulerend LDL-C-gehalte bereikt, en zijn ze goedgekeurd als eerstelijnsmedicijn om het risico van cardiovasculaire aandoeningen bij patiënten die geen statines kunnen verdragen te verminderen.

Statines en PCSK9-remmers werken in op hyperlipidemie, wat een bewezen risicofactor is voor plaque progressie, ruptuur en ongunstige cardiovasculaire aandoeningen. Geneesmiddelen die specifiek gericht zijn op het EC-metabolisme kunnen een nieuwe aanpak bieden om de ontwikkeling van atherosclerotische lesies te remmen door zich te richten op de onderliggende mechanismen van endotheliale disfunctie. Bovendien kan een gecombineerde manipulatie van EC's en het lipidenmetabolisme in gevestigde atherosclerose leiden tot minder cardiovasculaire complicaties als gevolg van kwetsbare plaques en tot een algemene verbetering van de overlevingskansen.

Curriculum Vitae

Paola Perrotta was born on 11 September 1986 in south of Italy (Puglia). After high-school, she moved to Tuscany to attend a 5-year Master Program at the School of Pharmacy of the University of Siena. During her course of study she became growingly interested in Pharmacology, and eventually joined the Pharmacology and Angiogenesis Laboratory under the supervision of Prof. Sandra Donnini and Prof. Marina Ziche. In 2012, after successfully defending her thesis about inflammatory angiogenesis, she graduated with a master degree in Pharmaceutical Chemistry. While continuing her research project with Prof. Ziche as post-graduate fellow, she also enrolled in an advanced master in oncological pharmacology at the University of Milan (academic year 2012-2013) where she graduated with a thesis discussion about monoclonal antibodies in cancer therapy. In 2013 she received a "Fellowship for Young Scientist" by the Italian Pharmacology Society to pursue of period of study and research in the Pharmacology laboratory directed by Prof. Sessa at Yale University (USA). In December 2015 she was selected for the MoGlyNet program, a Marie Curie European Joint doctoral program between the University of Antwerp and the University of Leiden. Paola started with a secondment in the laboratory of Prof. Paul Quax at LUMC and received initial training in advanced microsurgical techniques under the supervision of Dr. Margreet de Vries. After that she carried out her experimental doctoral thesis in the Physiopharmacology laboratory under the supervision of Prof. Wim Martinet at the University of Antwerp. Here she investigated the effect of glycolysis inhibition in endothelial cells in the context of atherosclerosis using advanced in vitro and in vivo models. During her doctoral period she attended multiple specialistic courses and presented scientific data at various international conferences. Paola is certified by Federation of European Laboratory Animal Science Associations (FELASA) for her skills in handling small laboratory animals. Other relevant professional experiences during her doctorate include an internship in a Contract Research Organization (PPD) in Milan (Italy) where she gained knowledge about clinical research and followed the development of clinical trials in various hospitals. In August 2020 she married with Federico, her long-term partner met in college, with whom she also shares the love for science. Currently, Paola is doing research activity in collaboration with the Yale Cardiovascular Research Center in the United States. *Erna Peters and Besa Emini Veseli, paranimfen*

List of publications

1. Emini Veseli, B., Perrotta, P., Van Wielendaele, P., Lambeir, A. M., Abdali, A., Bellosta, S., Monaco, G., Bultynck, G., Martinet, W., and De Meyer, G. R. Y. (2020) Small molecule 3PO inhibits glycolysis but does not bind to 6-phosphofructo-2-kinase/fructose-2,6-bisphosphatase-3 (PFKFB3). *FEBS Lett*
2. Perrotta, P., Pintelon, I., de Vries, M. R., Quax, P. H. A., Timmermans, J. P., De Meyer, G. R. Y., and Martinet, W. (2020) Three-Dimensional Imaging of Intraplaque Neovascularization in a Mouse Model of Advanced Atherosclerosis. J Vasc Res, 1-7
3. De Dominicis, C., Perrotta, P., Dall'Angelo, S., Wyffels, L., Staelens, S., De Meyer, G. R. Y., and Zanda, M. (2020) [(18)F]ZCDD083: A PFKFB3-Targeted PET Tracer for Atherosclerotic Plaque Imaging. ACS Med Chem Lett 11, 933-939
4. Perrotta, P., Van der Veken, B., Van Der Veken, P., Pintelon, I., Roosens, L., Adriaenssens, E., Timmerman, V., Guns, P. J., De Meyer, G. R. Y., and Martinet, W. (2020) Partial Inhibition of Glycolysis Reduces Atherogenesis Independent of Intraplaque Neovascularization in Mice. Arterioscler Thromb Vasc Biol 40, 1168-1181
5. Zhou, H., Mehta, S., Srivastava, S. P., Grabinska, K., Zhang, X., Wong, C., Hedayat, A., Perrotta, P., Fernandez-Hernando, C., Sessa, W. C., and Goodwin, J. E. (2020) Endothelial cell-glucocorticoid receptor interactions and regulation of Wnt signaling. JCI Insight 5
6. Perrotta, P., Emini Veseli, B., Van der Veken, B., Roth, L., Martinet, W., and De Meyer, G. R. Y. (2019) Pharmacological strategies to inhibit intra-plaque angiogenesis in atherosclerosis. Vascul Pharmacol 112, 72-78
7. Emini Veseli, B., Perrotta, P., De Meyer, G. R. A., Roth, L., Van der Donckt, C., Martinet, W., and De Meyer, G. R. Y. (2017) Animal models of atherosclerosis. Eur J Pharmacol 816, 3-13
8. Ulrich, V., Rotllan, N., Araldi, E., Luciano, A., Skroblin, P., Abonnenc, M., Perrotta, P., Yin, X., Bauer, A., Leslie, K. L., Zhang, P., Aryal, B., Montgomery, R. L., Thum, T., Martin, K., Suarez, Y., Mayr, M., Fernandez-Hernando, C., and Sessa, W. C. (2016) Chronic miR-29 antagonism promotes favorable plaque remodeling in atherosclerotic mice. EMBO Mol Med 8, 643-653
9. Landskroner-Eiger, S., Qiu, C., Perrotta, P., Siragusa, M., Lee, M. Y., Ulrich, V., Luciano, A. K., Zhuang, Z. W., Corti, F., Simons, M., Montgomery, R. L., Wu, D., Yu, J., and Sessa, W. C. (2015) Endothelial miR-17 approximately 92 cluster negatively regulates arteriogenesis via miRNA-19 repression of WNT signaling. Proc Natl Acad Sci U S A 112, 12812-12817

Acknowledgments

I would like to thank all the fantastic people and great scientists in Antwerp, Leiden and all over Europe who made my PhD an exciting scientific and personal journey.
I spent the first 7 months of my PhD in the laboratory of Prof. Paul Quax in Leiden. Paul, thank you very much for your constant guidance and encouragements. Your positive attitude and energy have always provided me with motivation throughout my PhD. Your enthusiasm for science and your ability to involve young scientists, taught me that science may begin with experiments but continues with the sharing of experiences and results. I have always been able to count on your support and for that, I am very thankful to you.
In Leiden I learned micro-surgery techniques with the extraordinary help of Dr. Margreet de Vries. Margreet, I want to thank for your guidance and for teaching me to be tenacious. I still remember when you came to Antwerp to help with my project, and our pleasant chats during dinner with pizza and Belgian soups. I have always appreciated your honesty in our scientific meetings and your feedback has greatly improved my scientific work.
I want to thank all the colleagues of the laboratory in Leiden. You are all very kind people and great scientists, I wish you all the best for your future!
I would like to thank my promoter in Antwerp, Prof. Wim Martinet. Wim you have been closely involved in my research and I have learned a lot from your scientific rigor. You have always helped me to overcome experimental hurdles and encouraged me to not give up. In our meetings, we talked a lot about cellular metabolism and autophagy and I gained a lot scientific knowledge from these discussions. Thanks for always being straightforward, I have always been able to count on your support. I thank you for everything!
Then, Prof. Guido De Meyer, who I also consider my supervisor. Guido, your positivity and your enthusiasm for science are contagious. I loved the words that you said when I was facing with difficult reviewers questions for the first time. You said "when the going gets tough, the tough get going!". Thank you for everything!
A big thank you to all the members of the Physiopharmacology laboratory (PhD students, Professors, technician and people from administration) who have become friends and with whom I have shared many great moments. This has contributed to make my PhD journey one of the most exciting and rewarding time of my life. Thank

you very much for your support and friendship. You all have conquered a special place in my heart!
Finally, I want to thank my family and my husband Federico. Thank you for always being there and for the love you always show me. Without you, everything would have been much more difficult!